Aus dem Institut für Arbeits-, Sozial- und Umweltmedizin
der Heinrich-Heine-Universität Düsseldorf
Direktor: Prof. Dr. med. Peter Angerer

Ambient Air Pollution and Cardiovascular Health

The Role of Exposure Assessment, Particle Size, and Co-Exposure with Noise

Dissertation

zur Erlangung des Grades eines Doktors der Public Health
der Medizinischen Fakultät der Heinrich-Heine-Universität Düsseldorf

vorgelegt von
Frauke Hennig

2021

Als Inauguraldissertation gedruckt mit Genehmigung der Medizinischen Fakultät der Heinrich-Heine-Universität Düsseldorf

gez.:

Dekan: Prof. Dr. Nikolaj Klöcker

Erstgutachterin: Prof. Dr.med Barbara Hoffmann MPH

Zweitgutachter: Prof. Dr.sc.hum Oliver Kuss

I am not a fan of PM_{10}

Für meine Großeltern.

Parts of this work have been published:

Hennig F, Sugiri D, Tzivian L, Fuks K, Moebus S, Jöckel KH, et al. 2016. Comparison of land-use regression modeling with dispersion and chemistry transport modeling to assign air pollution concentrations within the Ruhr area. Atmosphere (Basel) 7; doi:10.3390/atmos7030048.

Hennig F, Quass U, Hellack B, Küpper M, Kuhlbusch TAJ, Stafoggia M, et al. 2018. Ultrafine and fine particle number and surface area concentrations and daily cause-specific mortality in the Ruhr area, Germany, 2009–2014. Environ Health Perspect 126:1-10; doi:10.1289/EHP2054.

Hennig F, Moebus S, Reinsch N, Budde T, Erbel R, Jöckel KH, et al. 2019. Investigation of air pollution and noise on progression of thoracic aortic calcification: results of the Heinz Nixdorf Recall Study. Eur J Prev Cardiol 0:1–9; doi:10.1177/2047487319854818.

Hennig F, Geisel MH, Kälsch H, Lucht S, Mahabadi AA, Moebus S, et al. 2020. Air pollution and progression of atherosclerosis in different vessel beds—results from a prospective cohort study in the ruhr area, germany. Environ Health Perspect 128:1–9; doi:10.1289/EHP7077.

Zusammenfassung

Luftverschmutzung ist ein wichtiger umweltbedingter Risikofaktor für kardiovaskuläre Erkrankungen und Mortalität. Während eine kurzfristige Exposition akute Ereignisse auslösen kann, kann eine langfristige Exposition Atherosklerose begünstigen. Der Co-Exposition Lärm wird eine ähnliche Rolle zuteil. Im Ruhrgebiet in Deutschland leben etwa 5 Millionen Menschen, die einer ständigen Luftverschmutzung und möglicherweise Lärmbelastung, ausgesetzt sind, die nicht nur durch lokale, sondern auch umliegende Verkehrs-und Industriequellen hervorgerufen werden. Feinstaub mit einem aerodynamischen Durchmesser von $\leq$ 10 μm (PM_{10}), $\leq$ 2,5 μm ($PM_{2.5}$), und Stickstoffdioxid (NO_2) wird dort routinemäßig an ausgewählten Stationen gemessen, von denen eine Station zusätzlich, die möglicherweise besonders schädlichen, ultrafeinen Partikel (UFPs) misst. Um die langfristige Luftschadstoffkonzentration flächendeckend abzuschätzen, wurden zwei Modelle eingesetzt: Das zeitliche- und räumliche EURAD-Modell (European Air Pollution Dispersion) und das statische, aber räumliche Landnutzungs-Regressionsmodell (LUR). Hauptziele dieser Dissertation waren der Vergleich des EURAD- und des LUR-Modells im Studiengebiet; die Untersuchung von Assoziationen zwischen kurzfristiger Luftverschmutzungsexposition und kardiovaskulärer Mortalität; das Zusammenspiel von Luftverschmutzung und Lärm; und die Untersuchung der Assoziation zwischen langfristiger Luftverschmutzungsexposition und Progression der Atherosklerose. Kurzfristige Auswirkungen von Luftschadstoffen, insbesondere UFPs, auf die kardiovaskuläre Mortalität, wurden im Rahmen eine Zeitreihe mit denen vom zentralen Statistik- und IT-Dienstleister des Landes Nordrhein-Westfalen erhobenen Daten (2009-2014), untersucht. Langfristige Auswirkungen von Luftverschmutzung auf die Progression der Atherosklerose, d.h. koronarer Verkalkung (CAC), thorakaler Verkalkung (TAC) und der Intima-Media-Dicke der Halsschlagader (cIMT), wurden mit Daten der prospektiven (t_0: 2000-2003, t_1: 2006-2008) Heinz Nixdorf Recall-Kohortenstudie (Bochum, Mülheim und Essen), bestehend aus 4814 zufällig ausgewählten Männern und Frauen im Alter von 45-75 Jahren, untersucht. Die Übereinstimmung zwischen den mit dem EURAD-CTM und dem LUR-Modell geschätzten langfristigen Luftschadstoffkonzentrationen war schwach bis mäßig, wobei beide Modelle ihre Berechtigung haben. Kurzzeitige Exposition zeigte ähnliche, unmittelbare und verzögerte, Assoziationen für PM_{10} und UFPs mit kardiovaskulärer Mortalität. Luftverschmutzung war in der Gesamtpopulation nicht mit dem Fortschreiten der Atherosklerose (CAC, TAC und cIMT) assoziiert. Jedoch wurde eine konsistente Assoziation bei Teilnehmern mit keiner oder geringer atherosklerotischer Ausgangsbelastung beobachtet, die für $PM_{2.5}$ und CAC am konsistentesten war. Beobachtete Assoziationen waren robust gegenüber Lärmexposition und zeigten keine synergistische Wirkung. Ergebnisse für unterschiedliche Modellierungen für Luftverschmutzungskonzentrationen waren ähnlich. Zusammenfassend lässt sich sagen, dass Luftverschmutzung, insbesondere $PM_{2.5}$, sowohl mit akuten kardiovaskulären Ereignissen als auch mit chronischen Entwicklungen, wie Atherosklerose, assoziiert ist. Diese Ergebnisse ergänzen die epidemiologische Evidenz für die Notwendigkeit strengerer Vorschriften zur Reduzierung der Luftverschmutzung, um insbesondere in Ballungsräumen wie dem Ruhrgebiet die kardiovaskuläre Krankheitslast zu senken.

Summary

Air pollution is a major environmental risk factor for cardiovascular diseases (CVDs) and mortality (CVM). While short-term exposure to air pollution can trigger acute cardiovascular events, long-term exposure can contribute to atherosclerosis, the main underlying pathology of CVDs. Noise, a co-exposure of air pollution, has been shown to play a similar role regarding CVDs. The Ruhr Area is a metropolitan living and working environment in Western Germany, where roughly 5 million people are consistently exposed to air pollution and potentially noise, emitted not only from local, but also from surrounding traffic and industry. Air pollution, i.e. particulate matter with an aerodynamic diameter of $\leq 10\ \mu m$ (PM_{10}), $\leq 2.5\ \mu m$ ($PM_{2.5}$), nitrogen dioxide (NO_2), is routinely measured at selected traffic and urban background stations in the Ruhr Area, of which one station additionally measures ultrafine particles (UFPs), which are hypothesized to be particularly harmful for human health. In order to estimate long-term air pollution concentration in the whole Ruhr Area, two models were applied to estimate concentration levels at study participants residences: the temporal and spatial European Air Pollution Dispersion chemistry transport model (EURAD-CTM) and the temporally static but spatially variable land-use regression (LUR) model. The main objectives of this dissertation were to compare the EURAD and the LUR model; to investigate associations between short-term air pollution exposure and cardiovascular mortality; to evaluate the role of noise in the context of air pollution; and to evaluate the association between long-term exposure to air pollution and progression of atherosclerosis in different vessel beds. To study short-term effects of air pollution, particularly UFPs, cause-specific mortality, including CVM, was collected (2009-2014) from the central statistical and IT services provider of North Rhine-Westphalia for the three adjacent cities of Essen, Mülheim, and Oberhausen. Investigating effects of long-term exposure to air pollution on progression of atherosclerosis, namely coronary calcification (CAC), thoracic calcification (TAC), and carotid intima media thickness (cIMT), data of the prospective (t_0: 2000-2003, t_1: 2006-2008) Heinz Nixdorf Recall cohort study, located in the center of the Ruhr Area (Bochum, Mülheim, and Essen) was used, consisting of 4814 randomly selected males and females aged 45-75 years. Agreement between long-term air pollutant concentrations estimated with the EURAD-CTM and LUR model was weak to moderate, while both models have their justification. Short-term exposure showed immediate and delayed associations with with CVM, although UFPs were not shown to yield stronger effects. Air pollution was not associated with progression of atherosclerosis (CAC, TAC and cIMT) in the full population. However, a consistent association was observed in participants with no or minor initial atherosclerotic burden, which were most consistent for $PM_{2.5}$ and CAC. Observed associations were robust with regard to noise exposure and no synergistic effects of air pollution and noise exposure could be found. Overall associations between long-term exposure to air pollution and progression of atherosclerosis were fairly similar regarding air pollution modelling. In conclusion, air pollution, in particular $PM_{2.5}$, has shown to be associated with acute CV events, as well as with chronic developments, like atherosclerosis. These results add to the epidemiological evidence supporting the need for stricter regulations in air pollution reduction to lower CVDs and CVM, especially in metropolitan areas, like the Ruhr Area.

List of Abbreviations

Abbreviation	Definition
AAC	Abdominal aortic calcification
ATAC	Ascending thoracic aortic calcification
ATC	Anatomical Therapeutic Chemical classification system
BC	Black carbon
BImSchV	Verordnung zur Durchführung des Bundes-Immissionsschutzgesetzes (Federal Immission Control Act)
BMI	Body mass index
BS	Black smoke
CAC	Coronary calcification
CAD	Coronary artery disease
CCA	Common carotid artery
CHD	Coronary heart disease
CI	Confidence interval
cIMT	Carotid intima media thickness
CO	Carbon monoxide
CRP	C-reactive protein
CT	Computed tomography
CTM	Chemistry transport model
CV	Cardiovascular
CVD	Cardiovascular disease
CVM	Cardiovascular mortality
DCTM	Dispersion chemistry transport model
DM	Diabtes Mellitus
DTAC	Descending thoracic aortic calcification
EBCT	Electron beam computer tomography
EC	Elemental carbon
EEA	Europpean Environment Agency
ELAPSE	Effects of Low-Level Air Pollution: A Study in Europe
ESCAPE	European Study of Cohorts for Air Pollution Effects
ETS	Environmental tobacco smoke
EU	European Union
EURAD	European Air Pollution Dispersion
GIS	Geographic information system
GUAN	German Ultrafine Aerosol Network
HDL	High-density lipoprotein
HEI	Health Effects Institute
HNR	Heniz Nixdorf Recall
ICD-10	International Classification of diseases, 10th Revision
IND	Industry (industry-specific)
IQR	Interquartile range
IUTA	Institut für Energie- und Umwelttechnik (Institute of Energy and Environmental Technology)

(continued)

Abbreviation	Definition
LANUV	Landesamt für Natur, Umwelt und Verbraucherschutz Nordrhein-Westfalen (State Agency for Nature, Environment, and Consumer Protection)
L_{DEN}	Day-and-evening noise
LDL	Low-density lipoprotein
L_{Night}	Night-time noise
LOOCV	Leave one out cross validation
LUR	Land use regression
MESA	Multi-Ethnic Study of Atherosclerosis
NH_3	Ammonia
NM	Natural mortality
NMVOCs	Non-methane volatile organic compounds
NO	Nitric oxide
NO_2	Nitrogen dioxide
NRW	North Rhine-Westphalia
NSAM	Nanoparticle surface area monitor
nSES	Socioeconomical status within the neighbourhood
O_3	Ozone
OR	Odds Ratio
PM	Particulate matter
PM_1	Particulate matter with an areodynamic diameter $\leq 1\ \mu m$
PM_{10}	Particulate matter with an areodynamic diameter $\leq 10\ \mu m$
$PM_{2.5}$	Particulate matter with an areodynamic diameter $\leq 2.5\ \mu m$
PN_{acc}	PNC of accumulation mode particles
PNC	Particle number concentration
PSC	Particle surface concentration
Recall	Risk factors, Evaluation of coronary calcium and lifestyle
RM	Respiratory Mortality
RR	Relative Risk
SD	Standard deviation
SNAP-97	Selected Nomenclature for Sources of Air Pollution
SO_2	Sulfur dioxide
STYR	Mülheim Styrum Measurement station
t_0	Baseline examination
t_1	Follow-up examination
T2DM	Type-2 Diabetes Mellitus
TAC	Thoracic calcification
TRA	Traffic (traffic-specific)
UBA	Umweltbundesamt (Federal Environmental Agency)
UFPs	Ultrafine particles
VIF	Varicance inflation factor
WHO	World Health Organization

Table of Contents

1 Introduction

1.1 Role of Air Pollution regarding Public Health

Air pollution is not only the biggest environmental health risk in Europe, it has also been shown to be a major risk factor for chronic non-communicable diseases (WHO European Centre for Environment and Health 2013) and has been identified as a leading contributor to global morbidity and premature mortality (Gakidou et al. 2017). In particular, cardiovascular diseases (CVDs), combing disorders of the heart and blood vessels, do not only define the leading cause of death worldwide, but have also been ranked first among the causes of death from air pollution (Estol 2020). In fact, ambient air pollution is the fifth most common risk factor of (cardio-) vascular disease, following hypertension, smoking, diabetes, and obesity (Johnson et al. 2019).

Origins of epidemiological studies on health effects of air pollution date back to the 1930s in Meuse Valley, Belgium; 1952 in London, United Kingdom; and or 1962 in the Ruhr Area, Germany where increased mortality rates occurred during episodes of extreme elevations in urban pollution ("Smog") (Brook et al. 2004; Bruckmann et al. 2014). After the first legislation to fund air pollution studies in 1955, the "Clean Air Act" legislation of 1970 marked the beginning of governmental involvement reducing air pollution for a cleaner air and a healthier environment in the United States. Likewise, the first "Act on Air Pollution Control, Noise and Vibration Abatement" of the German state North Rhine-Westphalia (NRW) from April 1962 marked a big step toward governmental control of air pollution. In addition, the European Union (EU) has worked to reduce air pollution levels since the early 1970s by integrating environmental protection requirements into the transport and energy sectors (European Environment Agency (EEA) 2013). The first major instrument was the Air Quality Framework Directive 96/62/EC and its daughter Directives establishing standards for a range of air pollutants in the period up to the year 2004 (European Commission 2021).

Yet, despite consistent monitoring of air pollution concentrations (European Environmental Agency (EEA) 2017) and observed improvements in air quality over the past few decades, air pollution concentrations are partially still exceeding European standards (Kelly and Fussell 2015). Moreover, associations between current ambient pollution levels and elevated morbidity and mortality have consistently been detected (Brunekreef and Holgate 2002), such that today's environment is not considered safe with respect to the pathogenic role for vascular diseases (Estol 2020).

1.2 Air Pollution Exposure and Assessment

1.2.1 Air Pollutants and Sources

Air pollution is used as a general term for a heterogeneous mixture of gases, particulate matter (PM), and biological molecules from both natural and human-made sources.

Natural sources include emissions from volcanic eruptions, sea salt, forest fires, organic compounds, dust, or pollen, while human-made sources include road traffic, power and district heating plants, waste incineration plants, stoves and heaters in residential buildings or industrial processes. In metropolitan areas, road traffic defines the most meaningful source for particulate emissions. For example, particles are released by engines, primarily diesel engines, by brake and tire abrasion, or by dust swirled up from road surfaces (Umweltbundesamt 2009). Moreover, air pollutants can be transmitted over wide areas, which is known as long-range transmission of air pollutants. The term PM refers to solid and liquid aerosol particles with various chemical compositions, occurring in many sizes and shapes, which can either be directly emitted from anthropogenic or natural sources, or be formed in the atmosphere from emissions of sulfur dioxide (SO_2), nitrogen oxides (NO_x), ammonia (NH_3) or non-methane volatile organic compounds (NMVOCs). PM_{10} refers to particles with an aerodynamic diameter equal to or less than 10 μm, of which $PM_{2.5}$ defines a subset of finer particles with an aerodynamic diameter equal to or less than 2.5 μm (European Environmental Agency (EEA) 2013). The smallest particles are called ultrafine particles (UFPs) and have an aerodynamic diameter of less than 0.1 μm. Other air pollutants include SO_2, NO_x (nitrogen dioxide (NO_2) and nitrogen monoxide (NO)), ozone (O_3), NH_3, NMVOCs, carbon monoxide (CO), or methane. SO_2 emissions can be assigned to the electricity generation sector, NO_x and CO are emitted from industrial facilities and the road transport sector, NH_3 and methane emissions can be predominantly assigned to the agricultural sector, while O_3 is not directly emitted. Among different sources of air pollution, traffic-related air pollution has not only been considered as the most detectable form of air pollution, but also as the most substantial with regard to the global burden of disease (HEI Panel on the Health Effects of Traffic-Related Air Pollution 2009). The most prominently used surrogates for traffic-related pollution are CO, NO_2, benzene, particulate matter (PM_{10}, $PM_{2.5}$), UFPs, elemental carbon (EC) and black carbon or smoke (BC or BS). However, pollutants originating from traffic may not be easily distinguished from pollutants that contribute to ambient air pollution by other sources than traffic (HEI Panel on the Health Effects of Traffic-Related Air Pollution 2009). Furthermore, the impact of traffic-related pollutants on ambient air quality is defined on a broad spatial scale, ranging from roadside to urban and regional background, defining a major challenge to assess traffic-related air pollution in the context of epidemiological studies.

1.2.2 Assessment of Air pollution

While measured air pollution concentrations at central or stationary monitors have been used to link short-term air pollution exposure to acute events on a daily scale, they lack spatial resolution. Moreover, such time series analysis are able to capture air-pollution-related cases that are timely connected, while reduced life-expectancy, due to long-term morbidity enhanced by air pollution, may not be captured with this approach (Künzli et al. 2000). Hence, surrogates had to be developed to model air pollution exposure on a broader spatial scale in order to capture air pollution exposure on a population-based level (Hoek et al. 2008). The most common approaches for this are proximity-based,

land-use regression, dispersion, and hybrid approaches, including ambient and individual exposure. However, the latter has not prevailed in epidemiological research because of the cost. Although, proximity-based approaches are still used as an indicator for traffic in population-based cohorts (e.g. in Hoffmann et al. (2006), Künzli et al. (2010) or Lanki et al. (2015)), usage seems to be on a downward trend. This is likely due to legitimate concerns about exposure misclassification justified by the rapid decline of pollution with distance and the presence of upwind compared to downwind (HEI Panel on the Health Effects of Traffic-Related Air Pollution 2009) or the fact that it cannot be used as a basis for regulation. Moreover, model-based approaches have increasingly become available, aiming to capture air pollution exposure more accurately to study health effects of long-term exposure. The latter has especially become important in debates on air quality guidelines with respect to the protection of health (Künzli et al. 2000). Nevertheless, assessment of long-term exposure to air pollution remains a challenging task (Hoek et al. 2008) and until today, a gold standard method has not been identified. The two most common modelling approaches applied in epidemiological studies are land use regression model and dispersion (chemistry-transport) models.

Land-use regression defines a linear prediction model, developed using measured annual air pollution concentrations based on actual measurements at a small number of selected locations and a variety of land-use variables, obtained through geographic information systems (GIS), serving as predictor variables (features). The final prediction model is then applied to specific locations in the study area, for example participants' residences, to predict annually air pollution concentration based on land-use features (Hoek et al. 2008). The greatest advantage of this approach is its simplicity as well as its low costs of application. As a result, land-use regression is commonly applied in epidemiological studies, although its most common criticism is the lack of temporal variability.

Dispersion chemistry-transport models, on the other hand, assume a varying spatial distribution of air pollution concentrations over time due to changes in atmospheric conditions, land use or transport conditions. In contrast to statistical land-use regression models, dispersion models are based on mathematical formulations to characterize the atmospheric processes that disperse a pollutant emitted by a source. Taking into account emissions, meteorological conditions, atmospheric processes that lead to pollutant dispersion, transport, chemical conversion and removal from the atmosphere by deposition, air pollution concentration can be predicted at ground level.

With a growing body of knowledge about the environmental burden of air pollution on public health, especially in industrialized regions, air quality and hence air quality modelling have become important, not only for the sake of environmental research but also for policy questions (Jakobs et al. 2005). The EURAD (**Eur**opean **A**ir Pollution **D**ispersion) chemistry-transport model (CTM) is an example of a sophisticated dispersion and chemistry transport model, which has been developed for the simulation of air quality in Europe (Memmesheimer et al. 2004).

1.3 Air Pollution and Cardiovascular Health

1.3.1 Biological Mechanisms

The mechanisms of action of air pollutants on the cardiovascular system are central to the relationship between air pollution and cardiovascular disease. Not only does the size of the particles play a role, but also their mass and duration of exposure. While short-term exposure to air pollution can trigger acute cardiovascular events, longer-term exposure can contribute to cardiovascular risk to an even greater extent (Brook and Rajagopalan 2010). Brook and Rajagopalan (2010), revised by Franklin et al. (2015) have summarized three potential biological pathways, by which chronic inhalation of particles may lead to the development of CVDs: after inhalation, particles or components deposit in pulmonary tissues, from where they (1) spill-over to the systemic circulation by inducing pro-inflammatory or oxidative stress responses, (2) may cause an autonomic imbalance in the nervous system, or (3) penetrate directly into cardiovascular tissues, including endothelial cells. While none of these pathways are exclusive and complete knowledge about the interplay with respect to time, composition, and dose of particle inhalation can not be provided, air pollution-related inflammation can trigger the rupture of atherosclerotic plaques and promote tissue injury, potentially leading to myocardial infarction (Libby 2012). Biomarkers of inflammation, such as C-reactive protein (CRP) or interleukin-6, have not only been used for risk prediction of cardiovascular events, but they have also been shown to respond to inhalation of air pollution in European populations (Rückerl et al. 2007). Therefore, the activation of inflammatory mechanisms forms a major mediating pathway of air pollution-related cardiovascular effects.

Although, most robust evidence has been reported for cardiovascular effects of $PM_{2.5}$ (Franklin et al. 2015), epidemiological interest in health effects of UFPs has risen. Not only have UFPs received increased attention over the past decades due to their anthropogenic sources (e.g. motor vehicles powered by diesel engines), but they also have been considered to be more toxic. Due to their small size, UFPs can penetrate into the blood and lymph circulation more easily, and hence potentially reach sensitive targets, including the heart, more easily than larger particles. Moreover, the greater surface area per mass compared with larger-sized particles of the same chemistry was hypothesized to be responsible for greater biological activity, including inflammation (Oberdörster et al. 2005). Recently, there have been a growing number of studies investigating health effects of UFPs, suggesting that UFPs affect both, cardiovascular and respiratory health (HEI Review Panel on Ultrafine Particles 2013; Ohlwein et al. 2019).

In contrast to hypothesized mechanisms of particle exposure and cardiovascular disease, the role of NO_2 seems less well explored. Although a systemic vascular oxidative stress reaction causing vascular damage as a consequence of an oxidative reaction in the lung (1) could be related to NO_2 (Bourdrel et al. 2017), and NO_2 has been linked to increased cardiovascular mortality in epidemiological studies, a remaining research question is whether NO_2 is directly responsible for these observed adverse health effects or whether NO_2 serves only an indicator of other pollutants, e.g., PM (Faustini et al. 2014).

1.3.2 Atherosclerosis

Atherosclerosis is considered the major pathology regarding the development of CVDs and has also been hypothesized to play a major role in the causal chain of effects for cardiovascular events in the context of air pollution (Franklin et al. 2015). Atherosclerosis is an asymptomatic condition in which artery walls develop abnormalities, potentially leading to calcification or plaque and arterial congestion, causing myocardial infarction, stroke or peripheral artery disease. The biological function of arteries is the transport of oxygenated blood: coronary arteries, for example supply the heart muscle with oxygenated blood, the thoracic artery supplies the anterior chest wall and the breasts, while the common carotid arteries supply the head and neck. For the assessment of atherogenesis non-invasive imaging techniques can be used to directly capture the narrowing of arteries in terms of calcification, plaque or thickness. Common subclinical markers of atherosclerosis are coronary calcification (CAC), thoracic calcification (TAC) or carotid intima media thickness (cIMT). Due to the location within the human body, computed tomography (CT) is used to detect CAC and TAC, while ultrasound is used to capture the thickness of walls (intima media thickness) in the common carotid arteries, which lie superficially under the skin. Due to the ease of application and potentially lower costs, epidemiological studies investigating the association of air pollution and atherosclerosis have most often used cIMT as a surrogate for atherosclerosis. A meta-analysis, consisting of eight cross-sectional and three longitudinal studies, suggested evidence of a positive association between cIMT and long-term exposure to particulate air pollution (Provost et al. 2015).

1.3.3 Co-Exposure of Noise

Similar to air pollution exposure, epidemiological studies have shown adverse health effects from environmental noise regarding arterial hypertension, myocardial infarction, heart failure, and stroke (Münzel et al. 2018; World Health Organization 2011). Moreover, a growing body of evidence with regard to understanding the pathophysiological mechanisms of noise and the development of CVDs has shown that noise is associated with oxidative stress, vascular dysfunction, autonomic imbalance, and metabolic abnormalities, and may potentially contribute not only to cardiovascular risk factors, such as arterial hypertension and diabetes, but also to the progression of atherosclerosis (Münzel et al. 2018).

1.3.4 The Heinz-Nixdorf Recall Study

The Heinz Nixdorf Recall (**R**isk Factors, **E**valuation of Coronary **Cal**cium and **L**ifestyle) (HNR) study is a prospective cohort study executed to study cardiovascular disease and lifestyle in the general population (Schmermund et al. 2002). Participants were randomly selected from residents' registration offices of the three adjacent cities of Bochum, Mülheim, and Essen, located in the center of the Ruhr Area in Germany. All partici-

pants (or their legally authorised representative) provided written informed consent to undergo a program of examinations assessing preclinical atherosclerotic disease, an in-depth assessment of cardiovascular risk factors, including biomarkers (e.g. markers of inflammation), traditional risk factors (e.g. blood pressure, diabetes), as well as demographics (Schmermund et al. 2002). The HNR study complies with the Declaration of Helsinki and the study was approved by the institutional ethics committees (reference number: 99-69-1200).

Motivated by consistently high cardiovascular morbidity and mortality rates in an increasingly aging society, the HNR study has been part of international efforts to improve risk prediction in order to allow preventive treatment targeted at high-risk individuals.

In addition and motivated by the growing body of epidemiological and clinical evidence on adverse health effects of ambient air pollution and its relation to heart disease and stroke (Brook et al. 2004), the HNR study has also become a pioneering study regarding investigations on cardiovascular effects of air pollution in the general population in Germany and Europe. The first study in the HNR study investigating long-term exposure to traffic and coronary heart disease (coronary artery disease), which is the most common form among CVDs, was published in 2006, reporting adverse health effects (Hoffmann et al. 2006). In line, cross-sectional investigations have shown associations between particulate matter and atherosclerosis, in regard to CAC (Hoffmann et al. 2007), TAC (Kälsch et al. 2014), and cIMT (Bauer et al. 2010).

1.4 Air pollution in the Study Area

1.4.1 Air Quality in the Ruhr Area

The Ruhr Area, located in NRW, Germany, is a metropolitan living environment in Europe, which is not only affected by local rush-hour traffic and industrial hot spots, but also by traffic, industry, and shipping outside of the Ruhr Area or even outside of Germany. The Ruhr Area occupies an area of approximately 4,435 km^2, including four counties and 11 independent cities, of which Dortmund, Essen, Duisburg and Bochum are considered the core cities. As in many other major European cities, the air quality in the cities of the Ruhr Area is significantly affected by PM_{10} and NO_2 (Bezirksregierung Arnsberg 2011). Hence, the cities and the State Office for Nature, Environment and Consumer Protection (LANUV) have been carrying out measurements of air pollution concentrations for many years in order to monitor the air pollution situation. The legal foundation for binding air quality objectives is determined by the Air Quality Directive from 2008 of the European Union (EU) (European Union 2008). In Germany, a new directive was transposed into German law with effect from August 6, 2010 by amending the Federal Immission Control Act and by introducing the 39th Ordinance to the Federal Immission Control Act (39th BImSchV) (Bundesministerium der Justiz und für Verbraucherschutz 2010). With this, limit values for NO_2 and PM_{10} were confirmed, while first limit values were introduced for $PM_{2.5}$ (European Union 2008). PM_{10} mean concentration should not exceed 50 $\mu g/m^3$ (daily mean) or 40 $\mu g/m^3$ (annual mean).

For NO_2 concentrations, the 1-hour mean should not exceed 200 $\mu g/m^3$, and the annual mean should not exceed 40 $\mu g/m^3$. Mean annual $PM_{2.5}$ concentrations should not exceed 25 $\mu g/m^3$.

On the basis of these federal regulations, the air quality in the area of NRW has to be consistently monitored by measurement or model calculations. NRW is hence provided with 175 measurement locations of air quality monitoring by the LANUV (LANUV 2021). Of these, 15 stations are located in Essen (10 traffic station, 3 industry station, and 2 background stations), 4 traffic stations are located in Bochum, and one background as well as one traffic station is located in Mülheim. Among others, routinely monitored air pollutants are NO_2, PM_{10} and $PM_{2.5}$.

In addition, the German Ultrafine Aerosol Network (GUAN) was funded (Birmili et al. 2016) to continuously measure UFPs in selected areas of Germany, including the Ruhr Area, aiming to improve the understanding of atmospheric aerosol particles with regard to human particle exposure and climate effects. In cooperation with the Institute for Energy and Environmental Technology (IUTA), UFPs are continuously measured at the urban background station in Mülheim Styrum (STYR).

1.4.2 Air Pollution Modelling for the HNR Study Area

Based on a collaboration with the Rhenish Institute for Environmental Research (RIU) at the University of Cologne, it was possible to use the previously mentioned EURAD-CTM model (cf. Section 1.2.2) to estimate air pollution concentrations for several pollutants (PM_{10}, $PM2.5$, PM_1, NO, NO_2, NH_3, O_3, and SO_2) within the HNR study area, based on a resolution of one 1×1 km^2 (Nonnemacher et al. 2014). Using ArcView 9.2, location of residences were assigned to a 1×1 km^2-grid and then matched to the corresponding grid-based air pollutant concentration, including short-term (daily mean concentrations) and long-term (annual mean concentrations) exposure concentrations. Model runs for the EURAD-CTM within the Ruhr Area were executed for the examination periods of the HNR study (2000–2003, 2006–2008, and also 2011-2014).

Taking part in a large collaboration to generate epidemiological evidence with regard to air pollution within Europe, namely the **E**uropean **S**tudy of **C**ohorts for **A**ir **P**ollution **E**ffects (ESCAPE), a new air pollution model was developed for selected European regions, including the HNR study area. The ESCAPE study was funded by the European Commission to investigate multiple European studies simultaneously using a harmonized approach with respect to exposure assessment, definition of outcomes and covariates, as well as statistical modelling. As one result, LUR models were developed for annual concentrations of NO_2 and NO_x (Beelen et al. 2013), and PM_{10}, $PM_{2.5}$, $PM_{2.5\text{absorbance}}$, and PM_{coarse} (Eeftens et al. 2012) based on a standardized model approach in each area in which the original studies was located. Resulting prediction models were then applied to participants' residences, to estimate annual concentrations of respective air pollutants at the residences.

1.5 Aims of Thesis

1.5.1 Comparison of EURAD-CTM and LUR

The HNR study was provided with two modelling approaches to estimate long-term exposure to selected air pollutants at participants' residences. Within the scope of the ESCAPE study, a brief comparison showed only partial agreement, especially regarding total PM_{10} and $PM_{2.5}$ concentrations (Hoogh et al. 2014). Moreover different health effects have been detected in the HNR study: Bauer et al. (2010) reported a 4.9% (95% CI: 2.0%, 7.7%) difference in cIMT per 5 $\frac{\mu g}{m^3}$ change in annual-mean concentration of $PM_{2.5}$ estimated using the EURAD-CTM model, whereas Perez et al. (2015) reported a 0.57% (95% CI: –1.95%, 3.14%) difference in the same outcome per 5 $\mu g/m^3$ change in annual-mean concentration of $PM_{2.5}$ estimated using the LUR-model. Aiming for an in-depth comparison, the first publication includes quantitative and qualitative comparison between the EURAD-CTM and the LUR model with respect to air pollution concentrations in the HNR study area.

1.5.2 Effects of UFPs on Cardiovascular Mortality

The number of epidemiological studies investigating UFPs is still small compared to studies on PM_{10} and $PM_{2.5}$, limiting knowledge and evidence. Since UFPs are rarely measured, data collected within the GUAN (Birmili et al. 2016) provided a great chance to contribute to closing this knowledge gap. Because data on mortality is collected by the central statistical and IT services provider of North Rhine-Westphalia on a routine basis, it was possible to study short-term effects of UFPs on natural, cardiovascular and respiratory mortality. The second publication studied the effects of daily variations of different air pollution metrics, namely particle number concentrations (PNC) of particles in different sizes, including UFPs, and particle surface concentration (PSC), as well as the commonly used metrics PM_{10} and NO_2 on cause-specific daily mortality in the Ruhr Area between 2009 and 2014.

1.5.3 Air Pollution and Noise Exposure

Since both, environmental air pollution and environmental noise contribute to cardiovascular disease, and traffic have been identified as an important common source, noise defines a potential confounder in observational air pollution studies and *vice versa*. Prior investigations in the HNR study, however, have shown that long-term exposure to fine PM and noise exposure were both associated with subclinical atherosclerosis and remained associated after mutual adjustment (Kälsch et al. 2014). Aiming to investigate a potential synergism of air pollution and noise exposure that has not been investigated yet, the third paper studied the association of traffic-related air pollution, modelled using the EURAD-CTM and the co-exposure noise on progression of atherosclerosis in the thoracic aorta, concentrating on synergistic effects of simultaneous exposure.

1.5.4 Air Pollution and Atherosclerosis

In line with most epidemiological studies, cross-sectional findings within the HNR study were reported on one marker of subclinical atherosclerosis at a time. Considering that the HNR study is a population-based prospective cohort study with, to date, three examination periods (2000-2003, 2006-2008, 2011-2014), it not only seemed natural to confirm cross-sectional findings with longitudinal investigations but also use longitudinal observations in order to get a better understanding of atherogenesis, with regard to multiple markers of atherosclerosis. In addition, the applicable air pollution models, namely EURAD-CTM and LUR, had previously yielded different results regarding associations with cIMT (Perez et al. 2015). In order to investigate this observation in more depth, both model approaches were considered in this study. Therefore, the fourth publication examined the effects of long-term exposure to air pollution, using the EURAD-CTM as well as the LUR model, on progression of atherosclerosis in different vessel beds, namely TAC, CAC, and cIMT.

2 Comparison of land-use regression modeling with dispersion and chemistry transport modeling to assign air pollution concentrations within the Ruhr area. Hennig F, Sugiri D, Tzivian L, Fuks K, Moebus S, Jöckel KH, et al. Atmosphere (Basel) 7:1–19 (2016)

atmosphere

MDPI

Article

Comparison of Land-Use Regression Modeling with Dispersion and Chemistry Transport Modeling to Assign Air Pollution Concentrations within the Ruhr Area

Frauke Hennig [1,*], Dorothea Sugiri [1], Lilian Tzivian [1], Kateryna Fuks [1], Susanne Moebus [2], Karl-Heinz Jöckel [2], Danielle Vienneau [3,4], Thomas A.J. Kuhlbusch [5], Kees de Hoogh [3,4], Michael Memmesheimer [6], Hermann Jakobs [6], Ulrich Quass [5] and Barbara Hoffmann [1,7]

1 Working group of Environmental Epidemiology of Cardiovascular Aging and Allergies, IUF-Leibniz Research Institute for Environmental Medicine, Auf'm Hennekamp 50, Düsseldorf 40225, Germany; Dorothee.Sugiri@IUF-Duesseldorf.de (D.S.); Liliana.Tzivian@IUF-Duesseldorf.de (L.T.); Kateryna.Fuks@IUF-Duesseldorf.de (K.F.); B.Hoffmann@uni-Duesseldorf.de (B.H.)

2 Institute for Medical Informatics, Biometry and Epidemiology, University Hospital, University Duisburg-Essen, Essen 45141, Germany; Susanne.Moebus@uk-essen.de (S.M.); k-h.joeckel@uk-essen.de (K.-H.J.)

3 Department of Epidemiology and Public Health, Swiss Tropical and Public Health Institute, Socinstr. 57, Basel 4051, Switzerland; danielle.vienneau@unibas.ch (D.V.); c.dehoogh@unibas.ch (K.H.)

4 University of Basel, Basel 4003, Switzerland

5 IUTA e.V., Air Quality & Sustainable Nanotechnology Unit, Duisburg, Germany; tky@iuta.de (T.K.); quass@iuta.de (U.Q.)

6 Rhenish Institute for Environmental Research (RIU), Aachenerstr. 209, 50931 Köln, Germany; mm@eurad.uni-koeln.de (M.M.); Hermann.Jakobs@eurad.uni-koeln.de (H.J.)

7 Heinrich Heine University of Düsseldorf, Medical Faculty, Deanery of Medicine, Moorenstraße 5, Düsseldorf 40225, Germany

* Correspondence: Frauke.hennig@iuf-duesseldorf.de; Tel.: +49-211-3389-342; Fax: +49-211-3389-293

Academic Editor: Rebecca Sheesley
Received: 16 December 2015; Accepted: 15 March 2016; Published: 19 March 2016

Abstract: Two commonly used models to assess air pollution concentration for investigating health effects of air pollution in epidemiological studies are Land Use Regression (LUR) models and Dispersion and Chemistry Transport Models (DCTM). Both modeling approaches have been applied in the Ruhr area, Germany, a location where multiple cohort studies are being conducted. Application of these different modelling approaches leads to differences in exposure estimation and interpretation due to the specific characteristics of each model. We aimed to compare both model approaches by means of their respective aims, modeling characteristics, validation, temporal and spatial resolution, and agreement of residential exposure estimation, referring to the air pollutants $PM_{2.5}$, PM_{10}, and NO_2. Residential exposure referred to air pollution exposure at residences of participants of the Heinz Nixdorf Recall Study, located in the Ruhr area. The point-specific ESCAPE (European Study of Cohorts on Air Pollution Effects)-LUR aims to temporally estimate stable long-term exposure to local, mostly traffic-related air pollution with respect to very small-scale spatial variations ($\leqslant$100 m). In contrast, the EURAD (European Air Pollution Dispersion)-CTM aims to estimate a time-varying average air pollutant concentration in a small area (*i.e.*, 1 km^2), taking into account a range of major sources, e.g., traffic, industry, meteorological conditions, and transport. Overall agreement between EURAD-CTM and ESCAPE-LUR was weak to moderate on a residential basis. Restricting EURAD-CTM to sources of local traffic only, respective agreement was good. The possibility of combining the strengths of both applications will be the next step to enhance exposure assessment.

Keywords: air pollution; Land use regression; chemistry-transport dispersion-model

1. Introduction

A large number of epidemiological studies have shown associations between short-and/or long-term exposure to outdoor air pollution and adverse health effects [1]. Traditionally, adverse health effects of air pollution have been divided into effects of short-term variations in air pollution concentrations, mainly influenced by meteorology, and effects of long-term exposure to air pollution, where contrasts rely on spatial variation of air pollution concentrations. Early approaches on assessing exposure to air pollution used average air pollution concentrations of the nearest monitoring station as a surrogate of personal exposure, assuming homogeneity among air pollution concentrations within the area surrounding the monitoring station, or even within the whole city [2]. Considering short-term health effects in ecological time-series studies on air pollution and mortality, it seems reasonable to assume such a spatially-uniform temporal elevation or reduction in air pollution concentration because they are dependent on the underlying meteorological conditions. When considering long-term health effects on an individual basis, however, the spatial and spatio-temporal variations are of great importance given that outdoor air pollution concentrations vary on a small spatial scale, e.g., within 100 m of a busy road [3]. More recent epidemiological studies have, thus, approached such small-scale intra-urban variation of air pollution concentrations by using different types of models, such as Land Use Regression (LUR) models, Dispersion Models (DM), chemistry Transport Model Models (CTM), a combination of DM+CTM (DCTM), hybrid models, or other alternatives [4,5].

The LUR method, first developed by Briggs *et al.* [6] in the Small Area Variations In Air quality and Health (SAVIAH study), uses linear (least squared) regression models to predict monitoring air pollution data with Geographic Information System (GIS)-based data reflecting pollutant conditions. Compared to other approaches, LUR models were built to predict temporally-stable long-term air pollution concentrations applicable to the smallest spatial scale (point-specific), e.g., home residences.

DMs are in general mathematical simulation models to estimate air pollution concentrations by means of numerical descriptions of deterministic (physical, chemical, and fluid dynamical) processes of the dispersion of air pollutants in the ambient atmosphere, and typically include data on emissions, meteorological conditions, and topography [3].

CTMs model the variability in space and time of chemical concentrations in the atmosphere, using three-dimensional numerical models to simulate processes of emission, transport, chemical transformation, diffusion and deposition, using emissions, meteorological information, and land use as input. Most often DMs and CTMs (DCTM) are combined in practice, resulting in spatio-temporal estimations. Usually DMs and CTMs estimate air pollution concentrations on a coarser spatial scale compared to the point-specific LUR, e.g., a grid of 1 or 5 km^2.

LUR models were developed to estimate exposure concentration at the finest spatial resolution and have been increasingly used in epidemiological studies due to their relatively low cost and easy implementation, developed either on the basis of purpose-designed monitoring campaigns or routine monitoring measurements and appropriate geographic predictors of sources [7]. In contrast, DCTMs have been developed for air quality, *i.e.*, prediction, regulation and management, putting high demands on data requirements, costs and the complexity of modeling [6].

So far, only a few studies compared the performance of LUR and dispersion modeling for estimating exposure to nitrogen dioxide (NO_2). While some studies suggested that LUR models explained small-scale variations in air pollution concentrations as well or even better than various dispersion models [8–10], Beelen *et al.* [11] showed that the dispersion models performed better than LUR models regarding monitored and modeled concentrations on several validation sites. Most recently, de Hoogh *et al.* [12] investigated agreement between LUR and DM modeling approaches aiming to estimate residential exposure to NO_2 and particulate matter (PM) with an aerodynamic diameter $\leqslant$10 μm and $\leqslant$2.5 μm (PM_{10}, $PM_{2.5}$) within the European Study of Cohorts for Air Pollution Effects (ESCAPE). Comparisons across 4–13 cohorts, including the Heinz Nixdorf Recall (Risk Factors, Evaluation of Coronary calcium and Lifestyle) (HNR) study, located in the Ruhr area in Germany, yielded moderate to good correlations between LUR and DM (or DCTM) for NO_2 (0.39–0.90) and for

PM_{10} and $PM_{2.5}$ (0.23–0.81). However, single correlation coefficients for the HNR study were below 0.4 for all three pollutants [12], raising the question of comparability of the two different exposure modelling approaches. So far, most studies on the comparison of different modeling strategies focused on the residential agreement of estimated exposure concentrations, disregarding the potential reasons for the disagreement between different modelling approaches, as well as respective strengths and limitations. Although all exposure metrics are equally used as a surrogate of personal exposure in epidemiological studies, exposure modeling is strongly influenced by the spatial and temporal variation of exposure and exposure sources [5]. Furthermore, aims, application, input data but also the complexity of models might differ, yielding not only different exposure estimates but consequently different health effect estimates in terms of magnitude and/or statistical significance [5,13].

In the Ruhr area in Germany, the location of multiple epidemiological studies, e.g., the Heinz Nixdorf Recall study, air pollution concentrations have been modeled with a LUR model as part of the European Study of Cohorts for Air Pollution Effects (ESCAPE-LUR), as well as with a European Air Quality and Dispersion Model which is a DCTM (EURAD-CTM) as part of several research projects investigating health effects of residential air pollution exposure. In this article, we aim to compare the ESCAPE-LUR model and the EURAD-CTM model focusing on their respective strengths and limitations. To do so, we compare model approaches by means of their respective aim, application characteristics, validation, temporal, and spatial resolution and by means of residential agreement. In addition, we evaluated the agreement of modeled air pollution concentrations by EURAD-CTM and measured air pollution concentrations at ESCAPE-LUR monitoring sites for overlapping time windows. Air pollutants of interest are $PM_{2.5}$, PM_{10}, and NO_2.

2. Methods

2.1. Study Area

The Heinz Nixdorf Recall (Risk Factors, Evaluation of Coronary calcium and Lifestyle) (HNR) study area covers a region of approximately 600 km^2 and is located in the highly urbanized Ruhr Area in the west of Germany, including the cities of Mülheim, Essen, and Bochum. In addition to that the HNR study area is located within N3, one of the smallest sequential nests developed for the air pollution modelling purposes of EURAD-CTM. We used locations (x,y) (Gauss–Krüger coordinates) of 4809 residences, located within the HNR study area. According to the Ruhr Regional Association, land use in the area can be roughly divided into agricultural (~40%), built-up (~40%), and forest and other regions (e.g., water) (~20%) [14]. The population density of the Ruhr area is about 2100 inhabitants per 1 km^2, and in terms of traffic density the area is one of the densest in the whole of Europe (Figure 1). As an urban area, almost one fifth of the working population is occupied in the industrial sector. Among many industrial areas, the majority of steel and coal industry is located in Duisburg, in the west of the Ruhr area, including the biggest steelwork in Europe. Furthermore, Europe's largest inland harbor is located directly west of the study area in Duisburg. Intensive shipping takes place on the Rhine, which flows through Duisburg from south to north.

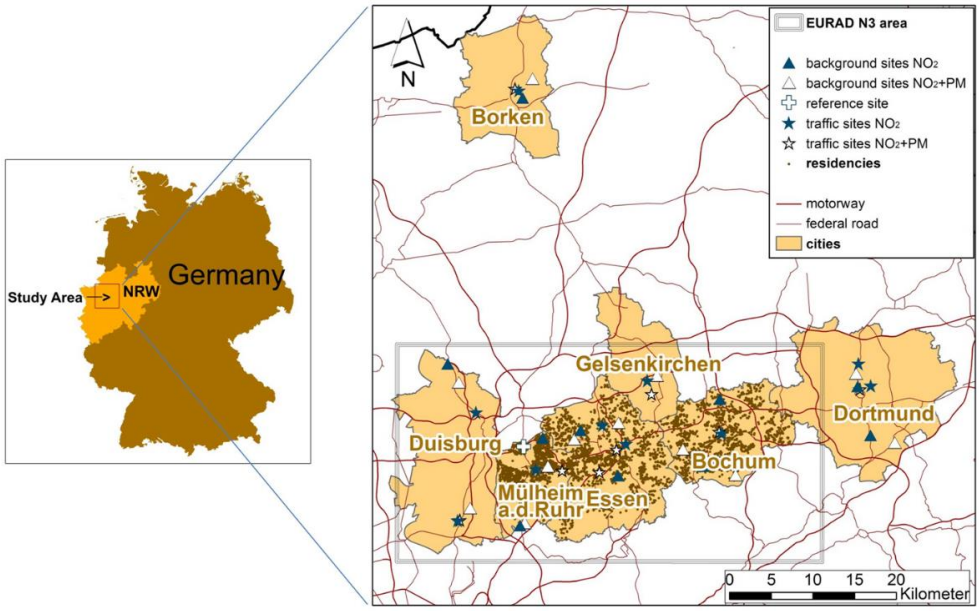

Figure 1. Study area, residences, and monitoring sites.

2.2. Exposure Assesment

2.2.1. EURAD-CTM

The EURAD-CTM model [15] is a validated time dependent three-dimensional chemistry transport model [16–19] developed to predict daily concentrations of air pollutants on a horizontal grid resolution of 1 km^2 (Table 1). The EURAD-CTM model system is a multi-layer, multi-grid model system for the simulation of transport, chemical transformation, and deposition of tropospheric constituents [20], and consists of five major parts (Figure S1): (1) the meteorological driver version 3 (MM5V3) [21]; (2) two pre-processors for preparation of meteorological fields and observational data; (3) the EURAD Emission Model EEM [22], and (4) the Chemistry Transport Model (CTM); including (5) a model for aerosol dynamics in Europe (MADE) [16,18,23,24]. An additional procedure includes data assimilation on an hourly basis, using routine measurement data of monitoring sites in North Rhine-Westphalia (NRW) provided by the local environmental agency: State Agency for Nature, Environment, and Consumer Protection (LANUV-NRW) [25–27] (intermitted 3d-var) (Figure S1). EURAD-CTM calculations are performed using a one-way nesting scheme to take long-range transport into account. Nested grid domains ranged from a European scale (N0: 125 km), to central Europe (N1: 25 km), to NRW (N2: 5 km) in Germany, to the Ruhr area (N3: 1 km), while the vertical resolution is the same for all model domains (40 m) ([18,20]). In addition to long-range transport, the formation of atmospheric gases and PM is also included in the model, *i.e.*, the formation of secondary particles in the atmosphere from primary emitted gaseous pollutants from NO_2, sulfur dioxide (SO_2), ammonia (NH_3), and Volatile Organic Compounds (VOC) during the transport [19]. Long-range transport and formation of secondary particles in the atmosphere can contribute considerably to the particle mass concentration in NRW and the Ruhr area, e.g., more than 50% [28]. The EURAD-CTM is driven by emissions due to anthropogenic and biogenic sources [29]. Anthropogenic emissions are taken from officially-available databases as EMEP-grid [30] for Europe and from the LANUV-NRW. The EURAD-CTM emission input is further structured with respect to different source categories according to the Selected Nomenclature for Sources of Air Pollution (SNAP-97) [31], including traffic, industry, and other source categories.

Table 1. Characteristics of the ESCAPE-LUR and EURAD-CTM approaches to estimate air pollution concentrations.

-	**Land use regression (ESCAPE-LUR)**	**European Air Quality and Dispersion Chemistry Transport Model (EURAD-CTM)**
Model Type	Linear regression model, to predict annual averages derived from selected monitored concentrations with land use data	Mesoscale chemistry transport model involving emissions, transport, diffusion, chemical transformation, wet and dry deposition, and sedimentation of gases and aerosols
Aim & Application	Estimation of long-term traffic-related air pollution for population-based exposure studies and epidemiological health outcome analyses	1) Air pollution modeling (forecasts, episode analysis, trend analysis, reduction scenarios) and Chemical data assimilation studies for Europe, Central Europe and several German States; 2) Exposure estimation in population-related exposure studies
Model Input	1) Data: • Annual mean AP concentration (for details see Table S1); • Land use density in 100, 300, 500, 1000, and 5000 m buffers: ○ Industry ○ Seaport ○ urban green ○ semi-natural ○ forested areas ○ number of inhabitants • Traffic data in 25, 50, 100, 300, 500, and 1000 m buffers: ○ distance ○ (heavy) traffic intensity on the nearest road and nearest major road ○ (heavy) traffic load on all roads and major roads)	1) Data: • Model area projection topography • Land use • Meteorological initial and boundary values • Anthropogenic emission data (according to the Selected Nomenclature for Sources of Air Pollution (SNAP-97)) • Chemical initial and boundary values, • Long-range transport, • Photolysis frequencies. 2) Procedures (Figure S3): • Mesoscale meteorological model (MM5) driven by global meteorological fields provided by NCEP (http://www.ncep.noaa.gov/), • EPC, anthropogenic and non-anthropogenic emission modules (EEM-A, EEM-B), • Aerosol dynamics module (MADE), • Data assimilation [a]
Modelled Air Pollutants	**$PM_{2.5}$, PM_{10}, NO_2** (additional pollutants: $PM_{2.5}$ absorbance, PM coarse, NO, NOx)	**$PM_{2.5}$, PM_{10}, NO_2** (additional pollutants: PM_1, O_3, SO_2, CO, PNC, NH_4, NO_3, SO_4, BC, EC)
Temporal Resolution (Output)	Yearly mean concentration (October16, 2008 until October 15, 2009)	Any temporal resolution > day within October 2000 until December 2003 and January 2006 until December 2008 is possible; e.g., 7-,14-, 21-,28-,91-,182-, and 365-day mean concentration
Model Validation	a) Goodness of fit (cf. Table S2): $PM_{2.5}$ (R^2 = 0.85), PM_{10} (R^2 = 0.66), NO_2 (R^2 = 0.88) b) Leave-one-out cross-validation: $PM_{2.5}$ (R^2 = 0.74), PM_{10} (R^2 = 0.59), NO_2 (R^2 = 0.82)	Validation for daily mean concentration in N3 area with routine measurements (mean bias, correlation); year: a) Before data assimilation: PM_{10} (−6.5, 0.45); 2006 NO_2 (4.0, 0.39); 2007 b) After data assimilation PM_{10} (−0.9, 0.93); 2006 NO_2 (0.6, 0.95); 2007
Spatial Resolution	Point-specific	1 km × 1 km grid
Additional Features	1) XRF-Model for air pollutant constituents 2) Back-extrapolating back in time and for specific time windows	Source-specific air pollutant concentrations (only local traffic (TRA), only local industry (IND))

[a] only for PM_{10} and NO_2 for the considered time period.

Output of the EURAD-CTM calculations consists of chemical compounds, such as atmospheric particle mass, number density, and particle size distribution, as well as concentration of atmospheric gases, photo oxidants, and a set of volatile organic compounds on an hourly basis for each grid. EURAD-CTM estimates of PM_{10} and NO_2 concentrations are assimilated using measurements from all available routine monitoring sites within the region of interest. For the Ruhr area there exists a maximum of ten monitoring sites, including different air pollution data bases [25]. Using ArcView 9.2, location of residences were assigned to a 1 × 1 km^2-grid and then matched to the corresponding grid-based air pollutant concentration, allowing both short-term (daily mean concentrations) and long-term (annual mean concentrations) assignment of exposure. The basis of daily mean concentration allows us to calculate exposure for any temporal resolution with a minimum of one day. Model runs for the EURAD-CTM within N3 were done for the examination periods of the HNR study (2000–2003

and 2006–2008). Thus, we are able to assign exposure concentrations of yearly-mean concentrations for the years 2001, 2002, 2003, 2006, 2007, and 2008 and personalized exposure concentrations of 1-, 7-, 28-, 91-, 182-, and 365-day mean concentrations prior to the date of examination.

As an add-on feature it was possible to model source-specific Air Pollution (AP) concentration with EURAD-CTM [28]. Briefly, within EURAD-CTM we estimated AP concentration suppressing local sources within the smallest grid domain (N3), such as traffic and industry by setting to them to zero (AP_{noTRA} or AP_{noIND} respectively). We then calculated local traffic-specific or industry-specific AP by taking the difference $AP_{TRA} = AP - AP_{noTRA}$ or $AP_{IND} = AP - AP_{noIND}$, respectively. In earlier studies, we applied this method to compare the health effects of PM, emitted from local traffic and local industrial sources within the Ruhr area on levels of highly-sensitive C-reactive protein, a marker of systemic inflammation [32].

2.2.2. ESCAPE-LUR

LUR models were developed to estimate temporally-stable spatial-variant concentrations of long-term exposure to traffic-related air pollutants as part of the ESCAPE study (Table 1). Following the definition of LUR describes a standardized model building procedure developed within the ESCAPE study, here the ESCAPE-LUR. The ESCAPE-LUR defines a linear prediction model for an air pollutant concentration, including annual mean air pollution concentrations as a dependent variable and geographic data on traffic, industry, and population density as potential predictors (independent variables). Predictor data were collected in a Geographical Information System (GIS), based on CORINE 2000 definitions [33]. The procedure of model development was standardized within the ESCAPE study and included a forward selection of predictors based on the incremental improvement in R^2 [34–36]. A predictor was added if addition of the predictor yielded an improvement of R^2 by more than 1%, if the coefficient conformed to the pre-specified direction, and if the direction of previously selected predictors did not change. In addition, predictors with a p-value > 0.1 were removed, while predictors with a variance inflation factor (VIF) > 3 and Cook's Distance (Cook's D) >1 were further investigated. To avoid extrapolation, estimated concentrations were truncated at the highest observed value. Annual air pollution concentrations were based on a measurement campaign in the study area of interest, including three periods of a 14-day measurement to cover all seasons (cold, warm, and one intermediate temperature season) from October 2008 until October 2009. The reason for the choice of 14-days was the settings design of the ESCAPE-LUR measurement campaign, which was conducted with discontinuous particle measurement devices (Harvard impactors). Measurements were conducted at 20–40 monitoring sites, placed at locations which were characteristic of traffic and background pollutant concentrations to measure PM (at 20 sites) and NO_2 (at 40 sites) (Figure 1, Table S1). One additional background reference site was chosen to measure PM and NO_2 continuously during a complete year (starting in October 2008) so that all discontinuous site-specific measurements could be adjusted to derive a long-term annual average. Measurement data from the reference site was only used for adjustment and not for ESCAPE-LUR model development. A separate LUR model was developed for each air pollutant and validated via Leave-One-Out Cross Validation (LOOCV), excluding one monitoring site at a time. Other choices of model validation are possible, e.g., hold-out cross validation, which has recently been proposed to perform better [37]. However, in this manuscript we hold onto the ESCAPE-LUR.

Since ESCAPE included two cohorts located within NRW, namely the HNR study and the Study on the influence of air pollution on lung function, inflammation, and aging (SALIA), the ESCAPE-LUR measurement campaign was combined for both studies and ranged from the urban Ruhr area to the more rural city of Borken (Figure 1) [34,36]. ESCAPE-LUR for $PM_{2.5}$ included heavy traffic load (1 km buffer), industry (5 km buffer), population density (1 km buffer), and the x-coordinate of the location of interest as predictors with an explained variance of $R^2 = 0.85$ (LOOCV-$R^2 = 0.74$) (Table S2) [34]. ESCAPE-LUR for PM_{10} included heavy traffic load (1 km buffer) and population density (1 km buffer) with an explained variance of $R^2 = 0.66$ (LOOVC-$R^2 = 0.59$) (Table S1) [34], ESCAPE-LUR for NO_2

included industry (5 km buffer), population density (100 m buffer), inland or seaport (5 km buffer) and traffic load (100 m buffer) with an explained variance of R^2 = 0.88 (LOOVC-R^2 = 0.82) (Table S1) [36]. (Heavy) traffic load referred to total (heavy-duty) traffic load of all roads in a buffer (sum of (traffic intensity × length of all segments)), industry referred to industrial, commercial, and transport units in a certain buffer; inland or seaport referred to the respective area within a buffer and population density to the number of inhabitants in a certain buffer. Uncertainty was evaluated as residuum's mean squared error in the LOOCV-approach, which was 0.61 for $PM_{2.5}$, 1.44 for PM_{10}, and 3.19 for NO_2.

Based on the coordinates of residence, located within the study area, annual mean concentrations were estimated using the ESCAPE-LUR prediction models and the relevant GIS predictors. In order to estimate AP concentration back in time, LUR modeling offers the method of back-extrapolation using a ratio or absolute difference method. Briefly, routine monitoring data should be available in order to account for differences of AP concentrations back in time [38]. Within the ESCAPE study, back-extrapolated AP estimations referred to a two year average (± 365 days of the examination day) in order to avoid any time-specific outliers. An additional feature offered by ESCAPE-LUR is the possibility to estimate exposure concentration as an average per month or trimester, e.g., before pregnancy, which might be of interest when investigating birth cohorts.

2.3. Statistical Analysis

Conducted statistical analysis referred to air pollutants $PM_{2.5}$, PM_{10}, and NO_2, estimated using the EURAD-CTM and the ESCAPE-LUR model. First, we described EURAD-CTM grid-based concentrations for the whole HNR study area for the years 2001–2003 and 2006–2008 by mean and standard deviation (mean ± SD) as well as minimum and maximum (Min, Max). Secondly, we described residence-based exposures derived from the EURAD-CTM and from the ESCAPE-LUR by mean ± SD (Min, Max) and Person's correlation coefficients for the most closely matched annual time-window: year 2008 for EURAD-CTM *vs.* annual mean ESCAPE-LUR (*i.e.*, based on measurements from October 2008 until October 2009). Considered air pollutants were $PM_{2.5}$, PM_{10}, and the gas NO_2. In addition, we calculated Spearman's correlation coefficient between 14-day mean air pollution concentrations measured at ESCAPE measurement sites (traffic and background) and 14-day mean air pollution concentrations calculated by EURAD-CTM for the grid cells that included an ESCAPE measurement site within the time period of October 2008–December 2008.

To evaluate an overall agreement between routinely measured air pollution concentrations, we compared annual mean concentrations of three routine monitoring stations provided by LANUV, located within the Ruhr area, and thus within EURAD specific grid cells (gc), with annual estimated air pollution concentrations estimated by EURAD-CTM and ESCAPE-LUR. Details of routine measurement stations are given in Table S3. Referred monitoring sites are the above mentioned reference site in Mülheim-Styrum (STYR) (gc: 679), an additional background site, located in Essen-Vogelheim (EVOG) (gc: 942), and one traffic site, located at a highly trafficked road in Essen (VESN) (gc: 690). For the comparison with the EURAD-CTM we considered annual mean concentrations from January 1, 2008 until December 31, 2008, while for the comparison with the ESCAPE-LUR we considered annual means from October 16, 2008 until October 15, 2009 in order to match the time window of the ESCAPE measurement campaign. Annual mean concentrations modeled by the ESCAPE-LUR referred to the location (coordinate points) of monitoring sites. In addition to that we calculated Pearson's correlation coefficients between daily measurements of LANUV monitoring sites and daily estimations by EURAD-CTM for the year 2008.

With regard to different temporal resolution, we compared EURAD-CTM air pollution concentration estimates to measured air pollution concentrations on a monthly basis to yearly mean concentrations (2006, 2007, and 2008) estimated by EURAD-CTM in two of the above mentioned grid cells (679 and 690). In contrast we visualized time-dependent measurements of the two corresponding routine monitoring sites (STYR and VESN) on a monthly basis as well as the temporally stable air pollution concentration estimated by ESCAPE-LUR for the specific locations of routine monitoring

sites. For ESCAPE-LUR values we used the original, not back-extrapolated values, since during the study period of 2006–2008, no substantial changes of long-term air pollutant concentrations were observed at the routine monitoring sites, therefore not having a meaningful influence on the back-extrapolated values.

With respect to the additional feature of source-specific estimation of air pollution concentrations, we further investigated the correlation of traffic-specific and industry-specific EURAD-CTM (EURAD-CTM_{TRA} and EURAD-CTM_{IND}, respectively) and ESCAPE-LUR concentrations at residence as well as at locations of specific ESCAPE measurement sites.

Statistical analysis were carried out with the statistical software R version 3.1.3 (2015-03-09) [39].

3. Results and Discussion

3.1. Comparison of Residence-Based EURAD-CTM and ESCAPE-LUR

Residence-based air pollution concentrations (for 4809 residences within the HNR study area) estimated by EURAD-CTM as yearly-mean air pollution concentrations for the years 2001–2003 (not including 2000 since modeling did not start before October 2000), 2006–2008 and estimated yearly mean air pollution concentrations by ESCAPE-LUR as well as back-extrapolated ESCAPE-LUR air pollution concentration estimates are presented in Table 2 for $PM_{2.5}$, PM_{10}, and NO_2 and visualized in Figure 2 for the year 2008 (EURAD-CTM) and October 2008–October 2009 (ESCAPE-LUR), respectively.

Table 2. Description of residence-based air pollutant exposure estimates $PM_{2.5}$, PM_{10}, and NO_2 from EURAD-CTM and ESCAPE-LUR for 4809 residences within the HNR study area.

–	$PM_{2.5}$ Mean ± SD (Min, Max)	PM_{10} Mean ± SD (Min, Max)	NO_2 Mean ± SD (Min, Max)
EURAD-CTM (μg/m³)			
2001 year-mean	16.6 ± 1.5 (14.0, 21.6)	21.2 ± 2.9 (17.0, 30.1)	42.2 ± 4.2 (28.2, 55.4)
2002 year-mean	16.8 ± 1.4 (14.3, 21.2)	20.4 ± 1.9 (16.7, 27.0)	39.3 ± 3.8 (27.5, 50.2)
2003 year-mean	18.2 ± 1.4 (15.5, 22.7)	22.4 ± 3.3 (17.8, 32.4)	42.7 ± 4.1 (30.1, 56.1)
2006 year-mean	16.2 ± 1.3 (13.9, 21.2)	21.0 ± 3.7 (16.5, 34.2)	40.0 ± 4.8 (27.1, 57.2)
2007 year-mean	15.7 ± 1.3 (13.4, 20.3)	19.8 ± 2.9 (15.7, 30.8)	37.7 ± 4.5 (26, 53.7)
2008 year-mean	14.6 ± 1.1 (12.5, 19.0)	18.0 ± 2.3 (14.9, 25.1)	37.5 ± 3.9 (26.3, 47.9)
ESCAPE-LUR (μg/m³)			
back-extrapolated (2-year averages) Year 2008–2009	–	30.3 ± 2.1 (25.5, 38.7)	30.5 ± 5.0 (19.3, 62.0)
	18.4 ± 1.0 (16.0, 21.4)	27.7 ± 1.8 (23.9, 34.7)	30.1 ± 4.9 (19.8, 62.4)
Difference (μg/m³)			
ΔESCAPE-LUR (2008–09) EURAD-CTM (2008)	3.7 ± 1.3 (−0.7, 7.0)	9.8 ± 2.4 (0.9, 16.5)	−7.4 ± 4.9 (−26.8, 18.9)

On a residential basis, estimated $PM_{2.5}$ and PM_{10} concentrations revealed a consistent decline since 2006 (Table 2). Considering the back-extrapolated ESCAPE-LUR and ESCAPE-LUR, we also observed a decline over time. Observed declines are accounted for by ongoing nation- and state-wide air quality regulations.

Comparing EURAD-CTM (2008) and ESCAPE-LUR (2008–09), however, we saw that the overall mean of the ESCAPE-LUR was considerably higher compared to the overall yearly-mean of EURAD-CTM ($\Delta PM_{2.5}$ = 3.7 ± 1.3 μg/m³ and ΔPM_{10} 9.8 ± 2.4 μg/m³, respectively). Ranges for $PM_{2.5}$ estimated by EURAD-CTM were slightly smaller than estimated by ESCAPE-LUR (5.4 *vs.* 6.5 μg/m³), while ranges for PM_{10} were more similar for both models (10.8 *vs.* 10.0 μg/m³). Smaller ranges of air pollution concentrations from EURAD-CTM are not unexpected due to the smoothing pattern within 1 km².

Explanations for the difference in mean concentrations for PM might be a consequence of the finer spatial resolution of the ESCAPE-LUR, since high exposure peaks in a very close proximity to busy

roads are better captured with this model than with the EURAD-CTM, especially considering that residences are usually located close to the roads and not randomly distributed across a certain area.

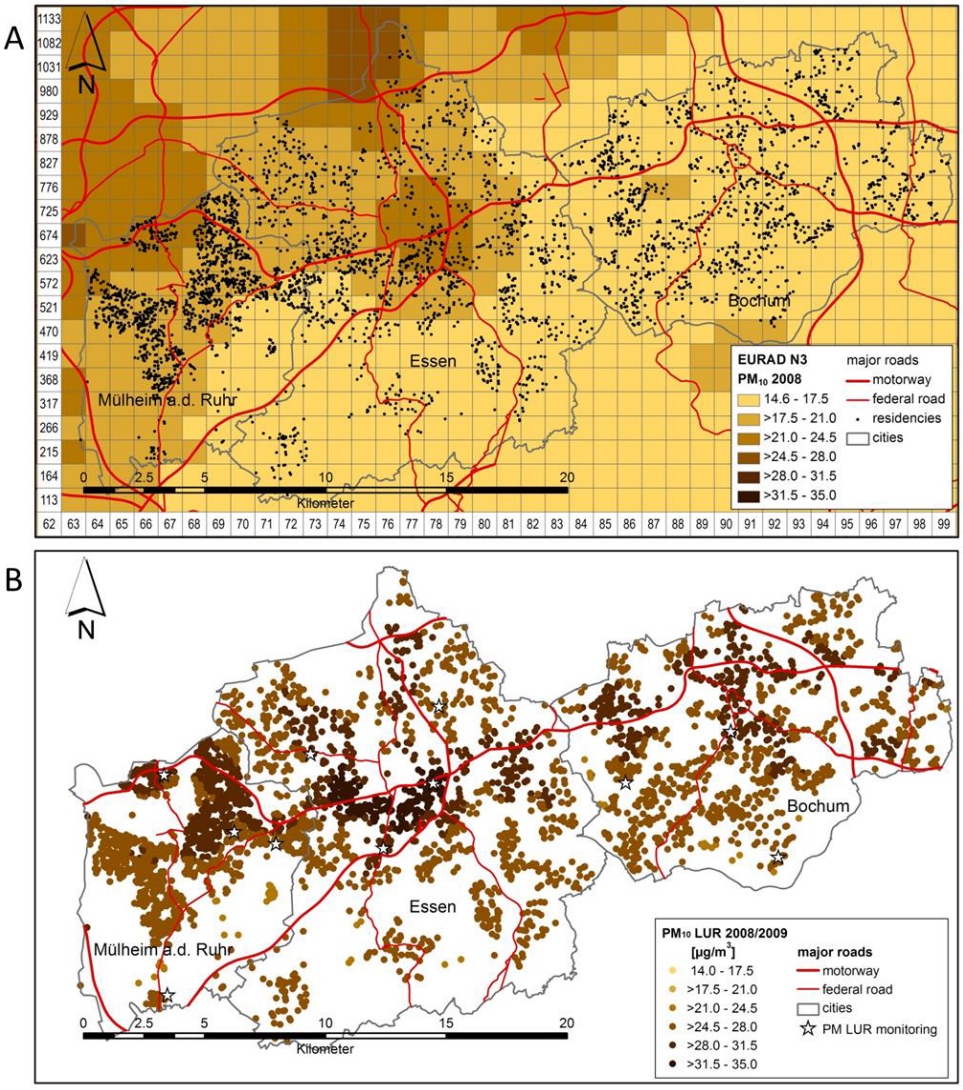

Figure 2. Spatial distribution of EURAD-CTM (1 km^2, yearly mean 2008, (**A**)) and ESCAPE-LUR (yearly mean October 2008–October 2009, (**B**)) at 4809 residences within the HNR study area for PM_{10}.

Pearson's correlation coefficients between models were rather weak for both, $PM_{2.5}$ and PM_{10}, with 0.33. This rather weak correlation has been reported earlier [12] and is not unexpected due to the different spatial resolution but also due to the different spatial distribution of PM concentrations for the two modelling approaches within the study area (Figure 2 and Figure S2): while we observed a west-to-east gradient for EURAD-CTM with higher concentrations in the west, estimated concentrations of ESCAPE-LUR revealed only a slight west-to-east gradient, which was prominently overlapped by an additional decreasing north-to-south and local hot spots, e.g., in Essen at a motorway intersection. In our study area the decreasing west-to-east gradient mirrors the distribution of industrial locations, e.g., metallurgical-industry and Europe's largest inland harbour in Duisburg, located to the west of the study area (Figure 1), as well as transported emissions from other countries in the west

of study area, e.g., the Netherlands or Great Britain. The decreasing north-to-south gradient on the other hand is consistent with the population density and the location of major arterial roads within our study area [32].

NO_2 concentrations estimated by EURAD-CTM showed an overall decrease between 2001 with 42.2 $\mu g/m^3$ and 2008 with 37.7 $\mu g/m^3$, while a change between the ESCAPE-LUR and the back-extrapolated ESCAPE-LUR was not observed. Yet, in contrast to PM, temporally-stable NO_2 concentrations estimated by ESCAPE-LUR were systematically lower than estimated by EURAD-CTM ($\Delta NO_2 = -7.4 \pm 4.9$ $\mu g/m^3$). One explanation for this difference could be a misrepresentation of industrial sources within the ESCAPE modeling approach: "industry" referred to industrial, commercial and transport units in a certain buffer, giving no information of the emission of such sources. Ranges of concentrations, however, were twice as big for the ESCAPE-LUR compared to the EURAD-CTM (42.4 *vs.* 21.9 $\mu g/m^3$), probably driven by greater small-scale variations due to point-specific estimates and the consideration of traffic load within a buffer of 100 m. Unlike spatial gradients for $PM_{2.5}$ and PM_{10}, we observed a more pronounced northwest-to-southeast-gradient for EURAD-CTM for NO_2, while the distribution of NO_2 by ESCAPE-LUR did not reveal a clear gradient, but local hot spots near major roads or motorway intersections (Figure S2). Similar to PM, correlation between EURAD-CTM NO_2 and ESCAPE-LUR NO_2 was rather weak with a correlation coefficient of 0.4.

3.2. Comparison of Estimated and Measured Air Pollution Concentrations

3.2.1. Comparison between 14-Day Mean ESCAPE-LUR Measurements and EURAD-CTM Estimates

In order to evaluate EURAD-CTM estimates we compared estimated 14-day mean AP concentrations by EURAD-CTM to available 14-day measurements taken during the ESCAPE measurement campaign. Descriptive statistics and correlation coefficients of these 14-day mean measured air pollution concentrations at ESCAPE measurement sites (background, traffic (*cf.* Table S2), and both) and the respective 14-day mean air pollution concentrations estimated by EURAD-CTM in the corresponding grid cells are shown in Table 3 for air pollutants $PM_{2.5}$, PM_{10}, and NO_2.

Table 3. Description of 14-day mean measured air pollution concentrations at ESCAPE measurement sites (background and/or traffic) and 14-day mean air pollution concentration estimations of EURAD-CTM in the corresponding grid cells for $PM_{2.5}$, PM_{10}, and NO_2.

Background	ESCAPE Site ($\mu g/m^3$)	EURAD-CTM ($\mu g/m^3$)	Spearman Correlation Coefficient (*r*)
	Mean ± SD	Mean ± SD	
$PM_{2.5}$ (N = 9)	17.78 ± 2.40	19.80 ± 5.80	0.34
PM_{10} (N = 9)	26.12 ± 4.70	23.29 ± 5.98	0.93
NO_2 (N = 16)	37.85 ± 6.21	50.82 ± 10.07	0.34
traffic			
$PM_{2.5}$ (N = 6)	19.75 ± 3.75	21.78 ± 6.96	0.43
PM_{10} (N = 6)	29.26 ± 4.95	26.97 ± 7.68	0.37
NO_2 (N = 13)	50.43 ± 9.83	58.04 ± 10.33	0.60
Background + traffic			
$PM_{2.5}$ (N = 15)	18.57 ± 3.05	20.59 ± 6.13	0.45
PM_{10} (N = 15)	27.37 ± 4.89	24.77 ± 6.71	0.77
NO_2 (N = 29)	43.49 ± 10.13	54.06 ± 10.65	0.55

Overall, 14-day mean EURAD-CTM estimates for $PM_{2.5}$ are slightly higher than mean of 14 daily measurements at the ESCAPE sites, while EURAD-CTM estimates for PM_{10} are slightly lower and EURAD-CTM estimates for NO_2 are considerably higher, especially regarding the ESCAPE background site (Table 3).

The highest correlation coefficient (r) was observed for PM_{10} between EURAD-CTM and ESCAPE background sites (r = 0.93), while the lowest correlation was observed for PM_{10} between EURAD-CTM and ESCAPE traffic sites (r = 0.37). This finding is not unexpected, regarding the aim, input, and construction of the two modeling approaches (Table 1): the EURAD-CTM aims to assess an average concentration in a 1 km^2 grid cell, taking into account long-range transport rather than locally-emitted pollution, in contrast to the ESCAPE-LUR, which was specifically designed to assess mostly traffic-related differences in exposure concentration. For $PM_{2.5}$, however, we did not observe a clear distinction between background and traffic sites, whereas correlation coefficients for NO_2 were higher between EURAD-CTM and ESCAPE traffic sites (r = 0.60) than between EURAD-CTM and ESCAPE background sites (r = 0.34). One reason for the low to moderate correlation between $PM_{2.5}$ modeled by EURAD-CTM and $PM_{2.5}$ measured at ESCAPE sites could be the lack of the assimilation procedure within EURAD-CTM, since $PM_{2.5}$ has only been measured at routine monitoring sites since 2009. So, for the considered period of time, estimated $PM_{2.5}$ was only assimilated indirectly taking a (constant) proportion of PM_{10} and $PM_{2.5}$ into account.

Overall, correlations between EURAD-CTM estimates and measured concentrations at all ESCAPE measurement sites were moderate for $PM_{2.5}$ (r = 0.45) and NO_2 (r = 0.55), and high for PM_{10} (r = 0.77) and, therefore, slightly better than comparing residence-based modeled air pollution concentrations between EURAD-CTM and ESCAPE-LUR.

3.2.2. Comparison between Routinely-Monitored and Estimated Air Pollution Concentrations

Overall correlations between daily measurements at routine monitoring sites and EURAD-CTM estimations over one year (2008) were strong for PM_{10} and NO_2 (>0.8) and moderate for $PM_{2.5}$ (0.66–0.74) for both, background and traffic monitoring site (Table 4). This finding is a consequence of the assimilation procedure within EURAD-CTM for PM_{10} and NO_2.

Taking into account absolute annual values, we observed several findings: annual averages for January 2008 until December 2008 differ considerably from annual averages from 16 October 2008 to 15 October 2009 (ESCAPE measurement period), for PM (Table 4). Generally, PM concentrations throughout Germany were at a minimum in 2008, as reported by the Federal Environment Agency [40]. This finding points to the importance of a fine temporal resolution even in medium- and long-term exposure estimations.

Considering uncertainty, the EURAD-CTM estimations underestimated PM and overestimated NO_2 at background monitoring sites, while the ESCAPE-LUR estimations agreed well for $PM_{2.5}$ (all sites) and PM_{10} (background sites), but tended to underestimate NO_2 concentrations considerably (Table 4). The latter is supported by mean squared errors of the LOOCV, which were remarkably higher for NO_2 than for PM. Furthermore, we observed considerable disagreement between predicted ESCAPE-LUR PM_{10} and measured PM_{10} at the routine monitoring traffic-site. This finding might be a consequence of the disagreement between PM_{10} measured at the routine monitoring site and the measured PM_{10} at the closest ESCAPE site (26.64 *vs.* 32.70 $\mu g/m^3$), which were located only 2.2 m away from each other.

Table 4. Yearly mean air pollution concentrations measured at routine monitoring sites (background (BG) and traffic (TRAFFIC)), provided by LANUV, modeled by EURAD-CTM (for the respective grid cell), modeled by ESCAPE-LUR (at the location of the routine monitoring sites) and measured adjusted yearly mean at the closest ESCAPE site plus Pearson's correlation coefficient between LANUV daily measurements and EURAD-CTM daily estimations for $PM_{2.5}$, PM_{10}, and NO_2.

Air Pollutant ($\mu g/m^3$)	LANUV Monitor (2008)	EURAD-CTM (2008)	Pearson Correlation Coefficient (LANUV*EURAD-CTM)	LANUV Monitor (October 2008–October 2009)	ESCAPE-LUR Prediction (October 2008-October 2009)	Closest ESCAPE-Measurement Site
Mülheim-Styrum (BG) (grid cell: 679)						
$PM_{2.5}$	17.90	16.33	0.66	20.71	19.50	19.00 [a]
PM_{10}	25.24	23.21	0.88	28.20	28.86	29.00 [a]
NO_2	34.17	39.33	0.80	34.67	31.42	33.00 [a]
Essen-Vogelheim (BG) (grid cell: 942)						
$PM_{2.5}$	22.08	16.21	0.74	20.18	19.31	18.50 [b]
PM_{10}	27.66	23.79	0.81	27.32	26.64	26.40 [b]
NO_2	35.17	41.56	0.76	35.70	28.75	53.30 [c]
Essen-Ost city (TRAFFIC) (grid cell: 690)						
$PM_{2.5}$	20.08	14.72	0.69	20.51	21.05	20.90 [d]
PM_{10}	26.61	23.77	0.81	26.64	33.38	32.70 [d]
NO_2	46.36	44.97	0.87	47.65	42.01	43.50 [d]

[a] 6.7 m; [b] 2665.0 m; [c] 4060.1 m, [d] 2.2 m.

3.3. Temporal Resolution of Air Pollution Concentrations

Regarding different years (2006–2008) we saw a weak time-dependent decline in PM concentrations (Table 2), in line with the observed overall decline in PM concentrations from the year 2001 to 2008 within the HNR study area [29]. To examine the temporal resolution on a monthly basis, Figure 3 and Figure S3 present monthly distributions of EURAD-CTM estimated air pollution concentrations of PM_{10}, $PM_{2.5}$, and NO_2 respectively, in two grid cells, including one background grid cell (679) and one traffic routine monitoring site grid cell (690), presenting spatial variation. For the purpose of comparison, yearly mean air pollution concentrations estimated with EURAD-CTM for the two grid cells as well as the temporally-stable ESCAPE-LUR air pollution concentrations estimated at the locations of the monitoring sites, and monthly-based measured air pollution concentration at routine monitoring sites are presented as lines. Overall, we observed strong seasonal variation (high in winter and low in summer) for estimated EURAD-CTM air pollution concentrations and measured air pollution concentrations, which cannot be detected when using the temporally stable ESCAPE-LUR estimates. While ESCAPE-LUR estimates are primarily designed to yield long-term exposure estimates without temporal resolution, the integration of other measurements (*i.e.*, from routine monitoring sites), or other measurement periods (e.g., three month instead of one year), can be used to derive LUR-data for the analysis of medium-term health effects [41], although not covered in this manuscript.

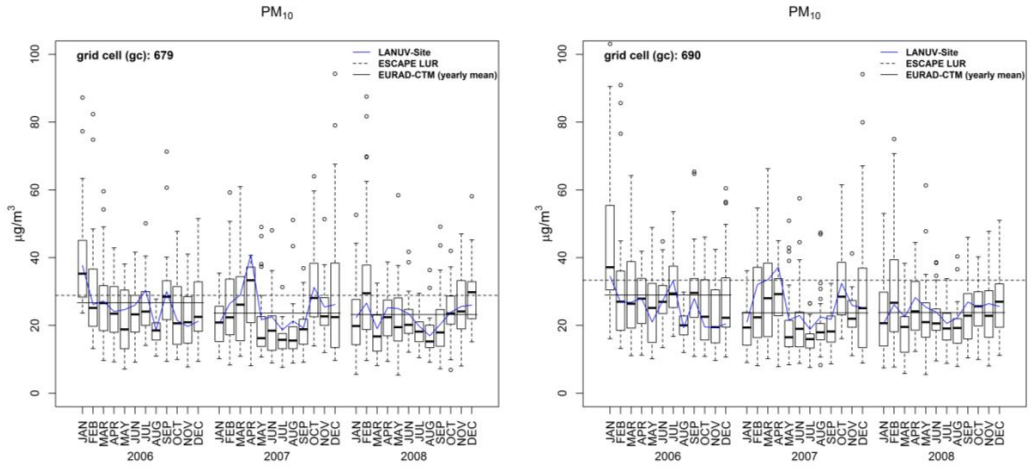

Figure 3. Box plots of air pollution concentrations of PM_{10} over time for two grid cells (gc), representing background (gc: 679) and traffic (gc: 690), estimated by EURAD-CTM on a monthly and yearly basis, long-term ESCAPE-LUR estimation and measured at monitoring sites on a monthly basis (median per month).

The seasonal patterns differed slightly across years and air pollutants (Figure 3 and Figure S3). Reasons for such differences might be specific meteorological conditions during the observation period as well as different chemical processes differentially influencing the concentration of the examined air pollutants, e.g., regarding transport, deposition or physical and chemical aging. These observed seasonal changes underscore the importance of time-dependent air pollution models for the analysis of short- and medium-term health effects. When using a LUR for short- and medium-term exposures, a finer temporal resolution can be achieved using back-extrapolation based on routine monitoring sites, as has been applied for birth outcomes in the framework of ESCAPE [41]. Furthermore, estimated $PM_{2.5}$ by EURAD-CTM, although following the seasonal pattern of measured $PM_{2.5}$, was considerably under-estimated, reflecting the lack of data assimilation within this modeling procedure. In contrast to the temporal variation over the considered time period, the spatial variation, presented by the two locations of a background and traffic site, is considerably smaller. This finding is in line with earlier

findings, indicating a slightly higher temporal, than spatial, variation of particle number concentrations within the Ruhr area [42].

3.4. Source-Specific EURAD-CTM

Estimated local traffic-specific (TRA) and local industry-specific (IND) air pollution concentrations take up only a small amount of all sources: for $PM_{2.5}$ local traffic takes up 3.4% and local industry 9.6%; for PM_{10} it is 2.7% and 10.5%, respectively, and for NO_2 it is 21.4% and 2.4%, respectively. Correlation coefficients between PM concentrations, including all sources and including only local traffic, were weak (0.34–0.43), while all-sources PM and industry-specific PM correlated well (0.73–0.96) (Figure 4). Correlation coefficients for NO_2 were, in contrast to PM, higher between all sources and local-traffic (0.63) and lower for industry-specific (0.44). The rather small amount of local traffic-and industry-specific concentrations is not surprising considering that long-range transport and formation of secondary particles in the atmosphere can contribute considerably to the particle mass concentration in North-Rhine-Westphalia and the Ruhr area, sometimes more than 50% depending on the meteorological situation [28]. The spatial distribution within the study area, represented by quintiles of respective PM_{10} distributions (Figure 4), illustrates that the agreement between all sources and industry-specific sources is better than between all sources and traffic-specific PM. Due to substantial industrial emissions from the Duisburg inland harbor and the adjacent industrial area west of the study region, a strong west-east gradient can be observed for industry-specific PM and for all sources PM. The spatial distribution traffic-specific PM follows closely the population-density in the study area, with a strong north-to-south gradient.

The associations between residence-based exposure estimates derived from EURAD-CTM_{TRA} and ESCAPE-LUR are relatively high ($PM_{2.5}$: 0.69, PM_{10}: 0.58, and NO_2: 0.45), while they are expectedly considerably lower for EURAD-CTM_{IND} and ESCAPE-LUR ($PM_{2.5}$: 0.16, PM_{10}: 0.0, and NO_2: 0.25) (Table 5). Such patterns are displayed for PM_{10} in the spatial distribution of traffic-specific EURAD-CTM and ESCAPE-LUR and industry-specific EURAD-CTM and ESCAPE-LUR, respectively (Figure 4). A similar pattern is observed taking into account correlations for 14-day mean measurements at ESCAPE monitoring stations (background and traffic) and estimated 14-day mean EURAD-CTM_{TRA} within respective grid cells (Table 5).

Table 5. Spearman correlation coefficients between 14-day series of measurements at ESCAPE-LUR-monitoring stations and 14-day mean estimations of EURAD-CTM_{TRA} in respective grid cells.

EURAD-CTM_{TRA} (Traffic-Specific)	ESCAPE Background Sites	ESCAPE Traffic Sites	All ESCAPE Sites
$PM_{2.5}$	0.69 (n = 9)	0.88 (n = 6)	0.77 (n = 15)
PM_{10}	0.02 (n = 9)	0.83 (n = 6)	0.32 (n = 15)
NO_2	0.57 (n = 16)	0.79 (n = 13)	0.63 (n = 29)

These observations indicate that EURAD-CTM and ESCAPE-LUR do not represent identical aspects of air pollution: while EURAD-CTM represents an area average similar to urban background concentrations, the ESCAPE-LUR was designed to predominantly estimate variability in local traffic-related air pollution, leading to a comparatively high correlation with local traffic-specific air pollution concentrations modeled by EURAD-CTM. The very low correlation with local industry-specific air pollution concentration at the residences indicates, that ESCAPE-LUR represents industry rather poorly compared to EURAD-CTM, where the overall spatial distribution (Figure 3) is mainly driven by industrial sources as has been observed in a previous study [32].

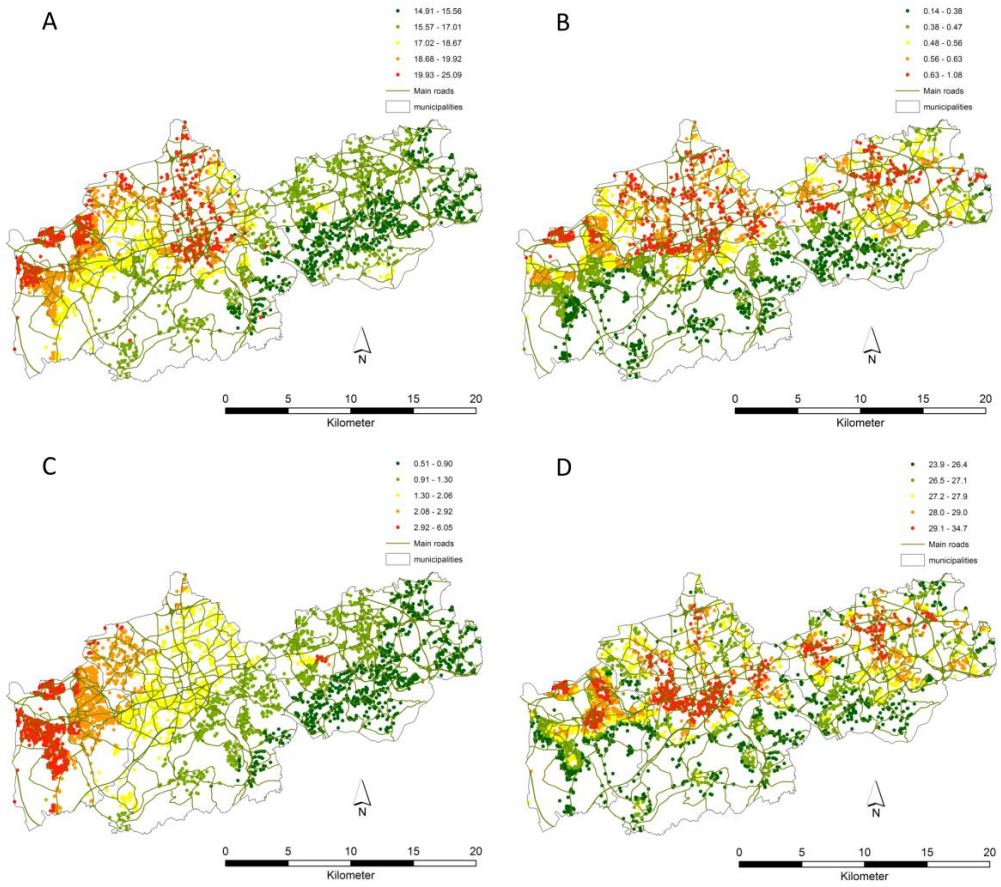

Figure 4. Residence-based spatial distribution of PM_{10} concentrations from EURAD-CTM: all-sources (**A**); local traffic (**B**) and local industry (**C**); and ESPCAPE-LUR (**D**).

4. Conclusions

Based on the comparison between air pollution concentrations modeled by ESCAPE-LUR and EURAD-CTM within the HNR study area, we showed that both model types have different input data as well as different temporal and spatial resolutions, driven by their different aims and application. While the point-specific ESCAPE-LUR primarily aims to estimate temporally stable and spatial variable long-term exposure to locally-emitted (mostly traffic-related) air pollution with a very high spatial resolution, the EURAD-CTM aims to estimate a spatio-temporal average air pollutant concentration in a small area (*i.e.*, 1 km^2), taking into account a range of major sources, e.g., traffic, industry, meteorological condition, and transport. While the observed weak to moderate overall agreement between the ESCAPE-LUR and the EURAD-CTM supports earlier findings [12], our analysis showed that the agreement between the two models improved considerably after restricting the EURAD-CTM to local traffic only. This finding was further supported by results comparing 14-day mean concentrations estimated by EURAD-CTM and measured at purpose-specific ESCAPE monitoring sites, yielding the highest correlations for traffic-specific EURAD-CTM estimates and measurements at traffic sites.

One of the principal strengths of the point-specific ESCAPE-LUR is to capture very small-scale variations in air pollution. Yet, this accuracy may be more error-prone than the coarser spatial resolution of 1 km^2 used by EURAD-CTM, regarding exposure assignment in cases of high personal mobility within small distances, like daily chores around the residence. The biggest strength of an LUR approach in general is the wide-ranging applicability, like the relatively small requirements on

measurement sites (low cost), the individual location of measurement sites, the easy assessment of land use data, and the straight forward model building procedure, based on linear regression modeling. In contrast, the EURAD-CTM, or chemical transport and dispersion modeling approaches in general, are less accessible to changes by the user due to the highly complex underlying mathematical, physical, and chemical modelling procedures. These complex procedures are, however, accompanied with benefit of including chemical transport actions, which allow modeling air pollution components that have not been measured. The LUR, on the other hand, is limited to modelling measured air pollutants. Moreover, CTMs enable the investigation of the role of meteorology and the prediction of air pollutant concentrations under hypothetical emission situations.

The comparatively easy applicability of LUR modeling and statistical model building procedure may come along with potential costs of wrong decisions: the initial choice of locations of the measurement sites limits the specificity of the model to capture those emission sources, whose concentration gradients are well captured by the chosen sites and may fail to capture all important source-specific concentration gradients across a study area, especially if important sources change over time. Restricting predictors to land use data might neglect important predictors of air pollution concentrations from other sources and processes, like chemical interaction and transport. Similarly, CTMs are only valid if based on a comprehensive and detailed emission database. To overcome limitations of each of the models and optimally make use of the respective strengths, we propose to combine the two approaches into a hybrid model [43,44]. These hybrid models are usually based on the LUR model since LURs are by design much easier to modify.

To conclude, our results show that ESCAPE-LUR and the EURAD-CTM are constructed to estimate complementary aspects of air pollution and both approaches have respective strengths and limitations, which need to be considered especially when investigating health effects. The possibility of combining the strengths of both, e.g., using hybrid models will be the next step to enhance exposure assessment.

Supplementary Materials: The following are available online at www.mdpi.com/2073-4433/7/3/48/s1. Figure S1: Flowchart of the EURAD model system containing the meteorological driver MM5, the pre-processors ECP and PREP, the emission model EEM and the chemistry transport model EURAD (input parameters are shaded in blue, output parameters are shaded in yellow and procedural parts are shaded in green or magenta), Figure S2: Spatial distribution of EURAD-CTM (1 km^2, yearly mean 2008) and ESCAPE-LUR (point-specific yearly mean October 2008–October 2009) at 4809 residences within the HNR study area for PM_{10} (A+C) and NO_2 (B+D), Figure S3: Boxplots of air pollution concentrations of monthly-mean PM_{10} and NO_2 concentrations over three year for a traffic-specific (grid cell: 690), and a background-specific location (grid cell: 679) with annual mean ESCAPE-LUR estimates and annual measurements at LANUV monitoring sites, Table S1: Time and locations of the ESCAPE-measurement campaign, Table S2: ESCAPE-LUR for $PM_{2.5}$, PM_{10} and NO_2, Table S3: Time and Location of routine monitoring sites, provided by LANUV, within the HNR study area.

Acknowledgments: The research leading to these results has received funding from the European Community's Seventh Framework Program (FP7/2007–2011) under grant agreement number: 211250; The study was supported by the Heinz Nixdorf Foundation (chairman: M. Nixdorf; former chairman: G. Schmidt (deceased)) and the German Ministry of Education and Science, the German Research Foundation (DFG: HO 3314/2-1, HO 3314/2-3, HO 3314/4-3). Lilian Tzivian gratefully acknowledges support by a post-doctoral fellowship from the Environmental and Health Fund, Jerusalem, Israel.

Author Contributions: Frauke Hennig contributed to the design of study, the analysis and interpretation of the results and preparation of manuscript. Dorothea Sugiri contributed to the analysis and preparation of the manuscript. Kateryna Fuks, Lilian Tzivian, Danielle Vienneau, Kees de Hoogh, Susanne Moebus, Karl-Heinz Jöckel, Ulrich Quass and Thomas Kuhlbush contributed to the interpretation of results and preparation of manuscript. Hermann Jakobs and Michael Memmesheimer contributed to the preparation of the manuscript. Barbara Hoffmann contributed to the design of study, interpretation of the results and preparation of manuscript.

Conflicts of Interest: The authors declare no conflict of interest.

References

1. World Health Organization. *The World Health Report 2013: Research for Universal Health Coverage*; WHO: Geneva, Switzerland, 2013.

2. Dockery, D.W.; Pope, C.A.; Xu, X.; SPrengler, J.D.; Ware, J.H.; Fay, M.E.; Ferris, B.G.; Speizer, F.E. An association between air pollution and mortality in six U.S. cities. *New Engl. J. Med.* **1993**, *329*, 1753–1759. [CrossRef] [PubMed]
3. Jerrett, M.; Arain, A.; Kanaroglou, P.; Beckerman, B.; Potoglou, D.; Sahsuvaroglu, T.; Morrison, J.; Giovis, C. A review and evaluation of intraurban air pollution exposure models. *J. Expo. Anal. Environ. Epidemiol.* **2005**, *15*, 185–204. [CrossRef] [PubMed]
4. Health Effects Institute. *HEI Panel on the Health Effect of Traffic-Related Air Pollution: A Critical Review of the Literature on Emissions, Exposure, and Health Effects*; Health Effects Institute: Boston, MA, USA, 2010.
5. Özkaynak, H.; Baxter, L.K.; Dionisio, K.L.; Burke, J. Air pollution exposure prediction approaches used in air pollution epidemiology studies. *J. Expo. Sci. Environ. Epidemiol.* **2013**, *23*, 566–572. [CrossRef] [PubMed]
6. Briggs, D.J. The use of GIS to evaluate traffic-related pollution. *Occup. Environ. Med.* **2007**, *64*, 1–2. [CrossRef] [PubMed]
7. Hoek, G.; Beelen, R.; de Hoogh, K.; Vienneau, D.; Gulliver, J.; Fischer, P.; Briggs, D. A review of land-use regression models to assess spatial variation of outdoor air pollution. *Atmos. Environ.* **2008**, *42*, 7561–7578. [CrossRef]
8. Cyrys, J.; Hochadel, M.; Gehring, U.; Hoek, G.; Diegmann, V.; Brunekreef, B.; Heinrich, J. GIS-based estimation of exposure to particulate matter and NO_2 in an urban area: Stochastic *versus* dispersion modeling. *Environ. Health Perspect.* **2005**, *113*, 987–992. [CrossRef] [PubMed]
9. Marshall, J.D.; Nethery, E.; Brauer, M. Within-urban variability in ambient air pollution: Comparison of estimation methods. *Atmos. Environ.* **2008**, *42*, 1359–1369. [CrossRef]
10. Briggs, D.J.; Collins, S.; Elliott, P.; Fischer, P.; Kingham, S.; Lebret, E.; Pryl, K.; Van Reeuwijk, H.; Smallbone, K.; van Der Veen, A. Mapping urban air pollution using GIS: A regression-based approach. *Int. J. Geogr. Inf. Sci.* **1997**, *11*, 699–718. [CrossRef]
11. Beelen, R.; Voogt, M.; Duyzer, J.; Zandveld, P.; Hoek, G. Comparison of the performances of land use regression modelling and dispersion modelling in estimating small-scale variations in long-term air pollution concentrations in a Dutch urban area. *Atmos. Environ.* **2010**, *44*, 4614–4621. [CrossRef]
12. De Hoogh, K.; Korek, M.; Vienneau, D.; Keuken, M.; Kukkonen, J.; Nieuwenhuijsen, M.J.; Badaloni, C.; Beelen, R.; Bolignano, A.; Cesaroni, G.; *et al*. Comparing land use regression and dispersion modelling to assess residential exposure to ambient air pollution for epidemiological studies. *Environ. Int.* **2014**, *73*, 382–392. [PubMed]
13. Perez, L.; Wolf, K.; Hennig, F.; Penell, J.; Basagaña, X.; Aguilera, I.; Agis, D.; Beelen, R.; Brunekreef, B.; Cyrys, J.; *et al*. Air pollution and atherosclerosis: A cross-sectional analysis of four European cohort studies in the ESCAPE study. *Environ. Health Perspect.* **2015**, *123*, 597–605. [PubMed]
14. Duisburg-Essen University. Ruhr & Culture. Available online: https://www.uni-due.de/welcome-services/en/rk_index.php (accessed on 3 December2015).
15. Ebel, A. The Eurad Project. Available online: http://www.uni-koeln.de/math-nat-fak/geomet/eurad/index_e.html (accessed on 30 November 2015).
16. Hass, H.; Ebel, A.; Feldmann, H.; Jakobs, H.J.; Memmesheimer, M. Evaluation studies with a regional chemical transport model (EURAD) using air quality data from the EMEP monitoring network. *Atmos. Environ. A. Gen. Top.* **1993**, *27*, 867–887. [CrossRef]
17. Ebel, A.; Elbern, H.; Feldmann, H.; Jakobs, H.; Kessler, C.; Memmesheimer, M. *Air Pollution Studies with the EURAD Model System (3): EURAD-European Air Pollution Dispersion Model SYSTEM*; University of Cologne: Cologne, Germany, 1997.
18. Memmesheimer, M.; Friesse, E.; Ebel, A.; Jakobs, H.; Feldmann, H.; Kessler, C. Long-term simulations of particulate matter in Europe on different scales using sequential nesting of a regional model. *Int. J. Environ. Pollut.* **2004**, *22*, 108–132. [CrossRef]
19. Schell, B.; Ackermann, I.; Hass, H.; Binkowski, F.; Ebel, A. Modeling the formation of secondary organic aerosol within a comprehensive air quality modeling system. *J. Geophys. Res.* **2001**, *106*, 28275–28293. [CrossRef]
20. Büns, C.; Klemm, O.; Wurzler, S.; Hebbinghaus, H.; Steckelbach, I.; Friesel, J.; Ebel, A.; Friese, E.; Jakobs, H.; Memmesheimer, M. Comparison of four years of air pollution data with a mesoscale model. *Atmos. Res.* **2012**, *118*, 404–417. [CrossRef]

21. Grell, G.A.; Oceanic, N.; Administr, A.; Dudhia, J. *A Description of the Fifth-Generation Penn State/NCAR Mesoscale Model (MM5)*; University Corporation for Atmospheric Research (UCAR): Boulder, CO, USA, 2016.
22. Memmesheimer, M.; Tippke, J.; Ebel, A.; Hass, H.; Jakobs, H.; Laube, M. On the use of EMEP emission inventories for European scale air pollution modelling with the EURAD model. In Proceedings of the 1991 EMEP Workshop on Photooxidant Modelling for Long Range Transport in Relation to Abatement Strategies, Berlin, Germany, 16–19 April 1991; pp. 307–324.
23. Elbern, H.; Strunk, A.; Schmidt, H.; Talagrand, O. Emission rate and chemical state estimation by 4-dimensional variational inversion. *Atmos. Chem. Phys.* **2007**, *7*, 3749–3769. [CrossRef]
24. Petry, H.; Ebel, A.; Franzkowiak, V.; Hendricks, J.; Lippert, E.; Möllhoff, M. Impact of aircraft exhaust on atmosphere: Box model studies and 3-d mesoscale numerical case studies of seasonal differences. In Proceedings of 1996 Impact of Aircraft Emissions upon the Atmosphere, Paris, France, 15–18 October 1996; pp. 241–246.
25. Current concentrations of air pollutants in Germany. Available online: http://www.umweltbundesamt.de/daten/luftbelastung/aktuelle-luftdaten (accessed 30 November 30 2015).
26. Stationen und Messwerte. Available online: http://www.lanuv.nrw.de/umwelt/luft/immissionen/stationen-und-messwerte/ (accessed on 30 November 2015).
27. Elbern, H. The Objectives of Chemical Data Assimilation. Available online: http://db.eurad.uni-koeln.de/en/research/working_group_he/data_assimilation.php (accessed on 16 December 2015).
28. Hebbinghaus, H.; Wurzler, S.; Friese, E.; Jakobs, H.J.; Kessler, C.; Ebel, A. Determination of the contribution of different groups of emission sources on the concentration of PM10, PM2.5, and NO2 in North Rhine-Westphalia—A whodunnit. In Proceedings of the 2009 European Aerosol Conference, Karlsruhe, Germany, 6–11 September 2009.
29. Nonnemacher, M.; Jakobs, H.; Viehmann, A.; Vanberg, I.; Kessler, C.; Moebus, S.; Möhlenkamp, S.; Erbel, R.; Hoffmann, B.; Memmesheimer, M. Spatio-temporal modelling of residential exposure to particulate matter and gaseous pollutants for the Heinz Nixdorf Recall Cohort. *Atmos. Environ.* **2014**, *91*, 15–23. [CrossRef]
30. Fagerli, H.; Dutcheak, S.; Torseth, K.; QAmman, M.; Ritter, M. EMEP. Available online: http://www.emep.int/ (accessed on 30 November 2015).
31. European Environment Agency. Index to methodology chapters ordered by SNAP97 Activity. Available online: http://www.eea.europa.eu/publications/EMEPCORINAIR4/page009-a.html (accessed on 30 November 2015).
32. Hennig, F.; Fuks, K.; Moebus, S.; Weinmayr, G.; Memmesheimer, M.; Jakobs, H.; Bröcker-Preuss, M.; Führer-Sakel, D.; Möhlenkamp, S.; Erbel, R.; *et al*. Association between Source-Specific Particulate Matter Air Pollution and hs-CRP: Local Traffic and Industrial Emissions. *Environ. Health Perspect.* **2014**, *122*, 703–710. [PubMed]
33. Keil, M.; Bock, M.; Esch, T.; Metz, A.; Nieland, S.; Pfitzner, A. CORINE Land Cover Aktualisierung 2006 für Deutschland. Available online: http://www.uba.de/uba-info-medien/4086.html (accessed on 16 December 2015).
34. Eeftens, M.; Beelen, R.; de Hoogh, K.; Bellander, T.; Cesaroni, G.; Cirach, M.; Declercq, C.; Dedele, A.; Dons, E.; de Nazelle, A.; *et al*. Development of Land Use Regression Models for $PM_{2.5}$, $PM_{2.5}$ Absorbance, PM_{10} and PM_{coarse} in 20 European Study Areas; Results of the ESCAPE Project. *Environ. Sci. Technol.* **2012**, *46*, 11195–11205.
35. Cyrys, J.; Eeftens, M.; Heinrich, J.; Ampe, C.; Armengaud, A.; Beelen, R.; Bellander, T.; Beregszaszi, T.; Birk, M.; Cesaroni, G.; *et al*. Variation of NO_2 and NO_x concentrations between and within 36 European study areas: Results from the ESCAPE study. *Atmos. Environ.* **2012**, *62*, 374–390.
36. Beelen, R.; Hoek, G.; Vienneau, D.; Eeftens, M.; Dimakopoulou, K.; Pedeli, X.; Tsai, M.Y.; Künzli, N.; Schikowski, T.; Marcon, A.; *et al*. Development of NO_2 and NO_x land use regression models for estimating air pollution exposure in 36 study areas in Europe—The ESCAPE project. *Atmos. Environ.* **2013**, *72*, 10–23.
37. Wang, M.; Brunekreef, B.; Gehring, U.; Szpiro, A.; Hoek, G.; Beelen, R. A New Technique for Evaluating Land-use Regression Models and Their Impact on Health Effect Estimates. *Epidemiology* **2016**, *27*, 51–56. [CrossRef] [PubMed]
38. ESCAPE manuals. Available online: http://www.escapeproject.eu/manuals/ (accessed on 16 December 2015).
39. R Development Core Team. *R: A Language and Environment for Statistical Computing*; R Foundation for Statistical Computing: Vienna, Austria, 2015.

40. Auswertung der Luftbelastungssituation 2009. Available online: http://www.umweltbundesamt.de/sites/default/files/medien/515/dokumente/3895.pdf (accessed on 16 December 2015).
41. Pedersen, M.; Giorgis-Allemand, L.; Bernard, C.; Aguilera, I.; Andersen, A.M. N.; Ballester, F.; Beelen, R.M.J.; Chatzi, L.; Cirach, M.; Danileviciute, A.; *et al*. Ambient air pollution and low birthweight: A European cohort study (ESCAPE). *Lancet Respir. Med.* **2013**, *1*, 695–704. [PubMed]
42. Hertel, S.; Viehmann, A.; Moebus, S.; Mann, K.; Bröcker-Preuss, M.; Möhlenkamp, S.; Nonnnemacher, M.; Erbel, R.; Jakobs, H.; Memmesheimer, M.; *et al*. Influence of short-term exposure to ultrafine and fine particles on systemic inflammation. *Eur. J. Epidemiol.* **2010**, *25*, 581–592. [PubMed]
43. Akita, Y.; Baldasano, J.M.; Beelen, R.; Cirach, M.; de Hoogh, K.; Hoek, G.; Nieuwenhuijsen, M.; Serre, M.L.; de Nazelle, A. Large Scale Air Pollution Estimation Method Combining Land Use Regression and Chemical Transport Modeling in a Geostatistical Framework. *Environ. Sci. Technol.* **2014**, *48*, 4452–4459. [CrossRef] [PubMed]
44. Vienneau, D.; de Hoogh, K.; Bechle, M.J.; Beelen, R.; van Donkelaar, A.; Martin, R.V.; Millet, D.B.; Hoek, G.; Marshall, J.D. Western European land use regression incorporating satellite- and ground-based measurements of NO_2 and PM_{10}. *Environ. Sci. Technol.* **2013**, *47*, 13555–13564.

Supplementary Materials: Comparison of Land-Use Regression Modelling with Dispersion and Chemistry Transport Modelling to Assign Air Pollution Concentrations within the Ruhr Area *Atmosphere* 2016, *7*, 48

Frauke Hennig, Dorothea Sugiri, Lilian Tzivian, Kateryna Fuks, Susanne Moebus, Karl-Heinz Jöckel, Danielle Vienneau, Thomas Kuhlbusch, Kees de Hoogh, Michael Memmesheimer, Hermann Jakobs, Ulrich Quass and Barbara Hoffmann

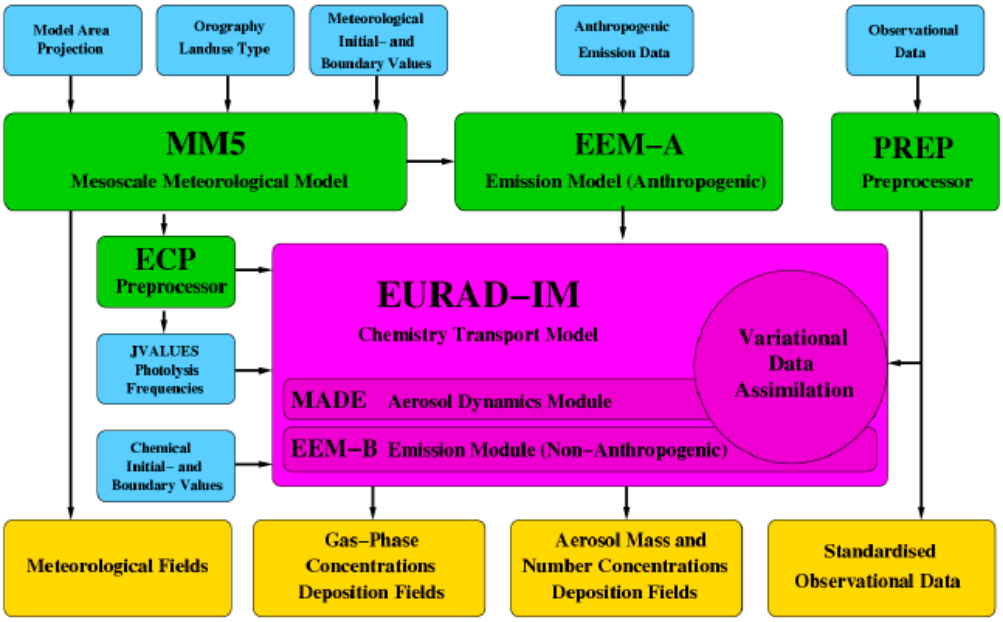

Figure S1. Flowchart of the EURAD model system containing the meteorological driver MM5, the pre-processors ECP and PREP, the emission model EEM and the chemistry transport model EURAD (input parameters are shaded in blue, output parameters are shaded in yellow and procedural parts are shaded in green or magenta) [1].

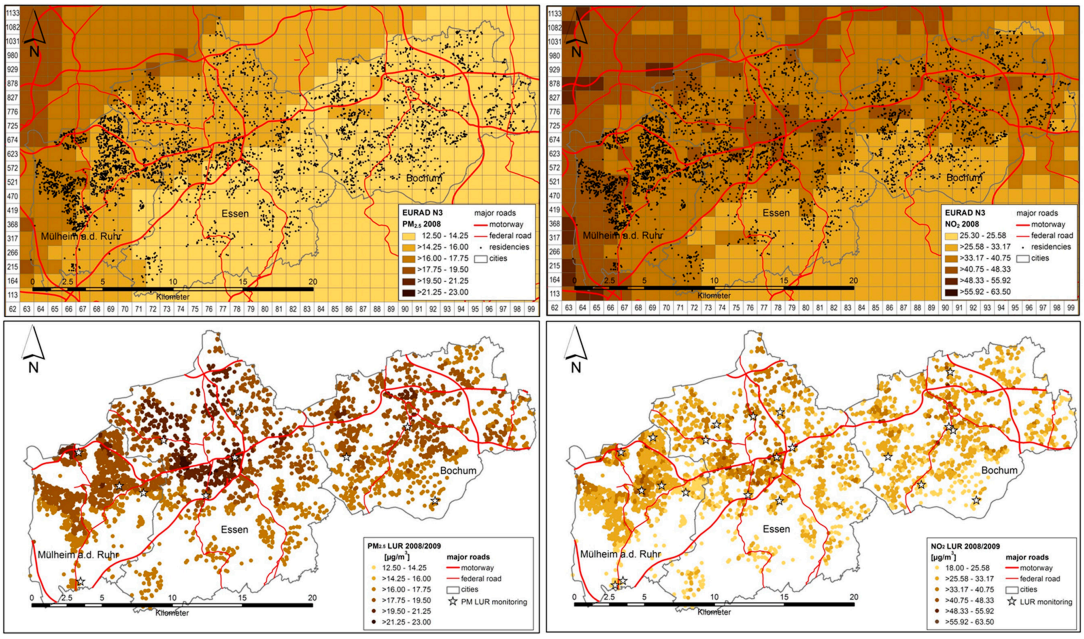

Figure S2. Spatial distribution of EURAD-CTM (1 km^2, yearly mean 2008) and ESCAPE-LUR (point-specific yearly mean October 2008–October 2009) at 4809 residences within the HNR study area for PM_{10} (A+C) and NO_2 (B+D).

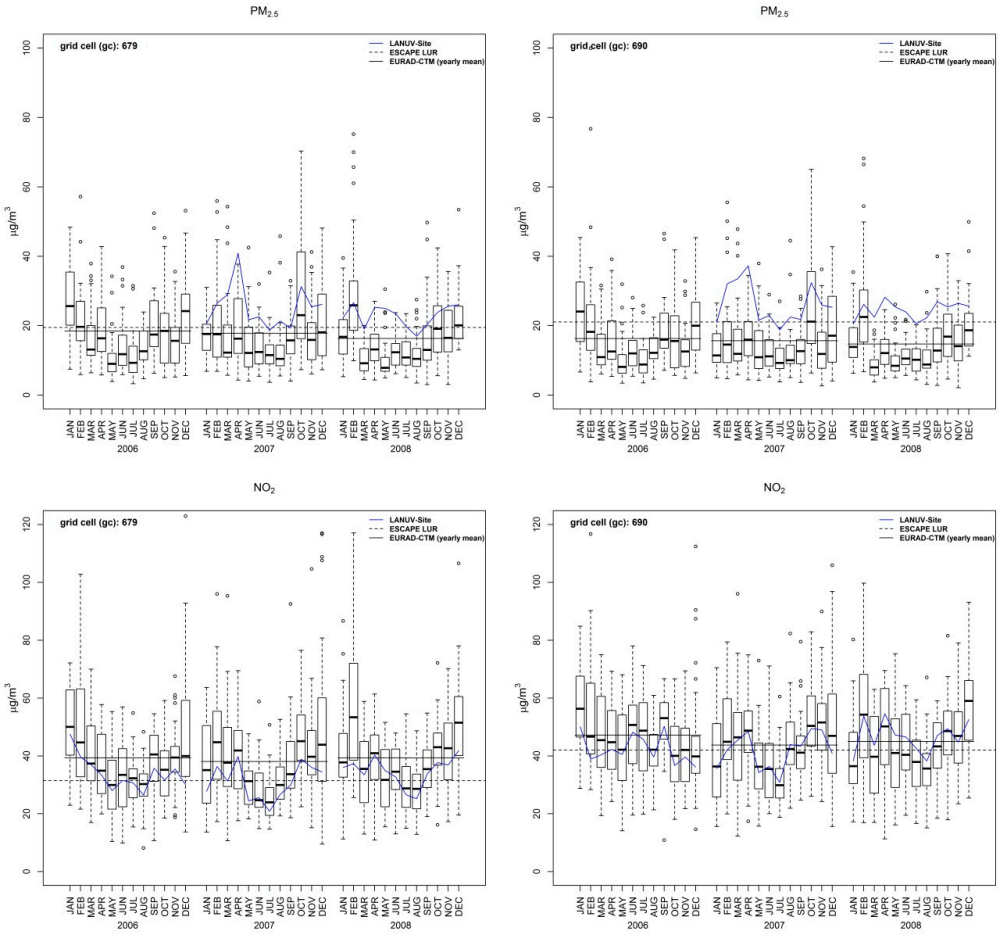

Figure S3. Boxplots of air pollution concentrations of monthly-mean PM_{10} and NO_2 concentrations over three year for a traffic-specific (grid cell: 690), and a background-specific location (grid cell: 679) with annual mean ESCAPE-LUR estimates and annual measurements at LANUV monitoring sites.

Table S1. Time and locations of the ESCAPE-measurement campaign.

Time of measurements	Autumn: • 16 October 2008–30 October 2008 • 3 November 2008–17 November 2008 • 19 November. 2009–3 December 2008 • 5 December 2008–19 December 2008 Winter: • 7 January 2009–21 January 2009 • 26 January 2009–9 Febuary 2009 • 11 Febuary 2009–25 Febuary 2009 • 27 Febuary 2009–13 March 2009 Spring/summer: • 24 June 2009–8 July 2009 • 10 July 2009–24 July 2009 • 28 Jul. 2009–11 August 2009 • 13 August 2009–27 August 2009
Characteristics of site	Background: • No influence by sources in the "direct vicinity" of site • No more than 3000 vehicles per day in a 50 m-buffer • No important sources of PM or NOx within a 100 m-buffer (combustion source, construction works, small industries, district heating plant, parking areas) and • Distance to large industries > 100 m. Traffic: • Traffic intensity > 10,000 vehicles per day at site location • Absence of other sources (preferable) • Ground level or first floor measurements (2–3 m).
Filter type of measurement sites	NO_2: Ogawa badges PM: Harvard Impactors

Table S2. ESCAPE-LUR for $PM_{2.5}$, PM_{10} and NO_2.

Air Pollutant	Linear Model	Predictors	Adj. R^2	LOOCV-R^2
$PM_{2.5}$	$81.73 + 5.61 \times 10^{-8} \times$ HEAVYTRAFLOAD_1000 + $1.20 \times 10^{-7} \times$ INDUSTRY_5000 + $1.04 \times 10^{-4} \times$ POP_1000 − $2.57 \times 10^{-5} \times$ XCOORD	Heavy traffic load in a 1000 m-buffer, Industry in a 5000m-buffer, Population in a 1000m-buffer, X-Coordinate of residential address	0.85	0.74
PM_{10}	$23.86 + 1.47 \times 10^{-7} \times$ HEAVYTRAFLOAD_1000 + $2.44 \times 10^{-4} \times$ POP_1000	Heavy traffic load in a 1000m-buffer, Population in a 1000m-buffer	0.66	0.59
NO_2	$19.66 + 3.48 \times 10^{-7} \times$ INDUSTRY_5000 + $0.022 \times$ POP_100 + $4.1 \times 10^{-6} \times$ PORT_5000 + $1.31 \times 10^{-6} \times$ TRAFLOAD_100	Industry in a 5000m-buffer, Population in a 100 m-buffer, inland sea-ports in a 5000 m-buffer, traffic load in a 100 m-buffer	0.88	0.82

Table S3. Time and Location of routine monitoring sites, provided by LANUV, within the HNR study area [2].

Name and Adress of Monitoring Site	Air Pollutant and Time of Monitoring	Frequency of Monitoring
Mülheim-Styrum (STYR) Neustadtstraße, 45476 Mülheim	NO_2 (since 1981)	Daily
	PM_{10} (since 2002)	Daily
	$PM_{2.5}$ (since 2007)	2-day-basis
Essen-Vogelheim (EVOG) Hafenstraße, 45356 Essen	NO_2 (since 1985)	Daily
	PM_{10} (since 2002)	Daily
	$PM_{2.5}$ (since 2008)	2-day-basis
Essen-Ost (VESN) Steelerstraße, 45138 Essen	NO_2 (since 1986)	Daily
	PM_{10} (since 2003)	Daily
	$PM_{2.5}$ (since 2003)	Daily

References

1. Elbern, H.; Friese, E. Eurad-IM Products, Quality and Background Information. Available online: http://www.uni-koeln.de/math-nat-fak/geomet/eurad/modell/eurad_descr_e.html (accessed on 16 December 2015).
2. Stationen und Messwerte. Available online: http://www.lanuv.nrw.de/umwelt/luft/immissionen/stationen-und-messwerte/ (accessed on 30 November 2015).

3 Ultrafine and fine particle number and surface area concentrations and daily cause-specific mortality in the Ruhr area, Germany, 2009–2014. Hennig F, Quass U, Hellack B, Küpper M, Kuhlbusch TAJ, Stafoggia M, et al. Environ Health Perspect 126:1-10 (2018)

A Section 508–conformant HTML version of this article is available at https://doi.org/10.1289/EHP2054.

Ultrafine and Fine Particle Number and Surface Area Concentrations and Daily Cause-Specific Mortality in the Ruhr Area, Germany, 2009–2014

Frauke Hennig,[1] Ulrich Quass,[2] Bryan Hellack,[2] Miriam Küpper,[2] Thomas A. J. Kuhlbusch,[3,4] Massimo Stafoggia,[5,6] and Barbara Hoffmann[1]

[1]Institute of Occupational, Social and Environmental Medicine, Center for Health and Society, Heinrich-Heine-University of Düsseldorf, Düsseldorf, Germany
[2]Institute of Energy and Environmental Technology e.V., Duisburg, Germany
[3]Federal Institute of Occupational Safety and Health, Dortmund, Germany
[4]Center for Nanointegration Duisburg-Essen (CENIDE), University Duisburg-Essen, Duisburg and Essen, Germany
[5]Department of Epidemiology, Lazio Region Health Service, Rome, Italy
[6]Institute of Environmental Medicine, Karolinska Institute, Stockholm, Sweden

Background: Although epidemiologic studies have shown associations between particle mass and daily mortality, evidence on other particle metrics is weak.

Objectives: We investigated associations of size-specific particle number concentration (PNC) and lung-deposited particle surface area concentration (PSC) with cause-specific daily mortality in contrast to PM_{10}.

Methods: We used time-series data (March 2009–December 2014) on daily natural, cardiovascular, and respiratory mortality (NM, CVM, RM) of three adjacent cities in the Ruhr Area, Germany. Size-specific PNC (electric mobility diameter of 13.3–750 nm), PSC, and PM_{10} were measured at an urban background monitoring site. In single- and multipollutant Poisson regression models, we estimated percentage change (95% confidence interval) [% (95% CI)] in mortality per interquartile range (IQR) in exposure at single-day (0–7) and aggregated lags (0–1, 2–3, 4–7), accounting for time trend, temperature, humidity, day of week, holidays, period of seasonal population decrease, and influenza.

Results: $PNC_{100–750}$ and PSC were highly correlated and had similar immediate (lag0–1) and delayed (lag4–7) associations with NM and CVM, for example, 1.12% (95% CI: 0.09, 2.33) and 1.56% (95% CI: 0.22, 2.92) higher NM with IQR increases in $PNC_{100–750}$ at lag0–1 and lag4–7, respectfully, which were slightly stronger then associations with IQR increases in PM_{10}. Positive associations between PNC and NM were strongest for accumulation mode particles (PNC 100–500 nm), and for larger UFPs (PNC 50–100 nm). Associations between NM and $PNC_{<100}$ changed little after adjustment for O_3 or PM_{10}, but were more sensitive to adjustment for NO_2.

Conclusion: Size-specific PNC (50–500 nm) and lung-deposited PSC were associated with natural and cardiovascular mortality in the Ruhr Area. Although associations were similar to those estimated for an IQR increase in PM_{10}, particle number size distributions can be linked to emission sources, and thus may be more informative for potential public health interventions. Moreover, PSC could be used as an alternative metric that integrates particle size distribution as well as deposition efficiency. https://doi.org/10.1289/EHP2054

Introduction

Increases of daily fine particulate matter [PM $\leq$2.5 μm and $\leq$10 μm, respectively, in aerodynamic diameter ($PM_{2.5}$ and PM_{10})] have been shown to be associated with natural mortality (NM) in several North American and European cities (HEI 2010; Katsouyanni and Samet 2009; Samoli et al. 2008). Epidemiological studies have further shown that PM is associated with adverse health effects, such as short- and long-term cardiovascular morbidity and mortality, diseases of the central nervous system, respiratory morbidity, and lung cancer (WHO 2013). Toxicological studies suggest that inhaled ultrafine particles (UFPs) might be particularly harmful, because they can pass the lung epithelium more easily and translocate into the blood to be transported to other organs (Oberdörster et al. 2005). However, epidemiological evidence on pathogenic health effects of UFPs is still limited and inconclusive (HEI Review Panel on Ultrafine Particles 2013; WHO 2013), mainly due to the lack of routinely monitored UFP data and few dedicated measurement campaigns in the framework of specific research projects. UFPs are commonly measured as particle number concentration (PNC), representing more than 85% of the total $PM_{2.5}$ particle number (Hinds 1999) while contributing little to the PM concentration. The latter is usually the only regulated ambient air particle metric worldwide. Although PM is a mixture composited by different particle sizes and numbers, particles of different size and number concentration are usually generated by different sources (Morawska et al. 1999) such that size and number distribution may provide a better understanding to identify sources as a potential basis for an intervention measure. The commonly used UFPs, defined as particles with an electric diameter <100 nm, for example, combine nucleation and Aitken mode particles (<30 nm and 30–100 nm respectively), whereas combustion-generated particles (from vehicle emissions) range from 30 nm to 500 nm (Vu et al. 2015). UFP concentration alone therefore does not inform about the different sources of the particles.

Another potentially important metric is the integrated measure of lung-deposited surface area concentration of airborne particles (PSC), which takes into account the surface area as well as the size-dependent deposition efficiency of respective particles in the respiratory system. This metric thus constitutes a proxy of the particle's reactivity, which is related to surface area, as well as its capacity to carry adsorbed chemical species, both possibly promoting oxidative stress, a precursor of inflammatory effects (Hussain et al. 2009). Besides PM, PNC in different size fractions and particle surface area may hence provide a better measurement regarding the toxicity of PM exposure (Noël et al. 2016; Oberdörster 2000) as well as the identification of sources (Morawska et al. 1999).

Address correspondence to F. Hennig, Universitätsklinikum Düsseldorf, AG Umweltepidemiologie, Postfach 101007, 40001 Düsseldorf, Germany. Telephone: 49 211 586729111. Email: Frauke.hennig@uni-duesseldorf.de

Supplemental Material is available online (https://doi.org/10.1289/EHP2054).

The authors declare they have no actual or potential competing financial interests.

Received 18 April 2017; Revised 19 December 2017; Accepted 21 December 2017; Published 15 February 2018.

In a European multicenter analysis on health effects of UFP number on natural and cardiorespiratory mortality including Finland, Sweden, Denmark, Germany, Italy, Spain, and Greece (Stafoggia et al. 2017), a weak delayed effect of UFP was estimated (>lag5). However, this multicenter study was limited by the heterogeneity of its exposure assessment methodology such as instrumentation capturing slightly different size ranges of particles or placement of monitors (background vs. traffic location) as well as by different measurement periods (time and duration) (Stafoggia et al. 2017). A slight difference in the size ranges of measured UFPs due to the use of different instruments has a great impact on the measured overall PNC because the number concentration of particles increases remarkably in the smallest size fractions. Moreover, the location of the monitoring equipment (height and placement of monitors with respect to local sources and the location of the study population) also substantially influence the representativeness of the exposure measurements and might introduce bias as a consequence of differential exposure measurement error (Stafoggia et al. 2017).

In this study we tried to overcome the aforementioned limitations by focusing on one large single study, located in the densely populated German Ruhr Area (Essen, Mülheim, and Oberhausen). Being part of the German Ultrafine Aerosol Network (GUAN) (Birmili et al. 2016), this time-series study benefits from a comparatively long measurement period of almost 6 y and an in-depth characterization of ultrafine (electric mobility diameter <100 nm, including the size ranges 13.3–30, 30–50, and 50–100 nm) and fine (electric mobility diameter 100–750 nm, including the size ranges 100–250, 250–500, and 500–750 nm) particles, including number concentration and lung-deposited PSC, a metric that has rarely been investigated in epidemiological studies to date. In addition, the measurement site is co-located with a central urban background monitoring station of the regional air quality network (Mülheim Styrum), enabling us to also make use of monitored PM_{10}, nitrogen dioxide (NO_2), and ozone (O_3), which potentially confound or modify ultrafine or fine particle effects on health. In a recent meta-analysis, NO_2 and $PM_{2.5}$ both were associated with mortality in multipollutant analyses (Faustini et al. 2014), whereas O_3 is highly correlated with temperature and sunlight, and hence might be an additional or even independent risk factor (Levy et al. 2012). Considering that multiple air pollutants originate from common sources, multiple air pollutants may interact with or confound each other. Results of the European study indicated that associations between UFPs and mortality were confounded by NO_2, $PM_{2.5}$, and $PM_{2.5–10}$; whereas adjusting for PM_{10} or O_3 had little influence on effect estimates (Stafoggia et al. 2017).

The objective of this study was to investigate the associations of size-specific PNC as well as lung-deposited PSC on natural, cardiovascular, and respiratory mortality in the Ruhr Area, based on a time-series study from March 2009 to December 2014. In addition to the toxicologically important novel particle metrics, we investigated the role of copollutants such as PM_{10}, NO_2, and O_3.

Methods

Mortality Data

We collected daily mortality counts based on the primary cause of death, defined as natural [*International Classification of Diseases, 10th Revision* (ICD-10) A00–R99], cardiovascular (ICD-10 I00–I99) and respiratory (ICD-10 J00–J99) mortality in the three adjacent cities of Essen, Mülheim, and Oberhausen between January 2008 and December 2014 from the central statistical and IT services provider of North Rhine-Westphalia. The three adjacent cities (in an area of $\sim 379\,km^2$) with a total of nearly 1 million inhabitants [Essen, $\sim 580{,}000$ ($210\,km^2$); Mülheim, $\sim 170{,}000$ ($91\,km^2$); and Oberhausen, $\sim 211{,}000$ ($77\,km^2$)] are located in the western part of the metropolitan Ruhr Area. As respective outcomes, we used the sum of city-specific natural and cause-specific deaths per day. The primary cause of deaths was assigned based on the underlying disease instead of the immediate cause of death.

Air Pollution Data

Exposure data was collected at the project-specific measurement site (i.e., GUAN) provided by the Institute of Energy and Environmental Technology (IUTA), co-located to an urban background monitoring site of the regional air quality network (code "STYR") operated by the North Rhine-Westphalia State Agency for Nature, Environment and Consumer Protection [Landesamt für Natur, Umwelt und Verbraucherschutz (LANUV) North Rhine-Westphalia (NRW), Essen, Germany] from March 2009 until December 2014. A detailed description of the measurement site and respective measurement techniques can be found elsewhere (Birmili et al. 2016). The measurement site is located close to the administrative border of the cities of Mülheim and Oberhausen. Within a 1-km buffer, the site is surrounded by highways with channel-like cross-sections (~ 10 m below site level) and traffic of approximately 50,000 vehicles/day (~ 250 m north), a railway yard (south/southwest), and a medium-trafficked street and its junction with a highway exit (west/northwest). Main wind directions are south/southwest and northeast. The mixed residential-, industrial-, and traffic-influenced character of the site is typical for many urban areas in the Ruhr Area and hence believed to be representative for a large part of the population living in the adjacent cities of Mülheim and Oberhausen, including their eastern neighbor Essen.

Measured particle characteristics included size-specific PNC of ultrafine, fine, and coarse particles (as well as their PSC) that deposit in the alveolar or tracheobronchial region of the lung (short: lung-deposited PSC). PNCs [number per cubic centimeter (n/cm^3)] were measured with a scanning mobility particle sizer (TSI Inc.) in the size ranges of 13.3–750 nm electrical mobility diameter (Wang and Flagan 1990). In an effort to understand the health effects of different particle sizes, potentially generated by different emission sources and reaction processes, we investigated six particle size fractions, including particles size ranges of 13.3–30 nm (reflecting the nucleation mode: <30 nm), 30–50 nm, 50–100 nm (reflecting the Aitken mode: 30–100 nm), 100–250 nm, 250–500 nm, and 500–750 nm (reflecting the accumulation mode: 100–1,000 nm). The PSC of lung-deposited particles with a diameter of 20–1,000 nm was measured in micrometers squared per cubic centimeter every second using a nanoparticle surface area monitor (NSAM; model 3550, TSI Inc.) (Asbach et al. 2009). The NSAM uses an opposed flow unipolar diffusion charger followed by an ion trap to remove excess ions. Particles >1 μm are withheld by means of an impactor located at the NSAM entrance. The voltage in the ion trap can be adjusted to manipulate the particle size distribution and therefore the response function; that is, if the ion trap voltage is set to 200 V, the NSAM delivers the surface area deposited in the alveolar region, whereas it delivers the surface area of particles deposited in the tracheobronchial region when the voltage is set to 100 V. In our study, alveolar-deposited particles were monitored. The accuracy of surface determination decreases substantially for particle diameters below 20 nm and above 400 nm (Asbach et al. 2009). However, typical outdoor aerosol particles <20 nm in diameter and >400 nm in aerodynamic diameter contribute little to the total surface area.

Routinely monitored air pollutants at the central state-run (LANUV) monitoring site (STYR) included PM_{10} (β-attenuation), NO_2 (chemiluminescence method), and O_3 (ultraviolet absorption).

Covariates

Daily temperature [in degrees Celsius (°C), daily mean] and relative humidity were measured according to standardized protocols (VDI-guidelines 3786, parts 3 and 4; Verein Deutscher Ingenieure 2009, 2012) at a state-run monitoring site (Duisburg-Walsum), located 11 km northeasterly from the study site. External information on periods of influenza was collected from the central statistical and information technology services provider of North Rhine-Westphalia. In addition, we defined an indicator for population decrease during summer, following the definition in Stafoggia et al. (2017): namely a three-level variable assuming value "1" for the time of school holidays in North Rhine-Westphalia (6 wk within July and September; e.g., 9 July until 21 August in 2012 or 22 July until 3 September in 2013), and "2" in the 4-wk period around the school holidays; all other days stood for reference days and were assigned to "0"). Further variables included day of week (six indicator variables, with Sundays as the reference category), holiday (an indicator variable identifying the main bank holidays in North Rhine-Westphalia), and season (fall = September–November; spring = March–May, summer = June–August; and winter = December–February).

Statistical Analysis

The basic description of particle metrics, mortality, and meteorological data included visualizations of the time series, median [interquartile range (IQR)], and Spearman's correlation coefficients between respective exposure variables.

To estimate associations between exposures and daily cause-specific mortality, we used Poisson regression models allowing for overdispersion. Regression models included penalized regression splines as a smoothing function for time trend. We further included potential confounders based on a review of current literature (Stafoggia et al. 2017). Adjusted models included mean air temperature [day of death (lag0) and a moving average of 1–3 d prior to the observed death (lag1–3)], relative humidity, and indicator variables for day of the week, holidays, influenza epidemics, and the presence of a population decrease in the respective cities during the summer vacation period. Air temperature was modeled by fitting a natural cubic regression spline to allow for nonlinear confounder adjustment.

We investigated single-lags from the same day of death (lag0) up to 7 d prior to death (lag7). Moreover, we investigated aggregated lags, representing immediate effects (0–1 d prior to the death; lag0–1), medium-term effects (lag2–3), and delayed effects (lag4–7). We chose single-lag models as well as aggregated 2- to 4-d lags over distributed lag-models because of multiple missing data in the PNC series and the respective loss of power, especially in the underlying small study population. By ending up with 11 models per investigated pollutant, we aimed to look for a general pattern of associations rather than identifying adverse health effects based on single-day lags that could be observed in such a multiple testing situation.

The main exposure metrics of interest were size-specific PNC, aggregated as ultrafine ($PNC_{<100}$) and fine particles ($PNC_{100–750}$), as well as PSC and PM_{10}. In addition, we also investigated size-specific PNC in finer resolved size fractions ($PNC_{13.3–30}$, $PNC_{30–50}$, $PNC_{50–100}$, $PNC_{100–250}$, $PNC_{250–500}$, and $PNC_{500–750}$). All health effect estimates are presented as mean percentage increase [95% confidence interval (CI)] [% (95% CI)] in mortality per IQR of the respective exposure.

We calculated two-pollutant models in order to investigate whether results for UFPs ($PNC_{<100}$) were independent of other pollutants or metrics: *a*) $PNC_{<100}$ and PM_{10}, *b*) $PNC_{<100}$ and NO_2, *c*) $PNC_{<100}$ and O_3, *d*) $PNC_{<100}$ and $PNC_{100–750}$, and *e*) $PNC_{<100}$ and PSC. In addition we investigated two-pollutant models including *a*) $PNC_{100–750}$ and PM_{10}, *b*) $PNC_{100–750}$ and NO_2, *c*) $PNC_{100–750}$ and O_3, and *d*) $PNC_{100–750}$ and PSC.

Furthermore, we investigated effect modification of UFPs and particles ($PNC_{100–750}$) by cold and warm periods of the year (October–March vs. April–September), and by high or low concentration of PM_{10}, O_3, NO_2 and PSC by including interaction terms between the potential effect modifier and the exposure of interest. High levels of PM_{10}, O_3, NO_2, and PSC referred to concentrations above the 75th percentile of the respective distribution. Effect modification was checked based on a 5% significance level regarding the coefficient of the respective interaction term.

Results

Because particle metrics (PNC and PSC) were only measured beginning in March 2009, our analysis was based on the time period from March 2009 until December 2014 (2,132 d). We observed different missing patterns among exposures ranging from 266 missing days for PNC, 125 d for PSC, 110 d for O_3, and 91 d for NO_2 to 29 d for PM_{10}. The majority of missing exposure data for PNC resulted from a sampling pump failure of the scanning mobility particle sizer during specific time windows (data not shown) and hence was assumed to be missing at random. Because of different missing patterns, the number of observations slightly changed between the analysis for each metric and lag.

Medians (IQRs) of daily cause-specific mortality per approximately 946,000 inhabitants in Essen, Mülheim, and Oberhausen were 32 (8) death/day for natural, 12 (5) for cardiovascular (corresponding to 37.5% of the overall deaths), and 3 (2) for respiratory mortality (corresponding to 9.4% of the overall deaths) (Table 1 and Figure 1). The city of Essen contributed most to the observed mortality (approximately 60%). Median (IQR) PNC of UFPs ($PNC_{<100}$) was 9,871 n/cm^3 (4,900), with the smallest size fraction ($PNC_{13.3–30}$) contributing the most to PNC (4,623 n/cm^3; 2,438). Median PSC was 36.1 $\mu m^2/cm^3$ (21.7) and PM_{10} was 20.2 $\mu g/m^3$ (13.3), which is well below the European annual limit value of 40 $\mu g/m^3$. In total, the PM_{10} 24-h limit (50 $\mu g/m^3$; EU 2008) was exceeded on 108 d (Figure 1). The median for

Table 1. Median (IQR) daily mortality, particle metrics, and meteorology in the Ruhr Area (Essen, Mülheim, and Oberhausen) between March 2009 and December 2014 (2,132 days).

Variable	Median (IQR)	Days (n)[a]
Mortality		
Natural[b]	32.0 (8.0)	2,132
Cardiovascular[c]	12.0 (5.0)	2,132
Respiratory[d]	3.0 (2.0)	2,132
Exposure PNC (n/cm^3)		
$PNC_{13.3–30}$	4,623.1 (2438.2)	1,866
$PNC_{30–50}$	2,673.1 (1492.5)	1,866
$PNC_{50–100}$	2,368.7 (1608.7)	1,866
$PNC_{<100}$ (UFP)	9,870.6 (4900.2)	1,866
$PNC_{100–250}$	1,209.7 (903.2)	1,866
$PNC_{250–500}$	195.8 (180.8)	1,866
$PNC_{500–750}$	9.0 (14.0)	1,866
$PNC_{100–750}$ (FP)	1,437.3 (1060.9)	1,866
PSC ($\mu m^2/cm^3$)	36.1 (21.7)	2,007
PM_{10} ($\mu g/m^3$)	20.2 (13.3)	2,103
NO_2 ($\mu g/m^3$)	29.2 (16.2)	2,041
O_3 ($\mu g/m^3$)	54.0 (37.0)	2,022
Meteorology		
Temperature (°C)	11.9 (9.9)	2,124
Relative humidity	78.8 (18.5)	2,124

[a]The number of days differs because of inconsistencies in measurements.
[b]Essen: 19.0 (6.0); Oberhausen 7.0 (4.0); Mülheim: 5.0 (3.0).
[c]Essen: 7.0 (4.0); Oberhausen 2.0 (3.0); Mülheim: 2.0 (2.0).
[d]Essen: 2.0 (2.0); Oberhausen 0.0 (1.0); Mülheim: 0.0 (1.0).

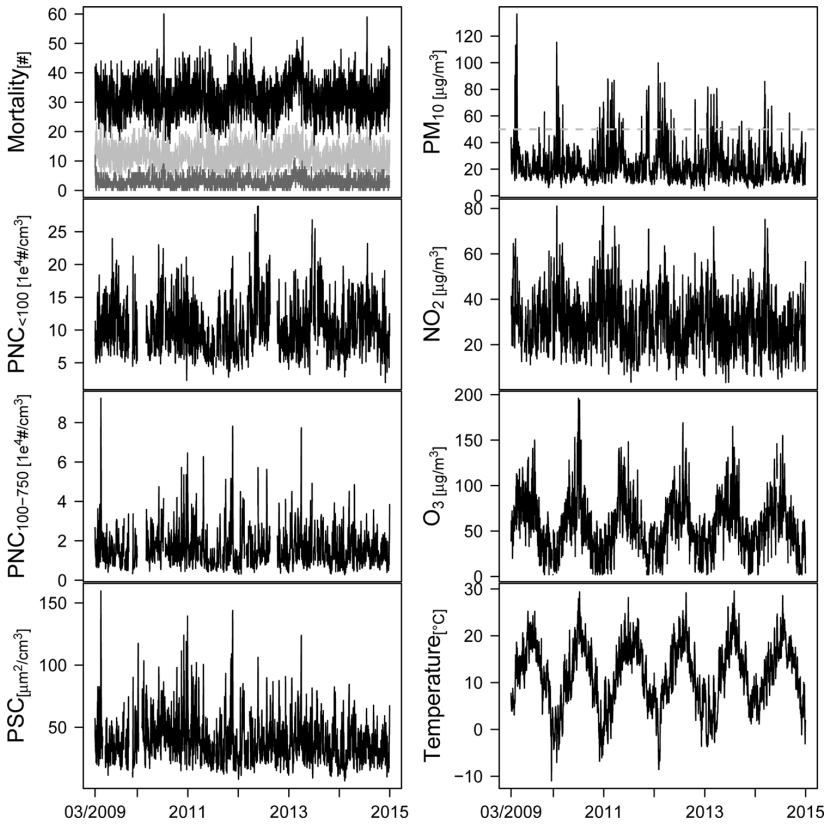

Figure 1. Time series of daily cause-specific mortality (top left panel: natural mortality is shown in black, cardiovascular mortality is shown in gray, and respiratory mortality is shown in dark gray), $PNC_{<100}$, $PNC_{100–750}$, PSC, PM_{10} (top right panel: the dashed horizontal line indicates the 24-h limit of 50 $\mu g/m^3$), NO_2, O_3, and temperature in the Ruhr Area. Note: NO_2, nitrogen dioxide; O_3, ozone; PM_{10}, particulate matter $\leq$10 µm in aerodynamic diameter; $PNC_{<100}$, size-specific particle number concentration of particles <100 nm electrical mobility diameter; $PNC_{100–750}$, PNC of particles with 100–750 nm electrical mobility diameter; PSC, particle surface area concentration.

NO_2 was 29.2 $\mu g/m^3$ (16.2), which was also below the annual limit value of 40 $\mu g/m^3$. The median temperature was 11.9°C (9.9), and relative humidity 78.8% (18.5).

Spearman correlation (r) between air pollutants ranged from −0.39 (for NO_2 and O_3) to 0.99 ($PNC_{100–250}$ and $PNC_{100–750}$) (Table 2; based on data for 1,669 d with complete measurement data for all exposure metrics and pollutants.). $PNC_{<100}$ (UFPs) generally correlated moderately with PSC and NO_2 ($r = 0.63$ and $r = 0.42$), and correlated considerably more weakly with PM_{10} and O_3 ($r = 0.26$ and $r = 0.14$). The smallest size fraction ($PNC_{13.3–30}$) correlated weakly with other particle metrics and pollutants ($0.00 \leq r \leq 0.28$). $PNC_{100–750}$ revealed overall high correlations with the particle metrics PSC ($r = 0.94$) and PM_{10} ($r = 0.74$). $PNC_{100–750}$ correlated slightly weaker with NO_2 than $PNC_{<100}$ ($r = 0.65$), whereas no correlation was observed between $PNC_{100–750}$ and O_3.

Table 2. Correlation coefficients (Spearman r) between exposure metrics and pollutants ($n = 1{,}669$) in the Ruhr Area between March 2009 and December 2014 based on daily-based complete case data for all exposures, $n = 1{,}669$.

	$PNC_{<100}$	$PNC_{100–750}$	$PNC_{13.3–30}$	$PNC_{30–50}$	$PNC_{50–100}$	$PNC_{100–250}$	$PNC_{250–500}$	$PNC_{500–750}$	PSC	PM_{10}	NO_2
$PNC_{<100}$	1										
$PNC_{100–750}$	0.56	1									
$PNC_{13.3–30}$	0.86	0.25	1								
$PNC_{30–50}$	0.92	0.53	0.67	1							
$PNC_{50–100}$	0.79	0.85	0.43	0.82	1						
$PNC_{100–250}$	0.60	0.99	0.28	0.57	0.87	1					
$PNC_{250–500}$	0.27	0.82	0.03*	0.26	0.56	0.74	1				
$PNC_{500–750}$	0.21	0.71	−0.01*	0.21	0.49	0.64	0.9	1			
PSC	0.63	0.94	0.28	0.66	0.90	0.93	0.76	0.68	1		
PM_{10}	0.26	0.74	0.00*	0.28	0.55	0.69	0.82	0.81	0.73	1	
NO_2	0.42	0.65	0.22	0.41	0.57	0.63	0.59	0.58	0.70	0.63	1
O_3	0.14	−0.01*	0.15	0.13	0.06	0.03*	−0.19	−0.25	−0.04*	−0.12	−0.39

*$p > 0.05$, all other $p \leq 0.05$.

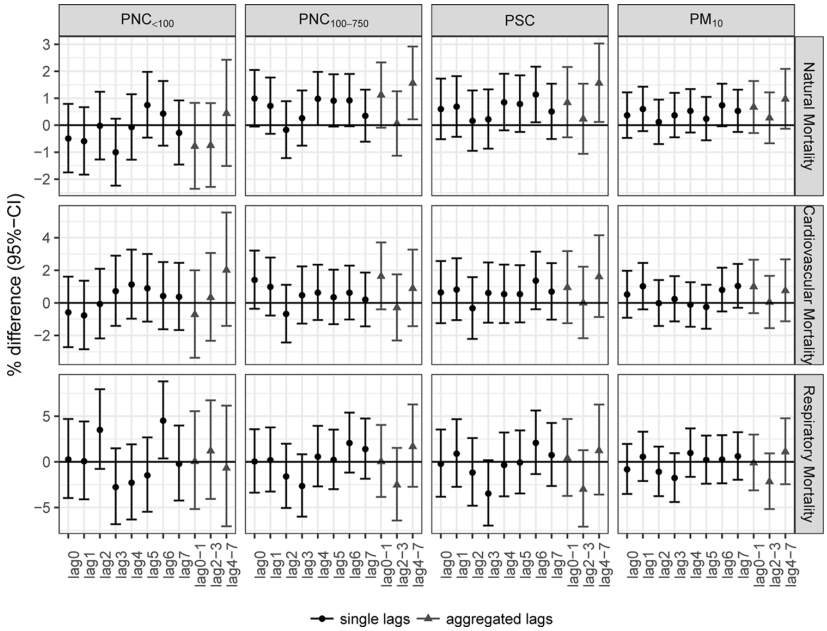

Figure 2. Short-term associations per IQR increase of air pollutant concentration and daily natural and cause-specific mortality in the Ruhr Area between March 2009 and December 2014, estimated for different particle metrics ($PNC_{<100}$, $PNC_{100–750}$, PSC, and PM_{10}) at single-day lags (lag0–lag7) and for aggregated lags (lag0–1, lag2–3, lag4–7) in Poisson regression models, adjusted for time trend, temperature, humidity, day of week, holidays, period of seasonal population decrease, and influenza. (Corresponding numeric data are provided in Table S1.) Note: IQR, interquartile range; NO_2, nitrogen dioxide; PM_{10}, particulate matter ≤10 μm in aerodynamic diameter; $PNC_{<100}$, size-specific particle number concentration of particles <100 nm electrical mobility diameter; $PNC_{100–750}$, PNC of particles with 100–750 nm electrical mobility diameter; PSC, particle surface area concentration.

Main Effects

Estimated associations of exposure with mortality showed different patterns for the different particle metrics and causes of mortality (Figure 2). Overall patterns of $PNC_{100–750}$ and PSC were similar and comparable to those of PM_{10}, showing immediate (lag0–1) and delayed (lag4–7) associations for NM and cardiovascular mortality (CVM) (Figure 2). Point estimates for immediate associations (lag0–1) of $PNC_{100–750}$ were 1.12% (95% CI: −0.09, 2.33) for NM and 1.63% (95% CI: −0.40, 3.71) for CVM (see Table S1), and for more delayed associations (lag4–7) 1.56% (95% CI: 0.22, 2.92) for NM and 0.89% (95% CI: −0.43, 3.27) for CVM (see Table S1). These effect estimates were slightly stronger than those of PM_{10} on an IQR basis with an immediate (lag0–1) increase in NM and CVM of 0.67% (95% CI: −0.29, 1.64) and 0.99% (95% CI: −0.63, 2.65) or a more delayed (lag4–7) increase in NM and CVM of 0.97% (95% CI: −0.13, 2.09) and 0.75 (95% CI: −1.13, 2.67) (Figure 2; see also Table S1). We did not observe clear associations between $PNC_{<100}$ (UFP) and NM or CVM, although the observed pattern suggested a more delayed association (lag4–7) with a slightly higher point estimate of 2.01% (95% CI: −1.41, 5.55), yet estimated less precisely (Figure 2; see also Table S1). For respiratory mortality (RM) we observed comparatively strong single-day associations at lag2 and lag6 with $PNC_{<100}$ of 3.50% (95% CI: −0.77, 7.95) and 4.51% (95% CI: 0.37, 8.81), respectively. However, there were no conclusive patterns linking RM with aggregated lag-exposures of the considered pollutants.

When looking at size-specific associations in more detail (Figure 3; see also Table S2), we observed immediate inverse associations of $PNC_{13.3–30}$ with NM and CVM (−1.81% (95% CI: −3.30, −0.30) and −1.63% (95% CI: −4.16, 0.97), respectively; whereas for lag4–7, the estimate for NM moved close to the null and that for CVM was positive (95% CI: −0.55% (−2.40, 1.34) and 1.43% (95% CI: −1.86, 4.83) respectively). In contrast, patterns for PNC with an electric diameter >50–500 nm pointed to positive immediate (lag0–1) and delayed (lag4–7) associations with NM and CVM, similar to associations of $PNC_{100–750}$, PSC and PM_{10}. Clearest associations were observed for particles of 100–250 and 250–500 nm size and NM. For RM, patterns were less conclusive, yet somewhat different from NM and CVM, indicating only delayed associations with larger particles (electric diameter >250 nm).

Adjustment for Copollutants

Effect estimates for NM and CVM in association with $PNC_{<100}$ and $PNC_{100–750}$ were similar after adjustment for O_3 (Figure 4). In general, effect estimates were mostly robust towards adjustment for PM_{10}, though associations between lag 4–7 $PNC_{<100}$ and NM became more negative. Adjustment for NO_2 on the other hand showed a slightly different pattern: Although effect estimates for UFP on CVM were unaffected by NO_2 adjustment, effect estimates for $PNC_{<100}$ and NM became more negative over all considered lags. Effect estimates for $PNC_{100–750}$ on both NM and CVM were essentially unchanged after NO_2 adjustment. After adjustment for PSC or $PNC_{100–750}$, associations for $PNC_{<100}$ and NM or CVM were similar to those adjusted for NO_2. Associations between $PNC_{100–750}$ and both outcomes at lag0–1 became more positive with adjustment for PSC, whereas the association between $PNC_{100–750}$ and CVM at lag4–7 became negative, although confidence intervals were wide.

Associations between $PNC_{13.3–30}$ and mortality remained unchanged after adjustment for other metrics (see Figure S1),

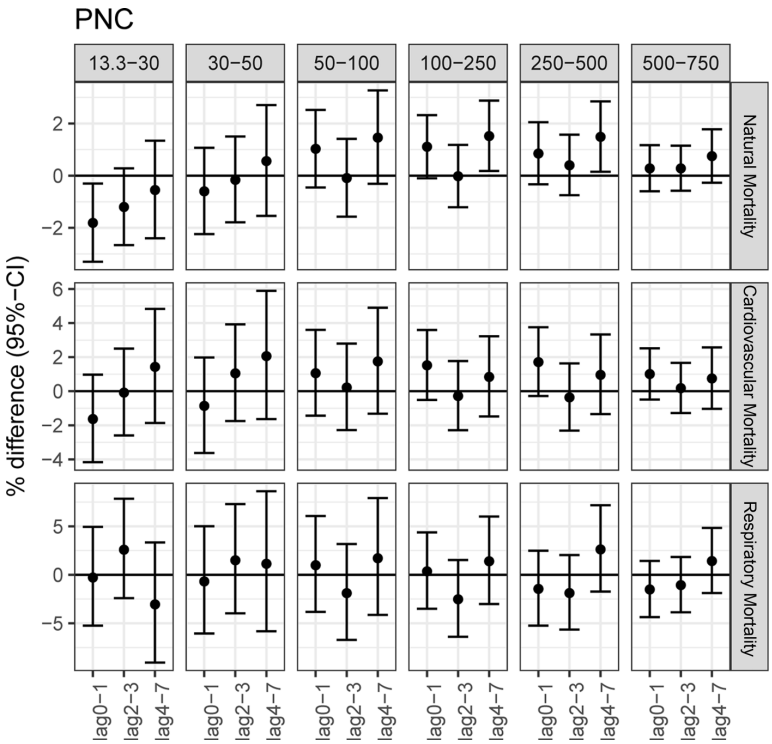

Figure 3. Short-term associations (lag0–1, lag2–3, lag4–7) per IQR increase of size-specific particle number concentrations and daily natural and cause-specific mortality in the Ruhr Area between March 2009 and December 2014, estimated in Poisson regression models, adjusted for time trend, temperature, humidity, day of week, holidays, period of seasonal population decrease, and influenza and presented as percentage differences (95% confidence interval) [% (95% CI)] in mortality. (Corresponding numeric data are provided in Table S2.) IQR, interquartile range.

consistent with expectations given the weak correlations with other pollutants (Table 2).

Effect Modification

Effect modification of associations between fine or ultrafine PNCs and natural or CV mortality were significant only for NM in association with O_3 and $PNC_{<100}$ at lag4–7 (interaction $p = 0.03$), where $PNC_{<100}$ was positively associated with NM when O_3 was below the 75th percentile (1.31%; 95% CI: −0.46, 3.11), and negatively associated with NM when O_3 was high (−1.94%; 95% CI: −4.63, 0.83) (Figure 5; see also Table S3). A similar pattern was observed for CVM in association with high or low O_3 and $PNC_{<100}$ at lag0–1 (interaction $p = 0.03$). We did not observe significant (defined as interaction $p < 0.05$) effect modification by season or higher levels of co-exposure (PM_{10}, NO_2, or PSC) regarding associations between fine or ultrafine PNCs and NM or CVM. However, at lag4–7, point estimates for $PNC_{<100}$ were positive among those with lower levels of PM_{10}, NO_2, and PSC, but closer to the null among those with higher levels of co-exposure (interaction p: 0.17–0.67). Similarly, for NM and CVM, associations with $PNC_{100–750}$ at lag0–1 were stronger for those with higher versus lower levels of PM_{10}, NO_2, and PSC co-exposure (interaction $p = 0.15$–0.72). The effect estimate between lag2–3 $PNC_{<100}$ and CVM was positive during the warmer season (April–September, 2.30%; 95% CI: −1.28, 6.06) but negative during colder months (October–March, −2.07%; 95% CI: −5.44, 1.43; interaction $p = 0.08$).

Discussion

Our findings suggest that short-term exposures to lung-deposited PSC and PNC in the ultrafine (electric mobility diameter <100 nm) and fine (100–750 nm) particle size ranges (especially PNC 50–500 nm), are associated with small increases in daily NM and CVM. Associations suggested immediate (lag0–1) and slightly delayed (lag4–7) effects, and effect estimates were more precise for all NM than for the smaller subset of deaths due to cardiovascular disease. Associations of size-specific PNC were mostly robust to the adjustment for PM_{10} and O_3, and slightly changed when adjusted for NO_2. Effect estimates for $PNC_{100–750}$ and PSC were similar to those observed for PM_{10}, suggesting immediate as well as delayed effects on NM and CVM. Based on an IQR increase in respective exposure concentration, positive associations for PNC in the 50–500 nm range were stronger than positive associations for PM_{10}.

In this study, we were able to investigate size-dependent PNC, including three size fractions in the UFP size range (13.3–30, 30–50, 50–500 nm) and three size fractions in the fine range (100–250, 250–500, 500–750 nm), aiming to identify the most pathogenic size fraction. We observed that the PNC of the smallest size ranges (13.5–50 nm) was inversely associated with natural and cause-specific mortality. This immediate inverse association of UFPs with natural and cause-specific mortality has been observed before in a German time-series study, showing inverse associations at lag1 and lag2, mainly driven by the smallest particle size, yet less pronounced than shown in our results (Stölzel et al. 2007). In contrast to the inverse association

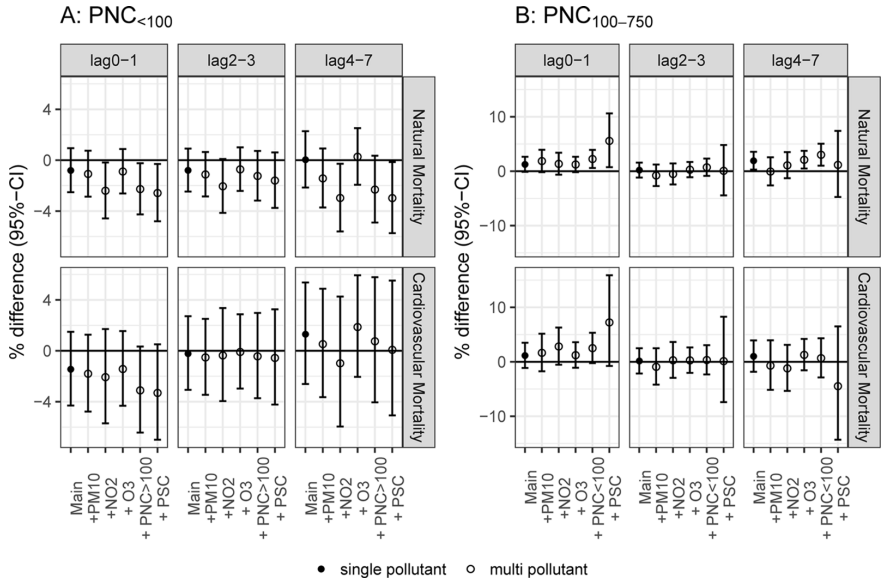

Figure 4. Effect estimates for percentage differences (95% confidence interval) [% (95% CI)] in natural and cardiovascular-specific mortality in the Ruhr Area between March 2009 and December 2014 per IQR increase in (*A*) ultrafine particles ($PNC_{<100}$) and (*B*) fine particles ($PNC_{100–750}$, short: $PNC_{>100}$) for averaged lags (lag0–1, lag2–3, lag4–7), estimated in Poisson regression models, adjusted for time trend, temperature, humidity, day of week, holidays, period of seasonal population decrease, and influenza with additional adjustment for PM_{10}, NO_2, O_3, $PNC_{>100}$ ($PNC_{<100}$), and PSC. Note: IQR, interquartile range; NO_2, nitrogen dioxide; O_3, ozone; PM_{10}, particulate matter ≤10 μm in aerodynamic diameter; $PNC_{<100}$, size-specific particle number concentration of particles <100 nm electrical mobility diameter; $PNC_{100–750}$, PNC of particles with 100–750 nm electrical mobility diameter; PSC, particle surface area concentration.

of the smallest size fraction, we observed positive immediate and delayed associations between UFP with an electric mobility diameter of 50–100 nm and daily mortality, which were similar to associations of other fine particle metrics ($PNC_{100–750}$, PSC, and PM_{10}). Among the fine to submicrometer particle size fractions ($PNC_{100–750}$), particles with an electric mobility diameter from 100 to 250 and 250 to 500 nm revealed the clearest health effect estimates. Moreover, and in contrast to the inverse immediate associations, UFPs indicated delayed associations with CVM, as has been reported by others (Lanzinger et al. 2016; Stafoggia et al. 2017).

Typically, specific size ranges are related to major emission sources. Particles in the nucleation mode (<30 nm) reflect mainly new particles formed by gas-to-particle conversion, including particles originating from gaseous precursors in vehicle exhaust such as NO_2 (Vu et al. 2015). Particles in the Aitken (30–100 nm) and accumulation (100 nm–1 μm) mode with an electric mobility diameter of 30–500 nm contain soot particles from combustion processes, including coal burning power plants, oil combustion, and combustion-engine powered vehicles (Vu et al. 2015). The modal size of vehicle-generated soot particles is in the size range of 100–250 nm (Harrison et al. 2010). Moreover, the particle size fraction 50–250 nm contains diesel exhaust particles, which have been shown to be specifically pathogenic in experimental settings (Mills et al. 2007). Particles from gasoline-powered engines, on the other hand, are typically smaller than diesel soot and mainly form particles <80 nm (Vu et al. 2015). Particles from mechanical abrasion processes such as brake, tire, and road wear are larger and can be found in the accumulation and coarse (>1 μm) mode (Vu et al. 2015). Moreover, accumulation mode particles encompass mostly long-range transported aerosols, whereas nucleation and Aitken mode particles usually have short lifetimes. From a biologic point of view, particles below 50 nm have the highest deposition efficiency, whereas Aitken and specifically accumulation mode particles deposit less efficiently (Kreyling et al. 2006). Moreover, particles below 50 nm contain a higher amount of soluble constituents.

Based on our findings, which show the largest associations for particles sized 50–500 nm, we concluded that primary combustion-generated soot particles might be more harmful than secondary particles formed via nucleation and condensation. This poses the question of whether the PNC in the size range from 50 to 500 nm might actually be a more important metric than the commonly used UFPs, which are defined as particles with a diameter <100 nm.

The repeatedly observed inverse associations for UFP ($PNC_{<100}$) in temperature- and humidity-adjusted models seemed to be driven by the smallest particle size fraction (13.5–30 nm) and remained striking. From a biologic point of view, it seems implausible that the particles contained in the nucleation mode have a true protective effect on mortality. Associations with $PNC_{<100}$ at lag0–1 remained inverse when additionally adjusted for NO_2 and O_3 in separate models, and they could not be explained through any investigated effect modification. In fact, point estimates became even more negative when O_3 was below the 75th percentile.

Most time-series studies on short-term mortality effects of UFPs today have conducted single pollutant analyses. The important question remains, whether the observed effects of ultrafine or any other specific particle size fraction act independently of other pollutants considering that they are sharing potential sources. The answer to this question is of great interest with regard to the regulation of exposure and prevention of adverse health effects. In our study, inverse associations between UFP and natural and cause-specific mortality were robust to adjustment for O_3 or PM_{10}, but tended to move further from the null (i.e., became more negative) with adjustment for NO_2, $PNC_{100–750}$, or PSC. Similar patterns of for UFP-associations have been observed after adjustment for NO_2, and also for $PM_{2.5}$ before (Stafoggia et al. 2017), whereas

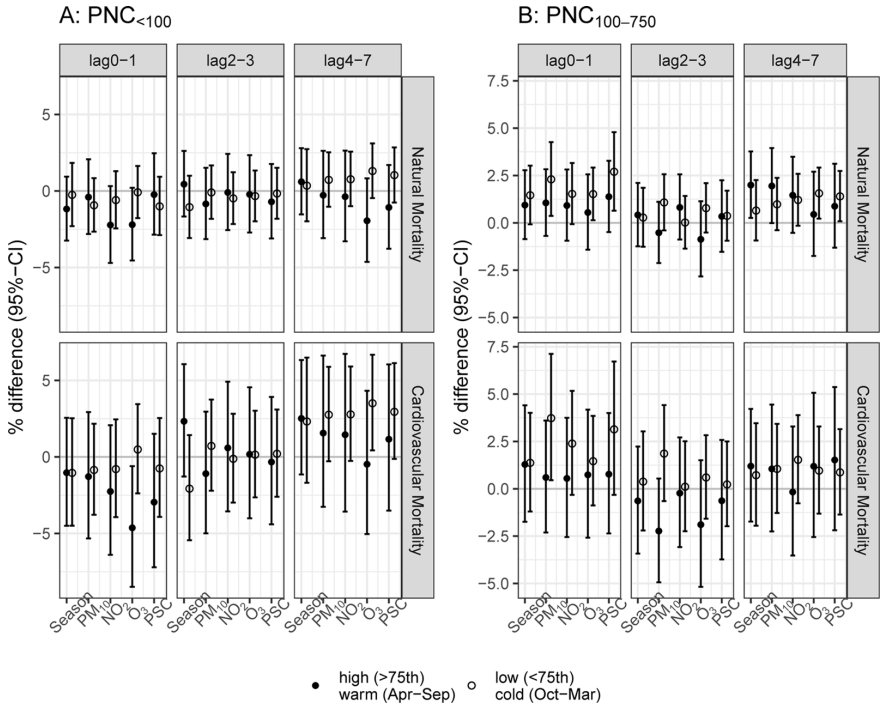

Figure 5. Estimated effect modification by season and copollutants for short-term (lag0–1, lag2–3, lag4–7) percentage differences in natural and cardiovascular mortality based on an IQR increase in the ultrafine particle concentration ($PNC_{<100}$) in the Ruhr Area between March 2009 and December 2014 using Poisson regression models, adjusted for time trend, temperature, humidity, day of week, holidays, period of seasonal population decrease, and influenza. (Corresponding numeric data are provided in Table S3.) Note: IQR, interquartile range; $PNC_{<100}$, size-specific particle number concentration of particles <100 nm electrical mobility diameter; $PNC_{100–750}$, PNC of particles with an electrical mobility diameter between 100 and 750 nm.

others reported associations between prolonged exposure to UFP independent of particle mass exposures (Lanzinger et al. 2016). These contrary findings probably reflect important differences across studies caused by the different mixture of particles and sources due to the region of interest.

The rarely investigated lung-deposited PSC showed similar results as $PNC_{100–750}$ or PM_{10}, namely immediate and delayed associations with NM and CVM. Moreover, PSC correlated highly (>0.7) with PNC of particles sized 50–500 nm, which were the size-classes revealing the most clearly observed (immediate and delayed) health effect estimates.

Despite a strong correlation between $PNC_{100–750}$, PM_{10} and PSC, PSC constitutes an integrated measure of reactive particle surface and deposition efficiency, which serve as a better marker understanding effect mechanisms between the inhalation of particles and health outcomes than solely mass-based or number-based metrics. It has been discussed that particle area surface plays a greater role in oxidative stress and pro-inflammatory effects than particle mass or particle number because the surface is the relevant location for oxidative processes (Hussain et al. 2009). Within this study, however, we were not able to disentangle biological effects of the mass, the number, and the surface of particles.

Season did not affect effect estimates of UFPs in the Ruhr Area consistently in terms of lag-time and cause of mortality, although season clearly affected effect estimates of UFPs on natural and cause-specific mortality and hospital admissions in other European regions (Samoli et al. 2016; Stafoggia et al. 2017). However, in comparison with the Mediterranean climate, the Ruhr Area has a more temperate climate with cool summers and mild and rainy winters, not displaying the strong seasonal pattern observed in Italy or Greece. Overall, we did not observe a consistent pattern among selected effect modifiers regarding associations between fine or ultrafine PNCs and natural or CV mortality.

Overall, our results are in line with results of other time-series studies, showing immediate (lag 0–1) and delayed effects (≥lag 4) of fine particles, while observing more delayed effects of UFPs on natural and cause-specific mortality (Breitner et al. 2009; Ibald-Mulli et al. 2002; Lanzinger et al. 2016; Stafoggia et al. 2017; Stölzel et al. 2007; Wichmann and Peters 2000). One of the first studies on UFPs reported the largest associations between UFPs and nonaccidental mortality for delayed (lag4) exposures in Erfurt, Germany (Wichmann et al. 2000). These results were confirmed in a reanalysis of an extended data base (Breitner et al. 2009; Stölzel et al. 2007). A European study including five cities (Augsburg, Chernovtsy, Dresden, Ljubljana, and Prague) reported an increase in respiratory mortality after 6 d (lag0–5) (Lanzinger et al. 2016). Another European study including eight cities (Helsinki, Stockholm, Copenhagen, Ruhr Area, Augsburg, Rome, Barcelona, and Athens) observed weak delayed associations (lag5–7) with NM and cardiovascular and respiratory mortality (Stafoggia et al. 2017). In contrast, several large multicenter time-series studies on fine particle mass showed primarily immediate effects on daily mortality (HEI 2010; Katsouyanni and Samet 2009; Samoli et al. 2008). Possible biological explanations for these different temporal patterns between size-specific particles could be local inflammation induced by fine particles in the bronchi and lung tissue, which may lead to immediate effects on mortality. In contrast, smaller particles such as UFPs may partly escape pulmonary clearing mechanisms, translocate across biologic

membranes, and gain access to the vasculature and systemic circulation, stimulating systemic inflammatory mechanisms. This process can lead to an increased risk for cardiovascular events after several days. The overall reported delayed associations of UFPs and cardiovascular health seem plausible from this biological perspective. Supporting our findings, Stölzel et al. (2007) reported slightly higher delayed effect estimates with CVM than with NM for the UFPs.

Several limitations should be acknowledged in our study. The most obvious one is the small number of mortality events, limiting the statistical power of our results, especially regarding cause-specific mortality. Moreover, we have fitted several models to estimate adverse health effects of multiple pollutants regarding multiple lags and time windows, yielding a higher possibility of rejecting a null effect. However, in this study we aimed to identify a temporal pattern of different sized particles on the different causes of death instead of focusing on associations of single-day lags. In addition, this study used only one monitor as the reference exposure for three adjacent cities. Although PM_{10} and $PM_{2.5}$ tend to be more homogeneously distributed over wider spatial regions with daily changes primarily dependent on meteorology, daily UFP concentration changes might differ considerably depending on location and local sources, especially in proximity to major roads or highways (Cyrys et al. 2008; Pekkanen and Kulmala 2004). For our study we assumed that the central monitor, placed at an urban background station, properly captured the day-to-day variability relevant for the surrounding population, as was assumed by others as well (Cyrys et al. 2008). Moreover, the high correlation of several exposure metrics limited our power to disentangle individual metric effects. Another limitation includes the lack of daily measurements of $PM_{2.5}$, which has been shown to confound health effects of UFPs (Stafoggia et al. 2017).

The main strength of this study is the consistent exposure assessment throughout the study period of approximately 6 y. Furthermore, the study benefits from an in-depth characterization of particles, with the aim to specifically capture toxicologically important particle characteristics, including size-specific PNC and total lung-deposited PSC, a metric that has rarely been investigated in epidemiological studies to date. Moreover, the measurement site was located next to a routine monitoring site, enabling us to make use of monitored copollutants such as PM_{10}, NO_2, or O_3, which can potentially confound or modify UFP effects on health.

Conclusions

Size-specific PNC (50–500 nm) and lung-deposited PSC indicated an association with NM and CVM in the Ruhr Area, showing immediate (lag0–1) and delayed (lag4–7) effect estimates revealing slightly higher point estimates than these of PM_{10} based on an IQR increase of exposure concentration. Although results from PM, PNC, and PSC could not be disentangled, it might be beneficial to investigate particle number size distributions, which can be linked to emission sources, in addition to the particle mixture captured by the measurement of PM_{10} only. Moreover, PSC could be used as an alternative metric that integrates particle size distribution as well as deposition efficiency. Further investigations are needed to establish the different temporal patterns among different particles sizes and surfaces.

Acknowledgments

We thank the Central statistical and IT services provider of North Rhine-Westphalia (Information und Technik NRW, Düsseldorf, Germany) and the North Rhine-Westphalia State Agency for Nature, Environment and Consumer Protection (Landesamt für Natur, Umwelt und Verbraucherschutz (LANUV) NRW, Essen, Germany) for providing, respectively, mortality and exposure data for the three cities of the Ruhr Area. We also thank D. Sugiri for the data management.

References

Asbach C, Fissan H, Stahlmecke B, Kuhlbusch TAJ, Pui DYH. 2009. Conceptual limitations and extensions of lung-deposited Nanoparticle Surface Area Monitor (NSAM). J Nanopart Res 11(1):101–109, https://doi.org/10.1007/s11051-008-9479-8.

Birmili W, Weinhold K, Rasch F, Sonntag A, Sun J, Merkel M. 2016. Long-term observations of tropospheric particle number size distributions and equivalent black carbon mass concentrations in the German Ultrafine Aerosol Network (GUAN). Earth Syst Sci Data 8(2):355–382, https://doi.org/10.5194/essd-8-355-2016.

Breitner S, Stölzel M, Cyrys J, Pitz M, Wölke G, Kreyling W. 2009. Short-term mortality rates during a decade of improved air quality in Erfurt, Germany. Environ Health Perspect 117(3):448–454, PMID: 19337521, https://doi.org/10.1289/ehp.11711.

Cyrys J, Pitz M, Heinrich J, Wichmann HE, Peters A. 2008. Spatial and temporal variation of particle number concentration in Augsburg, Germany. Sci Total Environ 401(1–3):168–175, PMID: 18511107, https://doi.org/10.1016/j.scitotenv.2008.03.043.

EU (European Commission). 2008. Directive 2008/50/EC of the European Parliament and of the Council of 21 May 2008 on ambient air quality and cleaner air for Europe. Off J Eur Union L 152/1.

Faustini A, Rapp R, Forastiere F. 2014. Nitrogen dioxide and mortality: review and meta-analysis of long-term studies. Eur Respir J 44(3):744–753, PMID: 24558178, https://doi.org/10.1183/09031936.00114713.

Harrison RM, Giorio C, Beddows DCS, Dall'Osto M. 2010. Size distribution of airborne particles controls outcome of epidemiological studies. Sci Total Environ 409(2):289–293, PMID: 21109288, https://doi.org/10.1016/j.scitotenv.2010.09.043.

HEI (Health Effects Institute). 2010. HEI Panel on the Health Effect of Traffic-Related Air Pollution: A Critical Review of the Literature on Emissions, Exposure, and Health Effects. HEI Spec Rep 17. Boston, MA:Health Effects Institute.

HEI Review Panel on Ultrafine Particles. 2013. *HEI Perspectives 3: Understanding the Health Effects of Ambient Ultrafine Particles*. Boston, MA:Health Effects Institute.

Hinds WC. 1999. *Aerosol Technology*. New York, NY:John Wiley & Sons.

Hussain S, Boland S, Baeza-Squiban A, Hamel R, Thomassen LCJ, Martens JA, et al. 2009. Oxidative stress and proinflammatory effects of carbon black and titanium dioxide nanoparticles: role of particle surface area and internalized amount. Toxicology 260(1-3):142–149, PMID: 19464580, https://doi.org/10.1016/j.tox.2009.04.001.

Ibald-Mulli A, Wichmann HE, Kreyling W, Peters A. 2002. Epidemiological evidence on health effects of ultrafine particles. J Aerosol Med 15(2):189–201, PMID: 12184869, https://doi.org/10.1089/089426802320282310.

Katsouyanni K, Samet JM. 2009. Air Pollution and Health: A European and North American Approach (APHENA). Health Effects Institute Research Report 142. Boston, MA:Health Effects Institute.

Kreyling WG, Semmler-behnke M, Möller W. 2006. Health implications of nanoparticles. J Nanopart Res 8(5):543–562, https://doi.org/10.1007/s11051-005-9068-z.

Lanzinger S, Schneider A, Breitner S, Stafoggia M, Erzen I, Dostal M, et al. 2016. Associations between ultrafine and fine particles and mortality in five central European cities - Results from the UFIREG study. Environ Int 88:44–52, PMID: 26708280, https://doi.org/10.1016/j.envint.2015.12.006.

Levy JI, Diez D, Dou Y, Barr CD, Dominici F. 2012. A meta-analysis and multisite time-series analysis of the differential toxicity of major fine particulate matter constituents. Am J Epidemiol 175(11):1091–1099, PMID: 22510275, https://doi.org/10.1093/aje/kwr457.

Mills NL, Törnqvist H, Gonzalez MC, Vink E, Robinson SD, Söderberg S. 2007. Ischemic and thrombotic effects of dilute diesel—exhaust inhalation in men with coronary heart disease. N Engl J Med 357(11):1075–1082, PMID: 17855668, https://doi.org/10.1056/NEJMoa066314.

Morawska L, Thomas S, Jamriska M, Johnson G. 1999. The modality of particle size distributions of environmental aerosols. Atmos Environ 33(27):4401–4411, https://doi.org/10.1016/S1352-2310(99)00217-4.

Noël A, Truchon G, Cloutier Y, Charbonneau M, Maghni K, Tardif R. 2016. Mass or total surface area with aerosol size distribution as exposure metrics for inflammatory, cytotoxic and oxidative lung responses in rats exposed to titanium dioxide nanoparticles. Toxicol Ind Health, PMID: 27256293, https://doi.org/10.1177/0748233716651560.

Oberdörster G. 2000. Toxicology of ultrafine particles: *in vivo* studies. Philos Trans A Math Phys Eng Sci 358(1775):2719–2740, https://doi.org/10.1098/rsta.2000.0680.

Oberdörster G, Oberdörster E, Oberdörster J. 2005. Nanotoxicology: an emerging discipline evolving from studies of ultrafine particles. Environ Health Perspect 113(7):823–839, PMID: 16002369, https://doi.org/10.1289/ehp.7339.

Pekkanen J, Kulmala M. 2004. Exposure assessment of ultrafine particles in epidemiologic time-series studies. Scand J Work Environ Health 30(suppl 2):9–18, PMID: 15487681.

Samoli E, Andersen ZJ, Katsouyanni K, Hennig F, Kuhlbusch TAJ, Bellander T. 2016. Exposure to ultrafine particles and respiratory hospitalisations in five European cities. Eur Respir J ERJ-02108-2015, PMID: 27338189, https://doi.org/10.1183/13993003.02108-2015.

Samoli E, Peng R, Ramsay T, Pipikou M, Touloumi G, Dominici F, et al. 2008. Acute effects of ambient particulate matter on mortality in Europe and North America: results from the APHENA study. Environ Health Perspect 116(11):1480–1486, PMID: 19057700, https://doi.org/10.1289/ehp.11345.

Stafoggia M, Schneider A, Cyrys J, Samoli E, Andersen ZJ, Bedada GB, et al. 2017. Association between short-term exposure to ultrafine particles and mortality in eight European urban areas. Epidemiology 28(2):172–180, PMID: 27922535, https://doi.org/10.1097/EDE.0000000000000599.

Stölzel M, Breitner S, Cyrys J, Pitz M, Wölke G, Kreyling W, et al. 2007. Daily mortality and particulate matter in different size classes in Erfurt, Germany. J Expo Sci Environ Epidemiol 17(5):458–467, PMID: 17108895, https://doi.org/10.1038/sj.jes.7500538.

Verein Deutscher Ingenieure. 2009. Environmental Meteorology - Meteorological Measurements - Air Humidity. Verein Deutscher Ingenieure-Richtlinien 1–14.

Verein Deutscher Ingenieure. 2012. Environmental Meteorology Meteorological Measurements Air Humidity. Verein Deutscher Ingenieure-Richtlinien 1–4.

Vu TV, Delgado-saborit JM, Harrison RM. 2015. Review: particle number size distributions from seven major sources and implications for source apportionment studies. Atmos Environ 122:114–132, https://doi.org/10.1016/j.atmosenv.2015.09.027.

Wang SC, Flagan RC. 1990. Scanning electrical mobility spectrometer. Aerosol Sci Technol 13(2):230–240, https://doi.org/10.1080/02786829008959441.

WHO (World Health Organization Regional Office for Europe). 2013. Review of Evidence on Health Aspects of Air Pollution – REVIHAAP Project, http://www.euro.who.int/__data/assets/pdf_file/0004/193108/REVIHAAP-Final-technical-report-final-version.pdf?ua=1 [accessed 5 February 2018].

Wichmann H, Spix C, Tuch T, Wölke G, Peters A, Heinrich J, et al. 2000. Daily mortality and fine and ultrafine particles in Erfurt, Germany Part I: role of particle number and particle mass. Res Rep Health Eff Inst 87–94, PMID: 11918089.

Wichmann HE, Peters A. 2000. Epidemiological evidence of the effects of ultrafine particle exposure. R Soc 358(1775):2751–2769, https://doi.org/10.1098/rsta.2000.0682.

Environ Health Perspect

DOI: 10.1289/EHP2054

Supplemental Material

Ultrafine and Fine Particle Number and Surface Area Concentrations and Daily Cause-Specific Mortality in the Ruhr Area, Germany, 2009–2014

Frauke Hennig, Ulrich Quass, Bryan Hellack, Miriam Küpper, Thomas A. J. Kuhlbusch, Massimo Stafoggia, and Barbara Hoffmann

Table of Contents

Table S1: Estimated %-differences in daily natural and cause-specific mortality per IQR of air pollutant concentration for particle metrics ($PNC_{\leq 100}$, $PNC_{100\text{-}750}$, PSC, and PM_{10}) at single day lags (0-7) and aggregated lags (0-1, 2-3, 4-7) in the Ruhr area between March 2009 and December 2014, using Poisson regression models, adjusted for time trend, temperature, humidity, day of week, holidays, period of seasonal population decrease and influenza. (Corresponding results are visualized in Figure 2.)

Outcome	Lag	$PNC_{\leq 100}$ IQR=4900.2	$PNC_{100\text{-}750}$ IQR=1060.9	PSC IQR=21.7	PM_{10} IQR=13.3
Natural Mortality	lag0	-0.49 (-1.75, 0.79)	0.99 (-0.05, 2.05)	0.60 (-0.52, 1.73)	0.37 (-0.47, 1.22)
	lag1	-0.59 (-1.83, 0.67)	0.72 (-0.32, 1.77)	0.69 (-0.43, 1.82)	0.60 (-0.22, 1.43)
	lag2	-0.02 (-1.27, 1.24)	-0.17 (-1.22, 0.89)	0.16 (-0.95, 1.29)	0.12 (-0.70, 0.95)
	lag3	-1.00 (-2.24, 0.24)	0.26 (-0.76, 1.29)	0.22 (-0.87, 1.33)	0.37 (-0.45, 1.20)
	lag4	-0.07 (-1.28, 1.15)	0.98 (0.00, 1.98)	0.85 (-0.19, 1.91)	0.53 (-0.27, 1.34)
	lag5	0.75 (-0.46, 1.98)	0.91 (-0.05, 1.89)	0.79 (-0.25, 1.85)	0.24 (-0.56, 1.05)
	lag6	0.43 (-0.76, 1.64)	0.92 (-0.04, 1.90)	1.14 (0.11, 2.17)	0.74 (-0.04, 1.54)
	lag7	-0.28 (-1.46, 0.92)	0.35 (-0.61, 1.32)	0.51 (-0.51, 1.54)	0.53 (-0.25, 1.32)
	lag0-1	-0.78 (-2.36, 0.83)	1.12 (-0.09, 2.33)	0.84 (-0.45, 2.16)	0.67 (-0.29, 1.64)
	lag2-3	-0.75 (-2.29, 0.82)	0.06 (-1.13, 1.26)	0.23 (-1.06, 1.54)	0.27 (-0.67, 1.22)
	lag4-7	0.44 (-1.51, 2.43)	1.56 (0.22, 2.92)	1.56 (0.12, 3.03)	0.97 (-0.13, 2.09)
Cardiovascular Mortality	lag0	-0.58 (-2.72, 1.61)	1.41 (-0.36, 3.21)	0.64 (-1.25, 2.57)	0.52 (-0.91, 1.97)
	lag1	-0.77 (-2.85, 1.36)	0.98 (-0.78, 2.78)	0.82 (-1.06, 2.74)	1.02 (-0.40, 2.45)
	lag2	-0.07 (-2.18, 2.09)	-0.68 (-2.43, 1.11)	-0.33 (-2.21, 1.58)	-0.02 (-1.42, 1.40)
	lag3	0.72 (-1.41, 2.90)	0.47 (-1.27, 2.24)	0.61 (-1.22, 2.48)	0.24 (-1.14, 1.64)
	lag4	1.13 (-0.97, 3.27)	0.63 (-1.05, 2.34)	0.54 (-1.24, 2.35)	-0.11 (-1.47, 1.27)
	lag5	0.90 (-1.15, 3.00)	0.35 (-1.31, 2.04)	0.54 (-1.20, 2.31)	-0.25 (-1.59, 1.11)
	lag6	0.42 (-1.62, 2.51)	0.62 (-1.02, 2.29)	1.36 (-0.39, 3.14)	0.80 (-0.53, 2.16)
	lag7	0.37 (-1.67, 2.46)	0.20 (-1.44, 1.86)	0.69 (-1.03, 2.44)	1.04 (-0.30, 2.39)
	lag0-1	-0.72 (-3.37, 2.00)	1.63 (-0.40, 3.71)	0.94 (-1.25, 3.18)	0.99 (-0.63, 2.65)
	lag2-3	0.33 (-2.33, 3.06)	-0.30 (-2.31, 1.75)	0.00 (-2.17, 2.22)	0.04 (-1.55, 1.66)
	lag4-7	2.01 (-1.41, 5.55)	0.89 (-1.43, 3.27)	1.61 (-0.87, 4.15)	0.75 (-1.13, 2.67)
Respiratory Mortality	lag0	0.27 (-3.96, 4.69)	0.04 (-3.37, 3.57)	-0.21 (-3.82, 3.54)	-0.82 (-3.52, 1.96)
	lag1	0.07 (-4.10, 4.42)	0.19 (-3.26, 3.77)	0.90 (-2.73, 4.67)	0.56 (-2.10, 3.30)
	lag2	3.50 (-0.77, 7.95)	-1.60 (-5.05, 1.98)	-1.17 (-4.80, 2.60)	-1.08 (-3.76, 1.67)
	lag3	-2.76 (-6.83, 1.48)	-2.64 (-6.00, 0.83)	-3.47 (-6.98, 0.17)	-1.76 (-4.40, 0.95)
	lag4	-2.28 (-6.32, 1.92)	0.57 (-2.69, 3.94)	-0.35 (-3.78, 3.21)	0.97 (-1.64, 3.66)
	lag5	-1.48 (-5.47, 2.68)	0.22 (-2.99, 3.53)	-0.07 (-3.46, 3.44)	0.21 (-2.39, 2.88)
	lag6	4.51 (0.37, 8.81)	2.06 (-1.17, 5.39)	2.08 (-1.34, 5.62)	0.25 (-2.35, 2.92)
	lag7	-0.21 (-4.23, 3.98)	1.40 (-1.85, 4.75)	0.74 (-2.65, 4.26)	0.61 (-1.96, 3.25)
	lag0-1	0.04 (-5.17, 5.54)	0.02 (-3.84, 4.04)	0.39 (-3.73, 4.69)	-0.11 (-3.12, 2.99)
	lag2-3	1.20 (-4.06, 6.74)	-2.53 (-6.42, 1.53)	-3.00 (-7.10, 1.27)	-2.17 (-5.17, 0.93)
	lag4-7	-0.68 (-7.06, 6.15)	1.67 (-2.73, 6.28)	1.23 (-3.58, 6.27)	1.10-2.45, 4.77)

Table S2: Estimated %-differences in daily natural and cause-specific mortality per IQR increase in size-specific particle number concentrations ($PNC_{13.3-30}$, PNC_{30-50}, PNC_{50-100}, $PNC_{100-250}$, $PNC_{100-250}$, $PNC_{250-500}$, $PNC_{500-750}$) at aggregated (lags 0-1, 2-3, and 4-7) in the Ruhr area between March 2009 and December 2014, using Poisson regression models, adjusted for time trend, temperature, humidity, day of week, holidays, period of seasonal population decrease and influenza. (Corresponding results are visualized in Figure 3.)

Outcome	Lag	$PNC_{13.3-30}$ IQR=2438.2	PNC_{30-50} IQR=1492.5	PNC_{50-100} IQR=1608.7	$PNC_{100-250}$ IQR=903.2	$PNC_{250-500}$ IQR=180.8	$PNC_{500-750}$ IQR=14.0
Natural Mortality	lag0-1	-1.81 (-3.30, -0.30)	-0.60 (-2.24, 1.07)	1.03 (-0.45, 2.52)	1.11 (-0.10, 2.32)	0.85 (-0.33, 2.05)	0.28 (-0.60, 1.17)
	lag2-3	-1.20 (-2.66, 0.28)	-0.16 (-1.79, 1.50)	-0.09 (-1.57, 1.41)	-0.02 (-1.21, 1.18)	0.40 (-0.75, 1.57)	0.28 (-0.58, 1.15)
	lag4-7	-0.55 (-2.40, 1.34)	0.56 (-1.54, 2.71)	1.46 (-0.31, 3.27)	1.52 (0.18, 2.88)	1.49 (0.15, 2.85)	0.75 (-0.27, 1.78)
Cardiovascular Mortality	lag0-1	-1.63 (-4.16, 0.97)	-0.86 (-3.62, 1.98)	1.06 (-1.43, 3.60)	1.52 (-0.51, 3.59)	1.71 (-0.28, 3.75)	1.01 (-0.49, 2.52)
	lag2-3	-0.08 (-2.59, 2.50)	1.05 (-1.75, 3.92)	0.22 (-2.28, 2.79)	-0.28 (-2.29, 1.77)	-0.36 (-2.31, 1.63)	0.18 (-1.28, 1.66)
	lag4-7	1.43 (-1.86, 4.83)	2.06 (-1.63, 5.89)	1.75 (-1.32, 4.90)	0.84 (-1.48, 3.22)	0.96 (-1.34, 3.33)	0.75 (-1.03, 2.57)
Respiratory Mortality	lag0-1	-0.28 (-5.25, 4.95)	-0.68 (-6.06, 5.01)	0.99 (-3.83, 6.07)	0.36 (-3.50, 4.37)	-1.45 (-5.24, 2.49)	-1.51 (-4.36, 1.43)
	lag2-3	2.59 (-2.41, 7.85)	1.50 (-3.98, 7.29)	-1.89 (-6.71, 3.18)	-2.52 (-6.39, 1.52)	-1.88 (-5.65, 2.04)	-1.06 (-3.87, 1.83)
	lag4-7	-3.05 (-9.05, 3.34)	1.14 (-5.83, 8.62)	1.71 (-4.13, 7.92)	1.40 (-3.01, 6.01)	2.62 (-1.73, 7.17)	1.42 (-1.88, 4.84)

Figure S1: Effect Estimates for %-differences (95%-CI) in Natural-and Cardiovascular-specific mortality in the Ruhr area between March 2009 and December 2014 per IQR increase in ultrafine particles ($PNC_{13.3-30}$), estimated in Poisson regression models, adjusted for time trend, temperature, humidity, day of week, holidays, period of seasonal population decrease and influenza with additional adjustment for PM_{10}, NO_2, O_3, $PNC_{>100}$, and PSC.

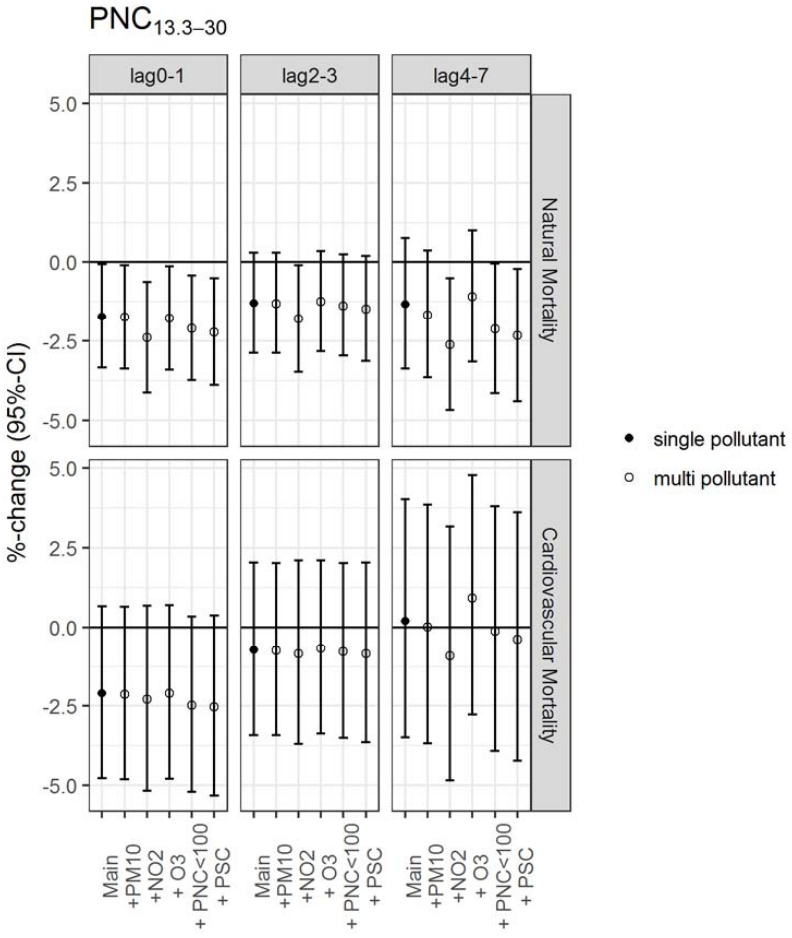

Table S3: Estimated %-differences in daily natural and cause-specific mortality per IQR increase in particle number concentrations ($PNC_{<100}$ and $PNC_{100-750}$) at aggregated (lags 0-1, 2-3, and 4-7) in the Ruhr area between March 2009 and December 2014 considering effect modification presented at group-specific exposure effect estimate [95%-CI] (p-value of the interaction term). (Corresponding results are visualized Figure 5).

Effect Modifier	Natural Mortality		Cardiovascular Mortality	
	$PNC_{<100}$	$PNC_{100-750}$	$PNC_{<100}$	$PNC_{100-750}$
		Lag0-1		
Season				
Oct-Mar	-0.25 [-2.30; 1.84] (p=0.53)	1.46 [-0.08; 3.02] (p=0.67)	-1.04 [-4.49; 2.53] (p=1.00)	1.37 [-1.20; 4.01] (p=0.97)
Apr-Sep	-1.17 [-3.24; 0.94] (p=0.53)	0.94 [-0.86; 2.78] (p=0.67)	-1.03 [-4.50; 2.56] (p=1.00)	1.29 [-1.74; 4.41] (p=0.97)
PM10				
>75th	-0.40 [-2.81; 2.07] (p=0.70)	1.06 [-0.69; 2.83] (p=0.33)	-1.28 [-5.32; 2.93] (p=0.85)	0.60 [-2.31; 3.60] (p=0.15)
≤ 75th	-0.93 [-2.66; 0.84] (p=0.70)	2.30 [0.37; 4.26] (p=0.33)	-0.85 [-3.78; 2.17] (p=0.85)	3.73 [0.45; 7.12] (p=0.15)
NO2				
>75th	-2.22 [-4.70; 0.32] (p=0.26)	0.92 [-0.94; 2.82] (p=0.61)	-2.25 [-6.40; 2.07] (p=0.55)	0.55 [-2.55; 3.75] (p=0.36)
≤ 75th	-0.59 [-2.44; 1.30] (p=0.26)	1.53 [-0.07; 3.16] (p=0.61)	-0.79 [-3.93; 2.45] (p=0.55)	2.39 [-0.32; 5.17] (p=0.36)
O3				
>75th	-2.20 [-4.54; 0.21] (p=0.12)	0.55 [-1.42; 2.56] (p=0.42)	-4.63 [-8.49; -0.60] (p=0.03)	0.74 [-2.58; 4.18] (p=0.72)
≤ 75th	-0.08 [-1.77; 1.64] (p=0.12)	1.52 [0.14; 2.92] (p=0.42)	0.49 [-2.38; 3.45] (p=0.03)	1.46 [-0.88; 3.85] (p=0.72)
PSC				
>75th	-0.23 [-2.85; 2.47] (p=0.61)	1.38 [-0.49; 3.28] (p=0.34)	-2.95 [-7.21; 1.51] (p=0.38)	0.77 [-2.36; 4.00] (p=0.31)
≤ 75th	-1.00 [-2.88; 0.93] (p=0.61)	2.70 [0.64; 4.79] (p=0.34)	-0.75 [-3.92; 2.54] (p=0.38)	3.14 [-0.32; 6.72] (p=0.31)
		Lag2-3		
Season				
Oct-Mar	-1.05 [-3.07; 1.00] (p=0.31)	0.28 [-1.26; 1.85] (p=0.91)	-2.07 [-5.44; 1.43] (p=0.08)	0.38 [-2.20; 3.03] (p=0.60)
Apr-Sep	0.45 [-1.67; 2.62] (p=0.31)	0.42 [-1.24; 2.11] (p=0.91)	2.33 [-1.28; 6.06] (p=0.08)	-0.64 [-3.42; 2.23] (p=0.60)
PM10				
>75th	-0.84 [-3.14; 1.52] (p=0.58)	-0.52 [-2.12; 1.11] (p=0.13)	-1.09 [-4.99; 2.96] (p=0.43)	-2.23 [-4.94; 0.54] (p=0.02)
≤ 75th	-0.09 [-1.82; 1.67] (p=0.58)	1.08 [-0.40; 2.57] (p=0.13)	0.72 [-2.21; 3.75] (p=0.43)	1.86 [-0.65; 4.42] (p=0.02)
NO2				
>75th	-0.09 [-2.55; 2.43] (p=0.78)	0.82 [-0.88; 2.56] (p=0.45)	0.59 [-3.56; 4.92] (p=0.77)	-0.23 [-3.08; 2.71] (p=0.85)
≤ 75th	-0.48 [-2.16; 1.23] (p=0.78)	0.02 [-1.36; 1.42] (p=0.45)	-0.12 [-2.98; 2.82] (p=0.77)	0.11 [-2.24; 2.51] (p=0.85)
O3				
>75th	-0.22 [-2.71; 2.34] (p=0.94)	-0.87 [-2.83; 1.14] (p=0.15)	0.18 [-4.01; 4.55] (p=0.99)	-1.89 [-5.18; 1.51] (p=0.20)
≤ 75th	-0.33 [-1.98; 1.34] (p=0.94)	0.78 [-0.51; 2.10] (p=0.15)	0.15 [-2.64; 3.02] (p=0.99)	0.60 [-1.58; 2.83] (p=0.20)
PSC				
>75th	-0.70 [-3.10; 1.77] (p=0.69)	0.34 [-1.53; 2.25] (p=0.98)	-0.33 [-4.40; 3.92] (p=0.82)	-0.63 [-3.73; 2.58] (p=0.64)
≤ 75th	-0.16 [-1.81; 1.52] (p=0.69)	0.37 [-0.94; 1.70] (p=0.98)	0.21 [-2.60; 3.10] (p=0.82)	0.23 [-1.98; 2.50] (p=0.64)
		Lag4-7		
Season				
Oct-Mar	0.35 [-1.98; 2.74] (p=0.88)	0.65 [-0.93; 2.26] (p=0.26)	2.32 [-1.69; 6.49] (p=0.94)	0.72 [-1.95; 3.46] (p=0.82)
Apr-Sep	0.61 [-1.53; 2.80] (p=0.88)	2.00 [0.26; 3.77] (p=0.26)	2.52 [-1.15; 6.33] (p=0.94)	1.20 [-1.73; 4.22] (p=0.82)
PM10				
>75th	-0.27 [-3.08; 2.63] (p=0.52)	1.95 [-0.01; 3.95] (p=0.41)	1.56 [-3.26; 6.62] (p=0.67)	1.05 [-2.25; 4.45] (p=1.00)
≤ 75th	0.73 [-1.03; 2.53] (p=0.52)	0.98 [-0.39; 2.38] (p=0.41)	2.76 [-0.28; 5.89] (p=0.67)	1.05 [-1.28; 3.43] (p=1.00)
NO2				
>75th	-0.37 [-3.29; 2.64] (p=0.49)	1.46 [-0.53; 3.49] (p=0.83)	1.45 [-3.57; 6.73] (p=0.65)	-0.17 [-3.52; 3.29] (p=0.40)
≤ 75th	0.77 [-0.99; 2.57] (p=0.49)	1.21 [-0.15; 2.59] (p=0.83)	2.78 [-0.26; 5.91] (p=0.65)	1.53 [-0.77; 3.89] (p=0.40)
O3				
>75th	-1.94 [-4.63; 0.83] (p=0.03)	0.45 [-1.75; 2.70] (p=0.39)	-0.47 [-5.04; 4.32] (p=0.13)	1.19 [-2.55; 5.07] (p=0.92)
≤ 75th	1.31 [-0.46; 3.11] (p=0.03)	1.56 [0.22; 2.92] (p=0.39)	3.51 [0.43; 6.68] (p=0.13)	0.96 [-1.31; 3.29] (p=0.92)
PSC				
>75th	-1.07 [-3.77; 1.70] (p=0.17)	0.88 [-1.31; 3.12] (p=0.68)	1.16 [-3.51; 6.05] (p=0.51)	1.52 [-2.19; 5.37] (p=0.76)
≤ 75th	1.04 [-0.75; 2.85] (p=0.17)	1.40 [0.08; 2.74] (p=0.68)	2.95 [-0.13; 6.13] (p=0.51)	0.87 [-1.36; 3.15] (p=0.76)

4 Investigation of air pollution and noise on progression of thoracic aortic calcification: results of the Heinz Nixdorf Recall Study. Hennig F, Moebus S, Reinsch N, Budde T, Erbel R, Jöckel KH, et al. Eur J Prev Cardiol 0:1–9 (2019)

European Journal of Preventive Cardiology

ESC European Society of Cardiology

Full research paper

European Journal of Preventive Cardiology
0(00) 1–10


Article reuse guidelines:
sagepub.com/journals-permissions
DOI: 10.1177/2047487319854818
journals.sagepub.com/home/ejpc


Investigation of air pollution and noise on progression of thoracic aortic calcification: results of the Heinz Nixdorf Recall Study

Frauke Hennig[1], Susanne Moebus[2], Nico Reinsch[3,4], Thomas Budde[3], Raimund Erbel[2], Karl-Heinz Jöckel[2], Nils Lehmann[2], Barbara Hoffmann[1] and Hagen Kälsch[3,4]; on behalf of the Heinz Nixdorf Recall Study Investigative Group

Abstract

Aims: Air pollution and noise are potential risk factors for subclinical atherosclerosis. Longitudinal analyses, especially on the interplay of these environmental factors, are scarce and inconsistent. Hence we investigated long-term traffic-related exposure to air pollution and noise with the development and progression of thoracic aortic calcification, a marker of subclinical atherosclerosis.

Methods: We used baseline (2000–2003) and follow-up (2006–2008) data from the German Heinz Nixdorf Recall cohort study, including 4814 middle-aged adults. Residence-based air pollution ($PM_{2.5}$ (aerodynamic diameter $\leq 2.5\,\mu m$), PM_{10}, nitrogen dioxide and particle number), and noise was assessed with dispersion models. Thoracic aortic calcification was quantified from non-contrast enhanced electron beam computed tomography. The presence and extent of thoracic aortic calcification progression were analysed with multiple logistic and linear regression models, respectively, adjusting for age, sex, lifestyle variables, socioeconomic status and respective co-exposure.

Results: We observed no association in the full study sample ($n = 3155$, mean age 59.1 ($\pm$7.6) years, 52.8% women). While an interquartile range in particle number and night-time noise yielded odds ratios of 1.20 (1.03, 1.40) and 1.21 (1.00, 1.46) for binary thoracic aortic calcification progression, and 0.02 (–0.01, 0.05) and 0.04 (0.00, 0.07) higher growth rates of thoracic aortic calcification in participants with baseline thoracic aortic calcification less than 10, negative findings were observed in those with baseline thoracic aortic calcification of 10 or greater. Results were similar for other pollutants and daytime noise.

Conclusion: Our study shows no overall associations. Subgroup analyses suggest independent associations of traffic-related air pollution and noise with the development and progression of subclinical atherosclerosis in participants with no or minor thoracic aortic calcification at baseline, in contrast to negative findings in those with advanced calcification.

Keywords

Atherosclerosis, epidemiology, air pollution, traffic noise

Received 11 March 2019; accepted 14 May 2019

Introduction

Environmental factors like air pollution and noise are associated with a higher risk of cardiovascular disease (CVD).[1–4] Moreover, noise was identified as an independent contributor to health risks in the context of air pollution,[5] while partly sharing similar sources and health effect mechanisms. One potential pathway linking both exposures to CVD includes a stress response

[1]Institute of Occupational, Social and Environmental Medicine, Heinrich-Heine University Düsseldorf, Germany
[2]Institute of Medical Informatics, Biometry and Epidemiology, University of Duisburg-Essen, Germany
[3]Alfried Krupp Hospital Essen, Department of Cardiology, Germany
[4]Medical Department, University Witten/Herdecke, Germany

Corresponding author:
Frauke Hennig, Institute of Occupational, Social and Environmental Medicine, Centre for Health and Society Medical Faculty, Heinrich-Heine-University Düsseldorf, POB 10 10 07, 40001 Düsseldorf, Germany.
Email: frauke.hennig@gmail.com

inducing inflammatory cascades, followed by vascular dysfunction or damage,[1,3] potentially developing into atherosclerosis, the underlying pathology for most CVD.[6] Another pathway specifically important for noise is sleep disturbance, which can influence cardiometabolic functions through decreased leptin secretion, potentially increasing appetite, obesity and impaired glucose tolerance.[7]

Correlating well with other markers of subclinical atherosclerosis, thoracic aortic calcification (TAC) independently predicts cardiovascular events and has a higher prevalence among middle-aged adults than coronary artery calcification (CAC).[8,9] It is therefore well suited for quantitative longitudinal analyses in middle-aged populations. Current epidemiological evidence on the association of traffic-related environmental exposures and the atherosclerotic burden remains inconclusive and is almost exclusively limited to air pollution effects. The majority of cross-sectional studies reported positive associations of air pollution on various markers of atherosclerosis, including carotid intima media thickness, CAC, abdominal aortic calcification (AAC), TAC and the ankle–brachial index;[10–14] however, evidence from longitudinal analysis is scarce. While a linear exposure-response for $PM_{2.5}$ (aerodynamic diameter $\leq 2.5\,\mu m$) and the progression of CAC was observed in the prospective Multi-Ethnic Study of Atherosclerosis (MESA) cohort,[13] the analysis of the Framingham Study did not support associations of living close to a major road or $PM_{2.5}$ exposure with the presence or extent of CAC, TAC or AAC progression.[15,16]

Road traffic noise has rarely been investigated in the context of air pollution and our previous cross-sectional investigation supported independent associations of air pollution and noise on TAC.[17] However, it remains unclear whether high air pollution exposure enhances the effect of noise on the cardiovascular system and vice versa.

Therefore, we expanded our previous work, investigating potential synergistic associations of long-term exposure to air pollution and noise, on the development and progression of TAC in a German, well-characterised, population-based cohort.

Methods

Study design

We used data from the baseline (t0: 2000–2003) and first follow-up (t1: 2006–2008) examination of the Heinz Nixdorf Recall (Risk Factors, Evaluation of Coronary Calcification, and Lifestyle; HNR) study, a population-based cohort study, initially including 4814 participants between 45 and 75 years of age, selected randomly from the mandatory population registries (age-stratified sampling), from three adjacent cities (Mülheim, Essen and Bochum) in the metropolitan Ruhr area, Germany, of which 4157 participated in the t1 examination. Traditional cardiovascular risk factors, demographics and addresses were assessed at both examinations using self-administered questionnaires, face-to-face interviews, clinical examinations and comprehensive laboratory tests according to standard protocols.[18] This study complies with the Declaration of Helsinki, all participants (or their legally authorised representative) provided written informed consent and the study was approved by the institutional ethics committees. The study design has been described in detail elsewhere.[19]

Thoracic aortic calcification

Computed tomography (CT) scans were performed for quantification of TAC at both examinations, using a C-100 (t0) and C-150 (t1) scanner (GE, Imatron, South San Francisco, CA, USA), following a standardised methodology for acquisition and interpretation of the scans, which has been reported previously.[18,19]

The CT was operated in the single-slice (3 mm) mode with an image acquisition time of 100 ms. Based on the Agatston algorithm,[20] TAC was quantified, including at least four contiguous pixels with a CT density of 130 or greater Hounsfield units for identifying calcified lesions. TAC was assessed by summation of all calcified lesions in the ascending (ATAC) and descending (DTAC) thoracic aorta visible in the CT scan.[9] While the aortic root was included, the aortic arch and the intrarenal abdominal aorta were excluded in the scan. TAC progression (yes/no) was operationalised as $TAC_{t1} - TAC_{t0} > 0$. Due to its exponential nature, the extent of TAC progression was operationalised as a growth rate of TAC, defined as $\left(\frac{\log(TAC_{t1}+1)-\log(TAC_{t0}+1)}{\text{years of follow-up}}\right)$.[21,22]

Air pollution

Long-term exposure to ambient air pollution, including PM with an aerodynamic diameter less than 10 or 2.5 μm (PM_{10} and $PM_{2.5}$ ($\mu g/m^3$)), particle number of accumulation mode particles (PN_{acc} (#/mL)) and nitrogen dioxide (NO_2 ($\mu g/m^3$)), was estimated using the validated European air pollution dispersion chemistry transport model (EURAD-CTM).[23,24] The EURAD-CTM uses input data from official emission inventories (i.e. traffic, industry, agriculture, energy production, etc.),[25] data on meteorology and regional topography, in combination with input on the dispersion of emissions, chemical reactivity and mass transport between horizontal strata and deposition to calculate daily exposure concentrations in a 1×1 km^2 grid[24] during

the examination years (2000–2003 and 2006–2008), which were assigned to participant' baseline and follow-up addresses using a geographical information system. Since exposure data from 2004–2005 was not available, long-term exposure was calculated as the mean of all daily values over both examination periods, reflecting long-term spatial exposure differences within our study area.

Road traffic noise

Long-term road traffic noise was modelled for the year 2007 according to the European Union Directive 2002/49/EC[26] and the validated national calculation method VBUS/RLS-90[2,7] for the year 2007 (supplied from the city administrations) considering small-scale topography of the area, dimensions of buildings, noise barriers, first order reflections, street axis, measured or estimated vehicle type-specific traffic density for all roads, speed limit and type of street surface. Average traffic noise values (A-weighted dB(A)) day-evening-night (24 hour) noise (L_{den}) and night-time noise (L_{night}, 22:00–06:00 hours) were estimated using the most exposed façade of participants' residences with a resolution of 0.1 dB.

Covariates

We classified education according to the international standard classification of education as total years of formal education grouped into four categories (<11, 11–13, 13–17 and > 17 years). Neighbourhood socioeconomic status was assessed as the unemployment rate (%). Smoking status defined current smoker (during the past year), ex-smoker and never-smoker. Lifetime cumulative smoking was assessed in pack-years at baseline. Exposure to environmental tobacco smoke (ETS) referred to ETS at home, at work or in other places. Body mass index (BMI; kg/m^2) was calculated using standardised height and weight measurements. Regular physical activity (yes/no) and alcohol intake (0, 1–3, 4–6, > 6 drinks per week) was assessed by questionnaire. High-density lipoprotein (HDL) and low-density lipoprotein (LDL) cholesterol, and high sensitivity C-reactive protein (hs-CRP) (all mg/dL) were measured with standard methods at the central laboratory of the University Hospital of Essen. Current medications were coded according to the anatomical therapeutic chemical classification index.[28] Blood pressure values were calculated as the mean of the second and third measurement of three measurements, using an oscillometric method according to a standard protocol. Hypertension was defined as systolic or diastolic blood pressure of 140 mmHg or greater or 90 mmHg or greater, respectively, or the use of antihypertensive medication. Diabetes mellitus was defined as a prior physician diagnosis of diabetes, anti-diabetic drug intake, a random blood glucose of 200 mg/dl or greater, or a fasting blood glucose of 126 mg/d or greater. Coronary artery disease (CAD) was defined by coronary artery bypass surgery and/or interventional revascularisation procedures and/or a history of prior myocardial infarction.

Statistical analyses

To assess the association between traffic-related continuous exposures and TAC progression we estimated: (a) odds ratios (ORs) (95% confidence intervals (CIs)) for having more TAC after 5 years using logistic regression; and (b) the change of growth rate in TAC (to be interpreted as a yearly change in percentage points, presented as a decimal number) using linear regression with respect to an interquartile range (IQR) of exposure. Because prior analyses have shown stronger associations of environmental risk factors and early atherosclerosis,[27,29,30] and our prior analysis has identified 10 as a cut-point for CAC,[30] we stratified the study population by baseline TAC value ($TAC_{t0} < 10$ vs. $TAC_{t0} \geq 10$). In a sensitivity analysis, we estimated ORs for incident TAC and change in growth rate among participants with $TAC_{t0} > 0$. Because prior analysis on TAC progression has shown a different susceptibility of segments of the thoracic aorta with regard to risk factors,[22] we also investigated ATAC and DTAC separately. The confounder-adjusted (main) model included age, sex, smoking status, pack-years of smoking, ETS, physical activity and follow-up time.

To investigate the interplay of air pollution and noise, we (a) estimated exposure effects adjusting for the respective co-exposure to evaluate potential confounding; (b) investigated effect modification including interaction terms between exposure and dichotomised co-exposure at the 75th percentile (low/high); and (c) investigated possible synergisms between co-exposures categorising participants into four groups based on the 75th percentile of each exposure: high air pollution and low noise, low air pollution and high noise, high exposure to both, and low exposure to both as a reference.

Sensitivity analysis

We evaluated the robustness of our main results with regard to additional covariates (neighbourhood unemployment rate, city and intake of statin or lipid-lowering medication). Moreover, we adjusted for hypothesised intermediates (systolic blood pressure, hypertension, hs-CRP and type 2 diabetes mellitus)[1] and (BMI and LDL-cholesterol/HDL-cholesterol (ratio), which have recently been discussed as potential

intermediates, especially regarding the health effects of noise).[31] We estimated ORs for TAC progression, defined as an absolute change greater than 10% and greater than 20% of the baseline value considering a potential mean interscan variability of 9.7%.[32] In this context, we also repeated the main analysis, excluding extreme outliers of TAC change (growth rate- > median + 3 IQR or < median − 3 IQR). Moreover, we restricted our sample to those less prone to exposure misclassification, namely those that have not moved within 5 years prior to the baseline examination and those that did not work full time. In addition, we repeated the analysis in never-smokers and those without incident statin medication. Finally, we investigated baseline and follow-up exposure separately.

Results

The study sample consisted of 3155 (52.8% women) participants, after excluding subjects with prior CAD, missing data on exposure, TAC measurements and covariates (Supplementary Figure 1). Participants were on average 59.1 (±SD 7.6) years old at baseline, well educated, mostly never smokers and slightly overweight (Table 1). Participants with $TAC_{t0} < 10$ ($n = 1433$) included more women, drank less alcohol and had a lower cardiac risk profile (overall Framingham risk score and its components) than those with $TAC_{t0} \geq 10$ ($n = 1722$).

TAC progression was observed in 53.0% with a mean (exponential) annual growth rate of $0.1 \pm$ SD 0.5 (equivalent to a 10% annual increase) (Table 1, Supplementary Figure 2), based on a median Agatston score of 15.5 (IQR 0.0–108.4) at t0 and 28.9 (0.0–306.5) at t1. Incident TAC was observed in 42.5% of 1171 participants.

Exposure concentrations were approximately normally distributed (Supplementary Figure 3) with mean (±SD) concentrations of 20.2 (±2.6) $\mu g/m^3$ PM_{10}, 16.7 (±1.2) $\mu g/m^3$ $PM_{2.5}$, 3399 (±382) #/mL PN_{acc}, 39.4 (±4.0) $\mu g/m^3$ NO_2, 53.9 (±9.3) dB(A) L_{den} and 45.0 (±9.1) dB(A) for L_{night}. Air pollution and noise correlated weakly (Table 2).

Association of traffic-related exposures with TAC progression

While observing no associations of PM_{10}, $PM_{2.5}$, PN_{acc}, NO_2 or noise with the presence or extent of TAC progression in the full study sample, results from participants with $TAC_{t0} < 10$ suggested exposure-related effects on the presence and degree of TAC progression (Figure 1, Supplementary Tables 1 and 2). In contrast, associations were negative for participants with $TAC_{t0} \geq 10$ (Figure 1).

Associations with the presence of TAC progression were strongest for PN_{acc} and L_{night}. For example, a 520 #/mL (IQR) increase in PN_{acc} yielded estimated ORs (95% CIs) of 1.03 (0.92, 1.14) for all participants, 1.20 (1.03, 1.40) for participants with $TAC_{t0} < 10$ and 0.90 (0.77, 1.04) for participants with $TAC_{t0} \geq 10$. Similarly, a 13.7 dB(A) increase in L_{night}, yielded estimated ORs (95% CIs) of 0.96 (0.85, 1.08), 1.15 (0.97, 1.37) and 0.80 (0.67, 0.95) for all participants, participants with $TAC_{t0} < 10$ and $TAC_{t0} \geq 10$ respectively (Figure 1, Supplementary Table 1). Defining TAC progression as a 10% or 20% change from TAC_{t0} did not affect the results (Supplementary Figure 4).

A similar pattern was observed for the TAC growth rate with strongest associations for IQR increases in $PM_{2.5}$ and L_{night}, yielding changes in TAC growth rates of 0.03 (0.00, 0.07) and 0.04 (0.00, 0.07) in participants with $TAC_{t0} < 10$, whereas negative associations were observed in those with $TAC_{t0} \geq 10$ (–0.06 (–0.08, –0.03) and –0.04 (–0.06, –0.01)) (Figure 1, Supplementary Table 2). For a subject with $TAC_{t0} = 5$ and an expected growth rate of 0.3, a 0.03 estimated increase in growth rate translates to a TAC score of $26.03 = 5 \times \exp(0.33 \times 5)$ instead of $22.41 = 5 \times \exp(0.30 \times 5)$.

Estimated ORs (95% CIs) for incident TAC were 1.19 (1.00, 1.41) and 1.21 (1.00, 1.46) for PN_{acc} and for $L_{night,}$ respectively (Supplementary Table 1), while negative changes in the growth rate were observed in participants with $TAC_{t0} \geq 0$ (–0.01 (–0.04, 0.01) and –0.03 (–0.06, –0.01)) (Supplementary Table 2).

The results were overall robust with regard to the extended adjustment and to potential intermediates such as hypertension, BMI or diabetes mellitus (Supplementary Figure 5). The only exception was adjustment for city enhancing effect estimates. Although not observing a clear pattern for separate segments of the thoracic aorta, noise seemed to be more strongly related to ATAC, while air pollutants seemed slightly more strongly related to DTAC (Supplementary Tables 1 and 2). Excluding outliers and further subgroup-specific sensitivity analysis overall supported our main results (Supplementary Tables 3 and 4). Restriction to never-smokers yielded slightly stronger effect estimates, particularly regarding PN_{acc}. Investigations of single baseline and follow-up air pollution exposure revealed similar results.

Interplay of air pollution and noise

Associations between air pollutants and TAC progression were not confounded or modified by co-exposure to noise and vice versa (Figure 2, Supplementary Table 5). Overall, we also did not find evidence for synergetic

Table 1. Baseline characteristics (mean ± SD, *N* (%)) of the full study sample ($n = 3155$) and stratified in subgroups of $TAC_{t0} < 10$ ($n = 1433$) and $TAC_{t0} \geq 10$ ($n = 1722$).

Variable	All	$TAC_{t0} < 10$	$TAC_{t0} \geq 10$	*P* value[a]
TAC (t0) (Agatston score)[b]	15.5 (108.4)	0.0 (0.0)	90.5 (239.8)	<0.001
TAC (t1) (Agatston score)[b]	28.9 (306.5)	0.0 (34.5)	168.1 (743.2)	<0.001
Incident TAC[c]	498 (42.5%)	498 (42.5%)		
TAC progression	1672 (53%)	594 (41.5%)	1078 (62.6%)	<0.001
TAC growth (rate)	0.1 ± 0.5	0.3 ± 0.5	–0.1 ± 0.4	<0.001
Age (years)	59.1 ± 7.6	56.4 ± 7.0	61.4 ± 7.4	<0.001
Sex				0.001
Male	1490 (47.2%)	631 (44.0%)	859 (49.9%)	
Female	1665 (52.8%)	802 (56.0%)	863 (50.1%)	
Education				0.003
≤10 years	302 (9.6%)	111 (7.7%)	191 (11.1%)	
11–13 years	1795 (56.9%)	820 (57.2%)	975 (56.6%)	
14–17 years	701 (22.2%)	319 (22.3%)	382 (22.2%)	
≥18 years	357 (11.3%)	183 (12.8%)	174 (10.1%)	
Neigbourhood unemploymentrate (%)	12.4 ± 3.4	12.5 ± 3.4	12.4 ± 3.4	0.501
Smoking status				0.354
Never smoker	1411 (44.7%)	651 (45.4%)	760 (44.1%)	
Ex-smoker	1043 (33.1%)	455 (31.8%)	588 (34.1%)	
Current smoker	701 (22.2%)	327 (22.8%)	374 (21.7%)	
Packyears (years)	19.5 (28.3)	17.0 (26.0)	21.0 (29.4)	<0.001
ETS	1099 (34.8%)	541 (37.8%)	558 (32.4%)	0.002
Regular physical activity	1379 (43.7%)	606 (42.3%)	773 (44.9%)	0.153
BMI (kg/m^2)	27.6 ± 4.3	27.2 ± 4.4	28.0 ± 4.2	<0.001
LDL (mg/dl)	146.3 ± 35.7	141.3 ± 34.4	150.5 ± 36.2	<0.001
HDL (mg/dl)	59.3 ± 17.3	60.1 ± 17.4	58.6 ± 17.2	0.014
Alcohol consumption				0.049
Never	1519 (48.1%)	683 (47.7%)	836 (48.5%)	
1–3 drinks/week	490 (15.5%)	246 (17.2%)	244 (14.2%)	
>3–6 drinks/week	348 (11%)	166 (11.6%)	182 (10.6%)	
>6–14 drinks/week	412 (13.1%)	182 (12.7%)	230 (13.4%)	
>14 drinks/week	386 (12.2%)	156 (10.9%)	230 (13.4%)	
Intake of statins at baseline[c]	213 (7.2%)	59 (4.5%)	154 (9.3%)	<0.001
Incident statin use[c]	348 (11.8%)	114 (8.7%)	234 (14.2%)	<0.001
Incident lipid-lowering meds[c]	375 (12.7%)	131 (10.0%)	244 (14.8%)	<0.001
Framingham risk[c]				<0.001
Low	1713 (54.6%)	931 (65.5%)	782 (45.7%)	
Medium	1014 (32.3%)	392 (27.6%)	622 (36.3%)	
High	408 (13%)	99 (7.0%)	309 (18.0%)	
Prevalent hypertension[c]	1677 (53.2%)	631 (44.1%)	1046 (60.7%)	<0.001
Incident hypertension[c]	524 (35.5%)	241 (30.1%)	283 (41.9%)	<0.001
Type 2 diabetes	364 (11.5%)	125 (8.7%)	239 (13.9%)	<0.001
Incident type 2 diabetes	240 (8.6%)	103 (7.9%)	137 (9.2%)	0.225
Incident CAD[c]	99 (3.1%)	25 (1.7%)	74 (4.3%)	<0.001

[a]*t*-test: Wilcoxon test or χ^2 independence test.
[b]Median (interquartile range).
[c]Additional missing observations.

Table 2. Summary statistics and Pearson correlation coefficients for traffic-related long-term exposures for 3155 participants of the Heinz Nixdorf Recall Study.

Exposure	Mean ± SD	IQR	$PM_{2.5}$	PN_{acc}	NO_2	L_{den}	L_{night}
PM_{10} ($\mu g/m^3$)[a]	20.2 ± 2.6	3.8	0.81	0.76	0.57	0.21	0.23
$PM_{2.5}$ ($\mu g/m^3$)[b]	16.7 ± 1.2	2.0		0.69	0.69	0.10	0.14
PN_{acc} (#/mL)[c]	3399 ± 382	520			0.69	0.20	0.21
NO_2 ($\mu g/m^3$)[d]	39.4 ± 4.0	5.3				0.18	0.21
L_{den} (dB(A))[e]	53.9 ± 9.3	14.4					0.99
L_{night} (dB(A))[f]	45.0 ± 9.1	13.7					1.00

PM_x: particulate matter with an aerodynamic diameter < x μm; PN_{acc}: particle number of accumulation mode particles; NO_2: nitrogen dioxide; L_{den}: day-evening-night noise; L_{night}: night-time noise; IQR: interquartile range.
[a]PM10: particulate matter with an aerodynamic diameter <10 μm.
[b]PM2.5: particulate matter with an aerodynamic diameter < 2.5 μm.
[c]PNacc: particle number of accumulation mode particles.
[d]NO2: nitrogen dioxide
[e]Lden: day-evening-night noise.
[f]Lnight: night-time noise; IQR: interquartile range.

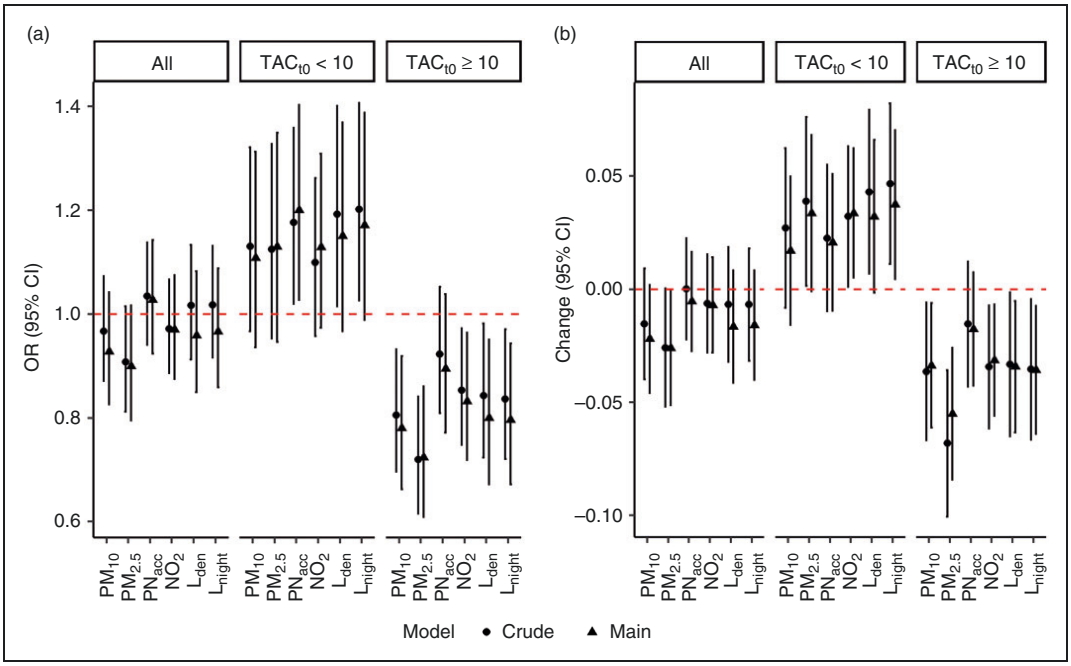

Figure 1. Crude and main effect estimates (95% confidence interval) per interquartile range (IQR) exposure increase on thoracic aortic calcification (TAC) progression in the Heinz Nixdorf Recall study sample and stratified by TACt0, adjusted for age, sex, smoking, physical activity, alcohol consumption, education and follow-up years. (a) Odds ratios (ORs) for TAC progression; (b) change of TAC growth rate. Complementing numbers are presented in Supplementary Tables 1 and 2.

effects of air pollution and noise levels (Supplementary Figure 6, Supplementary Table 6).

Discussion

In the full study sample our study shows no association of long-term exposure to both air pollution and road traffic noise, with the development and progression of TAC. However, a subgroup analysis of participants with no or only minor calcification at baseline suggests independent associations of long-term exposure to both air pollution and road traffic noise with the development and progression of TAC, while a lower risk was observed in those with advanced baseline calcification.

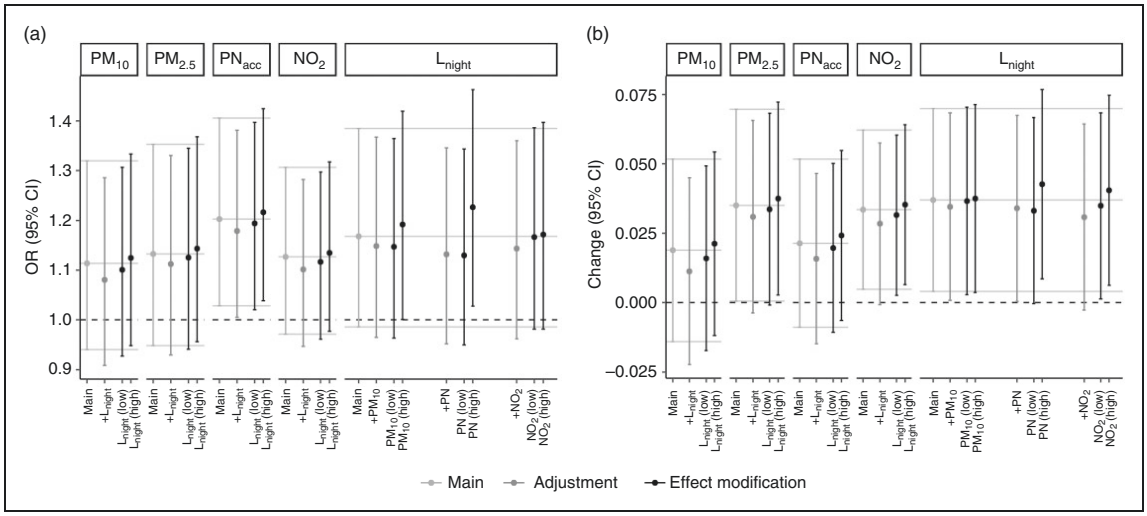

Figure 2. Effect estimates (95% confidence intervals) per interquartile range (IQR) exposure increase on thoracic aortic calcification (TAC) progression in participants with TACt0 < 10: co-exposure adjustment (dark grey) and effect modification (black). (a) TAC progression; (b) change of TAC growth rate. Models are adjusted for age, sex, smoking, alcohol consumption, physical activity, education and follow-up time. Complementing numbers are presented in Supplementary Table 7.

In this study, we were able to expand our previous investigation with a longitudinal design enabling us to analyse the development and progression of atherosclerosis. Moreover, we were able to investigate different traffic-related air pollutants, such as particle mass, particle number and NO_2, in the context of traffic-related noise.

The clearest effect estimates for the development, presence and extent of TAC progression were seen for particle number concentrations and noise exposure, which are also the most accurate surrogates of environmental pollution from road traffic. While road traffic has been shown to be related to numerous cardiovascular health effects,[33] most studies were not able to differentiate between air pollution and noise effects due to missing information on both exposures. This study fills this gap by showing independent associations of two traffic-related exposures on the development of subclinical atherosclerosis, the underlying pathology for most CVDs. In contrast, our study shows counterintuitive results in those participants with already advanced atherosclerosis.

There are two pathological processes leading to the formation of vascular calcifications, which often occur simultaneously,[34] yet can be affected differently by different environmental factors. Noise has been postulated to act on the cardiovascular system primarily by causing a stress reaction with the secretion of corticosteroids, accompanied by elevated blood pressure, dyslipidemia, elevated blood glucose and vascular dysfunction, which may all contribute to the progression of atherosclerosis.[3] Next to a sympathetic arousal that can be noted already within hours after the rise of air pollution concentrations, air pollutants have been shown to increase blood pressure and systemic inflammatory responses, which may also contribute to atherogenesis.[1] Previous studies observed cardiovascular-related health effects, like subclinical changes in left ventricular performance, most likely caused by decreased ventricular function in response to $PM_{2.5}$ exposure.[35]

Although still lacking a complete understanding of the health effect mechanisms, our findings can be linked to the public health risk of air pollution and road traffic noise on cardiovascular health.[36] Lacking safe levels of air pollutants, large parts of the population may be subjected to these adverse environmental effects on the vasculature, especially when not given personal risk (e.g. smoking). Importantly, associations were observed at air pollution levels below the European limit values,[26] while mean noise levels were also at or only slightly above the current World Health Organization (WHO) recommendations of 53 dB for L_{den} and 45 dB for L_{night},[37] indicating that these regulations and recommendations may not sufficiently protect the European population.

Our results show negative associations in participants with a more advanced atherosclerosis burden. Negative findings were also observed in the Framingham Heart Study, investigating associations of traffic proximity and $PM_{2.5}$ with abdominal or thoracic aortic calcification.[15,16] However, other recent studies reported that pathological subjects are

more vulnerable to the environmental effects, such as an increased risk of cancer induced by long-term exposure to traffic-related air pollution in myocardial infarction survivors reported by Cohen et al.[38] From a statistical point of view random variations in TAC measurements may have caused regression to the mean at the second examination time, leading to counterintuitive findings. A possible biological explanation for this finding is that subjects with a higher extent of TAC are more likely to be symptomatic. They will therefore more likely be diagnosed with cardiovascular risk factors and will consequently receive aggressive cardio-protective interventions such as statin therapy, antihypertensive therapy and tight control of blood glucose. Indeed, in our study participants with a higher TAC at baseline had higher incidences of cardiovascular-related mortality, as well as higher rates of incident statin medication. Although air pollution exposure may contribute more to the development of early soft plaque than to progression to arterial calcification,[15] which is in line with results from our prior analysis of second-hand smoke and CAC in the Heinz Nixdorf Recall study,[30] negative associations remain to be explained.

In line with our previous cross-sectional investigation[17] and results from a recent review,[5] air pollution and noise revealed independent health effect estimates. Moreover, our results did not indicate that the association of air pollutants on TAC progression was enhanced in those with high noise exposure or vice versa. This is different to a prior analysis of cognitive function in the same study population, in which susceptibility to adverse associations with air pollution was increased in those with high levels of noise exposure and vice versa, and the associations were over-additive in those with high levels of both exposures.[39] The lack of effect modification in the present analysis suggests that air pollution and noise action affect atherosclerosis through biological pathways which do not potentiate each other.[1,3,5]

The major strengths of this analysis include standardised measurements of classic cardiovascular risk factors, as well as of TAC. The CT scans were repeated with the same scanner technology and identical scanning protocols, so that we avoided the use of any correction factors. Moreover, a potential bias by therapy was eradicated because participants and their physicians were blinded to the results of the calcification scoring at the baseline examination. The detailed information on lifestyle factors, socioeconomic status and potential cardiovascular risk factors allowed an appropriate control of confounding.

Limitations were the relatively short time of follow-up (5 years) with respect to a life-time exposure and atherosclerotic changes. Moreover, measurement of TAC progression can suffer from unsystematic measurement error due to an underestimation of TAC burden at the slice border of each 3 mm CT slice, which most likely biases the effects towards the null. Unfortunately, we do not have repeated measures to assess study-specific interscan variability. Exposure assessment to noise and air pollution was conducted by modelling at participants' addresses, leading to exposure measurement error. Moreover, grid-based exposure estimation is more prone to measurement error for air pollutants with greater small-scale variation (NO_2 and PN_{acc}) than the more homogeneous PM_{10} and $PM_{2.5}$.

Conclusion

While our study does not show overall associations, subgroup analyses suggest independent associations of traffic-related air pollution and road traffic noise with the development and progression of subclinical atherosclerosis in participants with no or only minimal thoracic aortic calcification at baseline that may contribute to the development of environmentally caused CVD. The observed lower risk of the development and progression of TAC in participants with advanced calcification remains to be explained.

Acknowledgements

The authors are indebted to all study participants and both to the dedicated personnel of the study centre of the Heinz Nixdorf Recall study and the EBT-scanner facilities and to the investigative group, in particular to U Roggenbuck, U Slomiany, EM Beck, A Öffner, S Münkel, S Schrader, R Peter and H Hirche. They also thank Anna Buschka for the data management.

Author contribution

Frauke Hennig: Conceived and designed the research, performed statistical analysis, drafted the manuscript, made critical revision of the manuscript for key intellectual content.

Susanne Moebus: Acquired the data, made critical revision of the manuscript for key intellectual content.

Nico Reinsch: Made critical revision of the manuscript for key intellectual content.

Thomas Budde: Made critical revision of the manuscript for key intellectual content.

Raimund Erbel: Acquired the data. Made critical revision of the manuscript for key intellectual content.

Karl-Heinz Jöckel: Acquired the data. Made critical revision of the manuscript for key intellectual content.

Barbara Hoffmann: Conceived and designed the research, drafted the manuscript. Made critical revision of the manuscript for key intellectual content.

Hagen Kälsch: Conceived and designed the research, acquired the data, drafted the manuscript.

Nils Lehmann: Made critical revision of the manuscript for key intellectual content.

Declaration of conflicting interests

The author(s) declared no potential conflicts of interest with respect to the research, authorship, and/or publication of this article.

Funding

The author(s) disclosed receipt of the following financial support for the research, authorship, and/or publication of this article: the authors wish to thank the Heinz Nixdorf Foundation Germany, for their generous support of this study. This study was also supported by the German Ministry of Education and Science (BMBF), and the German Aerospace Center (Deutsches Zentrum für Luft und Raumfahrt, DLR), Bonn, Germany. They acknowledge the support of Sarstedt AG & Co. (Nümbrecht, Germany) concerning laboratory equipment. This work was supported by the German Research Council (DFG; projects (SI 236/8-1, SI 236/9-1, 3314/4-3, 3314/2-3)).

References

1. Franklin BA, Brook R and Arden Pope C. Air pollution and cardiovascular disease. *Curr Probl Cardiol* 2015; 40: 207–238.
2. World Health Organization. *Global health risks mortality and burden of disease attributable to selected major risks*. Switzerland: WHO Library Cataloguing-in-Publication Data Global, 2009.
3. Münzel T, Schmidt FP, Steven S, et al. Environmental noise and the cardiovascular system. *J Am Coll Cardiol* 2018; 71: 688–697.
4. Münzel T, Gori T, Babisch W, et al. Cardiovascular effects of environmental noise exposure. *Eur Heart J* 2014; 35: 829–836.
5. Stansfeld SA. Noise effects on health in the context of air pollution exposure. *Environ Res Public Health* 2015; 12: 12735–12760.
6. Roquer J and Ois A. Atherosclerotic Burden and Mortality. In: Preedy VR and Watson RR (eds) *Handbook of Disease Burdens and Quality of Life Measures*. New York, NY: Springer New York, 2010, pp.899–918.
7. Grandner MA, Seixas A, Shetty S, et al. Sleep duration and diabetes risk: population trends and potential mechanisms. *Curr Diabetes Rep* 2016; 16: 1–27.
8. Budoff MJ, Nasir K, Katz R, et al. Thoracic aortic calcification and coronary heart disease events: the multi-ethnic study of atherosclerosis (MESA). *Thorac Aortic Calcif* 2011; 215: 196–202.
9. Kälsch H, Lehmann N, Möhlenkamp S, et al. Prevalence of thoracic aortic calcification and its relationship to cardiovascular risk factors and coronary calcification in an unselected population-based cohort: the Heinz Nixdorf Recall Study. *Int J Cardiovasc Imaging* 2013; 29: 207–216.
10. Provost EB, Madhloum N, Panis LI, et al. Carotid intima-media thickness, a marker of subclinical atherosclerosis, and particulate air pollution exposure: the meta-analytical evidence. *PLoS One* 2015; 10: 1–12.
11. Hoffmann B, Moebus S, Stang A, et al. Residence close to high traffic and prevalence of coronary heart disease. *Eur Heart J* 2006; 27: 2696–2702.
12. Hoffmann B, Moebus S, Kröger K, et al. Residential exposure to urban air pollution, ankle-brachial index, and peripheral arterial disease. *Epidemiology* 2009; 20: 280–288.
13. Kaufman JD, Adar SD, Barr RG, et al. Association between air pollution and coronary artery calcification within six metropolitan areas in the USA (the Multi-Ethnic Study of Atherosclerosis and Air Pollution): a longitudinal cohort study. *Lancet* 2016; 6736: 1–9.
14. Allen RW, Criqui MH, Diez Roux AV, et al. Fine particulate matter air pollution, proximity to traffic, and aortic atherosclerosis. *Epidemiology* 2009; 20: 254–264.
15. Dorans KS, Wilker EH, Li W, et al. Residential proximity to major roads, exposure to fine particulate matter and aortic calcium: the Framingham Heart Study, a cohort study. *BMJ Open* 2017; 7: 1–12.
16. Dorans KS, Wilker EH, Li W, et al. Residential proximity to major roads, exposure to fine particulate matter, and coronary artery calcium. *Arterioscler Thromb Vasc Biol* 2016; 36: 1679–1685.
17. Kälsch H, Hennig F, Moebus S, et al. Are air pollution and traffic noise independently associated with atherosclerosis: the Heinz Nixdorf Recall Study. *Eur Heart J* 2013; 35: 1–8.
18. Erbel R, Möhlenkamp S, Moebus S, et al. Coronary risk stratification, discrimination, and reclassification improvement based on quantification of subclinical coronary atherosclerosis: the Heinz Nixdorf Recall study. *J Am Coll Cardiol* 2010; 56: 1397–1406.
19. Schmermund A, Möhlenkamp S, Stang A, et al. Assessment of clinically silent atherosclerotic disease and established and novel risk factors for predicting myocardial infarction and cardiac death in healthy middle-aged subjects: rationale and design of the Heinz Nixdorf RECALL Study. *Am Heart J* 2002; 144: 212–218.
20. Agatston AS, Janowitz FWR, Hildner FJ, et al. Quantification of coronary artery calcium using ultrafast computed tomography. *J Am Coll Cardiol* 1990; 15: 827–832.
21. Lehmann N, Erbel R, Mahabadi AA, et al. Value of progression of coronary artery calcification for risk prediction of coronary and cardiovascular events result of the HNR Study (Heinz Nixdorf Recall). *Circulation* 2018; 137: 665–679.
22. Kälsch H, Lehmann N, Moebus S, et al. Aortic calcification onset and progression: association with the development of coronary atherosclerosis. *J Am Heart Assoc* 2017; 6(4): 1–12.
23. Nonnemacher M, Jakobs H, Viehmann A, et al. Spatio-temporal modelling of residential exposure to particulate matter and gaseous pollutants for the Heinz Nixdorf Recall Cohort. *Atmos Environ* 2014; 91: 15–23.
24. Memmesheimer M, Friese E, Ebel A, et al. Long-term simulations of particulate matter in Europe on different scales using sequential nesting of a regional model. *Int J Environ Pollut* 2004; 22: 108–132.

25. European Environment Agency. *Index to methodology chapters ordered by SNAP97 Activity*, 2011. www.eea.europa.eu/publications/EMEPCORINAIR4/page009-a.html (2015, accessed 25 May 2019).
26. EU Directive 2008/50/EC of the European Parliament and of the Council of 21 May 2008 on ambient air quality and cleaner air for Europe. *Off J Eur Union* 2008; L152: 1–44.
27. Araujo JA and Nel AE. Particulate matter and atherosclerosis: role of particle size, composition and oxidative stress. *Part Fibre Toxicol* 2009; 6: 24.
28. World Health Organization. *ATC/DDD Index 2019*. www.whocc.no/atc_ddd_index/ (2013, accessed 25 May 2019).
29. Mills NL, Donaldson K, Hadoke PW, et al. Adverse cardiovascular effects of air pollution. *Nat Clin Pract Cardiovasc Med* 2009; 6: 36–44.
30. Peinemann F, Moebus S, Dragano N, et al. Secondhand smoke exposure and coronary artery calcification among nonsmoking participants of a population-based cohort. *Environ Health Perspect* 2011; 119: 1556–1561.
31. Dzhambov AM, Gatseva PD, Tokmakova MP, et al. Association between community noise and adiposity in patients with cardiovascular disease. *Noise Health* 2017; 19: 270–277.
32. Budoff MJ, Takasu J, Katz R, et al. Reproducibility of CT measurements of aortic valve calcification, mitral annulus calcification, and aortic wall calcification in the Multi-Ethnic Study of Atherosclerosis. *Acad Radiol* 2006; 13: 166–172.
33. HEI. *HEI Panel on the Health Effect of Traffic-Related Air Pollution: A Critical Review of the Literature on Emissions, Exposure, and Health Effects*. HEI Special Report 17, 2010. Boston, MA: Health Effects Institute.
34. Wasilewski J, Glowacki J and Poloński L. Not at random location of atherosclerotic lesions in thoracic aorta and their prognostic significance in relation to the risk of cardiovascular events. *Polish J Radiol* 2013; 78: 38–42.
35. Yang W, Zhang Z, Thijs L, et al. Left ventricular function in relation to chronic residential air pollution in a general population. *Eur J Prev Cardiol* 2017; 24: 1416–1428.
36. Van Kempen E, Casas M, Pershagen G, et al. WHO Environmental Noise Guidelines for the European Region: a systematic review on environmental noise and cardiovascular and metabolic effects: a summary. *Environ Res Public Health* 2018; 15: 1–59.
37. World Health Organization. *Environmental noise guidelines for the European Region*. Copenhagen, Denmark: World Health Organization, Regional Office for Europe, 2018.
38. Cohen G, Levy I, Kark JD, et al. Long-term exposure to traffic-related air pollution and cancer among survivors of myocardial infarction: a 20-year follow-up study. *Eur J Prev Cardiol* 2017; 24: 92–102.
39. Tzivian L, Dlugaj M, Winkler A, et al. Long-term air pollution and traffic noise exposures and mild cognitive impairment in older adults: a cross-sectional analysis of the Heinz Nixdorf Recall Study. *Environ Health Perspect* 2016; 124: 1361–1368.

Investigation of air pollution and noise on progression of thoracic aortic calcification – Results of the Heinz Nixdorf Recall Study

Short title: Traffic-related exposures and progression of thoracic aortic calcification

Frauke Hennig[1], Susanne Moebus[2], Nico Reinsch[3,4], Thomas Budde[3], Raimund Erbel, [2], Karl-Heinz Jöckel[2], Nils Lehmann[2] , Barbara Hoffmann[1] and Hagen Kälsch[3,4], on behalf of the Heinz Nixdorf Recall Study Investigative Group.

1. Institute of Occupational, Social and Environmental Medicine, Centre for Health and Society, Medical Faculty, Heinrich-Heine University Düsseldorf, Germany
2. Institute of Medical Informatics, Biometry and Epidemiology, University of Duisburg-Essen, Essen, Germany
3. Alfried Krupp Hospital Essen, Department of Cardiology, Essen, Germany
4. University Witten/Herdecke, Witten, Germany

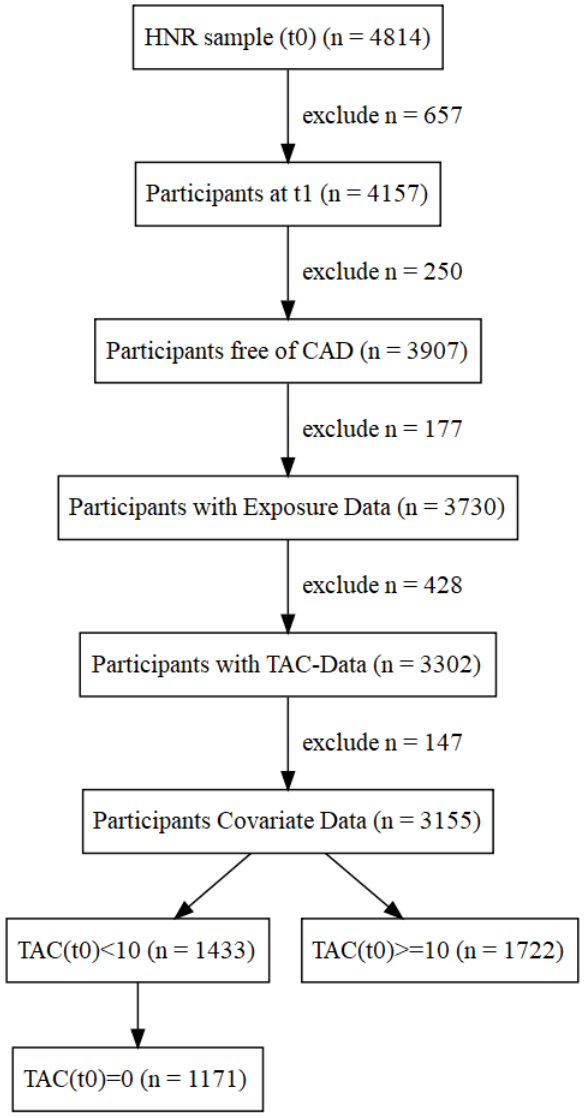

Figure S1: Flowchart visualizing the sample size reduction of the Heinz Nixdorf Recall Study cohort for the analysis samples investigating the association of air pollution and noise exposure on TAC-progression.

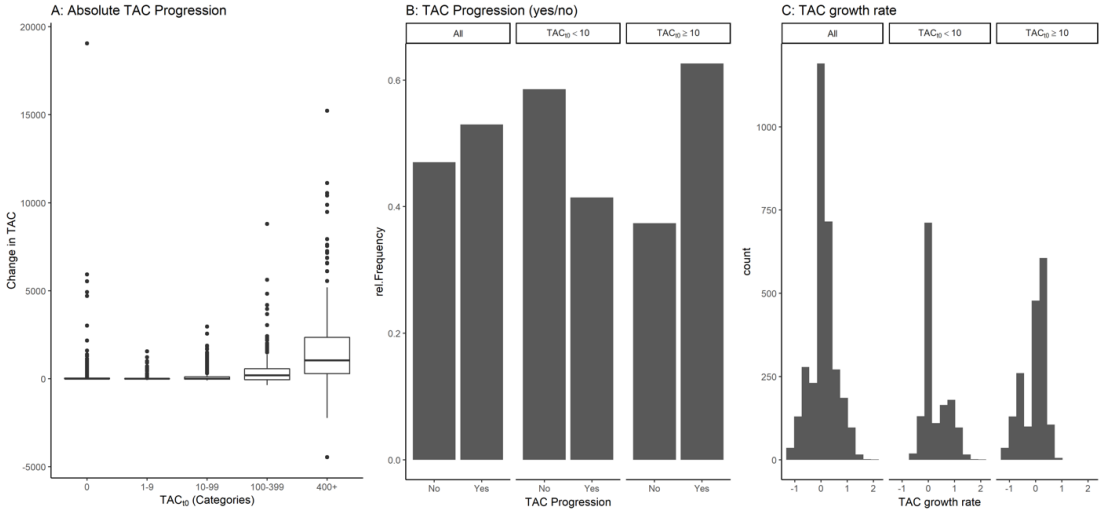

Figure S2: Distribution of TAC-progression for the study sample of the Heinz Nixdorf Recall Study cohort (n=3,155).visualized as A: Boxplot of absolute TAC-change according to baseline TAC categories; B: Barplot of TAC progression stratified by TAC=10, C: Histogram of TAC growth rates.

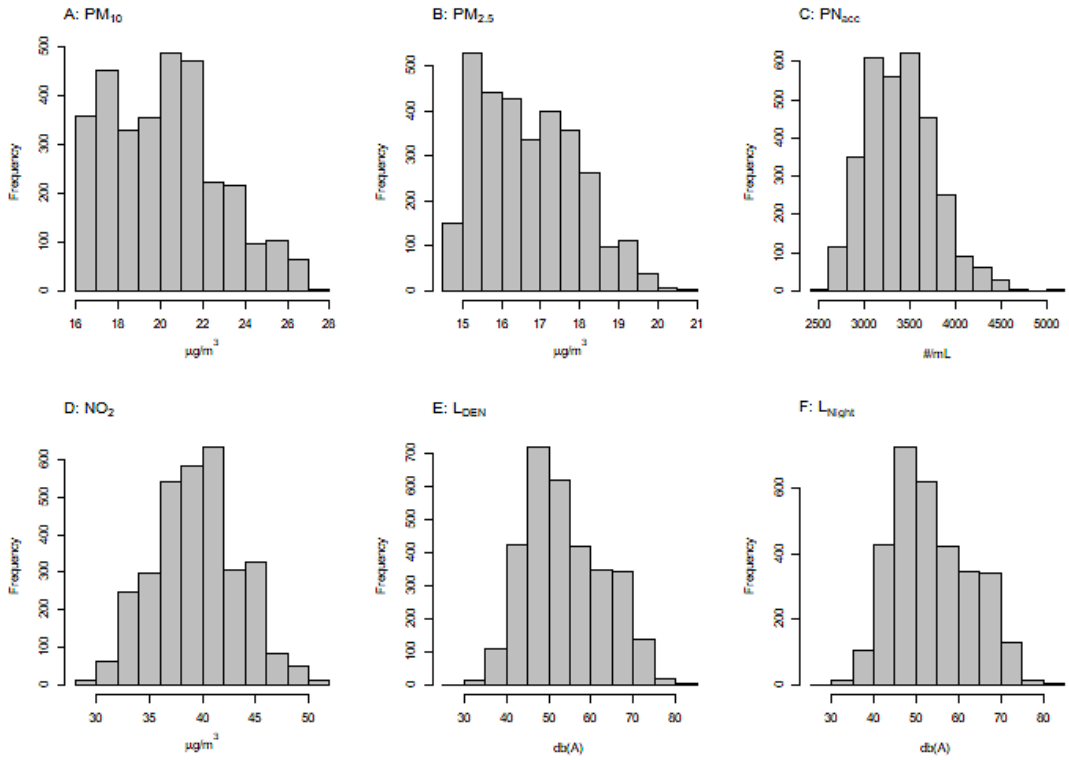

Figure S3: Residence-based modelled exposure distribution visualized as histogram for the study sample of the Heinz Nixdorf Recall Study cohort (n=3,155).

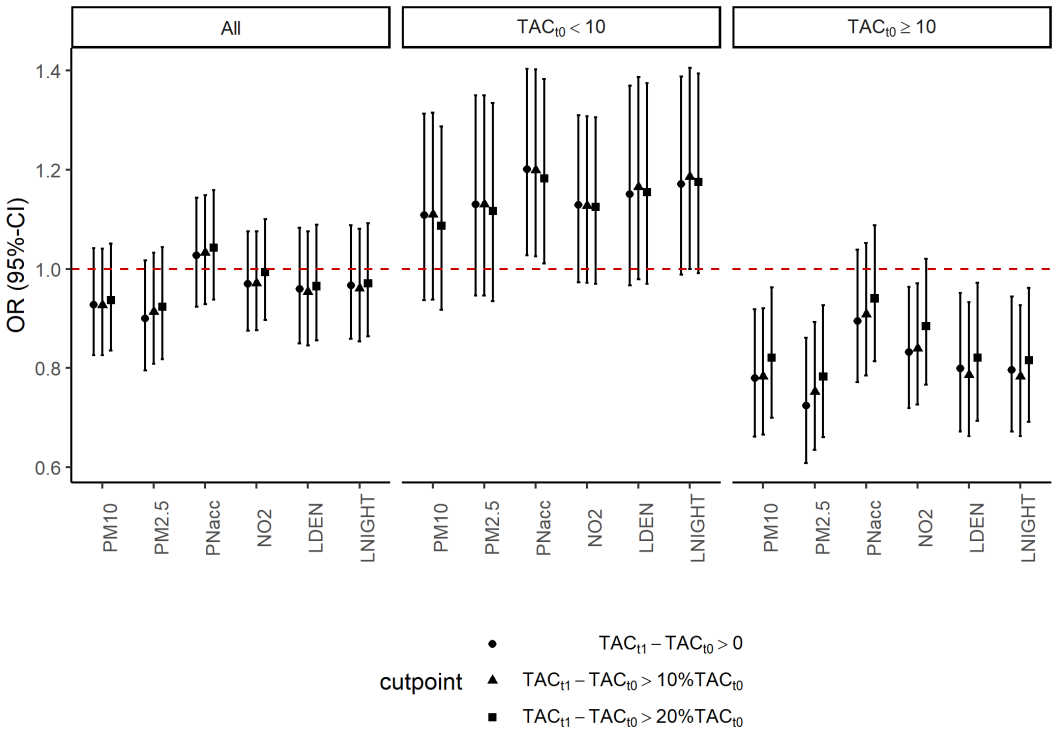

Figure S4: Main effect estimates (95%-CI) per IQR exposure increase on TAC-progression, using a cutpoint of 0 compared to 10% and 20% from baseline TAC value. Effects are estimated in the Heinz Nixdorf Recall study sample (n=3,155) and stratified by TAC_{t0} (TAC_{t0}<10, n=1,433 and TAC_{t0}≥10, n=1,722), adjusted for age, sex, smoking, physical activity, alcohol status, education and follow-up years.

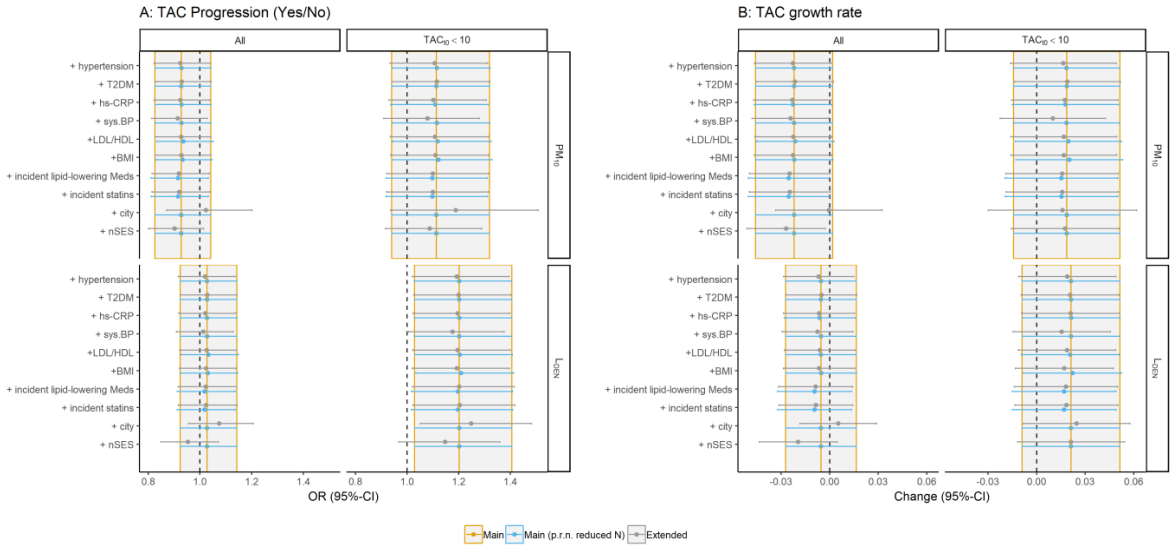

Figure S5: Exposure effect estimates per IQR increase in exposure (here PM_{10} and L_{DEN}) on TAC-progression after adding respective covariates to the main adjustment set (age, sex, smoking status, physical activity, and education), estimated in all participants of the Heinz Nixdorf Recall Study feasible for this analysis (n=3,125) and in participants with low baseline TAC (n=1,433). A: OR (95%-CI) for a TAC-progression, B: Change (95%-CI) of growth rate of TAC.

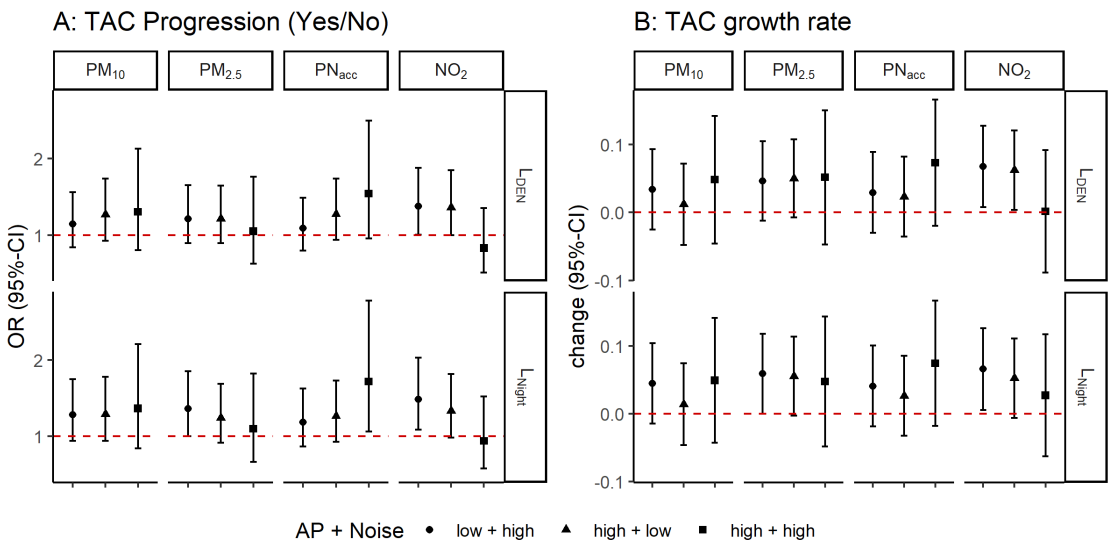

Figure S6: Synergism of co-exposure. Effect estimates of high and/or low co-exposure of air pollution (AP) and noise on TAC-progression in participants of the Heinz Nixdorf Recall Study with minimal/no baseline (TACt0 <10; n=1,417). A: RR (95%-CI) for a TAC-progression, B: Change (95%-CI) of growth rate of TAC. Models are adjusted for age, sex, smoking status, physical activity, BMI, LDL/HDL, education, and follow-up time. Complementing numbers are described in Table S6.

Table S1: Odds Ratios (95%-CI) per IQR increase in exposure on TAC-progression (TAC, ATAC and DTAC) in participants of the Heinz Nixdorf Recall Study (All, n=3,155; $TAC_{t0}<10$, n=1,433; $TAC_{t0}\geq10$, n=1,722; $TAC_{t0}=0$, n=1,158) in crude and main models (adjustment: age, sex, smoking status, physical activity and education). Complementing Figure is Figure 1 (A) in the main text.

Exposure	IQR	Outcome	Model	All	$TAC_{t0}<10$	$TAC_{t0}\geq10$	$TAC_{t0}=0$
PM_{10}	3.8 $\mu g/m^3$	TAC	crude	0.97 (0.87, 1.07)	1.13 (0.97, 1.32)	0.81 (0.70, 0.93)	1.18 (0.99, 1.41)
			Main	0.93 (0.83, 1.04)	1.11 (0.94, 1.31)	0.78 (0.66, 0.92)	1.12 (0.92, 1.36)
		ATAC	crude	0.91 (0.81, 1.01)	0.99 (0.82, 1.19)	0.82 (0.71, 0.95)	1.06 (0.87, 1.30)
			Main	0.88 (0.79, 0.99)	0.97 (0.80, 1.17)	0.81 (0.70, 0.95)	1.00 (0.81, 1.24)
		DTAC	crude	1.01 (0.91, 1.12)	1.14 (0.96, 1.34)	0.89 (0.77, 1.03)	1.17 (0.98, 1.41)
			Main	0.97 (0.87, 1.10)	1.09 (0.91, 1.31)	0.89 (0.75, 1.04)	1.08 (0.89, 1.33)
$PM_{2.5}$	2.0 $\mu g/m^3$	TAC	crude	0.91 (0.81, 1.01)	1.13 (0.95, 1.33)	0.72 (0.62, 0.84)	1.16 (0.97, 1.39)
			Main	0.90 (0.80, 1.02)	1.13 (0.95, 1.35)	0.72 (0.61, 0.86)	1.14 (0.94, 1.39)
		ATAC	crude	0.90 (0.80, 1.01)	1.01 (0.83, 1.23)	0.81 (0.69, 0.94)	1.08 (0.88, 1.34)
			Main	0.90 (0.80, 1.02)	1.00 (0.82, 1.22)	0.83 (0.71, 0.97)	1.06 (0.85, 1.32)
		DTAC	crude	0.95 (0.85, 1.06)	1.08 (0.90, 1.28)	0.83 (0.71, 0.97)	1.07 (0.89, 1.30)
			Main	0.95 (0.83, 1.07)	1.06 (0.88, 1.28)	0.86 (0.73, 1.02)	1.03 (0.83, 1.27)
PN_{acc}	520 #/mL	TAC	crude	1.03 (0.94, 1.14)	1.18 (1.02, 1.36)	0.92 (0.81, 1.05)	1.18 (1.00, 1.38)
			Main	1.03 (0.92, 1.14)	1.20 (1.03, 1.40)	0.90 (0.77, 1.04)	1.19 (1.00, 1.41)
		ATAC	crude	0.99 (0.89, 1.09)	1.02 (0.86, 1.20)	0.96 (0.84, 1.09)	1.05 (0.87, 1.26)
			Main	0.97 (0.87, 1.08)	1.02 (0.86, 1.21)	0.94 (0.82, 1.07)	1.04 (0.86, 1.25)
		DTAC	crude	1.05 (0.96, 1.16)	1.13 (0.97, 1.31)	1.00 (0.88, 1.14)	1.11 (0.94, 1.31)
			Main	1.05 (0.94, 1.17)	1.13 (0.96, 1.34)	1.00 (0.86, 1.16)	1.09 (0.91, 1.31)
NO_2	5.3 µg/m3	TAC	crude	0.97 (0.89, 1.07)	1.10 (0.96, 1.26)	0.85 (0.75, 0.97)	1.07 (0.92, 1.25)
			Main	0.97 (0.87, 1.08)	1.13 (0.97, 1.31)	0.83 (0.72, 0.96)	1.09 (0.93, 1.29)
		ATAC	crude	1.00 (0.91, 1.10)	1.05 (0.90, 1.24)	0.95 (0.84, 1.08)	1.08 (0.91, 1.29)
			Main	1.00 (0.90, 1.11)	1.07 (0.91, 1.26)	0.95 (0.83, 1.09)	1.09 (0.91, 1.31)
		DTAC	crude	0.98 (0.89, 1.08)	1.07 (0.93, 1.24)	0.90 (0.79, 1.02)	1.02 (0.87, 1.20)
			Main	0.98 (0.88, 1.09)	1.09 (0.93, 1.28)	0.89 (0.77, 1.03)	1.02 (0.85, 1.22)
L_{DEN}	14.4 dB(A)	TAC	crude	1.02 (0.91, 1.13)	1.19 (1.01, 1.40)	0.84 (0.72, 0.98)	1.21 (1.01, 1.45)
			Main	0.96 (0.85, 1.08)	1.15 (0.97, 1.37)	0.80 (0.67, 0.95)	1.18 (0.97, 1.43)
		ATAC	crude	1.05 (0.94, 1.18)	1.23 (1.02, 1.49)	0.91 (0.79, 1.06)	1.27 (1.03, 1.56)
			Main	1.01 (0.90, 1.14)	1.21 (1.00, 1.47)	0.88 (0.75, 1.03)	1.24 (1.00, 1.54)
		DTAC	crude	1.00 (0.89, 1.11)	1.15 (0.97, 1.36)	0.85 (0.74, 0.99)	1.16 (0.96, 1.40)
			Main	0.93 (0.82, 1.06)	1.08 (0.90, 1.30)	0.82 (0.69, 0.97)	1.10 (0.89, 1.36)
L_{Night}	13.7 dB(A)	TAC	crude	1.02 (0.92, 1.13)	1.20 (1.03, 1.41)	0.84 (0.72, 0.97)	1.22 (1.03, 1.46)
			Main	0.97 (0.86, 1.09)	1.17 (0.99, 1.39)	0.80 (0.67, 0.94)	1.21 (1.00, 1.46)
		ATAC	crude	1.05 (0.94, 1.17)	1.24 (1.03, 1.49)	0.90 (0.78, 1.04)	1.29 (1.05, 1.57)
			Main	1.01 (0.90, 1.14)	1.22 (1.01, 1.48)	0.88 (0.75, 1.02)	1.27 (1.02, 1.56)
		DTAC	crude	1.00 (0.90, 1.11)	1.15 (0.98, 1.36)	0.85 (0.73, 0.98)	1.17 (0.97, 1.41)
			Main	0.94 (0.83, 1.06)	1.10 (0.92, 1.32)	0.82 (0.69, 0.97)	1.13 (0.92, 1.38)

Table S2: Change (95%-CI) in growth rate of TAC (ATAC and DTAC) per IQR increase in exposure in participants of the Heinz Nixdorf Recall Study (all: n=3,155; TAC_{t0}<10, n=1,433; TAC_{t0}≥10, n=1,722). Models are adjusted for age, sex, smoking status, physical activity, and education. Complementing Figure is Figure 1 (B) in the main text.

Exposure	IQR	Outcome	Model	All	TAC_{t0}<10	TAC_{t0}≥10	TAC_{t0}>0
PM_{10}	3.8 $\mu g/m^3$	TAC	crude	-0.02 (-0.04, 0.01)	0.03 (-0.01, 0.06)	-0.04 (-0.07, -0.01)	-0.03 (-0.06, -0.01)
			Main	-0.02 (-0.05, 0.00)	0.02 (-0.02, 0.05)	-0.03 (-0.06, -0.01)	-0.03 (-0.06, -0.01)
		ATAC	crude	0.01 (-0.02, 0.03)	0.03 (0.00, 0.06)	-0.01 (-0.06, 0.03)	-0.01 (-0.05, 0.03)
			Main	0.00 (-0.03, 0.03)	0.02 (-0.01, 0.05)	-0.01 (-0.05, 0.04)	0.00 (-0.04, 0.04)
		DTAC	crude	-0.02 (-0.05, 0.01)	0.03 (-0.01, 0.06)	-0.05 (-0.08, -0.01)	-0.04 (-0.07, -0.01)
			Main	-0.03 (-0.05, 0.00)	0.01 (-0.02, 0.05)	-0.04 (-0.08, -0.01)	-0.04 (-0.07, -0.01)
$PM_{2.5}$	2.0 $\mu g/m^3$	TAC	crude	-0.03 (-0.05, 0.00)	0.04 (0.00, 0.08)	-0.07 (-0.10, -0.04)	-0.06 (-0.09, -0.03)
			Main	-0.03 (-0.05, 0.00)	0.03 (0.00, 0.07)	-0.06 (-0.08, -0.03)	-0.05 (-0.08, -0.03)
		ATAC	crude	0.00 (-0.04, 0.03)	0.03 (-0.01, 0.06)	-0.03 (-0.08, 0.02)	-0.02 (-0.06, 0.03)
			Main	0.00 (-0.03, 0.03)	0.02 (-0.01, 0.05)	-0.02 (-0.06, 0.03)	-0.01 (-0.05, 0.03)
		DTAC	crude	-0.04 (-0.06, -0.01)	0.03 (-0.01, 0.06)	-0.08 (-0.12, -0.05)	-0.07 (-0.11, -0.04)
			Main	-0.04 (-0.06, -0.01)	0.02 (-0.01, 0.06)	-0.07 (-0.10, -0.03)	-0.06 (-0.09, -0.03)
PN_{acc}	520 #/mL	TAC	crude	0.00 (-0.02, 0.02)	0.02 (-0.01, 0.06)	-0.02 (-0.04, 0.01)	-0.01 (-0.04, 0.01)
			Main	-0.01 (-0.03, 0.02)	0.02 (-0.01, 0.05)	-0.02 (-0.04, 0.01)	-0.01 (-0.04, 0.01)
		ATAC	crude	0.01 (-0.02, 0.03)	0.02 (-0.01, 0.05)	0.00 (-0.04, 0.04)	0.00 (-0.03, 0.04)
			Main	0.00 (-0.02, 0.03)	0.01 (-0.01, 0.04)	0.00 (-0.04, 0.04)	0.01 (-0.03, 0.04)
		DTAC	crude	0.00 (-0.03, 0.02)	0.02 (-0.02, 0.05)	-0.02 (-0.05, 0.01)	-0.01 (-0.04, 0.02)
			Main	-0.01 (-0.03, 0.01)	0.01 (-0.02, 0.04)	-0.02 (-0.05, 0.01)	-0.02 (-0.04, 0.01)
NO_2	5.3 µg/m3	TAC	crude	-0.01 (-0.03, 0.02)	0.03 (0.00, 0.06)	-0.03 (-0.06, -0.01)	-0.03 (-0.05, 0.00)
			Main	-0.01 (-0.03, 0.01)	0.03 (0.01, 0.06)	-0.03 (-0.06, -0.01)	-0.03 (-0.05, 0.00)
		ATAC	crude	-0.01 (-0.03, 0.02)	0.02 (-0.01, 0.05)	-0.03 (-0.07, 0.01)	-0.02 (-0.06, 0.02)
			Main	-0.01 (-0.03, 0.02)	0.02 (-0.01, 0.04)	-0.03 (-0.07, 0.01)	-0.02 (-0.06, 0.02)
		DTAC	crude	-0.02 (-0.04, 0.01)	0.03 (0.00, 0.05)	-0.05 (-0.08, -0.02)	-0.04 (-0.07, -0.01)
			Main	-0.02 (-0.04, 0.00)	0.02 (0.00, 0.05)	-0.05 (-0.08, -0.02)	-0.04 (-0.07, -0.01)
L_{DEN}	14.4 dB(A)	TAC	crude	-0.01 (-0.03, 0.02)	0.04 (0.01, 0.08)	-0.03 (-0.06, 0.00)	-0.03 (-0.05, 0.00)
			Main	-0.02 (-0.04, 0.01)	0.03 (0.00, 0.07)	-0.03 (-0.06, -0.01)	-0.03 (-0.06, 0.00)
		ATAC	crude	0.00 (-0.03, 0.03)	0.03 (0.00, 0.06)	-0.02 (-0.07, 0.02)	-0.02 (-0.06, 0.02)
			Main	-0.01 (-0.04, 0.02)	0.02 (-0.01, 0.05)	-0.02 (-0.07, 0.03)	-0.02 (-0.06, 0.02)
		DTAC	crude	-0.02 (-0.05, 0.01)	0.03 (0.00, 0.07)	-0.05 (-0.09, -0.02)	-0.04 (-0.08, -0.01)
			Main	-0.03 (-0.06, -0.01)	0.02 (-0.01, 0.05)	-0.05 (-0.09, -0.02)	-0.05 (-0.08, -0.02)
L_{Night}	13.7 dB(A)	TAC	crude	-0.01 (-0.03, 0.02)	0.05 (0.01, 0.08)	-0.04 (-0.07, 0.00)	-0.03 (-0.06, 0.00)
			Main	-0.02 (-0.04, 0.01)	0.04 (0.00, 0.07)	-0.04 (-0.06, -0.01)	-0.03 (-0.06, -0.01)
		ATAC	crude	0.00 (-0.03, 0.03)	0.03 (0.00, 0.06)	-0.03 (-0.07, 0.02)	-0.02 (-0.06, 0.02)
			Main	-0.01 (-0.04, 0.02)	0.02 (-0.01, 0.05)	-0.02 (-0.07, 0.02)	-0.02 (-0.06, 0.02)
		DTAC	crude	-0.02 (-0.05, 0.01)	0.04 (0.00, 0.07)	-0.06 (-0.09, -0.02)	-0.05 (-0.08, -0.01)
			Main	-0.03 (-0.06, -0.01)	0.03 (-0.01, 0.06)	-0.06 (-0.09, -0.02)	-0.05 (-0.08, -0.02)

Table S3: Odds Ratios (95%-CI) per IQR increase in exposure on TAC-progression in participants of the Heinz Nixdorf Recall Study (All, n=3,155; $TAC_{t0}<10$, n=1,433; $TAC_{t0}\geq10$, n=1,722; $TAC_{t0}=0$, n=1,158), estimated in specific subgroup (adjustment: age, sex, smoking status, physical activity and education).

Exposure	Subgroup	n	All	n	TAC<10	n	TAC≥10
PM_{10}	Main (no CAD)	3155	0.93 (0.83; 1.04)	1435	1.11 (0.94; 1.31)	1720	0.78 (0.66; 0.92)
	with CAD	3347	0.92 (0.83; 1.04)	1472	1.10 (0.93; 1.31)	1875	0.78 (0.67; 0.91)
	non-movers	2752	0.95 (0.84; 1.08)	1234	1.13 (0.95; 1.36)	1518	0.81 (0.69; 0.96)
	non-employees	1882	0.86 (0.75; 1.00)	683	1.17 (0.92; 1.47)	1199	0.70 (0.58; 0.85)
	Never-Smoker	1411	0.94 (0.79; 1.11)	652	1.29 (1.00; 1.67)	759	0.70 (0.55; 0.90)
	No incident Statin	2610	0.94 (0.83; 1.06)	1194	1.09 (0.91; 1.31)	1416	0.80 (0.67; 0.95)
	excluding outliers	3065	0.96 (0.85; 1.07)	1403	1.10 (0.93; 1.30)	1662	0.83 (0.71; 0.97)
$PM_{2.5}$	Main (no CAD)	3155	0.90 (0.80; 1.02)	1435	1.12 (0.95; 1.34)	1720	0.73 (0.62; 0.86)
	with CAD	3347	0.91 (0.81; 1.02)	1472	1.12 (0.94; 1.32)	1875	0.74 (0.63; 0.87)
	non-movers	2752	0.93 (0.82; 1.06)	1234	1.16 (0.97; 1.39)	1518	0.76 (0.64; 0.91)
	non-employees	1882	0.84 (0.72; 0.98)	683	1.12 (0.88; 1.43)	1199	0.69 (0.57; 0.85)
	Never-Smoker	1411	0.92 (0.77; 1.10)	652	1.27 (0.98; 1.65)	759	0.68 (0.53; 0.88)
	No incident Statin	2610	0.91 (0.80; 1.04)	1194	1.11 (0.92; 1.34)	1416	0.76 (0.64; 0.91)
	excluding outliers	3065	0.94 (0.84; 1.06)	1403	1.10 (0.92; 1.30)	1662	0.81 (0.68; 0.96)
PN_{acc}	Main (no CAD)	3155	1.03 (0.92; 1.15)	1435	1.21 (1.03; 1.41)	1720	0.89 (0.77; 1.04)
	with CAD	3347	1.03 (0.93; 1.15)	1472	1.20 (1.02; 1.40)	1875	0.90 (0.78; 1.05)
	non-movers	2752	1.04 (0.93; 1.17)	1234	1.21 (1.03; 1.43)	1518	0.92 (0.79; 1.07)
	non-employees	1882	0.94 (0.82; 1.08)	683	1.09 (0.87; 1.37)	1199	0.86 (0.72; 1.03)
	Never-Smoker	1411	1.08 (0.92; 1.27)	652	1.43 (1.13; 1.82)	759	0.85 (0.68; 1.06)
	No incident Statin	2610	1.05 (0.93; 1.18)	1194	1.18 (0.99; 1.40)	1416	0.94 (0.80; 1.11)
	excluding outliers	3065	1.06 (0.95; 1.19)	1403	1.21 (1.03; 1.42)	1662	0.95 (0.82; 1.11)
NO_2	Main (no CAD)	3155	0.97 (0.87; 1.08)	1435	1.13 (0.97; 1.31)	1720	0.83 (0.72; 0.96)
	with CAD	3347	0.98 (0.88; 1.08)	1472	1.12 (0.97; 1.30)	1875	0.85 (0.74; 0.98)
	non-movers	2752	0.98 (0.88; 1.09)	1234	1.15 (0.98; 1.34)	1518	0.84 (0.72; 0.97)
	non-employees	1882	0.92 (0.80; 1.05)	683	1.07 (0.86; 1.32)	1199	0.82 (0.69; 0.98)
	Never-Smoker	1411	0.98 (0.85; 1.15)	652	1.16 (0.93; 1.44)	759	0.83 (0.66; 1.03)
	No incident Statin	2610	0.98 (0.88; 1.09)	1194	1.12 (0.95; 1.32)	1416	0.85 (0.72; 0.99)
	excluding outliers	3065	1.01 (0.91; 1.12)	1403	1.11 (0.96; 1.29)	1662	0.91 (0.78; 1.05)
L_{DEN}	Main (no CAD)	3155	0.96 (0.85; 1.08)	1435	1.15 (0.97; 1.37)	1720	0.80 (0.67; 0.95)
	with CAD	3347	0.97 (0.86; 1.09)	1472	1.15 (0.97; 1.36)	1875	0.82 (0.69; 0.97)
	non-movers	2752	0.99 (0.87; 1.12)	1234	1.14 (0.95; 1.38)	1518	0.87 (0.72; 1.04)
	non-employees	1882	0.97 (0.83; 1.13)	683	1.21 (0.94; 1.56)	1199	0.83 (0.68; 1.02)
	Never-Smoker	1411	0.97 (0.81; 1.17)	652	1.21 (0.93; 1.58)	759	0.78 (0.60; 1.01)
	No incident Statin	2610	1.00 (0.88; 1.15)	1194	1.20 (0.99; 1.45)	1416	0.85 (0.70; 1.02)
	excluding outliers	3065	0.98 (0.87; 1.11)	1403	1.15 (0.97; 1.37)	1662	0.83 (0.70; 0.98)
L_{Night}	Main (no CAD)	3155	0.97 (0.86; 1.09)	1435	1.18 (0.99; 1.40)	1720	0.79 (0.67; 0.94)
	with CAD	3347	0.97 (0.87; 1.10)	1472	1.17 (0.99; 1.39)	1875	0.81 (0.69; 0.96)
	non-movers	2752	0.99 (0.87; 1.13)	1234	1.16 (0.96; 1.40)	1518	0.86 (0.72; 1.03)
	non-employees	1882	0.97 (0.83; 1.13)	683	1.25 (0.98; 1.61)	1199	0.81 (0.67; 0.99)
	Never-Smoker	1411	0.97 (0.81; 1.17)	652	1.24 (0.95; 1.62)	759	0.76 (0.59; 0.98)
	No incident Statin	2610	1.01 (0.89; 1.15)	1194	1.22 (1.01; 1.47)	1416	0.84 (0.70; 1.01)
	excluding outliers	3065	0.99 (0.88; 1.11)	1403	1.18 (0.99; 1.40)	1662	0.82 (0.70; 0.98)

Table S4: Change (95%-CI) in TAC growth rate per IQR increase in exposure in participants of the Heinz Nixdorf Recall Study (All, n=3,155; TAC_{t0}<10, n=1,433; TAC_{t0}≥10, n=1,722; TAC_{t0}=0, n=1,158), estimated in specific subgroup (adjustment: age, sex, smoking status, physical activity and education).

Exposure	Subgroup	n	All	n	TAC<10	n	TAC≥10
PM_{10}	Main (no CAD)	3155	-0.02 (-0.05; 0.00)	1435	0.02 (-0.02; 0.05)	1720	-0.03 (-0.06; -0.01)
	with CAD	3347	-0.02 (-0.05; 0.00)	1472	0.02 (-0.01; 0.05)	1875	-0.03 (-0.06; -0.01)
	non-movers	2752	-0.02 (-0.04; 0.01)	1234	0.02 (-0.01; 0.06)	1518	-0.03 (-0.06; 0.00)
	non-employees	1882	-0.02 (-0.05; 0.01)	683	0.03 (-0.02; 0.09)	1199	-0.04 (-0.07; -0.01)
	Never-Smoker	1411	-0.01 (-0.05; 0.02)	652	0.05 (0.00; 0.10)	759	-0.04 (-0.08; 0.00)
	No incident Statin	2610	-0.03 (-0.06; -0.01)	1194	0.01 (-0.03; 0.04)	1416	-0.04 (-0.06; -0.01)
	excluding outliers	3065	-0.01 (-0.03; 0.01)	1403	0.01 (-0.02; 0.05)	1662	-0.01 (-0.04; 0.01)
$PM_{2.5}$	Main (no CAD)	3155	-0.03 (-0.05; 0.00)	1435	0.03 (0.00; 0.07)	1720	-0.05 (-0.08; -0.03)
	with CAD	3347	-0.03 (-0.05; 0.00)	1472	0.03 (0.00; 0.07)	1875	-0.05 (-0.08; -0.03)
	non-movers	2752	-0.02 (-0.04; 0.01)	1234	0.04 (0.01; 0.08)	1518	-0.05 (-0.08; -0.02)
	non-employees	1882	-0.03 (-0.06; 0.00)	683	0.04 (-0.02; 0.09)	1199	-0.05 (-0.08; -0.02)
	Never-Smoker	1411	-0.03 (-0.06; 0.01)	652	0.05 (0.00; 0.10)	759	-0.07 (-0.11; -0.02)
	No incident Statin	2610	-0.03 (-0.06; -0.01)	1194	0.02 (-0.01; 0.06)	1416	-0.05 (-0.08; -0.02)
	excluding outliers	3065	-0.01 (-0.03; 0.01)	1403	0.02 (-0.01; 0.06)	1662	-0.02 (-0.05; 0.00)
PN_{acc}	Main (no CAD)	3155	-0.01 (-0.03; 0.02)	1435	0.02 (-0.01; 0.05)	1720	-0.02 (-0.04; 0.01)
	with CAD	3347	-0.01 (-0.03; 0.02)	1472	0.02 (-0.01; 0.05)	1875	-0.02 (-0.04; 0.01)
	non-movers	2752	0.00 (-0.02; 0.02)	1234	0.03 (0.00; 0.07)	1518	-0.01 (-0.04; 0.01)
	non-employees	1882	-0.01 (-0.04; 0.01)	683	0.01 (-0.04; 0.06)	1199	-0.02 (-0.05; 0.01)
	Never-Smoker	1411	0.00 (-0.03; 0.04)	652	0.05 (0.01; 0.10)	759	-0.02 (-0.06; 0.02)
	No incident Statin	2610	-0.01 (-0.03; 0.01)	1194	0.01 (-0.02; 0.04)	1416	-0.01 (-0.04; 0.01)
	excluding outliers	3065	0.01 (-0.01; 0.03)	1403	0.02 (0.00; 0.05)	1662	0.00 (-0.02; 0.02)
NO_2	Main (no CAD)	3155	-0.01 (-0.03; 0.01)	1435	0.03 (0.01; 0.06)	1720	-0.03 (-0.06; -0.01)
	with CAD	3347	-0.01 (-0.03; 0.01)	1472	0.03 (0.01; 0.06)	1875	-0.03 (-0.05; -0.01)
	non-movers	2752	0.00 (-0.02; 0.02)	1234	0.05 (0.01; 0.08)	1518	-0.03 (-0.06; -0.01)
	non-employees	1882	-0.02 (-0.04; 0.01)	683	0.03 (-0.02; 0.08)	1199	-0.03 (-0.06; 0.00)
	Never-Smoker	1411	-0.01 (-0.04; 0.02)	652	0.04 (0.00; 0.08)	759	-0.04 (-0.07; 0.00)
	No incident Statin	2610	-0.01 (-0.03; 0.01)	1194	0.03 (0.00; 0.06)	1416	-0.03 (-0.06; 0.00)
	excluding outliers	3065	0.00 (-0.02; 0.02)	1403	0.03 (0.00; 0.06)	1662	-0.01 (-0.03; 0.01)
L_{DEN}	Main (no CAD)	3155	-0.02 (-0.04; 0.01)	1435	0.03 (0.00; 0.07)	1720	-0.03 (-0.06; -0.01)
	with CAD	3347	-0.02 (-0.04; 0.01)	1472	0.03 (0.00; 0.06)	1875	-0.03 (-0.06; 0.00)
	non-movers	2752	-0.02 (-0.04; 0.01)	1234	0.03 (-0.01; 0.07)	1518	-0.02 (-0.05; 0.01)
	non-employees	1882	-0.01 (-0.04; 0.02)	683	0.04 (-0.02; 0.09)	1199	-0.02 (-0.05; 0.01)
	Never-Smoker	1411	-0.02 (-0.06; 0.02)	652	0.04 (-0.01; 0.09)	759	-0.04 (-0.08; 0.00)
	No incident Statin	2610	-0.01 (-0.04; 0.01)	1194	0.04 (0.00; 0.08)	1416	-0.02 (-0.05; 0.01)
	excluding outliers	3065	-0.01 (-0.03; 0.01)	1403	0.03 (0.00; 0.06)	1662	-0.02 (-0.05; 0.00)
L_{Night}	Main (no CAD)	3155	-0.02 (-0.04; 0.01)	1435	0.04 (0.00; 0.07)	1720	-0.04 (-0.07; -0.01)
	with CAD	3347	-0.02 (-0.04; 0.01)	1472	0.04 (0.00; 0.07)	1875	-0.03 (-0.06; -0.01)
	non-movers	2752	-0.02 (-0.04; 0.01)	1234	0.04 (0.00; 0.07)	1518	-0.02 (-0.05; 0.00)
	non-employees	1882	-0.01 (-0.04; 0.02)	683	0.04 (-0.01; 0.10)	1199	-0.02 (-0.05; 0.01)
	Never-Smoker	1411	-0.02 (-0.06; 0.02)	652	0.05 (0.00; 0.10)	759	-0.05 (-0.09; 0.00)
	No incident Statin	2610	1.01 (0.89; 1.15)	1194	1.22 (1.01; 1.47)	1416	0.84 (0.70; 1.01)
	excluding outliers	3065	0.99 (0.88; 1.11)	1403	1.18 (0.99; 1.40)	1662	0.82 (0.70; 0.98)

Table S5: Effect estimates per IQR increase in exposure on TAC-progression with regard to the interplay of air pollution and noise exposure (OR (95%-CI) for a TAC-progression and Change (95%-CI) of growth rate of TAC). Models are estimated participants with TACt0<10 (n=1,433), adjusted for age, sex, smoking status, alcohol consumption, physical activity, education, and follow-up time. Complementing Figure is Figure 2.

Exposure	Model	OR (95%-CI)	Change (95%-CI)
PM_{10}	Main	1.11 (0.94; 1.32)	0.02 (-0.01; 0.05)
	+L_{DEN}	1.09 (0.92; 1.29)	0.01 (-0.02; 0.05)
	L_{DEN} (high)	1.11 (0.93; 1.31)	0.02 (-0.02; 0.05)
	L_{DEN} (low)	1.12 (0.94; 1.33)	0.02 (-0.01; 0.05)
	+L_{Night}	1.08 (0.91; 1.29)	0.01 (-0.02; 0.04)
	L_{Night} (high)	1.10 (0.93; 1.31)	0.02 (-0.02; 0.05)
	L_{Night} (low)	1.12 (0.95; 1.33)	0.02 (-0.01; 0.05)
$PM_{2.5}$	Main	1.13 (0.95; 1.35)	0.04 (0.00; 0.07)
	+L_{DEN}	1.12 (0.94; 1.34)	0.03 (0.00; 0.07)
	L_{DEN} (high)	1.13 (0.94; 1.35)	0.03 (0.00; 0.07)
	L_{DEN} (low)	1.14 (0.95; 1.36)	0.04 (0.00; 0.07)
	+L_{Night}	1.11 (0.93; 1.33)	0.03 (0.00; 0.07)
	L_{Night} (high)	1.13 (0.94; 1.35)	0.03 (0.00; 0.07)
	L_{Night} (low)	1.14 (0.96; 1.37)	0.04 (0.00; 0.07)
PN_{acc}	Main	1.20 (1.03; 1.41)	0.02 (-0.01; 0.05)
	+L_{DEN}	1.18 (1.01; 1.39)	0.02 (-0.01; 0.05)
	L_{DEN} (high)	1.20 (1.02; 1.40)	0.02 (-0.01; 0.05)
	L_{DEN} (low)	1.21 (1.03; 1.42)	0.02 (-0.01; 0.05)
	+L_{Night}	1.18 (1.01; 1.38)	0.02 (-0.01; 0.05)
	L_{Night} (high)	1.19 (1.02; 1.40)	0.02 (-0.01; 0.05)
	L_{Night} (low)	1.22 (1.04; 1.42)	0.02 (-0.01; 0.05)
NO_2	Main	1.13 (0.97; 1.31)	0.03 (0.00; 0.06)
	+L_{DEN}	1.11 (0.95; 1.29)	0.03 (0.00; 0.06)
	L_{DEN} (high)	1.12 (0.97; 1.30)	0.03 (0.00; 0.06)
	L_{DEN} (low)	1.13 (0.97; 1.31)	0.03 (0.01; 0.06)
	+L_{Night}	1.10 (0.95; 1.28)	0.03 (0.00; 0.06)
	L_{Night} (high)	1.12 (0.96; 1.30)	0.03 (0.00; 0.06)
	L_{Night} (low)	1.13 (0.98; 1.32)	0.04 (0.01; 0.06)
L_{DEN}	Main	1.15 (0.96; 1.36)	0.03 (0.00; 0.07)
	+PM_{10}	1.13 (0.94; 1.35)	0.03 (-0.01; 0.06)
	PM_{10} (high)	1.13 (0.94; 1.34)	0.03 (0.00; 0.07)
	PM_{10} (low)	1.17 (0.98; 1.40)	0.03 (0.00; 0.07)
	+$PM_{2.5}$	1.14 (0.95; 1.35)	0.03 (0.00; 0.06)
	$PM_{2.5}$ (high)	1.14 (0.96; 1.36)	0.03 (0.00; 0.06)
	$PM_{2.5}$ (low)	1.17 (0.97; 1.40)	0.04 (0.00; 0.08)
	+PN	1.11 (0.93; 1.33)	0.03 (-0.01; 0.06)
	PN (high)	1.11 (0.93; 1.33)	0.03 (-0.01; 0.06)
	PN (low)	1.20 (1.00; 1.43)	0.04 (0.00; 0.07)
	+NO_2	1.12 (0.94; 1.34)	0.03 (-0.01; 0.06)
	NO_2 (high)	1.14 (0.96; 1.36)	0.03 (0.00; 0.06)
	NO_2 (low)	1.15 (0.96; 1.38)	0.04 (0.00; 0.07)
L_{Night}	Main	1.17 (0.99; 1.38)	0.04 (0.00; 0.07)
	+PM_{10}	1.15 (0.96; 1.37)	0.03 (0.00; 0.07)
	PM_{10} (high)	1.15 (0.96; 1.36)	0.04 (0.00; 0.07)
	PM_{10} (low)	1.19 (1.00; 1.42)	0.04 (0.00; 0.07)
	+$PM_{2.5}$	1.15 (0.97; 1.37)	0.03 (0.00; 0.07)
	$PM_{2.5}$ (high)	1.16 (0.98; 1.38)	0.03 (0.00; 0.07)
	$PM_{2.5}$ (low)	1.19 (0.99; 1.42)	0.05 (0.01; 0.08)
	+PN	1.13 (0.95; 1.35)	0.03 (0.00; 0.07)
	PN (high)	1.13 (0.95; 1.34)	0.03 (0.00; 0.07)
	PN (low)	1.23 (1.03; 1.46)	0.04 (0.01; 0.08)
	+NO_2	1.14 (0.96; 1.36)	0.03 (0.00; 0.06)
	NO_2 (high)	1.17 (0.98; 1.39)	0.03 (0.00; 0.07)
	NO_2 (low)	1.17 (0.98; 1.40)	0.04 (0.01; 0.07)

Table S6: Effect estimates for indicator variables of co-exposure levels on TAC-progression (OR (95%-CI) for a TAC-progression and Change (95%-CI) of growth rate of TAC). Models are estimated participants with TACt0<10 (n=1,433), adjusted for age, sex, smoking status, alcohol consumption, physical activity, education, and follow-up time. Complementing Figure is Figure S7.

AP	Noise	AP+Noise	OR (95%-CI)	Change (95%-CI)
PM_{10}	**L_{DEN}**	**low + high**	1.14 (0.84; 1.55)	0.03 (-0.03; 0.09)
		high + low	1.26 (0.92; 1.72)	0.01 (-0.05; 0.07)
		high + high	1.22 (0.75; 1.98)	0.03 (-0.06; 0.13)
	L_{Night}	**low + high**	1.28 (0.94; 1.74)	0.04 (-0.02; 0.10)
		high + low	1.28 (0.94; 1.76)	0.01 (-0.05; 0.08)
		high + high	1.29 (0.81; 2.07)	0.04 (-0.05; 0.13)
$PM_{2.5}$	**L_{DEN}**	**low + high**	1.20 (0.88; 1.62)	0.04 (-0.02; 0.10)
		high + low	1.24 (0.92; 1.67)	0.06 (0.00; 0.11)
		high + high	1.03 (0.62; 1.72)	0.05 (-0.05; 0.15)
	L_{Night}	**low + high**	1.35 (1.00; 1.84)	0.06 (0.00; 0.12)
		high + low	1.27 (0.94; 1.72)	0.06 (0.01; 0.12)
		high + high	1.08 (0.66; 1.78)	0.05 (-0.05; 0.14)
PN_{acc}	**L_{DEN}**	**low + high**	1.08 (0.79; 1.48)	0.03 (-0.03; 0.09)
		high + low	1.31 (0.97; 1.78)	0.04 (-0.02; 0.09)
		high + high	1.47 (0.92; 2.37)	0.07 (-0.03; 0.16)
	L_{Night}	**low + high**	1.19 (0.87; 1.62)	0.04 (-0.02; 0.10)
		high + low	1.30 (0.96; 1.77)	0.04 (-0.02; 0.10)
		high + high	1.65 (1.03; 2.65)	0.07 (-0.02; 0.16)
NO_2	**L_{DEN}**	**low + high**	1.37 (1.01; 1.87)	0.07 (0.01; 0.13)
		high + low	1.39 (1.03; 1.88)	0.07 (0.02; 0.13)
		high + high	0.80 (0.49; 1.29)	-0.01 (-0.10; 0.08)
	L_{Night}	**low + high**	1.49 (1.09; 2.03)	0.07 (0.01; 0.13)
		high + low	1.36 (1.01; 1.85)	0.06 (0.01; 0.12)
		high + high	0.91 (0.57; 1.46)	0.02 (-0.07; 0.11)

5 Air pollution and progression of atherosclerosis in different vessel beds—results from a prospective cohort study in the Ruhr Area, Germany. Hennig F, Geisel MH, Kälsch H, Lucht S, Mahabadi AA, Moebus S, et al. Environ Health Perspect 128:1–9 (2020)

A Section 508–conformant HTML version of this article is available at https://doi.org/10.1289/EHP7077.

Air Pollution and Progression of Atherosclerosis in Different Vessel Beds—Results from a Prospective Cohort Study in the Ruhr Area, Germany

Frauke Hennig,[1] Marie Henrike Geisel,[2,3] Hagen Kälsch,[4,5] Sarah Lucht,[1] Amir Abbas Mahabadi,[6] Susanne Moebus,[7] Raimund Erbel,[2] Nils Lehmann,[2] Karl-Heinz Jöckel,[2] André Scherag,[3,8] and Barbara Hoffmann[1], on behalf of the Heinz Nixdorf Recall Study Investigative Group

[1]Institute of Occupational, Social and Environmental Medicine, Center for Health and Society, Medical Faculty, Heinrich-Heine University Düsseldorf, Düsseldorf, Germany
[2]Institute for Medical Informatics, Biometry and Epidemiology, University Hospital, University Duisburg-Essen, Essen, Germany
[3]Research Group Clinical Epidemiology, Center for Sepsis Control and Care (CSCC), Jena University Hospital, Jena, Germany
[4]Department of Cardiology, Alfried Krupp Hospital Essen, Essen, Germany
[5]Witten/Herdecke University, Witten, Germany
[6]Department of Cardiology and Vascular Medicine, West German Heart and Vascular Center, University Hospital Essen, Essen, Germany
[7]Center of Urban Epidemiology (Cue), Institute for Medical Informatics, Biometry and Epidemiology, University Hospital Essen, Essen, Germany
[8]Institute of Medical Statistics, Computer and Data Sciences, Jena University Hospital, Jena, Germany

Objectives: Due to inconsistent epidemiological evidence on health effects of air pollution on progression of atherosclerosis, we investigated several air pollutants and their effects on progression of atherosclerosis, using carotid intima media thickness (cIMT), coronary calcification (CAC), and thoracic aortic calcification (TAC).

Methods: We used baseline (2000–2003) and 5-y follow-up (2006–2008) data from the German Heinz Nixdorf Recall cohort study, including 4,814 middle-aged adults. Residence-based long-term air pollution exposure, including particulate matter (PM) with aerodynamic diameter ≤ 2.5 μm ($PM_{2.5}$), (PM_{10}), and nitrogen dioxide (NO_2) was assessed using chemistry transport and land use regression (LUR) models. cIMT was quantified as side-specific median IMT assessed from standardized ultrasound images. CAC and TAC were quantified by computed tomography using the Agatston score. Development (yes/no) and progression of atherosclerosis (change in cIMT and annual growth rate for CAC/TAC) were analyzed with logistic and linear regression models, adjusting for age, sex, lifestyle variables, socioeconomic status, and traffic noise.

Results: While no clear associations were observed in the full study sample (mean age 59.1 ($\pm$7.6) y; 53% female), most air pollutants were marginally associated with progression of atherosclerosis in participants with no or low baseline atherosclerotic burden. Most consistently for CAC, e.g., a 1.5 $\mu g/m^3$ higher exposure to $PM_{2.5}$ (LUR) yielded an estimated odds ratio of 1.19 [95% confidence interval (CI): 1.03, 1.39] for progression of CAC and an increased annual growth rate of 2% (95% CI: 1%, 4%).

Conclusion: Our study suggests that development and progression of subclinical atherosclerosis is associated with long-term air pollution in middle-aged participants with no or minor atherosclerotic burden at baseline, while overall no consistent associations are observed. https://doi.org/10.1289/EHP7077

Background

Outdoor air pollution defines a global environmental risk factor for mortality (WHO Regional Office for Europe 2013; WHO 2009), and has been identified as leading contributor to the burden of disease worldwide (Gakidou et al. 2017). In particular, air pollution exposure contributes to the development of cardiovascular diseases (CVD) (Franklin et al. 2015; Rückerl et al. 2011). Although short-term exposure to particulate matter (PM) can trigger acute cardiovascular events, long-term exposure to PM was linked to the development of underlying chronic cardiovascular pathologies (Franklin et al. 2015), of which atherosclerosis is considered the major one (Künzli et al. 2011). Although experimental animal studies provide strong evidence for air pollution causing atherosclerosis through oxidative stress and systemic inflammation (Araujo et al. 2008; Soares et al. 2009; Sun et al. 2005), epidemiological evidence on air pollution effects on the development and progression of atherosclerosis along the pathway to cardiovascular endpoints is less consistent (Adar et al. 2013; Gan et al. 2014; Hennig et al. 2019; Kaufman et al. 2016; Künzli et al. 2010; Wilker et al. 2013).

In epidemiological studies, the degree of atherosclerosis can be quantified by medical imaging [e.g., computed tomography (CT) or ultrasound] of the arteries, measuring coronary artery calcification (CAC), thoracic aortic calcification (TAC), and intima media thickness of the common carotid artery, which have all been identified as predictors of cardiovascular and cerebrovascular events (Defilippis et al. 2011; Den Ruijter et al. 2012; Erbel et al. 2010; Folsom et al. 2008; Geisel et al. 2017; Kälsch et al. 2017; Nair et al. 2012; Polak et al. 2011).

Due to ease of assessment, most epidemiological studies on air pollution and progression of atherosclerosis studied the change in cIMT (Adar et al. 2013; Gan et al. 2014; Kaufman et al. 2016; Künzli et al. 2010; Wilker et al. 2013). A meta-analysis, including three longitudinal studies, reported a positive association between particulate matter with an aerodynamic diameter less or equal than 2.5 μm ($PM_{2.5}$) and carotid intima media thickness (cIMT) (Provost et al. 2015), in line with a single longitudinal study reporting a positive association between black carbon and cIMT (Wilker et al. 2015). The most recent analyses conducted in the North American Multi-Ethnic Study of Atherosclerosis only found an association of ozone with cIMT (Wang et al. 2019), but not between $PM_{2.5}$ or NO_2 and cIMT progression (Kaufman et al. 2016). In contrast, the investigators observed positive association of $PM_{2.5}$ and NO_2 with CAC progression (Kaufman et al. 2016), but others did not (Dorans et al. 2016). TAC progression has been shown to be related to air pollution only in early stages of thoracic calcification, but not in more advanced stages of atherosclerosis (Hennig et al. 2019).

Address correspondence to Frauke Hennig on behalf of the Institute of Occupational, Social and Environmental Medicine, Center for Health and Society, Faculty of Medicine, University of Düsseldorf, Germany. Telephone: +49-211- 586729110. Email: frauke.hennig@gmail.com

Supplemental Material is available online (https://doi.org/10.1289/EHP7077).

The authors declare they have no actual or potential competing financial interests.

Received 16 March 2020; Revised 23 July 2020; Accepted 4 September 2020; Published 5 October 2020.

Although all existing studies provide considerable sources of heterogeneity (outcome definitions, air pollutants and exposure modeling, study populations and statistical methods) that could explain inconsistent epidemiological findings, we aimed to comprehensively investigate effects of air pollution on the development and progression of atherosclerosis. To that end, we investigated progression of atherosclerosis in three different vessel beds (coronary circulation, thoracic aorta, and carotid arteries) applying different imaging methods (CT and ultrasound) in participants from the Heinz Nixdorf Recall (HNR) cohort study. To investigate possible reasons for heterogeneity between studies due to selection of study populations, and motivated by our prior findings of stronger associations at lower baseline levels of atherosclerosis, we investigated subgroup effects based on atherosclerosis burden at baseline (t0) and explored individual susceptibility factors. Furthermore, we made use of two complementary air pollution exposure models, yielding *a*) point-specific estimates [land use regression (LUR) modeling], which capture small-scale differences in air pollution exposure specifically related to traffic, and *b*) urban background exposure [chemistry transport modeling (CTM)], which captures changes over time. Finally, we took ambient noise exposure into account, a potential confounder within the air pollution and cardiovascular framework (Münzel et al. 2018).

Methods

Study Design

The HNR (Risk Factors, Evaluation of Coronary Calcification, and Lifestyle) study is a population-based prospective cohort study, including 4,814 randomly selected participants of 45 to 75 years of age at baseline (t0: 2000–2003) from three large adjacent cities (Mülheim, Essen, and Bochum) in the metropolitan Ruhr area of Germany [recruitment efficacy proportion: 55.8%; (Stang et al. 2005)]. The study design has been described in detail elsewhere (Schmermund et al. 2002). The study was approved by the institutional ethics committees of the University of Duisburg-Essen and the University Hospital of Essen and adhered to strict internal and external quality assurance protocols. The follow-up examination (t1: 2006–2008) had a response of 86.4% ($n = 4{,}157$). Assessment for both examinations included a self-administered questionnaire, face-to-face interviews for personal risk factor assessment and clinical examinations, and comprehensive laboratory tests according to standard protocols. All participants gave informed consent.

Exposure Assessment

Long-term exposure to residential ambient air pollution was assessed using concentrations of particulate matter (PM) with an aerodynamic diameter ≤ 2.5 μm [$PM_{2.5}$ ($\mu g/m^3$)], and ≤ 10 μm [PM_{10} ($\mu g/m^3$)], the number of accumulation mode particles PN_{acc} (#/mL), $PM_{2.5}$ absorbance [$PM_{2.5\,abs}$ ($\mu g/m^3$)], and nitrogen dioxide [NO_2 ($\mu g/m^3$)]. To reflect long-term urban background exposure differences within our study area, we estimated mean long-term air pollution concentrations for $PM_{2.5}$, PM_{10}, PN_{acc}, and NO_2 in a spatial grid of 1×1 km^2 assigned to participant's addresses (Nonnemacher et al. 2014), using the European Air pollution Dispersion chemistry transport model (EURAD-CTM, short: CTM). The EURAD-CTM uses input data from official emission inventories (i.e., traffic, industry, agriculture, energy production, etc.) (European Environment Agency 2011) data on meteorology and regional topography, in combination with modeling the dispersion, chemical reactivity, and mass transport between horizontal strata and deposition to calculate daily exposure concentrations in a 1×1 km^2 grid (Memmesheimer et al. 2004). The EURAD-CTM includes data assimilation on an hourly basis for routinely measured air pollutants (PM_{10}, NO_2), using routine monitoring data in North Rhine-Westphalia (NRW) provided by the local environmental agency (State Agency for Nature, Environment, and Consumer Protection, LANUV-NRW). For this study, daily concentrations were assessed during the examination years (2000–2003 and 2006–2008), which were assigned to participants' baseline and follow-up addresses using a geographic information system. Because model data from 2004 to 2005 were not available, long-term exposure was calculated as the mean of all daily values over both examination periods (2000–2003 and 2006–2008).

In addition, annual exposure to $PM_{2.5}$, PM_{10}, $PM_{2.5abs}$, and NO_2 at point of participants' residences was estimated using land use regression (LUR) models that were locally developed as part of the European Study of Cohorts on Air Pollution Effects using a standardized protocol (Beelen et al. 2013; Eeftens et al. 2012). Each LUR model was locally cross-validated with the leave-one-out-cross-validation (LOOCV). Resulting explained variances (adjusted R^2) (and LOOCV-R^2) within the Ruhr Area were 85% (79%) for predicting $PM_{2.5}$, 66% (59%) for predicting PM_{10}, 97% (95%) for predicting $PM_{2.5abs}$, and 88% (82%) for predicting NO_2 (Beelen et al. 2013; Eeftens et al. 2012). The overall agreement between long-term urban background concentrations (estimated with the EURAD-CTM) and point-specific concentrations (estimated with the ESCAPE LUR) was moderate to low (Spearman correlations <0.45), reflecting different aspects of the air pollution exposure conditions within a densely populated and industrialized urban area (de Hoogh et al. 2014; Hennig et al. 2016).

Assessment of the Outcomes

CIMT was assessed by B-mode ultrasound (Vivid FiVe, GE Ultrasound Europe), using a linear array 10-MHz scan head, at the left and right common carotid artery (Bauer et al. 2009). The semiautomatic computer-based software Artery Measurement (AMS) II (version 1.151; Chalmers University of Technology) (Wendelhag et al. 1997) was used to determine median cIMT per ultrasound image (exported offline as bitmap file) at the far wall within the first 10 mm proximal to the bulb. To reduce measurement error, images were grouped into work packages of approximately 200 images, including 10 repeated images each, to monitor intrareader variability. If mean intrareader variability was >0.03 mm, the respective reader was trained again and the corresponding work package had to be remeasured to achieve high quality measurement data. Offline measurements were performed by six certified readers according to a standardized operation procedure.

Mean side-specific cIMT value (millimeters) for baseline and 5-y follow-up was calculated based on the median values of all available images for each examination. Progression (yes/no) was operationalized as $cIMT_{t1} - cIMT_{t0} > 0$, and the extent of progression was assessed as annual μm-change in cIMT: $\Delta CIMT = (cIMT_{t1} - cIMT_{t0})/\text{follow-up time}$ for the left and right body side. An early stage (no/minor) vs. a more advanced stage of atherosclerotic burden at baseline was defined by dichotomizing at a cut point of 0.7 mm (≤ 0.7 vs. >0.7 mm), which was identified as the upper value of a normal cIMT range for middle-aged adults (O'Leary et al. 1999).

Participants underwent cardiac CT as part of the primary study aim of the HNR Study. CAC and TAC were derived from non–contrast-enhanced electron-beam CT scans, using a C-100 (t0) and C-150 (t1) scanner (GE, Imatron), following a standardized methodology for acquisition and interpretation of the scans, which has been reported previously (Erbel et al. 2010; Schmermund et al. 2002). The CTs were operated in the single-slice (3 mm) mode with an image acquisition time of 100 ms. The Agatston algorithm was used for quantification of calcification, identifying a calcified lesion as at least 4 contiguous pixels

with a CT density ≥130 Hounsfield (Agatston et al. 1990). Analyses were performed using a Virtuoso workstation (Siemens Medical Solutions). The total CAC score was calculated, comprising all calcified lesions in the coronary system. A reassessment of CAC scoring was implemented as quality control when extreme progression or regression was observed (Lehmann et al. 2018). The total TAC score was calculated, comprising all calcified lesions, including segments of the ascending and descending portion of the thoracic aorta that were visible in the CT scan (Kälsch et al. 2013b). Progression (yes/no) of CAC and TAC was operationalized as $CAC_{t1} - CAC_{t0} > 0$ and $TAC_{t1} - TAC_{t0} > 0$, respectively. Due to its exponential nature, extent of progression was assessed as the annual growth rate in Agatston score: $(log\,(CAC_{t1}+1) - log\,(CAC_{t0}+1))$/years of follow-up (Lehmann et al. 2018) and $(log\,(TAC_{t1}+1) - log\,(TAC_{t0}+1))$/ years of follow-up respectively (Kälsch et al. 2017). A beta-coefficient of 0.01 in the linear regression model can be interpreted as an exposure-related 1% increase in annual growth rate. An early stage (no/minor) vs. a more advanced stage of atherosclerotic burden at baseline was defined by dichotomizing at cut point 10 (no/minor calcification 0–9 Agatston score units vs. more extensive calcification ≥10 Agatston score units).

Definition of Covariates

Long-term road traffic noise was modeled for the year 2006 according to the European Union Directive 2002/49/EC (EU 2008) and the validated national calculation method VBUS/RLS-90 (28) for the year 2006 (supplied from the city administrations), considering small-scale topography of the area, dimensions of buildings, noise barriers, first order reflections, street axis, measured or estimated vehicle-type specific traffic density for all roads, speed limit, and type of street surface. Average traffic noise values [A-weighted dB(A)] day–evening–night (24 h) noise (Lden) at the participant's residence was estimated at a height of 4 ± 0.2 m selecting the highest estimated noise level within a buffer of 10 m from the residence.

Individual socioeconomic status (SES) was defined as years of education in four categories (≤10, 11–13, 14–17, ≥18 y) according to the International Standard Classification of Education (UNESCO 1997). Neighborhood SES (nSES) was assessed by unemployment rate (%) for each administrative neighborhood (median size: 11,263 inhabitants) obtained from local census authorities for t0 (2000–2003) (Dragano et al. 2009). Smoking status was defined as current, ex- (>1 y since quitting), and never-smoker. Lifetime cumulative smoking was assessed in pack-years at baseline. Exposure to environmental tobacco smoke (ETS) referred to ETS at home, at work, or in other places. Physical activity (yes/no) was assessed as regular sporting activities at least once a week for a minimum of 30 min. Alcohol consumption was operationalized as drinks per week. Anthropometric measurements (height, weight) were conducted according to standardized protocols to calculate the body mass index [BMI (kg/m^2)]. Diabetes mellitus (DM) was defined as prior physician diagnosis of diabetes or taking an antidiabetic drug or having a blood glucose ≥200 mg/dL or having a fasting blood glucose ≥126 mg/dL. High-density lipoprotein (HDL), low-density lipoprotein (LDL) cholesterol, and high sensitivity C-reactive protein (hs-CRP) (all mg/dL) were measured with standard methods at the central laboratory of the University Hospital of Essen. In the analysis, we used quotient of LDL-C and HDL-C (LDL-C/HDL-C). Confirmed medication taken in the previous 7 d was assigned using the WHO Anatomical Therapeutic Chemical classification system (ATC) (WHO 2013). Blood pressure was calculated as the mean of the second and third of three measurements, using an oscillometric method according to a standard protocol. Hypertension was defined as systolic or diastolic blood pressure of 140 mmHg or greater or 90 mmHg or greater, respectively, or use of antihypertensive medication. Incident coronary heart disease (CHD) was based on self-reported incident coronary events that met predefined study criteria (Schmermund et al. 2002) and which were adjudicated with medical records by a study end point committee (Erbel et al. 2010). Updated information on all baseline characteristics were obtained at the first follow-up examination, with the exception of neighborhood unemployment rate, education, and cumulative smoking exposure, which were only obtained at baseline. Traffic was assessed as distance (in meters) to high-traffic roads [i.e., roads with a traffic count of >26,000 vehicles/day (upper quintile of traffic density)], using official digitized maps with a precision of at least 0.5 m and the median strip between the oncoming traffic lanes as reference.

Analytic Strategies

The statistical analysis was conducted in the study sample with participants of the baseline and first follow-up examination, free of CHD at baseline ($n = 3{,}907$), available exposure data for the complete follow-up ($n = 3{,}753$), nonmissing data on progression of atherosclerosis for at least one marker ($n = 3{,}625$) and nonmissing covariate data ($n = 3{,}480$) (Figure S1). Due to different sample sizes for atherosclerosis markers, the main analysis was conducted in marker-specific subsamples. For the analysis of cIMT, 2,116 participants had nonmissing information on left cIMT, 2,197 had nonmissing data on right cIMT, 3,220 had nonmissing data on CAC, and 3,126 had nonmissing data on TAC.

We *a*) used logistic regression models to estimate odds ratios [OR; and 95% confidence intervals (CI)] for progression (yes/no) per interquartile range (IQR) increase in air pollutant concentration; and *b*) estimated the effect of an IQR increase in concentrations of air pollution on annual change of atherosclerosis (wall thickening and growth rate of calcification), using linear regression models. All models were estimated for each marker separately in the total study population and in subgroups of participants with no/minor vs. advanced atherosclerotic burden at baseline. Subgroup effects were estimated by adding the subgroup indicator and an interaction term between the continuous exposure and the subgroup indicator. *c*) We estimated the 5-y risk of incident calcification in the coronaries and the thoracic aorta with logistic regression.

Confounder adjustment was based on a hypothesized directed acyclic graph (DAG; Figure S2), a qualitative method emphasized by Greenland et al. (1999), complemented with a quantitative evaluation of suggested minimal sufficient adjustment sets and covariate extensions (Figures S3 and S4). Our main model included age, sex, BMI, smoking status and quantity, environmental tobacco smoke (ETS), LDL-C/HDL-C, physical activity, education, traffic noise, and for dichotomous outcomes additionally years of follow-up. Moreover, we investigated extended models including nSES and city.

In a separate step, we added potentially mediating covariates along the hypothesized pathway linking air pollution to atherosclerosis as covariates to the analysis. These covariates included baseline atherosclerosis, incident intake of statins during follow-up, hs-CRP, blood pressure, prevalent and incident hypertension, and prevalent and incident DM.

We also investigated effect modification by categorized personal risk factors, including sex (male vs. female), age (≤65 y old vs. >65 y old), BMI (≤30 vs. >30), DM (yes vs. no), incident statin intake (yes vs. no), low education (≤10 y vs. >10 y), smoking (current vs. ex- and never-smoker), and high cardiovascular risk defined using Framingham risk score. Effect modification was investigated using interaction terms between categorical characteristics as described above and the respective continuous

exposure in the main model. Effect estimates were evaluated visually based on 95% CIs.

Sensitivity analyses included a more conservative cut point to identify progression (yes/no) in subclinical markers, namely 10% and 20% instead of 0. We conducted Poisson regression as an alternative approach to logistic regression to prevent overestimation of the relative risk (RR) in the highly frequent outcome. Moreover, we investigated an alternative metric of CAC progression, namely faster progression compared with internal expected reference values, defined by the percentile of CAC at baseline [$CAC_{expected\_t1} - CAC_{observed\_t1} < 0$ (Lehmann et al. 2018)], which was based on the hypothesis that the individual's CAC progresses exponentially with time, similar to CAC percentiles with age. We also investigated mean cIMT progression considering the mean of both (left and/or right) side.

In addition, we investigated whether a different time window of exposure (namely, baseline exposure (2001–2003), as well as mean exposure between 2006 and 2008, estimated by the EURAD-CTM), affected our main results. We also estimated exposure effect estimates for subgroups less likely affected by exposure misclassification due to mobility using employment status (nonemployees or part-time employees working $\leq$15 h/wk vs. full-time employees), and due to change of residence prior to baseline (nonmovers vs. movers).

Results

Out of 3,480 participants free of CAD at baseline with two valid measurements (one at baseline and one at follow-up examination) for at least one marker of subclinical atherosclerosis, complete exposure information and nonmissing covariate data, marker-specific subsamples were quite homogeneous with regard to personal characteristics (BMI, smoking status, education, or physical inactivity) (Table 1), including roughly 53% women and a mean age $\sim$59.0 [standard deviation (SD) 7.6] years of age at baseline.

Air pollutant concentrations at baseline were below current European air quality limit values, but clearly higher than World Health Organization recommendations (Table 2). Correlations between air pollutants were mostly moderate to high (Table 2). LUR modeling estimated higher long-term particle concentrations, but lower NO_2 concentrations than CTM (Figure S5). Mean air pollutant concentrations estimated by CTM decreased for all pollutants (Figure S6) during the follow-up period with overall high correlations between examination periods (>0.87) (Table S1).

Mean baseline cIMT (left) was 710.9 (172.1) μm with a calculated annual change of 21.1 (31.9) μm, resulting in 78% participants with positive progression after 5 y (Table 1, Figure S7). Mean baseline cIMT (right) was 693.3 (168.9) μm with a calculated annual change of 21.5 (29.8) μm, resulting in 81% participants with progression after 5 y. Median baseline CAC was 7.2 (IQR 0.0–88.2) Agatston Score units with an observed annual growth rate of 0.106 (SD 0.225) and 60% progression after 5 years of follow-up. Incident CAC was observed in 25.7% participants with no CAC add baseline ($n = 1{,}154$). Median baseline TAC was 16.0 (IQR 0.0–108.3) Agatston Score units with an observed annual growth rate of 0.091 (SD 0.470) and 53% progression after 5 years of follow-up. Incident TAC was observed in 42.2% participants with no TAC add baseline ($n = 1{,}161$). In all four markers, overall progression was more pronounced in participants with no or minor atherosclerotic burden (Figure S8).

Air Pollution and Progression of Atherosclerosis

In the full sample analysis, we observed no clear pattern of an association between any of the air pollutants and progression or degree of progression of atherosclerosis. Although most effect estimates for the crude and main (noise-adjusted) were positive, CI were wide and included the null effect (Figure 1, with complementing numbers in Table S2). Additional covariate adjustment (residence and nSES) as covariates did not substantially change effect estimates (Figures S3 and S4), nor did including potential mediating factors (Figures S9 and S10).

Baseline level of subclinical atherosclerosis had an impact on the association of air pollutants with progression of atherosclerosis (Figure 1 with complementing numbers in Tables S3). Most consistently, PM_{10}, $PM_{2.5}$, PN_{acc}, and NO_2 modeled by CTM were related to progression of left cIMT, CAC, and TAC in participants with no or minor burden of atherosclerosis at baseline (e.g., an estimated OR of 1.12 [0.96, 1.31] for progression of CAC per 3.8 $\mu g/m^3$ increase in PM_{10}). PM_{10} and $PM_{2.5}$ modeled by LUR were associated with left cIMT and CAC [e.g., a 1.5 $\mu g/m^3$ higher exposure to $PM_{2.5}$ (LUR) yielded an estimated OR of 1.19 (95% CI: 1.03, 1.39) for progression of CAC and an increased annual growth rate of 2% (95% CI: 1%, 4%)]. On the other hand, effect estimates for participants with more advanced atherosclerotic burden yielded inverse or null findings, most notably for TAC. For right cIMT, we observed no consistent associations across pollutants and outcome definition with regard to atherosclerotic burden at baseline. Supporting findings in participants with no or minor atherosclerotic burden, long-term air pollution exposure was consistently related to incident CAC, whereas CI for incident TAC were elevated but most often included the null (Table 3).

We did not observe clear and consistent effect modification by personal characteristics (Figure S11). In general, we found a pattern of stronger associations in participants who had diabetes, participants who were obese, and less-educated participants, whereas the analysis of cIMT suggests possible inverse associations in participants with a high baseline Framingham Risk Score and participants with incident statin intake during the follow-up period.

Sensitivity Analyses

Results of evaluating progression with a more conservative cut point of 10% change (and 20%) did not differ notably from the main results (Table S4). The alternative approach of applying a Poisson regression to estimate RR instead of OR, as expected, yielded smaller point estimates yet did not change our main conclusions (Table S4). Investigating progression of mean of left and/or right cIMT as expected yielded less consistent findings, and evaluating whether CAC progressed faster than following the expected percentile did not change the observed main findings (Table S5).

Inspecting different time windows of air pollutant exposures separately did not differ from the main approach of combining exposure time windows to one long-term exposure measure (Table S6). Exploring exposure misclassification based on variables of personal mobility and relocation prior to baseline showed that estimated effects were quite stable in the group of nonemployees and nonmovers (Figure S13).

Discussion

In this study of middle-aged adults in Germany, our analysis shows no consistent associations of long-term exposure to ambient particulate and gaseous air pollutants with the development and progression of atherosclerosis in different vessels beds in the full sample over a follow-up time of roughly 5 y. However, in those participants with no or only minor atherosclerotic burden at baseline, we observed associations of long-term exposure to

Table 1. Summary statistics for outcome-specific subpopulations within the Heinz-Nixdorf Recall Study sample at baseline unless otherwise indicated. Continuous variables with a symmetric distribution are displayed using mean ± standard deviation (SD), continuous variables with a skewed distribution are displayed using median (Q1, Q3), and categorical variables are displayed by absolute and relative frequencies [*n* (%)].

Variable	Value	cIMT (left) $n = 2{,}116$	cIMT (right) $n = 2{,}197$	CAC $n = 3{,}220$	TAC $n = 3{,}126$
cIMT, t0 (μm)	—	710.9 ± 172.1	693.3 ± 168.9	—	—
cIMT, t1 (μm)	—	817.2 ± 185.4	801.9 ± 161.1	—	—
Change in cIMT (μm)	—	21.1 ± 31.9	21.5 ± 29.8	—	—
cIMT progression	No	465 (22.0%)	426 (19.4%)	—	—
	Yes	1,651 (78.0%)	1,771 (80.6%)	—	—
Calcification, t0 (Agatston score)	—	—	—	7.2 (0.0, 88.2)	16.0 (0.0, 108.3)
Calcification, t1 (Agatston score)	—	—	—	26.8 (0.0, 193.9)	29.5 (0.0, 307.1)
Change in calcification (growth rate)	—	—	—	0.106 ± 0.225	0.091 ± 0.470
Calcification progression	No	—	—	1,291 (40.1%)	1,466 (46.9%)
	Yes	—	—	1,929 (59.9%)	1,660 (53.1%)
Incident calcification[a]	No	—	—	857 (26.6%)	671 (21.5%)
	Yes	—	—	297 (9.2%)	490 (15.7%)
Age (y)	—	58.9 ± 7.5	58.9 ± 7.6	59.0 ± 7.6	59.1 ± 7.6
Sex	Female	1,109 (52.4%)	1,156 (52.6%)	1,726 (53.6%)	1,663 (53.2%)
	Male	1,007 (47.6%)	1,041 (47.4%)	1,494 (46.4%)	1,463 (46.8%)
Education	≤10 y	204 (9.6%)	208 (9.5%)	318 (9.9%)	310 (9.9%)
	≥18 y	256 (12.1%)	266 (12.1%)	363 (11.3%)	349 (11.2%)
	11–13 y	1,169 (55.2%)	1,215 (55.3%)	1,821 (56.6%)	1,767 (56.5%)
	14–17 y	487 (23.0%)	508 (23.1%)	718 (22.3%)	700 (22.4%)
Unemployed rate (2001) (%)	—	12.5 ± 3.4	12.4 ± 3.4	12.4 ± 3.4	12.4 ± 3.4
Smoking status	Current smoker	481 (22.7%)	500 (22.8%)	729 (22.6%)	698 (22.3%)
	Ex-smoker	688 (32.5%)	717 (32.6%)	1,036 (32.2%)	1,026 (32.8%)
	Never smoker	947 (44.8%)	980 (44.6%)	1,455 (45.2%)	1,402 (44.8%)
Cumulative smoking (pack-years)	—	2.4 (0.0, 21.0)	2.7 (0.0, 21.8)	2.2 (0.0, 22.0)	2.4 (0.0, 22.0)
ETS (any exposure)	No	1,389 (65.6%)	1,437 (65.4%)	2,084 (64.7%)	2,039 (65.2%)
	Yes	727 (34.4%)	760 (34.6%)	1,136 (35.3%)	1,087 (34.8%)
Physical inactivity	No	1,196 (56.5%)	1,241 (56.5%)	1,809 (56.2%)	1,756 (56.2%)
	Yes	920 (43.5%)	956 (43.5%)	1,411 (43.8%)	1,370 (43.8%)
BMI (kg/m^2)	—	27.4 ± 4.4	27.4 ± 4.4	27.4 ± 4.4	27.6 ± 4.3
LDL-C (mg/dL)	—	146.5 ± 36.5	146.7 ± 35.8	146.2 ± 35.6	146.4 ± 35.7
HDL-C (mg/dL)	—	59.7 ± 17.4	59.5 ± 17.4	59.3 ± 17.1	59.3 ± 17.3
Statin medication[a]	No	1,902 (89.9%)	1,983 (90.3%)	2,805 (87.1%)	2,719 (87.0%)
	Yes	160 (7.6%)	152 (6.9%)	216 (6.7%)	215 (6.9%)
Incident statin use[a]	No	1,846 (87.2%)	1,896 (86.3%)	2,723 (84.6%)	2,603 (83.3%)
	Yes	216 (10.2%)	239 (10.9%)	298 (9.3%)	331 (10.6%)
Hs-CRP (mg/dL)[a]	—	0.1 (0.1, 0.3)	0.1 (0.1, 0.3)	0.1 (0.1, 0.3)	0.1 (0.1, 0.3)
Framingham Risk[a]	High	237 (11.2%)	244 (11.1%)	399 (12.4%)	398 (12.7%)
	Low	1,197 (56.6%)	1,229 (55.9%)	1,802 (56.0%)	1,715 (54.9%)
	Mediate	680 (32.1%)	723 (32.9%)	1,019 (31.6%)	1,012 (32.4%)
Hypertension[a]	No	1,034 (48.9%)	1,079 (49.1%)	1,515 (47.0%)	1,464 (46.8%)
	Yes	1,080 (51.0%)	1,117 (50.8%)	1,705 (53.0%)	1,661 (53.1%)
Incident hypertension[a]	No	688 (32.5%)	699 (31.8%)	988 (30.7%)	951 (30.4%)
	Yes	345 (16.3%)	380 (17.3%)	526 (16.3%)	512 (16.4%)
Diabetes	No	1,895 (89.6%)	1,954 (88.9%)	2,853 (88.6%)	2,764 (88.4%)
	Yes	221 (10.4%)	243 (11.1%)	367 (11.4%)	362 (11.6%)
Incident type 2 diabetes[a]	No	1,740 (82.2%)	1,798 (81.8%)	2,617 (81.3%)	2,529 (80.9%)
	Yes	155 (7.3%)	156 (7.1%)	236 (7.3%)	235 (7.5%)
Developed coronary heart disease	No	2,056 (97.2%)	2,126 (96.8%)	3,205 (99.5%)	3,051 (97.6%)
	Yes	60 (2.8%)	71 (3.2%)	15 (0.5%)	75 (2.4%)
Lden [dB(A)]	—	53.9 ± 9.4	53.8 ± 9.4	53.9 ± 9.3	53.9 ± 9.3
Distance to highly trafficked road (m)	—	1,018.0 ± 808.7	1,033.2 ± 817.2	1,023.7 ± 811.3	1,025.5 ± 818.4

[a]Including additional missing values. For subpopulation of cIMT (left): Statin medication ($n = 54$), Incident statin use ($n = 54$), Hs-CRP [mg/dl] ($n = 5$), Framingham Risk ($n = 2$), Hypertension ($n = 2$), Incident hypertension ($n = 1{,}083$), Incident type 2 diabetes ($n = 221$). For subpopulation of cIMT (right): Statin medication ($n = 62$), Incident statin use ($n = 62$), Hs-CRP (mg/dl) ($n = 6$), Framingham Risk ($n = 1$), Hypertension ($n = 1$), Incident hypertension ($n = 1{,}118$), Incident type 2 diabetes ($n = 243$). For subpopulation of CAC: Statin medication ($n = 199$), Incident statin use ($n = 199$), Hs-CRP (mg/dL) ($n = 8$), Incident hypertension ($n = 1{,}706$), Incident type 2 diabetes ($n = 367$), Incident calcification ($n = 2{,}066$). For subpopulation of TAC: Statin medication ($n = 192$), Incident statin use ($n = 192$), Hs-CRP (mg/dL) ($n = 8$), Framingham Risk ($n = 1$), Hypertension ($n = 1$), Incident hypertension ($n = 1{,}663$), Incident type 2 diabetes ($n = 362$), Incident calcification ($n = 1{,}965$). —, no data.

particulate air pollution with progression of atherosclerosis, whereas estimated effects in the group with more advanced atherosclerotic burden at baseline were null or inverse.

Long-term air pollution has been shown to be associated with cerebrovascular and cardiovascular events in multiple studies (U.S. EPA 2019; WHO 2013), including prior analyses of the HNR Study (Hoffmann et al. 2015). Therefore, our findings are important regarding the underlying hypothesis that ambient air pollution may lead to atherosclerosis on the pathway to CVD, possibly explaining the higher incidence and prevalence of cardiovascular and cerebrovascular disease observed in people with higher air pollution exposure. Our findings of associations limited to earlier stages of atherosclerosis point to a higher susceptibility to air pollution in the development of atherosclerosis, which has also been observed in our prior analysis of environmental tobacco smoke and CAC (Peinemann et al. 2011). In contrast, our findings did not support a susceptibility to air pollution exposure in people with a higher cardiac risk profile based on personal characteristics or with an advanced burden of atherosclerosis. These findings are in line with investigations based on the Framingham Heart Study, which also found null or inverse estimates in analyses of participants with apparent calcifications at baseline

Table 2. Summary statistics [mean ± standard deviation (SD)] of air pollutant concentrations (CTM during enrollment periods 2001–2003 and 2006–2008 and LUR) and pairwise Spearman correlation coefficients, estimated in 3,480 participants of the Heinz Nixdorf Recall Study population.

Exposure	Mean ± SD	IQR	PM_{10} (LUR)	$PM_{2.5}$ (CTM)	$PM_{2.5}$ (LUR)	PN_{acc} (CTM)	$PM_{2.5abs}$ (LUR)	NO_2 (CTM)	NO_2 (LUR)
PM_{10} (CTM) (μg/m^3)	20.3 ± 2.6	3.8	0.33	0.86	0.56	0.79	0.35	0.62	0.5
PM_{10} (LUR) (μg/m^3)	27.8 ± 1.9	2.1		0.18	0.89	0.46	0.9	0.34	0.55
$PM_{2.5}$ (CTM) (μg/m^3)	16.7 ± 1.3	2.0			0.38	0.72	0.14	0.69	0.4
$PM_{2.5}$ (LUR) (μg/m^3)	18.4 ± 1.1	1.5				0.73	0.89	0.46	0.66
PN_{acc} (CTM) (#/mL)	3,408.4 ± 387.6	527.5					0.55	0.74	0.56
$PM_{2.5abs}$ (LUR) (0.0001/m)	1.6 ± 0.4	0.4						0.34	0.63
NO_2 (CTM) (μg/m^3)	39.5 ± 4.0	5.4							0.41
NO_2 (LUR) (μg/m^3)	30.2 ± 4.9	6.2							

Note: CTM, chemistry transport modeling; IQR, interquartile range; LUR, land use regression.

(Dorans et. al 2016, 2017). One explanation for inverse associations in participants with advanced atherosclerosis at baseline could be the dominating effect of cardioprotective therapy, which is more common in participants with advanced atherosclerosis.

However, not all vessel beds and their markers of subclinical atherosclerosis were equally susceptible to the effects of long-term exposure to air pollution. We observed the most consistent associations for progression of CAC (dichotomous progression, annual growth rate, and incidence) and for the left cIMT. Although side-specific differences in cIMT have been mentioned in literature before (Foerch et al. 2003; Luo et al. 2011), we cannot explain the observed differences between left and right cIMT with regard to air pollution exposure, but we speculate that there could be different turbulence patterns leading to a higher susceptibility of the left common carotid vessel wall. Overall, results for cIMT vary greatly across studies (Perez et al. 2015). Only a few studies have investigated the association of air exposure with progression of cIMT, and these studies find striking differences in annual progression—from a mean of 1–5 μm/y in a selected group of participants in atherosclerosis prevention trials (Künzli et al. 2010), 10–13 μm/y in the MESA cohort (Wang et al. 2019), and 22 μm/y in general population of the HNR Study reported here. In addition to biological characteristics and medical interventions, assessment methods regarding location, technique, and inclusion of plaque, as well as different consideration of body side (using mean of left and right cIMT or only right cIMT), contribute to these differences and possibly mask associations with air pollution.

Fewer but also inconsistent results can be found for investigations of long-term air pollution exposure and development and progression of CAC or aortic calcification. Kaufman et al. (2016) and Wang et al. (2019) both observed associations of $PM_{2.5}$ and NO_2 with CAC progression. Wang et al. (2019) found similar results for long-term exposure to high levels of ozone. Two analyses of the Framingham Heart Study investigating progression of coronary and aortic calcification do not find any association with roadway proximity or $PM_{2.5}$ (Dorans et al. 2016, 2017), whereas we had already observed associations restricted to participants with no or only minor manifestation of TAC at baseline in our prior study (Hennig et al. 2019).

Despite the fundamental differences in the applied exposure models, we observed generally similar patterns of associations with subclinical atherosclerosis for both models, strengthening the fact that our findings are not dependent on a specific air

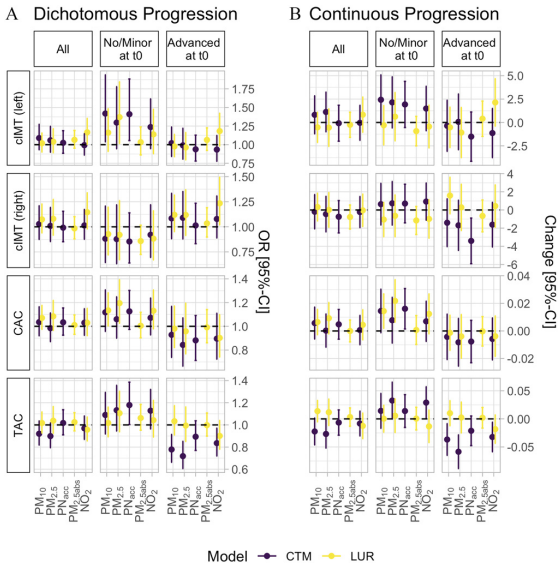

Figure 1. Main effect estimates for the associations between different air pollutants and progression of atherosclerosis in subpopulations of the Heinz Nixdorf Recall Study based on the marker of atherosclerosis, investing all participants (cIMT (left) = 2,116, cIMT(right) = 2,197, CAC = 3,220, TAC = 3,126), participants with no/minor atherosclerotic burden at baseline (t0) (cIMT(left) = 1,054, cIMT(right) = 1,017, CAC = 1,527, TAC = 1,761), and participants with advanced atherosclerotic burden at t0 (cIMT(left) = 1,203, cIMT(right) = 1,317, CAC = 1,693, TAC = 1,469). Main model is adjusted for age, sex, BMI, smoking status and quantity, ETS, LDL-C/HDL-C, physical activity, education, traffic noise and for dichotomous outcomes additionally years of follow-up. (A) This panel displays OR (95% CI) for any progression in atherosclerosis based on an IQR in exposure. (B) This panel displays change in thickness (μm) for cIMT and change in growth rate for CAC and TAC (complementing numbers are in Tables S2 and S3). Note: BMI, body mass index; CAC, coronary artery calcification; CI, confidence interval; cIMT, carotid intima media thickness; ETS, environmental tobacco smoke; HDL-C, high-density lipoprotein cholesterol; IQR, interquartile range; LDL-C, low-density lipoprotein cholesterol; OR, odds ratio; TAC, thoracic aortic calcification.

Table 3. Estimated odds ratio (95% CI) for incident CAC and TAC displayed per interquartile ranges of exposure based on participants of the Heinz-Nixdorf Recall Study sample (n = 1,154 for CAC, n = 1,161 for TAC).

Exposure	Incident CAC	Incident TAC
PM_{10} (CTM)	1.23 (1.00, 1.52)	1.09 (0.90, 1.33)
PM_{10} (LUR)	1.20 (1.02, 1.42)	0.98 (0.84, 1.13)
$PM_{2.5}$ (CTM)	1.06 (0.85, 1.33)	1.15 (0.94, 1.40)
$PM_{2.5}$ (LUR)	1.31 (1.06, 1.61)	1.06 (0.88, 1.28)
PNacc (CTM)	1.15 (0.95, 1.41)	1.15 (0.96, 1.37)
$PM_{2.5abs}$ (LUR)	1.11 (0.96, 1.29)	1.03 (0.91, 1.18)
NO_2 (CTM)	1.10 (0.91, 1.33)	1.08 (0.91, 1.28)
NO_2 (LUR)	1.21 (1.00, 1.47)	1.01 (0.84, 1.21)

Note: Main model is adjusted for age, sex, BMI, smoking status and quantity, ETS, LDL-C/HDL-C, physical activity, education, traffic noise and for dichotomous outcomes additionally years of follow-up; BMI, body mass index; CAC, coronary artery calcification; CI, confidence interval; CTM, chemistry transport modeling; ETS, environmental tobacco smoke; HDL-C, high-density lipoprotein cholesterol; LDL-C, low-density lipoprotein cholesterol; LUR, land use regression; TAC, thoracic aortic calcification.

quality model. The CTM models average daily concentration of air pollutants in a 1 km^2 grid cell, based on emission factors, daily meteorology, and the distribution and chemical transformation of emissions (Hennig et al. 2016), reflecting long-term urban background concentrations taking changes in emission into account. In contrast, the LUR model estimates time-stable long-term air pollution concentrations, using a linear regression model. Urban background air pollution in a highly industrialized area close to coal-burning power plants and neighboring areas characterized by intensive livestock farming is expected to differ from air pollution at hot spots close to heavily trafficked roads, possibly contributing to differences in health effect estimates. Moreover, depending on the individual mobility of the participants, models reflecting urban background concentrations might lead to less exposure misclassification than point-specific models, specifically if emission patterns change during a long observation period. However, similar patterns of associations with subclinical atherosclerosis for both models remained, even when investigating participants less vs. more likely to exposure misclassification.

The estimated air pollution concentrations in this study were well below current European regulatory limits (EU 2008), suggesting that, even at current air pollution levels, adverse effects on the underlying pathology of CVD cannot be ruled out. In addition, observed results were robust with regard to adjustment for road traffic noise, a coexposure that has been shown to affect blood pressure (Kempen et al. 2018; Münzel et al. 2018), a major risk factor for the development of atherosclerosis. This finding was observed for all markers and in line with earlier studies that investigated thoracic calcification only (Hennig et al. 2019; Kälsch et al. 2013a). However, residual confounding of air pollution and noise cannot be ruled out due to possible noise exposure misclassification when using façade values and lack of personal exposure measures. Moreover, noise annoyance, which might play an additional role with regard to CVD, was not taken into account.

Our study has several limitations. For the measurement of TAC, no remeasurements for assessment of reliability were conducted, and the size of the measured area varied according to anatomical conditions, resulting in potentially large measurement error and imprecision of health effect estimation. cIMT ultrasound measurements were conducted by different examiners and followed two slightly different measurement protocols at t0 and t1, preventing the reader to identify the same location for cIMT reading at both time points. These differences increased random outcome measurement error and thereby contributed to imprecise health effect estimation. In addition, the relatively short time period between baseline and follow-up measurements (roughly 5 y) may have limited power to detect associations between air pollution exposure and progression of atherosclerosis. Exposure measurement error may have biased our estimates. First, long-term prebaseline exposure, which probably contributes most to the development of atherosclerosis during the follow-up period, was not available, and we used exposure during the examination periods (CTM) and time-stable estimates (LUR) as a surrogate for long-term air pollution exposure. Second, for assessing personal mobility, we had information only on employment status and on relocations within 5 y prior to baseline.

An important strength of our study is the relatively large study population with a comprehensive assessment of markers of subclinical atherosclerosis, in-depth covariate data. In addition, we applied two different commonly used air pollution models for estimating long-term air pollution exposure, reflecting urban background and point-specific exposure. Moreover, we considered traffic and noise, and we conducted comprehensive sensitivity analysis.

Conclusions

Our study suggests that development and progression of subclinical atherosclerosis are associated with long-term air pollution in middle-aged participants with no or minor atherosclerotic burden at baseline, whereas overall no consistent associations are observed.

Acknowledgments

The authors express their gratitude to all study participants in the HNR Study; the personnel of the HNR study center and the EBT-scanner facilities, specifically D. Grönemeyer, R. Seidel, and T. Budde; and the investigative group and all former employees of the HNR study. The authors also thank the Advisory Board of the HNR Study: T. Meinertz, Hamburg, Germany (Chair); C. Bode, Freiburg, Germany; P.J. de Feyter, Rotterdam, Netherlands; B. Güntert, Hall i.T., Austria; F. Gutzwiller, Bern, Switzerland; H. Heinen, Bonn, Germany; O. Hess, Bern, Switzerland; B. Klein, Essen, Germany; H. Löwel, Neuherberg, Germany; M. Reiser, Munich, Germany; G. Schmidt, Essen, Germany; M. Schwaiger, Munich, Germany; C. Steinmüller, Bonn, Germany; T. Theorell, Stockholm, Sweden; and S.N. Willich, Berlin, Germany. The authors thank the North Rhine-Westphalia State Agency for Nature, Environment and Consumer Protection for providing emission and land use data for North Rhine-Westphalia.

The authors also thank U. Roggenbuck, U. Slomiany, and A. Buschka for their data management work. Furthermore, the authors thank the International Society of Environmental Epidemiology ISEE for providing a platform to exchange environmental research and for providing training opportunities in environmental epidemiology. This work was completed in partial fulfillment of the requirements of the doctoral thesis for F.H.

The authors thank the Heinz Nixdorf Foundation (M. Nixdorf, chairman; G. Schmidt, past chairman), for their generous support of this study. Parts of the study were also supported by the German Research Council (DFG) (DFG project: ER 155/6-1;6-2, HO 3314/2-3, SCHE 1648/1-3).

References

Adar SD, Sheppard L, Vedal S, Polak JF, Sampson PD, Diez Roux AV, et al. 2013. Fine particulate air pollution and the progression of carotid intima-medial thickness: a prospective cohort study from the multi-ethnic study of atherosclerosis and air pollution. PLoS Med 10(4):e1001430, PMID: 23637576, https://doi.org/10.1371/journal.pmed.1001430.

Agatston AS, Janowitz FWR, Hildner FJ, Zusmer NR, Viamonte M, Detrano R. 1990. Quantification of coronary artery calcium using ultrafast computed tomography. J Am Coll Cardiol 15(4):827–832, PMID: 2407762, https://doi.org/10.1016/0735-1097(90)90282-T.

Araujo J. A, Barajas B, Kleinman M, Wang X, Bennett BJ, Gong KW, et al. 2008. Ambient particulate pollutants in the ultrafine range promote early atherosclerosis and systemic oxidative stress. Circ Res 102(5):589–596, PMID: 18202315, https://doi.org/10.1161/CIRCRESAHA.107.164970.

Bauer M, Möhlenkamp S, Lehmann N, Schmermund A, Roggenbuck U, Moebus S, et al. 2009. The effect of age and risk factors on coronary and carotid artery atherosclerotic burden in males–results of the Heinz Nixdorf Recall Study. Atherosclerosis 205(2):595–602, PMID: 19200545, https://doi.org/10.1016/j.atherosclerosis.2009.01.005.

Beelen R, Hoek G, Vienneau D, Eeftens M, Dimakopoulou K, Pedeli X, et al. 2013. Development of NO_2 and NO*x* land use regression models for estimating air pollution exposure in 36 study areas in Europe – The ESCAPE project. Atmos Environ 72:10–23, https://doi.org/10.1016/j.atmosenv.2013.02.037.

de Hoogh K, Korek M, Vienneau D, Keuken M, Kukkonen J, Nieuwenhuijsen MJ, et al. 2014. Comparing land use regression and dispersion modelling to assess residential exposure to ambient air pollution for epidemiological studies. Environ Int 73:382–392, PMID: 25233102, https://doi.org/10.1016/j.envint.2014.08.011.

Defilippis AP, Blaha MJ, Ndumele CE, Budoff MJ, Lloyd-Jones DM, McClelland RL, et al. 2011. The association of Framingham and Reynolds Risk Scores with incidence and progression of coronary artery calcification in MESA (Multi-Ethnic Study of Atherosclerosis). J Am Coll Cardiol 58(20):2076–2083, PMID: 22051329, https://doi.org/10.1016/j.jacc.2011.08.022.

Den Ruijter HM, Peters SAE, Anderson TJ, Britton AR, Dekker JM, Eijkemans MJ, et al. 2012. Common carotid intima-media thickness measurements in cardiovascular risk prediction: a meta-analysis. JAMA 308(8):796–803, PMID: 22910757, https://doi.org/10.1001/jama.2012.9630.

Dorans KS, Wilker EH, Li W, Rice MB, Ljungman PL, Schwartz J, et al. 2016. Residential proximity to major roads, exposure to fine particulate matter, and coronary artery calcium. Arterioscler Thromb Vasc Biol 36(8):1679–1685, PMID: 27312220, https://doi.org/10.1161/ATVBAHA.116.307141.

Dorans KS, Wilker EH, Li W, Rice MB, Ljungman PL, Schwartz J, et al. 2017. Residential proximity to major roads, exposure to fine particulate matter and aortic calcium: the Framingham Heart Study, a cohort study. BMJ Open 7: e013455, PMID: 28302634, https://doi.org/10.1136/bmjopen-2016-013455.

Dragano N, Hoffmann B, Stang A, Moebus S, Verde PE, Weyers S, et al. 2009. Subclinical coronary atherosclerosis and neighbourhood deprivation in an urban region. Eur J Epidemiol 24(1):25–35, PMID: 18931923, https://doi.org/10.1007/s10654-008-9292-9.

Eeftens M, Beelen R, Hoogh K, De Bellander T, Cesaroni G, Cirach M, et al. 2012. Development of Land Use Regression models for PM(2.5), PM(2.5) absorbance, PM(10) and PM(coarse) in 20 European study areas; results of the ESCAPE project. Environ Sci Technol 46(20):11195–11205, PMID: 22963366, https://doi.org/10.1021/es301948k.

Erbel R, Möhlenkamp S, Moebus S, Schmermund A, Lehmann N, Stang A, et al. 2010. Coronary risk stratification, discrimination, and reclassification improvement based on quantification of subclinical coronary atherosclerosis: the Heinz Nixdorf Recall study. J Am Coll Cardiol 56(17):1397–1406, PMID: 20946997, https://doi.org/10.1016/j.jacc.2010.06.030.

EU (European Union). 2008. Directive 2008/50/EC of the European Parliament and of the Council of 21 May 2008 on ambient air quality and cleaner air for Europe. Off J Eur Union. http://data.europa.eu/eli/dir/2008/50/oj [accessed 24 September 2020].

European Environment Agency. 2011. Index to methodology chapters ordered by SNAP97 Activity. http://www.eea.europa.eu/publications/EMEPCORINAIR4/page009-a.html [accessed 30 November 2015].

Foerch C, Buehler A, von Kegler S, Sitzer M. 2003. Intima-media thickness side differences are limited to the common carotid artery. Hypertension 42(6):e17, PMID: 14674381, https://doi.org/10.1161/01.HYP.0000103164.73172.30.

Folsom AR, Kronmal RA, Detrano RC, O'Leary DH, Bild DE, Bluemke DA, et al. 2008. Coronary artery calcification compared with carotid intima-media thickness in the prediction of cardiovascular disease incidence: the Multi-Ethnic Study of Atherosclerosis (MESA). Arch Intern Med 168(12):1333–1339, PMID: 18574091, https://doi.org/10.1001/archinte.168.12.1333.

Franklin BA, Brook R, Arden Pope C 3rd. 2015. Air pollution and cardiovascular disease. Curr Probl Cardiol 40(5):207–238, PMID: 25882781, https://doi.org/10.1016/j.cpcardiol.2015.01.003.

Gakidou E, Afshin A, Abajobir AA, Abate KH, Abbafati C, Abbas KM, et al. 2017. Global, regional, and national comparative risk assessment of 84 behavioural, environmental and occupational, and metabolic risks or clusters of risks, 1990–2016: a systematic analysis for the Global Burden of Disease Study 2016. Lancet 390(10100):1345–1422, PMID: 28919119, https://doi.org/10.1016/S0140-6736(17)32366-8.

Gan WQ, Allen RW, Brauer M, Davies HW, Mancini GBJ, Lear S. A. 2014. Long-term exposure to traffic-related air pollution and progression of carotid artery atherosclerosis: a prospective cohort study. BMJ Open 4(4):e004743, PMID: 24710134, https://doi.org/10.1136/bmjopen-2013-004743.

Geisel MH, Bauer M, Hennig F, Hoffmann B, Lehmann N, Möhlenkamp S, et al. 2017. Comparison of coronary artery calcification, carotid intima-media thickness and ankle-brachial index for predicting 10-year incident cardiovascular events in the general population. Eur Heart J 38(23):1815–1822, PMID: 28379333, https://doi.org/10.1093/eurheartj/ehx120.

Greenland S, Pearl J, Robins JM. 1999. Causal diagrams for epidemiologic research. Epidemiology 10(1):37–48, PMID: 9888278.

Hennig F, Moebus S, Reinsch N, Budde T, Erbel R, Jo K, et al. 2019. Investigation of air pollution and noise on progression of thoracic aortic calcification: results of the Heinz Nixdorf Recall Study. Eur J Prev Cardiol 0:1–10, https://doi.org/10.1177/2047487319854818.

Hennig F, Sugiri D, Tzivian L, Fuks K, Moebus S, Jöckel K-H, et al. 2016. Comparison of land-use regression modeling with dispersion and chemistry transport modeling to assign air pollution concentrations within the Ruhr area. Atmosphere (Basel). 7(3):48, https://doi.org/10.3390/atmos7030048.

Hoffmann B, Weinmayr G, Hennig F, Fuks K, Moebus S, Weimar C, et al. 2015. Air quality, stroke, and coronary events. Dtsch Arztebl Int 195–201, https://doi.org/10.3238/arztebl.2015.0195.

Kälsch H, Hennig F, Moebus S, Möhlenkamp S, Dragano N, Jakobs H, et al. 2013a. Are air pollution and traffic noise independently associated with atherosclerosis: the Heinz Nixdorf Recall Study. Eur Heart J 35(13):853–860, PMID: 24194529, https://doi.org/10.1093/eurheartj/eht426.

Kälsch H, Lehmann N, Moebus S, Hoffmann B, Stang A, Jöckel, KH. 2017. Aortic calcification onset and progression: association with the development of coronary atherosclerosis. J Am Heart Assoc 6(4):e005093, https://doi.org/10.1161/JAHA.116.005093.

Kälsch H, Lehmann N, Möhlenkamp S, Hammer C, Mahabadi AA, Moebus S, et al. 2013b. Prevalence of thoracic aortic calcification and its relationship to cardiovascular risk factors and coronary calcification in an unselected population-based cohort: the Heinz Nixdorf Recall Study. Int J Cardiovasc Imaging 29(1):207–216, PMID: 22527262, https://doi.org/10.1007/s10554-012-0051-3.

Kaufman JD, Adar SD, Barr RG, Budoff M, Burke GL, Curl CL, et al. 2016. Association between air pollution and coronary artery calcification within six metropolitan areas in the USA (the Multi-Ethnic Study of Atherosclerosis and Air Pollution): a longitudinal cohort study. Lancet 388(10045):696–704, PMID: 27233746, https://doi.org/10.1016/S0140-6736(16)00378-0.

Kempen EV, Casas M, Pershagen G, Foraster M. 2018. WHO Environmental Noise Guidelines for the European Region: a systematic review on environmental noise and cardiovascular and metabolic effects: a summary. Int J Environ Res Public Health 15(2):379, PMID: 29470452, https://doi.org/10.3390/ijerph15020379.

Künzli N, Jerrett M, Garcia-Esteban R, Basagaña X, Beckermann B, Gilliland F, et al. 2010. Ambient air pollution and the progression of atherosclerosis in adults. PLoS One 5(2):e9096, PMID: 20161713, https://doi.org/10.1371/journal.pone.0009096.

Künzli N, Perez L, Klot SV, Baldassarre D, Bauer M, Basagana X, et al. 2011. Investigating air pollution and atherosclerosis in humans: concepts and outlook. Prog Cardiovasc Dis 53(5):334–343, PMID: 21414468, https://doi.org/10.1016/j.pcad.2010.12.006.

Lehmann N, Erbel R, Mahabadi AA, Rauwolf M, Möhlenkamp S, Moebus S, Kälsch H, et al. 2018. Value of progression of coronary artery calcification for risk prediction of coronary and cardiovascular events result of the HNR Study (Heinz Nixdorf Recall). Circulation 137(7):665–679, PMID: 29142010, https://doi.org/10.1161/CIRCULATIONAHA.116.027034.

Luo X, Yang Y, Cao T, Li Z. 2011. Differences in left and right carotid intima-media thickness and the associated risk factors. Clin Radiol 66(5):393–398, PMID: 21324442, https://doi.org/10.1016/j.crad.2010.12.002.

Memmesheimer M, Friese E, Ebel A, Jakobs HJ, Feldmann H, Kessler C, et al. 2004. Long-term simulations of particulate matter in Europe on different scales using sequential nesting of a regional model. Int J Environ Pollut 22(1/2):108–132, https://doi.org/10.1504/IJEP.2004.005530.

Münzel T, Schmidt FP, Steven S, Herzog J, Daiber A, Sørensen M. 2018. Environmental noise and the cardiovascular system. J Am Coll Cardiol 71(6):688–697, PMID: 29420965, https://doi.org/10.1016/j.jacc.2017.12.015.

Nair SB, Malik R, Khattar RS. 2012. Carotid intima-media thickness: ultrasound measurement, prognostic value and role in clinical practice. Postgrad Med J 88(1046):694–699, PMID: 22761324, https://doi.org/10.1136/postgradmedj-2011-130214.

Nonnemacher M, Jakobs H, Viehmann A, Vanberg I, Kessler C, Moebus S, et al. 2014. Spatio-temporal modelling of residential exposure to particulate matter and gaseous pollutants for the Heinz Nixdorf Recall Cohort. Atmos Environ 91:15–23, https://doi.org/10.1016/j.atmosenv.2014.03.052.

O'Leary DH, Polak JF, Kronmal RA, Manolio TA, Burke GL, Wolfson SK. 1999. Carotid-artery intima and media thickness as a risk factor for myocardial infarction and stroke in older adults. Cardiovascular Health Study Collaborative Research Group. N Engl J Med 340(1):14–22, PMID: 9878640, https://doi.org/10.1056/NEJM199901073400103.

Peinemann F, Moebus S, Dragano N, Möhlenkamp S, Lehmann N, Zeeb H, et al. 2011. Secondhand smoke exposure and coronary artery calcification among nonsmoking participants of a population-based cohort. Environ Health Perspect 119(11):1556–1561, PMID: 21742575, https://doi.org/10.1289/ehp.1003347.

Perez L, Wolf K, Hennig F, Penell J, Basagaña X, Aguilera I, et al. 2015. Air pollution and atherosclerosis: a cross-sectional analysis of four European cohort studies in the ESCAPE Study. Environ Health Perspect 123(6):597–605, PMID: 25625785, https://doi.org/10.1289/ehp.1307711.

Polak JF, Pencina MJ, Pencina KM, O'Donnell CJ, Wolf PA, D'Agostino RB. 2011. Carotid-wall intima-media thickness and cardiovascular events. N Engl J Med 365(3):213–221, PMID: 21774709, https://doi.org/10.1056/NEJMoa1012592.

Provost EB, Madhloum N, Panis LI, De Boever P, Nawrot TS. 2015. Carotid intima-media thickness, a marker of subclinical atherosclerosis, and particulate air pollution exposure: the meta-analytical evidence. PLoS One 10(5):e0127014, https://doi.org/10.1371/journal.pone.0127014.

Rückerl R, Schneider A, Breitner S, Cyrys J, Peters A. 2011. Health effects of particulate air pollution: a review of epidemiological evidence. Inhal Toxicol 23(10):555–592, PMID: 21864219, https://doi.org/10.3109/08958378.2011.593587.

Schmermund A, Möhlenkamp S, Stang A, Grönemeyer D, Seibel R, Hirche H, et al. 2002. Assessment of clinically silent atherosclerotic disease and established and novel risk factors for predicting myocardial infarction and cardiac death in healthy middle-aged subjects: rationale and design of the Heinz Nixdorf RECALL Study. Am Heart J 144(2):212–218, PMID: 12177636, https://doi.org/10.1067/mhj.2002.123579.

Soares RSC, Carvalho-Oliveira R, Ramos-Sanchez E, Catanozi S, Fernando L, Mauad T, et al. 2009. Air pollution and antibodies against modified lipoproteins are associated with atherosclerosis and vascular remodeling in hyperlipemic mice. Atherosclerosis 207(2):368–373, PMID: 19486979, https://doi.org/10.1016/j.atherosclerosis.2009.04.041.

Stang A, Moebus S, Dragano N, Beck EM, Mo S, Schmermund A, et al. 2005. Baseline recruitment and analyses of nonresponse of the Heinz Nixdorf Recall Study: identifiability of phone numbers as the major determinant of response. Eur J Epidemiol 20(6):489–496, PMID: 16121757, https://doi.org/10.1007/s10654-005-5529-z.

Sun Q, Wang A, Jin X, Natanzon A, Duquaine D, Brook RD. 2005. Acceleration of atherosclerosis and vascular inflammation in an animal model. JAMA 294(23):3003–3010, https://doi.org/10.1001/jama.294.23.3003.

U.S. EPA (U.S. Environmental Protection Agency). 2019. Integrated Science Assessment for Particulate Matter.

UNESCO (United Nations Educational, Scientific and Cultural Organisation). 1997. International standard classification of education ISCED 1997. https://unesdoc.unesco.org/ark:/48223/pf0000146967.locale=en [accessed 24 September 2020].

Wang M, Sampson PD, Sheppard LE, Stein JH, Vedal S, Kaufman JD. 2019. Long-term exposure to ambient ozone and progression of subclinical arterial disease: the Multi-Ethnic Study of Atherosclerosis and air pollution. Environ Health Perspect 127(5):57001, PMID: 31063398, https://doi.org/10.1289/EHP3325.

Wendelhag I, Liang Q, Gustavsson T, Wikstrand J. 1997. A new automated computerized analyzing system simplifies readings and reduces the variability in ultrasound measurement of intima-media thickness. Stroke 28(11):2195–2200, PMID: 9368564, https://doi.org/10.1161/01.str.28.11.2195.

WHO (World Health Organization). 2009. Global health risks mortality and burden of disease attributable to selected major risks: Technical Report [Internet]. Copenhagen: WHO Regional Office for Europe. https://www.ncbi.nlm.nih.gov/books/NBK361805/ [accessed 24 September 2020].

WHO Regional Office for Europe. 2013. Review of evidence on health aspects of air pollution—REVIHAAP Project. https://www.ncbi.nlm.nih.gov/books/NBK361805/ [accessed 24 September 2020].

WHO. 2013. ATC/DDD Index 2018. http://www.whocc.no/atc_ddd_index/ [accessed 24 September 2020].

Wilker EH, Mittleman M. A, Coull B. A, Gryparis A, Bots ML, Schwartz J, et al. 2013. Long-term exposure to black carbon and carotid intima-media thickness: the normative aging study. Environ Health Perspect 121(9):1061–1067, PMID: 23820848, https://doi.org/10.1289/ehp.1104845.

Wilker EH, Preis SR, Beiser AS, Wolf PA, Au R, Kloog I, et al. 2015. Long-term exposure to fine particulate matter, residential proximity to major roads and measures of brain structure. Stroke 46(5):1161–1166, PMID: 25908455, https://doi.org/10.1161/STROKEAHA.114.008348.

Environ Health Perspect

DOI: 10.1289/EHP7077

Supplemental Material

Air Pollution and Progression of Atherosclerosis in Different Vessel Beds—Results from a Prospective Cohort Study in the Ruhr Area, Germany

Frauke Hennig, Marie Henrike Geisel, Hagen Kälsch, Sarah Lucht, Amir Abbas Mahabadi, Susanne Moebus, Raimund Erbel, Nils Lehmann, Karl-Heinz Jöckel, André Scherag, and Barbara Hoffmann on behalf of the Heinz Nixdorf Recall Study Investigative Group

Table of Contents

Figure S5. Histograms and Scatterplots between long-term exposure concentration for PM10, PM2.5, and NO2 modelled via CTM and LUR.

Figure S6. Histograms and Scatterplots of CTM air pollutant concentrations (PM10, PM2.5, PNacc, and NO2) at baseline (2001-2003) and follow-up (2006-2008).

Table S1. Spearman correlation coefficients for CTM-modelled air pollutant concentrations PM10, PM2.5, PNacc, and NO2 between baseline (2001-2003) and follow-up (2006-2008).

Figure S7. Histograms of outcome distributions at baseline and follow-up in all four subclinical markers of atherosclerosis (cIMT (left), cIMT (right), CAC, and TAC in participants of the Heinz-Nixdorf-Recall Study.

Figure S8. Histograms of change in markers of atherosclerosis (cIMT (left), cIMT (right), CAC, and TAC) in participants of the Heinz-Nixdorf-Recall Study.

Table S2. Estimated Odds Ratio [95%-CI] for progression of atherosclerosis and estimated change [95%-CI] in cIMT (µm) and calcification (growth rate) displayed per interquartile ranges of exposure based on participants of the Heinz-Nixdorf Recall Study sample (N = 2116 for cIMT (left), N = 2197 for cIMT (right), N = 3220 for CAC, and N = 3126 for TAC).

Figure S9. Estimated Odds Ratios (OR) (95%-CI) for progression of atherosclerosis measured using different markers (cIMT (left), cIMT (right), CAC, TAC) per IQR increase in air pollution concentration based on participants of the Heinz Nixdorf Recall cohort study evaluating adjustment by potential mediating variables.

Figure S10. Estimated change (95%-CI) in carotid intima media thickniss (µm) (cIMT (left) and cIMT (right)) and calcification (growth rate) (CAC and TAC) per IQR increase in air pollution concentration based on participants of the Heinz Nixdorf Recall cohort study evaluating adjustment by potential mediating variables.

Table S3. Odds Ratio [95%-CI] for progression and change [95%-CI] in cIMT (µm) and calcification (growth rate) displayed per interquartile ranges of exposure estimated in participants of the Heinz-Nixdorf Recall Study with no/minor atherosclerotic burden at baseline (t0) (cIMT (left)=1054, cIMT (right)=1017, CAC=1527,TAC=1761) and participants with advanced atherosclerotic burden at t0 (cIMT (left)=1203, cIMT (right)=1317, CAC=1693,TAC=1469).

Figure S11. Subgroup effect estimates for the associations between different air pollutants and progression of atherosclerosis in subpopulations of the Heinz Nixdorf Recall Study based on the marker of atherosclerosis (cIMT (left)=2116, cIMT (right)=2197, CAC=3220, TAC=3126). Model is adjusted for age, sex, BMI, smoking status and quantity, environmental tobacco smoke (ETS), LDL-C/HDL-C, physical activity, education, traffic noise and for dichotomous outcomes additionally years of follow-up Panel A displays Odds Ratios (OR) (95%-CI) for any progression in atherosclerosis based on an interquartile range (IQR) in exposure. Panel B displays change in thickness (µm) for cIMT and change in growth rate for CAC and TAC.

Table S4. Estimated Odds Ratio (95%-CI) for progression of atherosclerosis in different markers defined by 10% increase (first column) and Relative Risks (95%-CI) for progression of atherosclerosis estimated using Poisson regression (second column) displayed per interquartile ranges of exposure based on participants of the Heinz-Nixdorf Recall Study sample (N = 2116 for cIMT (left), N = 2197 for cIMT (right), N = 3220 for CAC, and N = 3126 for TAC).

Table S5. Estimated Odds Ratio (95%-CI) for progression of atherosclerosis in different markers as a sensitivity analysis investigating mean of left and/or right cIMT, faster progression of CAC based on personal percentile, displayed per interquartile ranges of exposure based on participants of the Heinz-Nixdorf Recall Study sample (N = 2594 for cIMT (left/right), N = 3220 for faster CAC).

Table S6. Estimated Odds Ratio [95%-CI] for progression of atherosclerosis and estimated change [95%-CI] in cIMT (µm) and calcification (growth rate) displayed per interquartile ranges of exposure with regard to different time windows of exposure, modelled using the EURAD chemistry-transport model (CTM). Estimation are based on the main model and participants of the Heinz-Nixdorf Recall Study sample (N = 2116 for cIMT (left), N = 2197 for cIMT (right), N = 3220 for CAC, and N = 3126 for TAC).

Figure S12. Subgroup effect estimates for the associations between different air pollutants and progression of atherosclerosis in subpopulations of the Heinz Nixdorf Recall Study based on the marker of atherosclerosis with respect to exposure misclassification (cIMT (left)=2116, cIMT (right)=2197, CAC=3220, TAC=3126). Movers within subsamples: cIMT (left) = 13.3%; cIMT (right) = 12.8%; CAC = 12.9%; TAC = 12.8%. Non-Employees within subsamples: cIMT (left) = 57.9%; cIMT (right) = 58%; CAC = 58.8%; TAC = 59.9%. Panel A displays Odds Ratios (OR) (95%-CI) for any progression in atherosclerosis based on an interquartile range (IQR) in exposure. Panel B displays change in thickness (µm) for cIMT and change in growth rate for CAC and TAC.

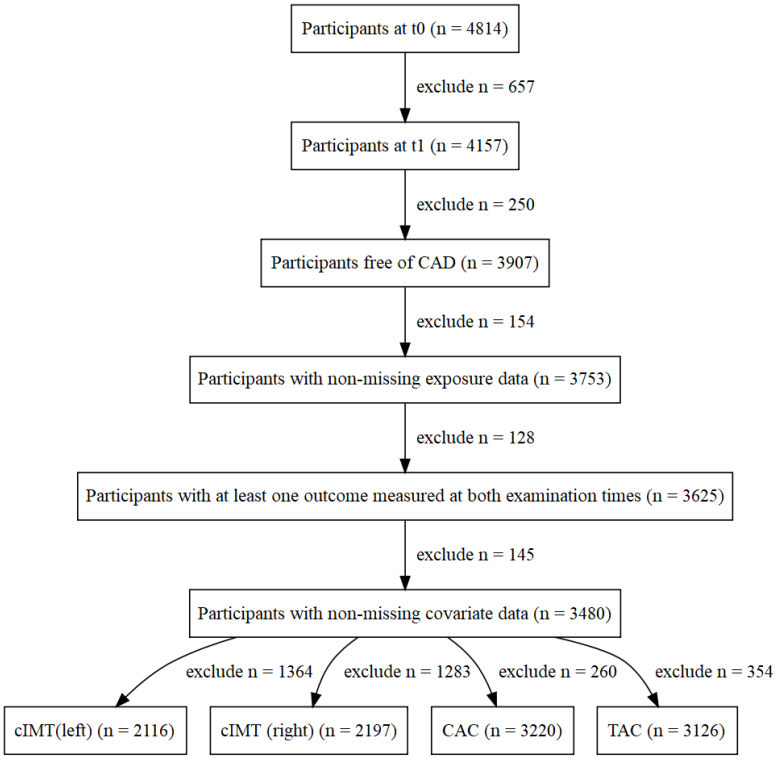

Figure S1: Flowchart visualizing the sample size reduction of the Heinz Nixdorf Recall Study cohort for the analysis sample investigating the association of air pollution on progression of atherosclerosis in different vessel beds/Markers (carotid intima media thickness cIMT (left); cIMT (right), coronary artery calcification (CAC); thoracic aortic calcification (TAC) in respective subpopulations.

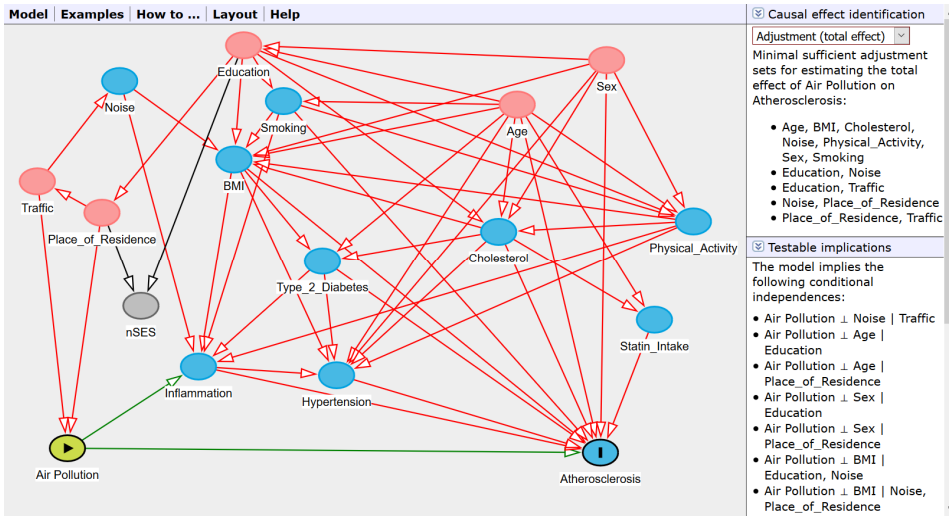

Figure S2: Directed acyclic graph describing hypothesized causal relationship between exposure, outcome and considered covariables.

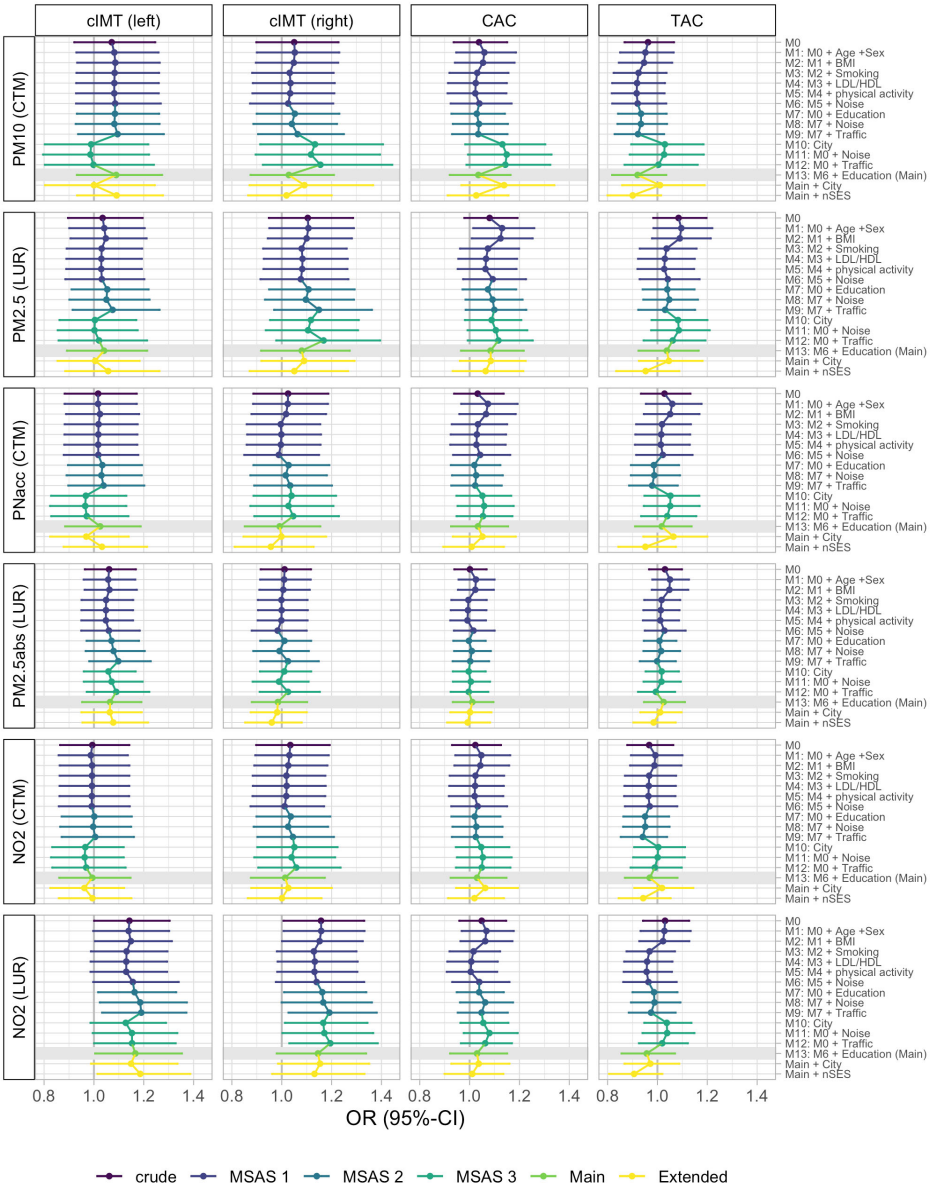

Figure S3: Estimated Odds Ratios (OR) (95%-CI) for progression of atherosclerosis measured using different markers (cIMT (left), cIMT (right), CAC, TAC) per IQR increase in air pollution concentration based on participants of the Heinz Nixdorf Recall cohort study (cIMT (left): n=2116; cIMT (right): n=2197; CAC: n=3220; TAC: n=3126) comparing different DAG-based adjustment sets. The first MSAS included personal characteristics, while the second and third included education or place of residence in combination with co-exposures noise or traffic. For each MSAS, variables were added subsequently. Main model combined 2 MSAS, before extended adjustment was applied.

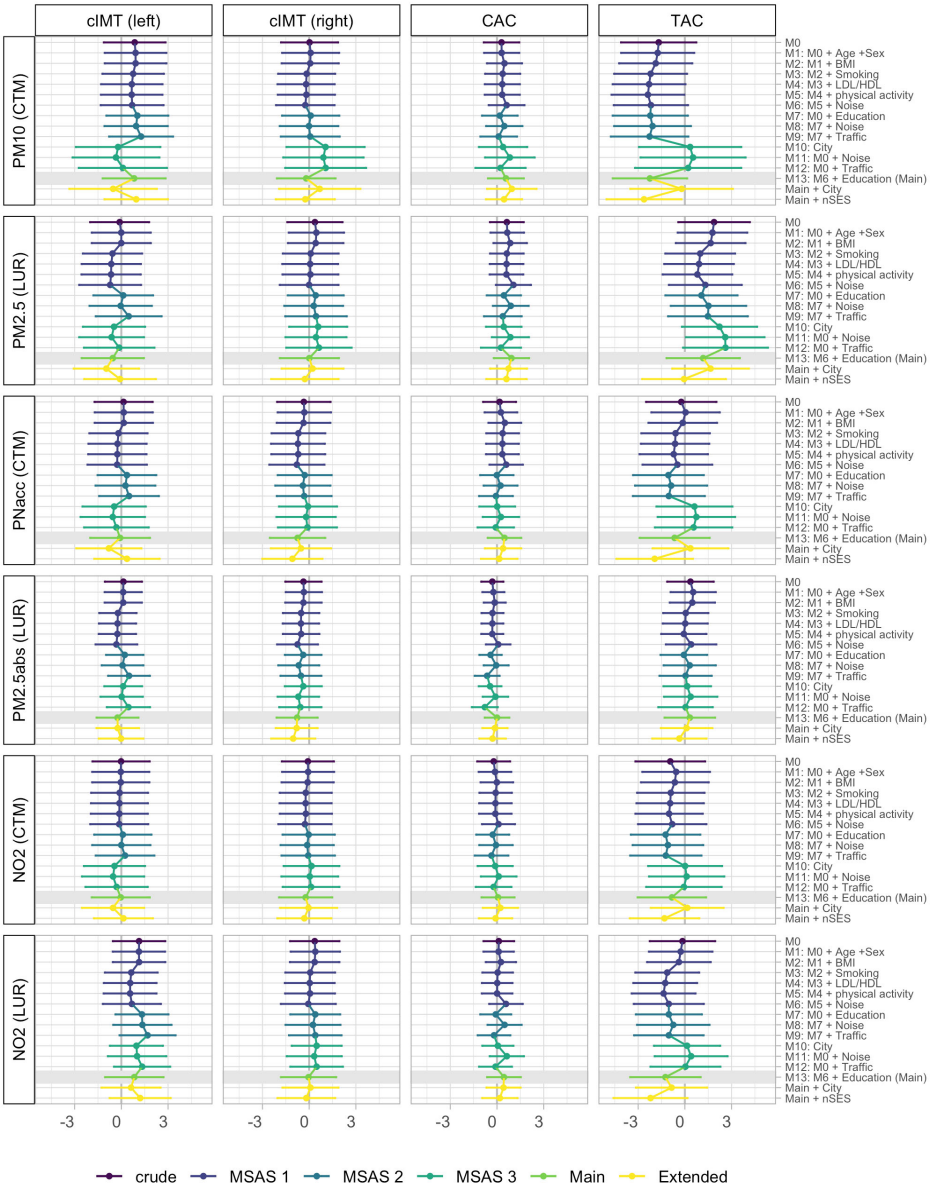

Figure S4: Estimated change (95%-CI) in intima media thickness (µm) and calcification (growth rate) per IQR increase in air pollution concentration based on participants of the Heinz Nixdorf Recall cohort study (cIMT (left): n=2116; cIMT (right): n=2197; CAC: n=3220; TAC: n=3126) comparing different DAG-based adjustment sets. The first MSAS included personal characteristics, while the second and third included education or place of residence in combination with co-exposures noise or traffic. For each MSAS, variables were added subsequently. Main model combined 2 MSAS, before extended adjustment was applied.

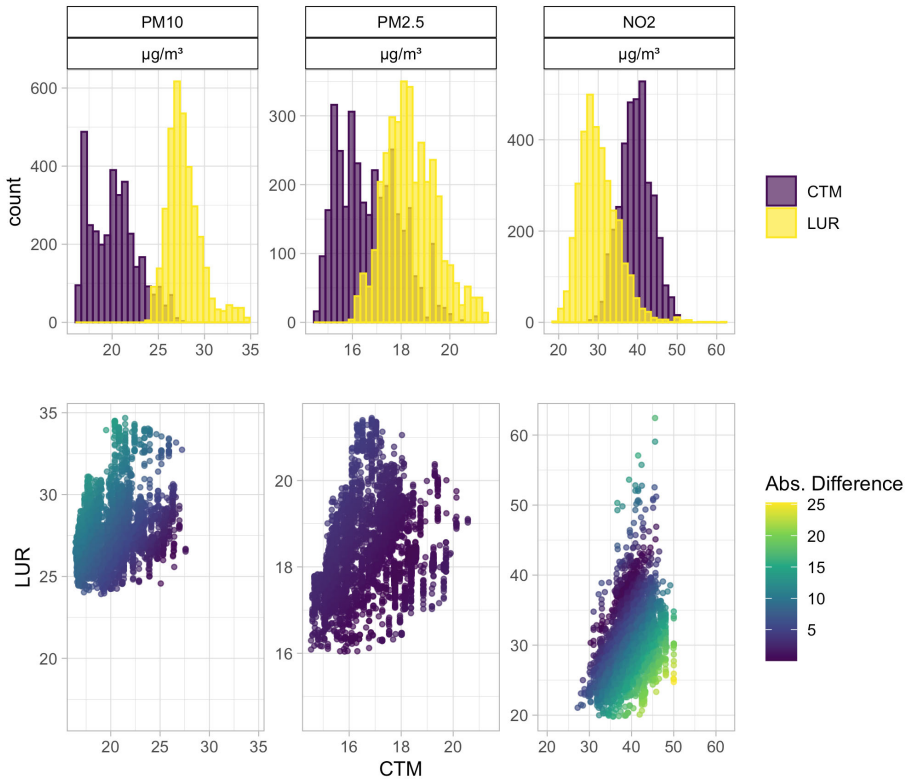

Figure S5: Histograms and Scatterplots between long-term exposure concentration for PM10, PM2.5, and NO2 modelled via CTM and LUR.

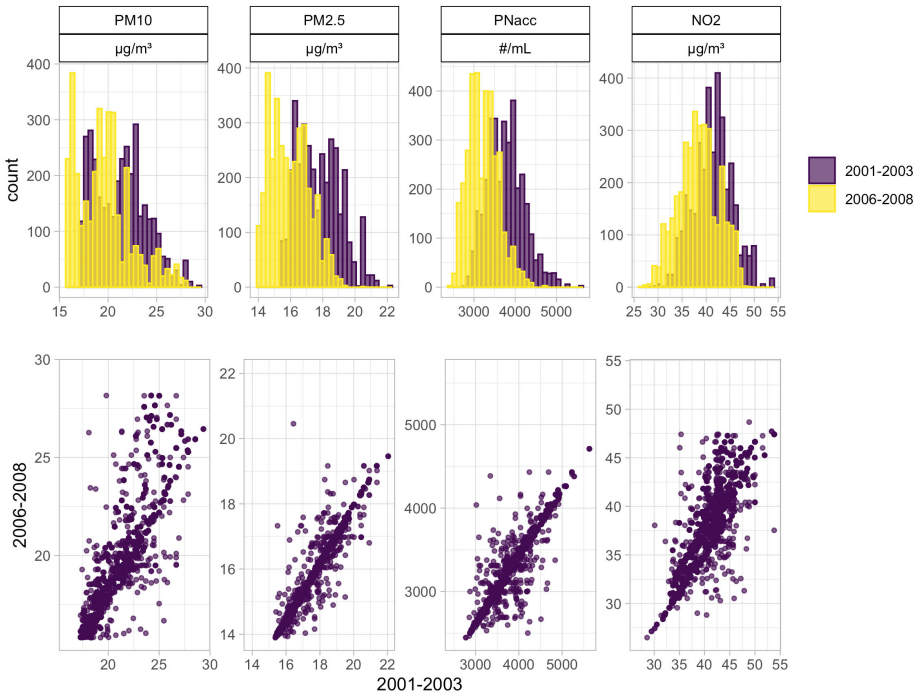

Figure S6: Histograms and Scatterplots of CTM air pollutant concentrations (PM10, PM2.5, PNacc, and NO2) at baseline (2001-2003) and follow-up (2006-2008).

Table S1: Spearman correlation coefficients for CTM-modelled air pollutant concentrations PM10, PM2.5, PNacc, and NO2 between baseline (2001-2003) and follow-up (2006-2008).

Variable 1	Variable 2	cor
PM10 (2001-2003), µg/m³	PM10 (2006-2008), µg/m³	0.93
PM2.5 (2001-2003), µg/m³	PM2.5 (2006-2008), µg/m³	0.98
PNacc (2001-2003), #/mL	PNacc (2006-2008), #/mL	0.95
NO2 (2001-2003), µg/m³	NO2 (2006-2008), µg/m³	0.87

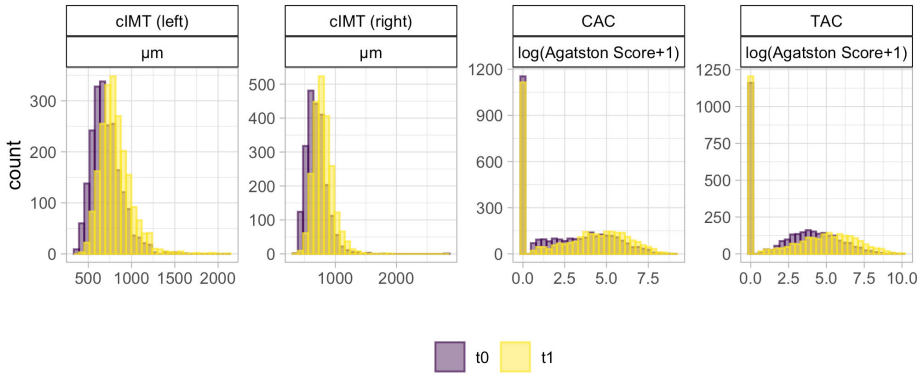

Figure S7: Histograms of outcome distributions at baseline and follow-up in all four subclinical markers of atherosclerosis (cIMT (left), cIMT (right), CAC, and TAC in participants of the Heinz-Nixdorf-Recall Study.

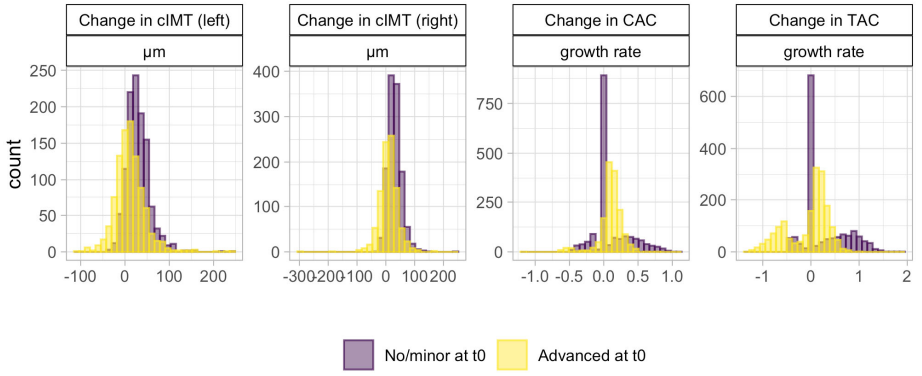

Figure S8: Histograms of change in markers of atherosclerosis (cIMT (left), cIMT (right), CAC, and TAC) in participants of the Heinz-Nixdorf-Recall Study.

Table S2: Estimated Odds Ratio [95%-CI] for progression of atherosclerosis and estimated change [95%-CI] in cIMT (µm) and calcification (growth rate) displayed per interquartile ranges of exposure based on participants of the Heinz-Nixdorf Recall Study sample (N = 2116 for cIMT (left), N = 2197 for cIMT (right), N = 3220 for CAC, and N = 3126 for TAC).

Marker	Exposure	Model	OR [95%-CI]	Change [95%-CI]
cIMT (left)	PM10 (CTM)	Crude	1.07 [0.92, 1.25]	0.86 [-1.13, 2.84]
		Main	**1.09 [0.93, 1.27]**	**0.82 [-1.20, 2.85]**
	PM10 (LUR)	Crude	1.02 [0.91, 1.15]	-0.18 [-1.72, 1.36]
		Main	**1.02 [0.90, 1.16]**	**-0.52 [-2.13, 1.10]**
	PM2.5 (CTM)	Crude	1.05 [0.89, 1.23]	1.10 [-1.01, 3.21]
		Main	**1.06 [0.90, 1.25]**	**1.12 [-0.99, 3.24]**
	PM2.5 (LUR)	Crude	1.03 [0.90, 1.20]	-0.11 [-2.01, 1.79]
		Main	**1.04 [0.89, 1.21]**	**-0.55 [-2.55, 0.45]**
	PNacc (CTM)	Crude	1.02 [0.88, 1.17]	0.14 [-1.73, 2.01]
		Main	**1.02 [0.88, 1.19]**	**-0.08 [-2.00, 1.84]**
	PM2.5abs (LUR)	Crude	1.06 [0.96, 1.17]	0.13 [-1.06, 1.33]
		Main	**1.06 [0.95, 1.19]**	**-0.25 [-1.59, 1.10]**
	NO2 (CTM)	Crude	0.99 [0.86, 1.14]	-0.02 [-1.86, 1.82]
		Main	**0.99 [0.86, 1.15]**	**-0.04 [-1.90, 1.83]**
	NO2 (LUR)	Crude	1.14 [1.00, 1.30]	1.14 [-0.54, 2.82]
		Main	**1.17 [1.00, 1.35]**	**0.83 [-1.05, 2.71]**
cIMT (right)	PM10 (CTM)	Crude	1.05 [0.90, 1.23]	0.02 [-1.81, 1.86]
		Main	**1.03 [0.87, 1.21]**	**-0.19 [-2.07, 1.69]**
	PM10 (LUR)	Crude	1.09 [0.96, 1.23]	0.51 [-0.92, 1.95]
		Main	**1.07 [0.94, 1.23]**	**0.32 [-1.20, 1.85]**
	PM2.5 (CTM)	Crude	1.03 [0.87, 1.21]	-0.33 [-2.27, 1.61]
		Main	**1.01 [0.85, 1.19]**	**-0.45 [-2.41, 1.50]**
	PM2.5 (LUR)	Crude	1.10 [0.95, 1.29]	0.37 [-1.41, 2.14]
		Main	**1.08 [0.92, 1.27]**	**0.01 [-1.89, 1.91]**
	PNacc (CTM)	Crude	1.03 [0.89, 1.19]	-0.34 [-2.06, 1.37]
		Main	**0.99 [0.85, 1.15]**	**-0.75 [-2.53, 1.04]**
	PM2.5abs (LUR)	Crude	1.01 [0.92, 1.12]	-0.37 [-1.53, 0.80]
		Main	**0.98 [0.88, 1.10]**	**-0.77 [-2.09, 0.55]**
	NO2 (CTM)	Crude	1.03 [0.90, 1.19]	-0.08 [-1.76, 1.59]
		Main	**1.01 [0.88, 1.17]**	**-0.23 [-1.94, 1.48]**
	NO2 (LUR)	Crude	1.16 [1.01, 1.33]	0.36 [-1.23, 1.94]
		Main	**1.15 [0.98, 1.34]**	**-0.04 [-1.81, 1.74]**
CAC	PM10 (CTM)	Crude	1.04 [0.94, 1.15]	0.00 [-0.01, 0.01]
		Main	**1.04 [0.92, 1.16]**	**0.01 [-0.01, 0.02]**
	PM10 (LUR)	Crude	1.07 [0.99, 1.16]	0.00 [0.00, 0.01]
		Main	**1.07 [0.97, 1.18]**	**0.01 [0.00, 0.02]**

Marker	Exposure	Model	OR [95%-CI]	Change [95%-CI]
	PM2.5 (CTM)	Crude	0.98 [0.88, 1.10]	0.00 [-0.01, 0.01]
		Main	**0.98 [0.87, 1.11]**	**0.00 [-0.01, 0.01]**
	PM2.5 (LUR)	Crude	1.08 [0.98, 1.19]	0.01 [0.00, 0.02]
		Main	**1.08 [0.97, 1.22]**	**0.01 [0.00, 0.02]**
	PNacc (CTM)	Crude	1.03 [0.94, 1.14]	0.00 [-0.01, 0.01]
		Main	**1.03 [0.93, 1.15]**	**0.00 [-0.01, 0.02]**
	PM2.5abs (LUR)	Crude	1.00 [0.94, 1.07]	0.00 [-0.01, 0.00]
		Main	**1.01 [0.93, 1.10]**	**0.00 [-0.01, 0.01]**
	NO2 (CTM)	Crude	1.02 [0.93, 1.13]	0.00 [-0.01, 0.01]
		Main	**1.03 [0.92, 1.15]**	**0.00 [-0.01, 0.01]**
	NO2 (LUR)	Crude	1.05 [0.96, 1.15]	0.00 [-0.01, 0.01]
		Main	**1.03 [0.92, 1.15]**	**0.00 [-0.01, 0.02]**
TAC	PM10 (CTM)	Crude	0.96 [0.87, 1.07]	-0.02 [-0.04, 0.01]
		Main	**0.92 [0.82, 1.04]**	**-0.02 [-0.05, 0.00]**
	PM10 (LUR)	Crude	1.06 [0.98, 1.14]	0.02 [0.00, 0.04]
		Main	**1.02 [0.93, 1.12]**	**0.01 [-0.01, 0.03]**
	PM2.5 (CTM)	Crude	0.91 [0.82, 1.02]	-0.03 [-0.05, 0.00]
		Main	**0.90 [0.79, 1.02]**	**-0.03 [-0.05, 0.00]**
	PM2.5 (LUR)	Crude	1.08 [0.98, 1.20]	0.02 [0.00, 0.04]
		Main	**1.04 [0.92, 1.17]**	**0.01 [-0.01, 0.04]**
	PNacc (CTM)	Crude	1.03 [0.93, 1.13]	0.00 [-0.02, 0.02]
		Main	**1.02 [0.91, 1.14]**	**-0.01 [-0.03, 0.02]**
	PM2.5abs (LUR)	Crude	1.03 [0.97, 1.10]	0.00 [-0.01, 0.02]
		Main	**1.02 [0.95, 1.11]**	**0.00 [-0.01, 0.02]**
	NO2 (CTM)	Crude	0.97 [0.88, 1.06]	-0.01 [-0.03, 0.01]
		Main	**0.97 [0.87, 1.08]**	**-0.01 [-0.03, 0.01]**
	NO2 (LUR)	Crude	1.03 [0.94, 1.13]	0.00 [-0.02, 0.02]
		Main	**0.96 [0.86, 1.07]**	**-0.01 [-0.04, 0.01]**

Note: Main model is adjusted for age, sex, BMI, smoking status and quantity, environmental tobacco smoke (ETS), LDL-C/HDL-C, physical activity, education, traffic noise and for dichotomous outcomes additionally years of follow-up.

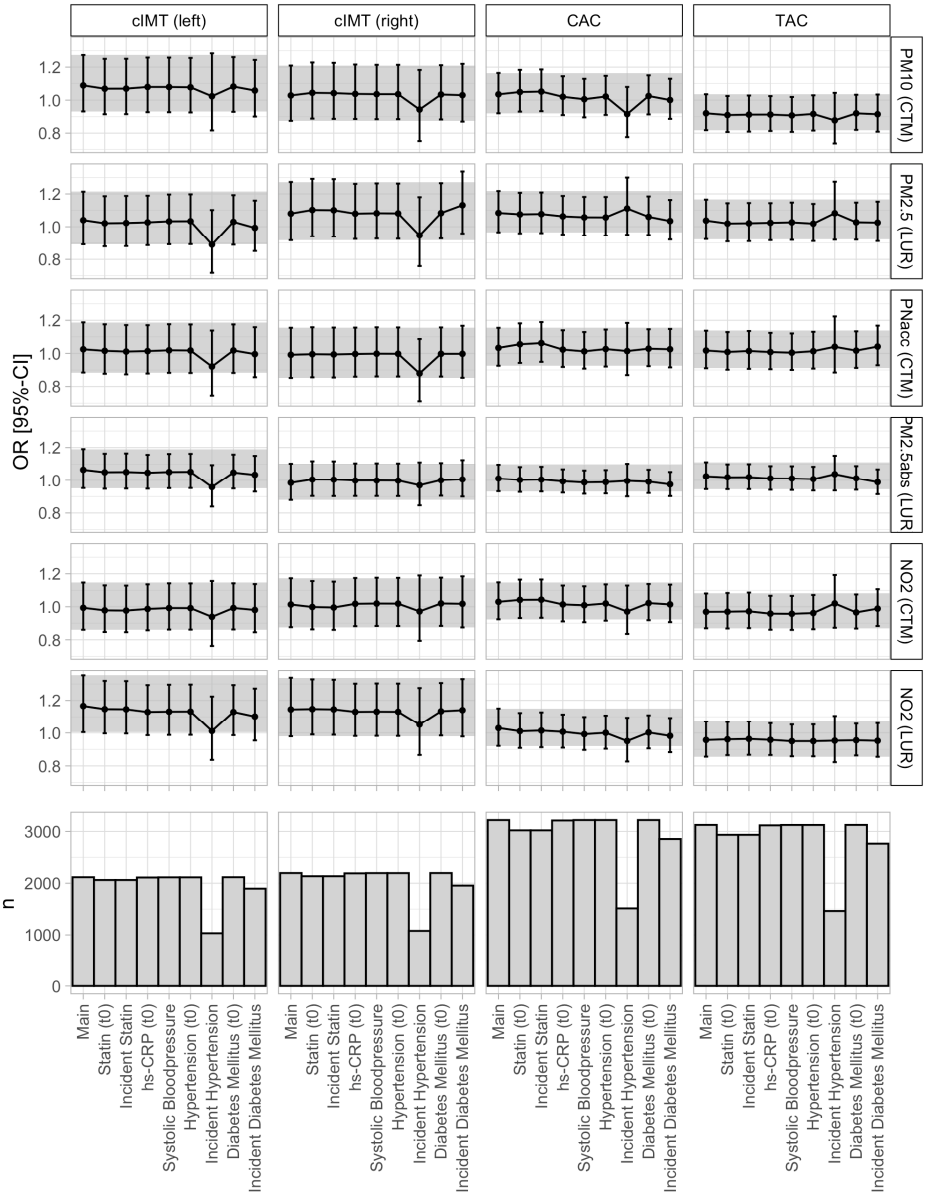

Figure S9: Estimated Odds Ratios (OR) (95%-CI) for progression of atherosclerosis measured using different markers (cIMT (left), cIMT (right), CAC, TAC) per IQR increase in air pollution concentration based on participants of the Heinz Nixdorf Recall cohort study evaluating adjustment by potential mediating variables.

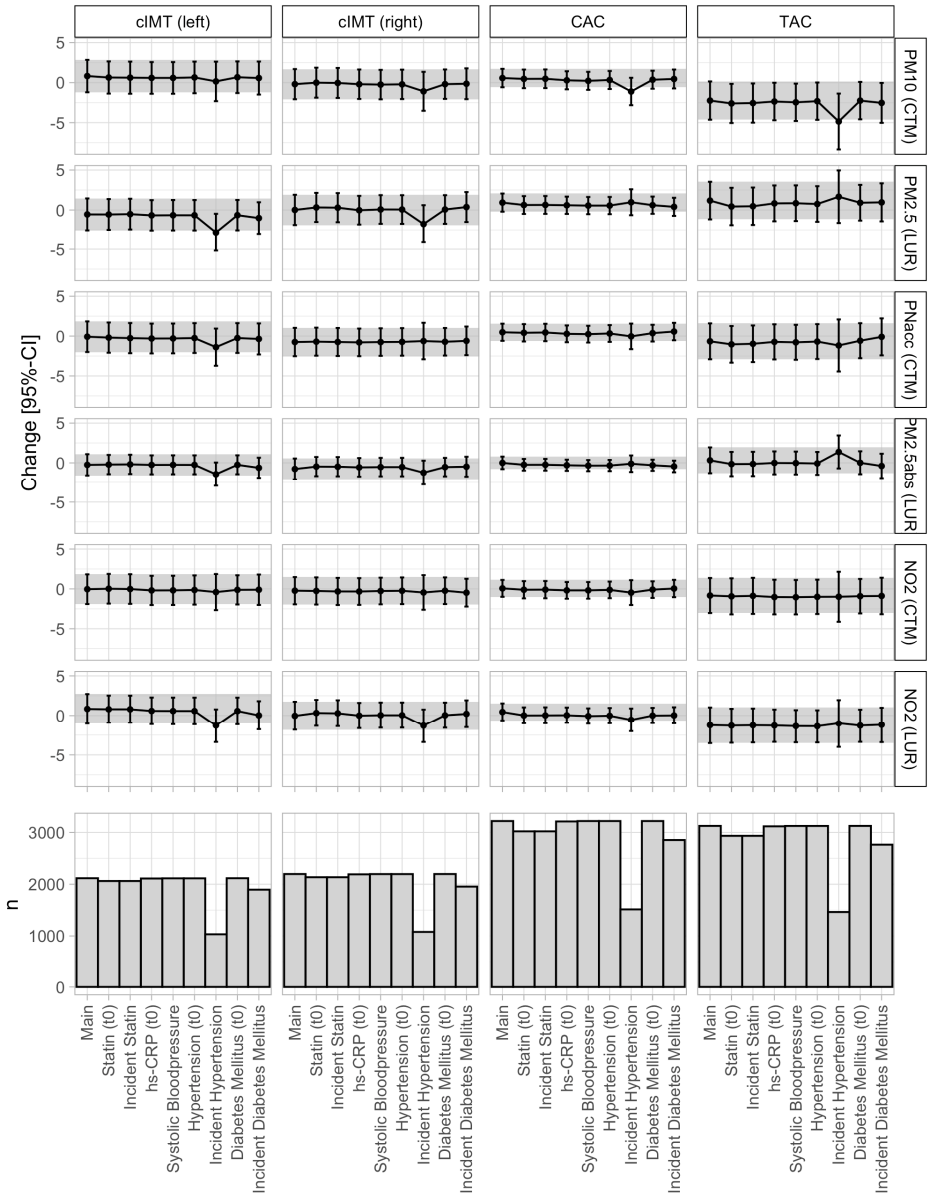

Figure S10: Estimated change (95%-CI) in carotid intima media thickniss (µm) (cIMT (left) and cIMT (right)) and calcification (growth rate) (CAC and TAC) per IQR increase in air pollution concentration based on participants of the Heinz Nixdorf Recall cohort study evaluating adjustment by potential mediating variables.

Table S3: Odds Ratio [95%-CI] for progression and change [95%-CI] in cIMT (µm) and calcification (growth rate) displayed per interquartile ranges of exposure estimated in participants of the Heinz-Nixdorf Recall Study with no/minor atherosclerotic burden at baseline (t0) (cIMT (left)=1054, cIMT (right)=1017, CAC=1527,TAC=1761) and participants with advanced atherosclerotic burden at t0 (cIMT (left)=1203, cIMT (right)=1317, CAC=1693,TAC=1469).

Marker	Exposure	Atherosclerotic burden[a]	OR [95%-CI]	Change [95%-CI]
cIMT (left)	PM10 (CTM)	No/Minor	1.42 [1.04, 1.94]	2.43 [-0.23, 5.09]
		Advanced	1.02 [0.84, 1.24]	-0.36 [-3.08, 2.37]
	PM10 (LUR)	No/Minor	1.16 [0.91, 1.48]	-0.30 [-2.39, 1.80]
		Advanced	0.98 [0.84, 1.14]	-0.52 [-2.68, 1.63]
	PM2.5 (CTM)	No/Minor	1.30 [0.95, 1.78]	2.15 [-0.58, 4.88]
		Advanced	0.99 [0.81, 1.22]	0.07 [-2.91, 3.04]
	PM2.5 (LUR)	No/Minor	1.37 [1.02, 1.84]	0.62 [-1.96, 3.20]
		Advanced	0.96 [0.80, 1.16]	-1.08 [-3.75, 1.60]
	PNacc (CTM)	No/Minor	1.41 [1.06, 1.88]	1.93 [-0.54, 4.39]
		Advanced	0.94 [0.78, 1.13]	-1.51 [-4.15, 1.12]
	PM2.5abs (LUR)	No/Minor	1.03 [0.86, 1.24]	-0.93 [-2.50, 0.65]
		Advanced	1.06 [0.92, 1.23]	0.40 [-1.49, 2.29]
	NO2 (CTM)	No/Minor	1.24 [0.95, 1.61]	1.49 [-0.88, 3.86]
		Advanced	0.93 [0.78, 1.12]	-1.13 [-3.76, 1.49]
	NO2 (LUR)	No/Minor	1.14 [0.88, 1.48]	-0.43 [-2.71, 1.84]
		Advanced	1.18 [0.98, 1.42]	2.14 [-0.39, 4.68]
cIMT (right)	PM10 (CTM)	No/Minor	0.88 [0.64, 1.21]	0.64 [-1.65, 2.93]
		Advanced	1.08 [0.88, 1.33]	-1.40 [-4.04,1.23]
	PM10 (LUR)	No/Minor	0.93 [0.72, 1.20]	-1.05 [-2.94, 0.83]
		Advanced	1.12 [0.95, 1.32]	1.59 [-0.42, 3.60]
	PM2.5 (CTM)	No/Minor	0.88 [0.63, 1.22]	0.74 [-1.66, 3.13]
		Advanced	1.09 [0.88, 1.35]	-1.69 [-4.45, 1.07]
	PM2.5 (LUR)	No/Minor	0.92 [0.67, 1.26]	-0.64 [-2.94, 1.66]
		Advanced	1.12 [0.91, 1.37]	0.29 [-2.26, 2.83]
	PNacc (CTM)	No/Minor	0.85 [0.64, 1.14]	0.71 [-1.42, 2.84]
		Advanced	1.01 [0.83, 1.23]	-3.40 [-5.92, -0.89]
	PM2.5abs (LUR)	No/Minor	0.86 [0.72, 1.02]	-1.15 [-2.70, 0.39]
		Advanced	1.03 [0.90, 1.19]	-0.65 [-2.41, 1.10]
	NO2 (CTM)	No/Minor	0.92 [0.69, 1.22]	0.93 [-1.12, 2.97]
		Advanced	1.08 [0.89, 1.31]	-1.62 [-4.08, 0.84]
	NO2 (LUR)	No/Minor	0.88 [0.67, 1.16]	-0.99 [-3.10, 1.12]
		Advanced	1.23 [1.02, 1.49]	0.44 [-1.89, 2.76]
CAC	PM10 (CTM)	No/Minor	1.12 [0.96, 1.31]	0.01 [0.00, 0.03]
		Advanced	0.93 [0.74, 1.17]	0.00 [-0.02, 0.01]
	PM10 (LUR)	No/Minor	1.13 [1.00, 1.28]	0.01 [0.00, 0.03]

Marker	Exposure	Atherosclerotic burden[a]	OR [95%-CI]	Change [95%-CI]
		Advanced	0.98 [0.82, 1.17]	0.00 [-0.01, 0.01]
	PM2.5 (CTM)	No/Minor	1.06 [0.90, 1.25]	0.01 [-0.01, 0.02]
		Advanced	0.84 [0.66, 1.07]	-0.01 [-0.03, 0.01]
	PM2.5 (LUR)	No/Minor	1.19 [1.03,1.39]	0.02 [0.01, 0.04]
		Advanced	0.96 [0.77, 1.19]	0.00 [-0.02, 0.01]
	PNacc (CTM)	No/Minor	1.13 [0.97, 1.30]	0.02 [0.00, 0.03]
		Advanced	0.88 [0.71, 1.09]	-0.01 [-0.02, 0.01]
	PM2.5abs (LUR)	No/Minor	1.00 [0.90, 1.12]	0.00 [-0.01, 0.01]
		Advanced	0.99 [0.86, 1.14]	0.00 [-0.01, 0.01]
	NO2 (CTM)	No/Minor	1.07 [0.93, 1.24]	0.01 [-0.01, 0.02]
		Advanced	0.90 [0.72, 1.11]	-0.01 [-0.02, 0.01]
	NO2 (LUR)	No/Minor	1.13 [0.98, 1.31]	0.01 [0.00, 0.03]
		Advanced	0.90 [0.74, 1.10]	0.00 [-0.02, 0.01]
TAC	PM10 (CTM)	No/Minor	1.09 [0.92, 1.29]	0.01 [-0.02, 0.05]
		Advanced	0.78 [0.66, 0.91]	-0.04 [-0.06, -0.01]
	PM10 (LUR)	No/Minor	1.02 [0.89, 1.16]	0.00 [-0.02, 0.02]
		Advanced	1.03 [0.91, 1.17]	0.01 [-0.01, 0.03]
	PM2.5 (CTM)	No/Minor	1.13 [0.95, 1.36]	0.03 [0.00, 0.07]
		Advanced	0.72 [0.61, 0.85]	-0.06 [-0.09, -0.03]
	PM2.5 (LUR)	No/Minor	1.11 [0.94, 1.30]	0.01 [-0.02, 0.04]
		Advanced	0.99 [0.85, 1.16]	0.00 [-0.02, 0.03]
	PNacc (CTM)	No/Minor	1.18 [1.00, 1.39]	0.01 [-0.02, 0.04]
		Advanced	0.89 [0.77, 1.04]	-0.02 [-0.05, 0.01]
	PM2.5abs (LUR)	No/Minor	1.06 [0.95, 1.18]	0.00 [-0.02, 0.02]
		Advanced	1.00 [0.90, 1.11]	0.00 [-0.02, 0.02]
	NO2 (CTM)	No/Minor	1.13 [0.96, 1.32]	0.03 [0.00, 0.06]
		Advanced	0.84 [0.72, 0.97]	-0.03 [-0.06, -0.01]
	NO2 (LUR)	No/Minor	1.04 [0.89, 1.22]	-0.01 [-0.04, 0.02]
		Advanced	0.90 [0.78, 1.04]	-0.02 [-0.04, 0.01]

Note: Main model is adjusted for age, sex, BMI, smoking status and quantity, environmental tobacco smoke (ETS), LDL-C/HDL-C, physical activity, education, traffic noise and for dichotomous outcomes additionally years of follow-up.

a. No/minor atherosclerotic burden is defined by baseline cIMT <=0.7mm and CAC/TAC <= 10 Agatston score units; Advanced atherosclerotic burden is defined by baseline cIMT > 0.7mm and CAC/TAC > 10 Agatston score units.

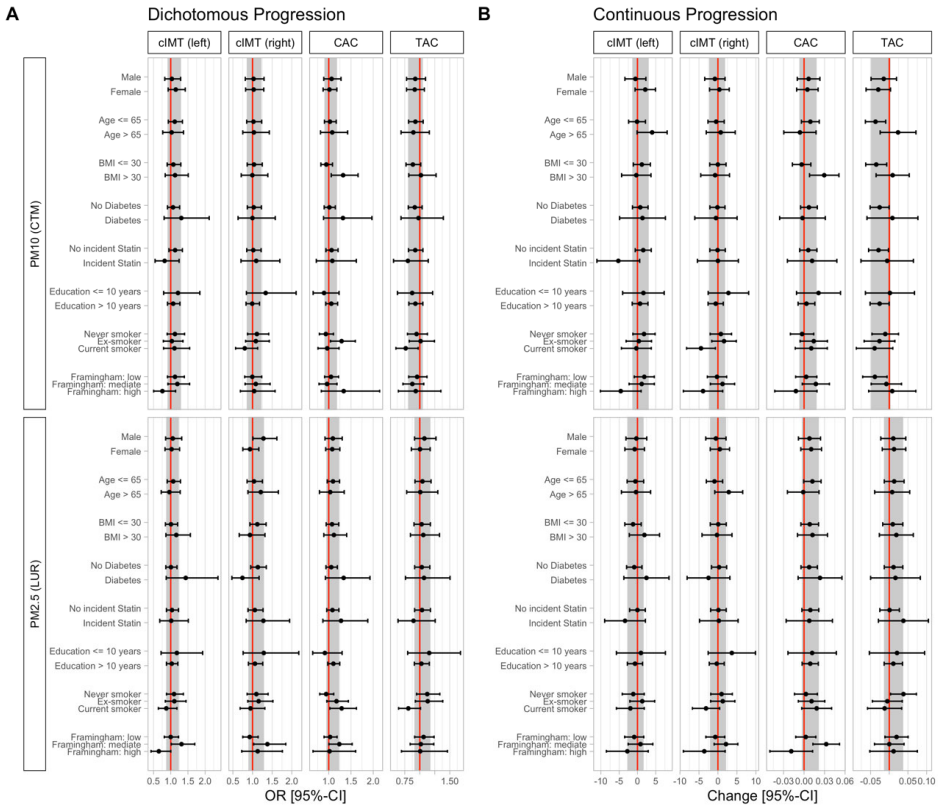

Figure S11: Subgroup effect estimates for the associations between different air pollutants and progression of atherosclerosis in subpopulations of the Heinz Nixdorf Recall Study based on the marker of atherosclerosis (cIMT (left)=2116, cIMT (right)=2197, CAC=3220, TAC=3126). Model is adjusted for age, sex, BMI, smoking status and quantity, environmental tobacco smoke (ETS), LDL-C/HDL-C, physical activity, education, traffic noise and for dichotomous outcomes additionally years of follow-up Panel A displays Odds Ratios (OR) (95%-CI) for any progression in atherosclerosis based on an interquartile range (IQR) in exposure. Panel B displays change in thickness (µm) for cIMT and change in growth rate for CAC and TAC.

Table S4: Estimated Odds Ratio (95%-CI) for progression of atherosclerosis in different markers defined by 10% increase (first column) and Relative Risks (95%-CI) for progression of atherosclerosis estimated using Poisson regression (second column) displayed per interquartile ranges of exposure based on participants of the Heinz-Nixdorf Recall Study sample (N = 2116 for cIMT (left), N = 2197 for cIMT (right), N = 3220 for CAC, and N = 3126 for TAC).

Marker	Exposure	OR (95%-CI), 10%	RR (95%-CI)
cIMT (left)	PM10 (CTM)	1.06 [0.93, 1.21]	1.02 [0.95, 1.09]
	PM10 (LUR)	1.00 [0.90, 1.11]	1.00 [0.95, 1.06]
	PM2.5 (CTM)	1.06 [0.92, 1.21]	1.01 [0.94, 1.09]
	PM2.5 (LUR)	0.99 [0.87, 1.13]	1.01 [0.94, 1.08]
	PNacc (CTM)	1.02 [0.90, 1.15]	1.01 [0.94, 1.08]
	PM2.5abs (LUR)	1.01 [0.93, 1.11]	1.01 [0.97, 1.06]
	NO2 (CTM)	0.99 [0.87, 1.11]	1.00 [0.93, 1.07]
	NO2 (LUR)	1.04 [0.92, 1.18]	1.03 [0.97, 1.10]
cIMT (right)	PM10 (CTM)	0.97 [0.85, 1.10]	1.01 [0.94, 1.08]
	PM10 (LUR)	0.95 [0.86, 1.06]	1.01 [0.96, 1.07]
	PM2.5 (CTM)	0.94 [0.82, 1.08]	1.00 [0.93, 1.08]
	PM2.5 (LUR)	0.94 [0.82, 1.07]	1.01 [0.95, 1.09]
	PNacc (CTM)	0.98 [0.87, 1.11]	1.00 [0.93, 1.07]
	PM2.5abs (LUR)	0.99 [0.90, 1.08]	1.00 [0.95, 1.05]
	NO2 (CTM)	0.96 [0.85, 1.08]	1.00 [0.94, 1.07]
	NO2 (LUR)	1.03 [0.91, 1.16]	1.03 [0.96, 1.10]
CAC	PM10 (CTM)	1.02 [0.91, 1.15]	1.01 [0.94, 1.08]
	PM10 (LUR)	1.08 [0.99, 1.19]	1.03 [0.98, 1.08]
	PM2.5 (CTM)	0.96 [0.85, 1.08]	0.99 [0.93, 1.07]
	PM2.5 (LUR)	1.10 [0.98, 1.23]	1.03 [0.97, 1.10]
	PNacc (CTM)	1.02 [0.92, 1.14]	1.01 [0.95, 1.07]
	PM2.5abs (LUR)	1.03 [0.95, 1.11]	1.00 [0.96, 1.05]
	NO2 (CTM)	1.00 [0.90, 1.11]	1.01 [0.95, 1.07]
	NO2 (LUR)	1.04 [0.93, 1.16]	1.01 [0.95, 1.08]
TAC	PM10 (CTM)	0.92 [0.82, 1.03]	0.96 [0.90, 1.04]
	PM10 (LUR)	1.02 [0.93, 1.12]	1.01 [0.95, 1.07]
	PM2.5 (CTM)	0.91 [0.81, 1.03]	0.95 [0.88, 1.03]
	PM2.5 (LUR)	1.04 [0.93, 1.17]	1.01 [0.94, 1.09]
	PNacc (CTM)	1.02 [0.92, 1.14]	1.00 [0.94, 1.07]
	PM2.5abs (LUR)	1.01 [0.94, 1.10]	1.01 [0.96, 1.06]
	NO2 (CTM)	0.97 [0.87, 1.08]	0.99 [0.92, 1.06]
	NO2 (LUR)	0.96 [0.86, 1.07]	0.98 [0.92, 1.05]

Marker	Exposure	OR (95%-CI), 10%	RR (95%-CI)

Note: Main model is adjusted for age, sex, BMI, smoking status and quantity, environmental tobacco smoke (ETS), LDL-C/HDL-C, physical activity, education, traffic noise and for dichotomous outcomes additionally years of follow-up; changing the cutpoint to 20% did not differ from using a cut point of 10%.

Table S5: Estimated Odds Ratio (95%-CI) for progression of atherosclerosis in different markers as a sensitivity analysis investigating mean of left and/or right cIMT, faster progression of CAC based on personal percentile, displayed per interquartile ranges of exposure based on participants of the Heinz-Nixdorf Recall Study sample (N = 2594 for cIMT (left/right), N = 3220 for faster CAC).

Marker	Exposure	OR [95%-CI]	Change [95%-CI]
cIMT (left or right)	PM10 (CTM)	1.04 [0.90, 1.22]	0.34 [-1.23, 1.90]
	PM10 (LUR)	1.06 [0.93, 1.20]	0.28 [-0.98, 1.54]
	PM2.5 (CTM)	1.01 [0.86, 1.18]	0.19 [-1.45, 1.82]
	PM2.5 (LUR)	1.04 [0.89, 1.21]	0.05 [-1.51, 1.62]
	PNacc (CTM)	0.96 [0.84, 1.11]	-0.40 [-1.87, 1.08]
	PM2.5abs (LUR)	1.04 [0.93, 1.17]	-0.26 [-1.33, 0.81]
	NO2 (CTM)	1.00 [0.87, 1.14]	-0.26 [-1.70, 1.17]
	NO2 (LUR)	1.11 [0.96, 1.28]	0.45 [-1.01, 1.92]
faster CAC	PM10 (CTM)	1.04 [0.91, 1.19]	
	PM10 (LUR)	1.08 [0.97, 1.19]	
	PM2.5 (CTM)	0.95 [0.83, 1.09]	
	PM2.5 (LUR)	1.10 [0.97, 1.25]	
	PNacc (CTM)	1.05 [0.93, 1.19]	
	PM2.5abs (LUR)	1.02 [0.93, 1.12]	
	NO2 (CTM)	0.99 [0.88, 1.12]	
	NO2 (LUR)	1.05 [0.93, 1.19]	

Note: Main model is adjusted for age, sex, BMI, smoking status and quantity, environmental tobacco smoke (ETS), LDL-C/HDL-C, physical activity, education, traffic noise and for dichotomous outcomes additionally years of follow-up.

Table S6: Estimated Odds Ratio [95%-CI] for progression of atherosclerosis and estimated change [95%-CI] in cIMT (µm) and calcification (growth rate) displayed per interquartile ranges of exposure with regard to different time windows of exposure, modelled using the EURAD chemistry-transport model (CTM). Estimation are based on the main model and participants of the Heinz-Nixdorf Recall Study sample (N = 2116 for cIMT (left), N = 2197 for cIMT (right), N = 3220 for CAC, and N = 3126 for TAC).

Marker	Exposure	OR [95%-CI]	Change [95%-CI]
cIMT (left)	PM10 (CTM)	1.09 [0.93, 1.27]	0.82 [-1.20, 2.85]
	PM10 (CTM, 2000-2003)	1.10 [0.93, 1.31]	1.21 [-1.01, 3.42]
	PM10 (CTM, 2006-2008)	1.07 [0.93, 1.24]	0.46 [-1.40, 2.31]
	PM2.5 (CTM)	1.06 [0.90, 1.25]	1.12 [-0.99, 3.24]
	PM2.5 (CTM, 2000-2003)	1.07 [0.91, 1.26]	1.34 [-0.80, 3.48]
	PM2.5 (CTM, 2006-2008)	1.04 [0.89, 1.23]	0.87 [-1.25, 2.99]
	PNacc (CTM)	1.02 [0.88, 1.19]	-0.08 [-2.00, 1.84]
	PNacc (CTM, 2000-2003)	1.04 [0.89, 1.21]	0.21 [-1.78, 2.21]
	PNacc (CTM, 2006-2008)	1.01 [0.86, 1.17]	-0.40 [-2.39, 1.59]
	NO2 (CTM)	0.99 [0.86, 1.15]	-0.04 [-1.90, 1.83]
	NO2 (CTM, 2000-2003)	1.00 [0.87, 1.14]	0.14 [-1.62, 1.90]
	NO2 (CTM, 2006-2008)	0.99 [0.86, 1.13]	-0.25 [-2.02, 1.52]
cIMT (right)	PM10 (CTM)	1.03 [0.87, 1.21]	-0.19 [-2.07, 1.69]
	PM10 (CTM, 2000-2003)	1.01 [0.85, 1.20]	-0.41 [-2.47, 1.65]
	PM10 (CTM, 2006-2008)	1.04 [0.90, 1.21]	0.00 [-1.72, 1.73]
	PM2.5 (CTM)	1.01 [0.85, 1.19]	-0.45 [-2.41, 1.50]
	PM2.5 (CTM, 2000-2003)	1.01 [0.85, 1.20]	-0.37 [-2.34, 1.60]
	PM2.5 (CTM, 2006-2008)	1.01 [0.85, 1.19]	-0.54 [-2.50, 1.42]
	PNacc (CTM)	0.99 [0.85, 1.15]	-0.75 [-2.53, 1.04]
	PNacc (CTM, 2000-2003)	0.99 [0.85, 1.16]	-0.71 [-2.55, 1.14]
	PNacc (CTM, 2006-2008)	0.98 [0.84, 1.15]	-0.88 [-2.72, 0.97]
	NO2 (CTM)	1.01 [0.88, 1.17]	-0.23 [-1.94, 1.48]
	NO2 (CTM, 2000-2003)	1.00 [0.87, 1.15]	-0.24 [-1.85, 1.38]
	NO2 (CTM, 2006-2008)	1.02 [0.89, 1.18]	-0.18 [-1.80, 1.44]
CAC	PM10 (CTM)	1.04 [0.92, 1.16]	0.01 [-0.01, 0.02]
	PM10 (CTM, 2000-2003)	1.03 [0.90, 1.17]	0.01 [-0.01, 0.02]
	PM10 (CTM, 2006-2008)	1.04 [0.93, 1.16]	0.01 [-0.01, 0.02]
	PM2.5 (CTM)	0.98 [0.87, 1.11]	0.00 [-0.01, 0.01]
	PM2.5 (CTM, 2000-2003)	0.98 [0.86, 1.11]	0.00 [-0.01, 0.01]
	PM2.5 (CTM, 2006-2008)	0.99 [0.88, 1.12]	0.00 [-0.01, 0.01]
	PNacc (CTM)	1.03 [0.93, 1.15]	0.00 [-0.01, 0.02]
	PNacc (CTM, 2000-2003)	1.02 [0.91, 1.15]	0.00 [-0.01, 0.02]
	PNacc (CTM, 2006-2008)	1.05 [0.93, 1.17]	0.01 [0.00, 0.02]
	NO2 (CTM)	1.03 [0.92, 1.15]	0.00 [-0.01, 0.01]
	NO2 (CTM, 2000-2003)	1.01 [0.91, 1.12]	0.00 [-0.01, 0.01]

Marker	Exposure	OR [95%-CI]	Change [95%-CI]
	NO2 (CTM, 2006-2008)	1.04 [0.94, 1.16]	0.00 [-0.01, 0.01]
TAC	PM10 (CTM)	0.92 [0.82, 1.04]	-0.02 [-0.05, 0.00]
	PM10 (CTM, 2000-2003)	0.91 [0.80, 1.04]	-0.02 [-0.05, 0.01]
	PM10 (CTM, 2006-2008)	0.93 [0.84, 1.04]	-0.02 [-0.05, 0.00]
	PM2.5 (CTM)	0.90 [0.79, 1.02]	-0.03 [-0.05, 0.00]
	PM2.5 (CTM, 2000-2003)	0.90 [0.79, 1.02]	-0.03 [-0.05, 0.00]
	PM2.5 (CTM, 2006-2008)	0.90 [0.80, 1.02]	-0.03 [-0.05, 0.00]
	PNacc (CTM)	1.02 [0.91, 1.14]	-0.01 [-0.03, 0.02]
	PNacc (CTM, 2000-2003)	1.02 [0.91, 1.15]	0.00 [-0.03, 0.02]
	PNacc (CTM, 2006-2008)	1.02 [0.91, 1.14]	-0.01 [-0.03, 0.02]
	NO2 (CTM)	0.97 [0.87, 1.08]	-0.01 [-0.03, 0.01]
	NO2 (CTM, 2000-2003)	0.99 [0.90, 1.10]	0.00 [-0.02, 0.02]
	NO2 (CTM, 2006-2008)	0.95 [0.86, 1.06]	-0.02 [-0.04, 0.01]

Note: Main model is adjusted for age, sex, BMI, smoking status and quantity, environmental tobacco smoke (ETS), LDL-C/HDL-C, physical activity, education, traffic noise and for dichotomous outcomes additionally years of follow-up.

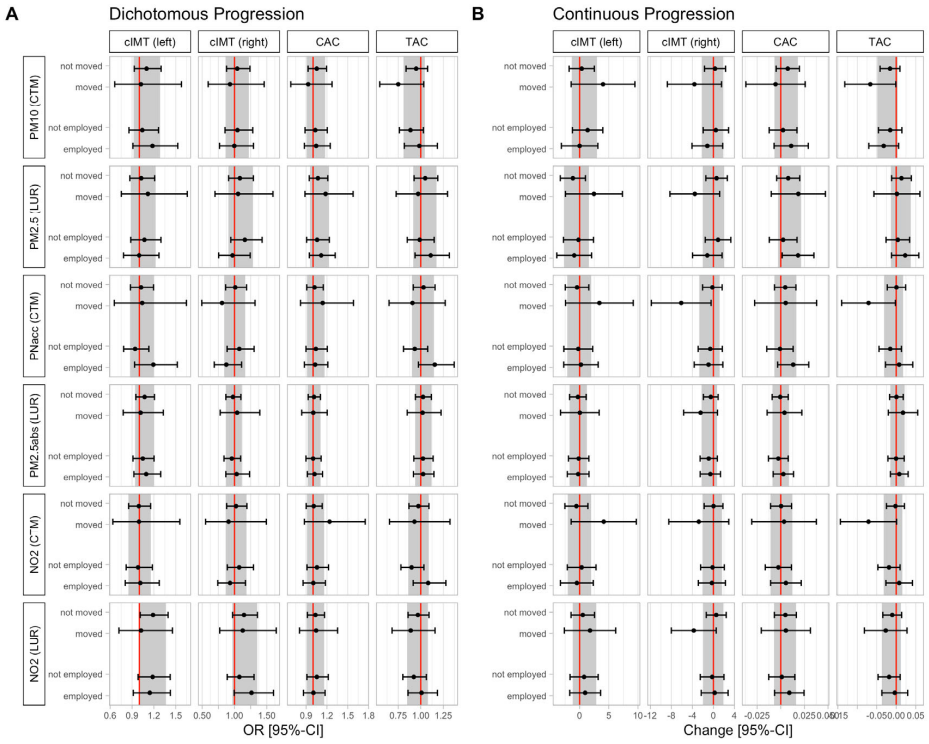

Figure S12: Subgroup effect estimates for the associations between different air pollutants and progression of atherosclerosis in subpopulations of the Heinz Nixdorf Recall Study based on the marker of atherosclerosis with respect to exposure misclassification (cIMT (left)=2116, cIMT (right)=2197, CAC=3220, TAC=3126). Movers within subsamples: cIMT (left) = 13.3%; cIMT (right) = 12.8%; CAC = 12.9%; TAC = 12.8%. Non-Employees within subsamples: cIMT (left) = 57.9%; cIMT (right) = 58%; CAC = 58.8%; TAC = 59.9%. Panel A displays Odds Ratios (OR) (95%-CI) for any progression in atherosclerosis based on an interquartile range (IQR) in exposure. Panel B displays change in thickness (µm) for cIMT and change in growth rate for CAC and TAC.

6 Discussion

Overall, the achievements of this thesis are its contributions to epidemiological evidence on associations between ambient short- as well as long-term air pollution exposure and cardiovascular disease in the Ruhr Area, representing a metropolitan living environment in Europe, which is not only affected by local rush-hour traffic and industrial hot spots, but also by traffic, industry, and shipping outside of the Ruhr Area or even outside of Germany.

6.1 Air Pollution Exposure Assessment

6.1.1 EURAD-CTM *versus* LUR

Long-term air pollution was characterized by concentrations of different air pollutants, including fine particulate matter ($PM_{2.5}$), mass of coarser particles (PM_{10}), $PM_{2.5\text{abs}}$ (absorbance), particle number concentration of particles in the accumulation mode ($0.035 - 0.14\ \mu m$ (Nonnemacher et al. 2014)), as well as NO_2, which were modelled using the EURAD-CTM and/or land-use regression models, developed within the ESCAPE study [Beelen et al. (2013); Eeftens2012]. Short-term air pollution was characterized by daily particle number concentrations of different sized particles, including UFPs, particle surface concentration (PSC), PM_{10}, NO_2, and O_3, at a single measurement site as part of the German Ultrafine Aerosol Network (Birmili et al. 2016). The EURAD-CTM was originally implemented to operationalize daily forecast air pollution concentrations in Germany, and was part of an extensive model comparison and evaluation study over a whole decade modelling air quality data (Colette et al. 2011). The cooperation with the RIU institute forecasting air quality in Europe, was a big milestone for studying health effects of air pollution studies in the general population, namely the HNR study, enabling a flexible exposure assessment with regard to time and space. The LUR model, on the other hand, has specifically been developed to estimate air pollution concentration on a population-based level, taking into account features of land-use within certain buffers and a statistical modelling approach to predict air pollution concentration. Reported investigations in Hennig et al. (2016) have shown that different approaches to estimate concentration for the same air pollutants (here $PM_{2.5}$, PM_{10}, and NO_2) in the same geographical area expectedly lead to different air pollution concentration due to the modelling design, aim, and strategy. Despite these differences, neither of the applied models is considered as wrong or as being better than the other. In fact, these two approaches can complement each other. While the the EURAD-CTM is a spatial and temporal approach, considering long-range transport on a broader scale (1×1 km^2), the LUR estimates static point-specific concentrations based on local land-use predictors. As has been pointed out in Hennig et al. (2016), agreement, for example, improved when the EURAD-CTM was restricted to sources of regional traffic. However, long-range transport and formation of secondary particles in the atmosphere can contribute considerably to the particle mass concentration in NRW and the Ruhr Area, e.g., more than 50%

(Hebbinghaus et al. 2014). Also, the NO_2 concentration can be attributed to long-range transportation by approximately 25%.

Moreover, an accurate population-representative estimation of air pollution exposure does not only depend on ambient exposure levels but also on the mobility and whereabouts of the population of interest. Yet, while a broader scale seemed more promising in terms of exposure misclassification, included sensitivity analyses with regard to employment and changes of residence, have not shown to noticeably change the reported main effects for both exposure models.

Motivated by the question of whether to use one or the other approach, a suggestion to use a hybrid model combining both modelling approaches was discussed in Hennig et al. (2016). A first approach to combine the EURAD-CTM with the LUR modelling has been performed in the Ruhr Area, improving the performance for $PM_{2.5}$ based on explained variation from 85% to 93% (Hennig et al. 2018a). However, despite a considerably better performance of the hybrid LUR compared to the original ESCAPE LUR model, more research is needed. In an additional European collaboration hybrid LUR models for $PM_{2.5}$, NO_2, O_3 and BC were developed in West-Europe to provide exposure assessment for 35 million participants from 18 European cohorts participating in the ELAPSE study (Effects of Low-Level Air Pollution: A Study in Europe), including the HNR cohort (Hoogh et al. 2018). They developed LUR models for monitored air pollution data based on satellite observations, dispersion model estimates, land use and traffic data, reaching an overall performance of 72% for $PM_{2.5}$ and 69% for NO_2 based on explained spatial variation in the measured concentrations.

6.1.2 Air Pollution Assessment and Health Effects

While in population-based studies there is often only one modelling approach available, the Ruhr Area benefited from two commonly used modelling approaches, enabling a direct comparison of health effects. While earlier findings pointed to inconsistent conclusions, the newer longitudinal investigation, including a re-assessment of cIMT measurement in order to follow a standardized approach for repeated measures, yielded only slightly different point estimates with largely overlapping confidence intervals (Hennig et al. 2020). Overall, slightly stronger associations were reported with the EURAD-CTM compared to the LUR with respect to point estimates.
An investigation in the Netherlands comparing the earlier mentioned hybrid LUR model developed within the ELAPSE study, with an LUR model and an dispersion model have reported an overall moderate agreement (Klompmaker et al. 2021). Nevertheless, although air pollution was overall positively associated with natural cause and cause-specific mortality, the strength of the associations differed between the three exposure models. Continued efforts to overcome potential inconsistencies between different exposure models, or at least transparently report respective strength and limitations, may reduce scientific uncertainties, which may hamper policy interventions to protect public health.

6.1.3 Future Perspectives

Although, CTMs and LURs both have their justification, hybrid approaches are gaining popularity and seem promising with regard to performance and application in population-based air-pollution studies. Due to their ease of use, hybrid models are predominantly based on the LUR modeling strategy. For example, EURAD-CTM estimates are used as an additional predictor to predict annual air pollutant concentrations based on the LUR model. However, a general concern regarding LUR models has rarely been discussed: it's own ambiguity. The LUR approach comes with a number of variables that have to be chosen *a priori*, possibly having an impact on the outcome performance. These variables include the choice of locations, as well as the duration and time of air pollution measurements on the one hand, and the choice of features (predictors), the selection strategy, and the statistical model assumption on the other hand. While a linear regression model has been the statistical model of choice, mostly due to its simplicity of understanding and application, overfitting, especially in the presence of only few monitoring sites to train a model based on a large number of potential predictor variables, is just one concern that has arisen (Basagaña et al. 2012). Methods of supervised machine learning, such as random forests (Breiman 2001), have become more popular over the last years and have often been shown to outperform linear regression regarding predictive performance, even in air pollution applications (Brokamp et al. 2017). Possible reasons for this are the avoidance of a predefined selection strategy and less strong assumptions (i.e. linearity) about the relationship between features and the respective outcome. With data from the EURAD-CTM, continuously monitored concentrations, as well as land-use data at hand, application of machine learning algorithms could provide more accurate estimates for air pollution exposure in the Ruhr Area.

6.2 Air Pollution and Cardiovascular Health

6.2.1 Cardiovascular Mortality and Cardiovascular Outcomes

Short-term levels of air pollution have been shown to be associated with acute natural and cardiovascular mortality within a few days in the Ruhr Area as outlined in Hennig et al. (2018b). In addition, long-term exposure to air pollution has previously been shown to be associated with events of stroke and a potentially increased risk of coronary events within the HNR study population and a follow-up time of roughly 8 years (Hoffmann et al. 2015). Results for stroke were confirmed in a study considering a follow-up time of 14 years, while associations with events of coronary heart disease were not observed (Rodins et al. 2020). An additional finding, however, was that stronger effects were observed for traffic-specific air pollution concentrations compared to all or industrial sources. Complementing results on cardiovascular mortality and cardiovascular events, associations between long-term ambient air pollution exposure (estimated using the EURAD-CTM) have been frequently reported for several cardiovascular-related outcomes in the HNR study, including biomarkers of systemic inflammation (Hennig et al. 2014; Hoffmann et al. 2009; Viehmann et al. 2015), hypertension (Fuks et al. 2016a), diabetes (Lucht et

al. 2018; Lucht et al. 2020; Weinmayr et al. 2015), and atherosclerosis [Hoffmann et al. (2007); (Bauer et al. 2010; Kälsch et al. 2014).

In addition to these local findings, the HNR study was part of the earlier introduced ESCAPE study, and hence contributed to observed cardiovascular health effects of air pollution on an European level: Fuks et al. (2016b) supported associations between annual air pollution exposure and noise and incident arterial hypertension; Cesaroni et al. (2014) reported that long term exposure to particulate matter is associated with incidence of coronary events, e.g. myocardial infarction; and Stafoggia et al. (2014) suggested an association between fine particles and the incidence of cerebrovascular events, i.e. strokes. While Perez et al. (2015) only indicated weak cross-sectional associations between long-term air pollution exposure and atherosclerosis, measured as cIMT, Lanki et al. (2015) was not able to support associations between particulate matter and markers of systemic inflammation (i.e. CRP or fibrinogen) but indicated weakly adverse effects for those living close to highly trafficked roads.

All these results reflect partial aspects of the causal chain between exposure to long-term air pollution and the occurrence of cardiovascular events hypothesized by Franklin et al. (2015). Yet, except the investigation of incident CV events, incident hypertension or incident diabetes, most of the mentioned results were based on cross-sectional findings.

6.2.2 Air pollution and Atherosclerosis

New results on air pollution and progression of atherosclerosis, reported in Hennig et al. (2019) and Hennig et al. (2020), widely supported cross-sectional findings, which reported that higher levels of air pollution or traffic-proximity are associated to higher levels of CAC (Hoffmann et al. 2007), TAC (Kälsch et al. 2014) and cIMT (Bauer et al. 2010). Although a direct relationship between air pollution and progression of markers has not been observed in the full study population, analyses in all three markers suggested associations with multiple air pollutant concentrations in participants with no or only minor atherosclerotic burden at baseline (Hennig et al. 2020, 2019). This supports the hypothesis that particle inhalation is associated with the development of atherosclerosis (Franklin et al. 2015). Associations between air pollution and CAC were the most consistent among those considered, and in line with results from Multi-Ethnic Study of Atherosclerosis (MESA), suggesting air-pollution induced progression of CAC (but not with cIMT) (Kaufman et al. 2016). The MESA study is a population-based cohort comparable to the HNR cohort, studying characteristics of subclinical cardiovascular disease, risk prediction and progression of the subclinical disease initiated in the year 2000 in the United States. Non air pollution studies have identified advanced CAC (CAC >100 Agatston score units) as a strong predictor for cardiovascular events in the HNR study and MESA study (Budoff et al. 2013; Erbel et al. 2010). Hence, an air pollution-related shift in the distribution of CAC is likely to have an impact on the occurrence of cardiovascular events.

In Hennig et al. (2020), the natural progression of CAC over time was taken into account by using a mathematical prediction equation, developed in Lehmann et al. (2018).

However, a faster progression, namely deviating upwards from the predicted value, was not observed for increased levels of air pollution, considering the whole population under study. Nevertheless, subgroup analyses in participants starting off with a smaller atherosclerotic burden, which was not reported in the published analyses, indicated a faster progression of CAC based on an 1.5 $\mu g/m^3$ increase in $PM_{2.5}$ (LUR) with an estimated Odds Ratio (OR) of 1.27 [95%-Confidence interval: 1.05; 1.54] in participants with no or minor atherosclerotic burden at baseline compared to participants with an advanced atherosclerotic burden at baseline with an estimated OR of 1.00 [0.83; 1.20]. These findings strengthen the reported findings on air pollution and incident CAC, and further support the cardiovascular burden of air pollution exposure.

One limitation is the relatively short follow-up time of only five years, hampering to study progression in such a non-symptomatic lifelong-changing condition like atherosclerosis. Hence, future investigations taking the 10-year follow-up examinations into account, could provide additional insight about air pollution-related progression of atherosclerosis.

6.2.3 Different Markers of Atherosclerosis and Challenges

While atherosclerosis is often used as a general term, without specifically differentiating between multiple surrogate measures, the majority of epidemiological studies on health effects of air pollution have made use of cIMT due to the low costs and an easy implementation of measurement. However, in the HNR study, as well as in the MESA study, more consistent effect estimates were observed between air pollution and CAC compared to air pollution and cIMT. TAC, probably due to its location and the subordinate clinical role compared to CAC, has rarely been studied in epidemiological studies.
Compared to the subclinical markers TAC and CAC, cIMT is more prone to measurement error. This may not only lead to confusion in the literature but also to somewhat inconsistent epidemiological findings (Touboul et al. 2012). While an agreement has been made to choose the common carotid artery (CCA) over the external and internal carotid artery because the CCA is less affected by the anatomical topography or the sonographer's expertise (Touboul et al. 2004), there are several important issues to consider. Compared to the thoracic artery or the coronary arteries, which are located in the center of the body, the CCAs are paired and located on the left and right body side, with different anatomic origins. While the left CCA arises from the arch of aorta, the right CCA arises from the brachiocephalic trunk, potentially leading to different flow patterns and turbulences. Luo et al. (2011) investigated left and right cIMT, reporting significantly thicker cIMT on the left compared to the right side, as well as a faster thickening by age. In addition, different side-specific correlations were observed between cIMT and haemodynamic parameters, including maximal velocity, which were stronger for right cIMT. In contrast, correlations between cIMT and biochemical indices, including pulse pressure, cholesterol or blood glucose, were stronger for left cIMT. A comparison of left and right cIMT focusing on their relationship with CVD has been carried out by Loizou et al. (2015), supporting a slightly higher left cIMT for the group with CVD. Although their collection of findings, taking into account multiple studies, did not yield strong evidence for side-specific differences, Loizou et al. (2015) suggested further research in

order to estimate differences and similarities between left and right cIMT regarding their complex structure, morphology, as well as their different vulnerability with respect to CVDs. Because epidemiological studies on air pollution often focus on only right cIMT measurements (Künzli et al. 2010) or an average of both sides (Bauer et al. 2010; Perez et al. 2015), they fail to enlighten differences with respect to side. The reported side-specific findings in Hennig et al. (2020) on the other hand contributed to the research on site-specific differences with respect to cIMT. While bigger values for cIMT on the left side compared to the right side for both examination time points were observed, in line with Luo et al. (2011) and Loizou et al. (2015), observed annual progression in cIMT did not support side-specific differences. In contrast, side-specific differences were, again, observed with respect to air pollution, especially in the subgroup analysis stratifying on the initial atherosclerotic burden: the association between air pollution and left cIMT showed a similar pattern to that of CAC and TAC, but with more variability. In contrast, the association between air pollution and right cIMT showed no such pattern (Hennig et al. 2020).

While sonography of the carotid arteries is readily available and comes at low cost and effort, correct and reliable measurement of cIMT is challenging. cIMT can be measured in offline ultrasound pictures manually or with the help of semi-automatic software, although semi-automatic tools have been used more widely lately. However, regarding cIMT measurements in the HNR study, a switch from manual to semi-automated measurements had to be conducted in order to guarantee reproducible, but mostly comparable measurements between baseline and follow-up measurements in order to calculate progression. Although Touboul et al. (2012) provided guidance on cIMT measurements based on a standard ultrasound image, independent of manual or semi-automatic technique, the choice of statistic metric (minimum, quartiles, median, mean or maximum) with respect to elemental measurements within a recommended length of 10 mm per longitudinal section, or with respect to the number of available images per side and with respect to an average over both sides remains to be chosen by the investigator. Therefore, re-measurements of cIMT at baseline, as well as new measurements of cIMT at the follow-up examination were conducted in alignment with the standardized procedure described in Hennig et al. (2020). Beyond the described technical difficulties, one has to carefully distinguish between the two phenotypes cIMT and plaque. While it is appropriate to use a 2-dimensional image to capture thickening of the intima-media-thickness, an appropriate capture of plaque requires demonstration from 2 different angles of intonation in longitudinal and cross-sectional views (Touboul et al. 2012). Maybe it is because of the complicated measurement that plaque has rarely been used in epidemiological studies on air pollution, as there has been only one study linking traffic-related air pollutants (NO_2) to carotid plaque (Johnson et al. 2020). However, from a clinical perspective, cIMT without plaque defines a significant marker of an increased risk of vascular events, with the potential to predict plaque occurrence (Touboul et al. 2012). In the HNR study, cIMT measurements did not include plaque formations. Occurrence of plaque formation (yes/no) in the bulb, external and internal carotid artery was recorded by the respective examiner, yet the data was too limited to be investigated in the conducted air pollution study.

6.2.4 Future Perspectives

While all of the reported studies mainly focussed on multiple air pollution exposures and one outcome at a time within the cardiovascular framework, investigations connecting the dots could yield a better understanding of reported associations and disease development with respect to the causal chain hypothesized by Franklin et al. (2015). Mediation analyses, like Lucht et al. (2020) performed for investigating the causal pathway between long-term exposure to air pollution and 10 year incidence of diabetes, are needed to investigate whether hypothetical mechanisms linking long-term air pollution exposure to cardiovascular morbidity and mortality, proposed by Franklin et al. (2015), can also be seen in observational data. Such information could add to the assessment of the cardiac health burden regarding air pollution.

6.3 Air Pollutants, Concentrations, and Particle Sizes

Of all reported estimated effects, associations were observed for coarser particles (PM_{10}), finer particles ($PM_{2.5}$), and quasi-UFPs (PN_{acc}), as well as for NO_2, of which $PM_{2.5}$ has shown the most consistent findings. This is consistent with previous research showing that the rather unspecific metric $PM_{2.5}$ is most commonly associated with CVD hospitalization and mortality (Franklin et al. 2015). In addition, the observed weaker but consistent indications for adverse health effects of NO_2, provide a contribution to the epidemiological evidence that is less well studied in relation to cardiovascular events. While NO_2 can be attributed to industrial facilities and the road transport sector and is a commonly used surrogate for traffic, PM can be emitted from many anthropogenic sources, including both combustion and non-combustion sources and hence, cannot be assigned to a single source (European Environmental Agency (EEA) 2013). As outlined in Hennig et al. (2018b) using other or additional particle metrics to PM, e.g. PSC or PNC for different particle sizes, could help to identify emission sources. This might be beneficial in order to tackle the problem of air pollution at the root cause.

Nevertheless, a remarkable finding from all reported analyses was that the majority of estimated adverse health effects were observed for air pollution levels below European standards (40 $\mu g/m^3$ for annual concentrations of PM_{10} and NO_2, and 25 $\mu g/m^3$ for annual concentrations of $PM_{2.5}$), which were defined in the European Union Air Quality Directive in 2008 (European Union 2008). Despite an overall achieved improvement in air quality (European Commission 2019; Hoffmann et al. 2020), which has also been observed within the Ruhr Area with consistently decreasing levels of air pollution (Hennig et al. 2020, 2016), the current European legislation regarding air pollution control has not fully succeeded in protecting the health of European citizens. Moreover, new studies have shown strong associations with health effects at levels below current legal standards in the general population, with no observable thresholds protecting human health (Papadogeorgou et al. 2019; Pope et al. 2020), despite a decline in air pollution levels and in the air pollution-attributable burden of disease in most European countries. In addition, the Health Effect Institute (HEI) has invested in studies to specifically ad-

dress adverse health effects of low levels of air pollution USA, Canada, and Europe. First studies have supported air pollution-associated mortality at low levels in the USA (Dominici et al. 2019) and Canada (Brauer et al. 2019), and associations between low-level air pollution and respiratory events, i.e. lung cancer or chronic obstructive pulmonary disease, in Europe (Hvidtfeldt et al. 2021; Liu et al. 2021). For Europe, however, it has to be said that the politically agreed currently applicable European standards for annual concentrations of PM are less stringent than the currently applicable target values suggested by the WHO (20 $\mu g/m^3$ for annual concentrations of PM_{10} and 10 $\mu g/m^3$ for annual concentrations of $PM_{2.5}$), which have explicitly been proposed to protect public health (World Health Organization 2005). Considering that air pollution travels across national boundaries, coordination at EU level is important for the health of Europeans, which cannot be guaranteed with the measures currently in force. Since the last implementation of target values took place in 2008 (European Union 2008), there are already plans in the EU to reach the values recommended by the WHO for particulate matter in large parts of the EU within ten years (European Commission 2019). In line, a promising European action is the European Green Deal, aiming for zero pollution with respect to air, water and soil and hence, a toxic-free environment in Europe (European Environmental Agency (EEA) 2020).

Alongside the pathogenic low levels of air pollution, UFPs have been given an increasingly important role due to their potential of not only getting deeper into the lungs but also into the bloodstream and the brain. Recent reviews concluded that particularly short-term exposures to UFPs contribute to respiratory, cardiovascular and nervous system health effects (HEI Review Panel on Ultrafine Particles 2013; Ohlwein et al. 2019; Schraufnagel 2020). The study on UFPs in the Ruhr Area, reported in Hennig et al. (2018b), could not attribute a greater role to UFPs compared to PM_{10} regarding acute (and slightly delayed) cause-specific mortality. However, this finding could be a result of the single-site measurement, which was related to mortality of three surrounding cities. PM_{10} concentrations have a higher spatial homogeneity than UFPs, such that health effects can be captured more accurately on a broader spatial scale. In addition, several strong indoor sources of UFPs, i.e. domestic cooking, complicate a precise exposure assessment. Time series analysis can only capture temporally connected air-pollution-related events instead of long-term morbidity, and few models for long-term concentrations of UFPs have been developed yet. This study can hence only contribute to the limited epidemiological evidence on acute health effects of UFPs.

6.4 Air Pollution and Noise

In addition to air pollution, traffic-related noise has been identified as an environmental risk factor for cardiovascular diseases (Münzel et al. 2018; World Health Organization 2011). Due to the potential common source of traffic, it is important to consider noise exposure in the context of air pollution studies whenever available. In line with most epidemiological studies on cardiovascular health taking into account simultaneous exposure to air pollution and noise (Tétreault et al. 2013), mutual confounding was not

observed in the HNR study regarding markers of atherosclerosis. However, confounding implies a reasonable correlation, which was not observed in the HNR study as reported in Hennig et al. (2019). While noise and air pollution did not confound each other, both exposures were almost equally associated with early development of TAC based on the population-based inter-quartile ranges with no signal of a synergistic effect. In contrast, investigations on mild cognitive impairment in the HNR study reported slightly stronger effects from noise compared to air pollution and observed an additive interaction of both exposures (Tzivian et al. 2016). Yet, there are uncertainties regarding the synergistic associations of air pollution and noise, as well as independent associations of noise with respect to mental health that remained to be investigated (Hahad et al. 2020). However, despite a non-additive effect, noise was shown to be associated with TAC progression and hence contributing to the importance of noise regarding cardiovascular risk, which has not been sufficiently studied in epidemiological studies up to date. Nevertheless, environmental is noise considered a health risk that affects quality of life and can lead to significant levels of stress, sleep disturbance and adverse health effects, including cardiovascular problems. Mainly as a result of increasing traffic volumes, intensifying industrial and recreational activities environmental noise levels are rising in urban areas. It is estimated that approximately 20% of the European population are subjected to noise levels that are considered unacceptable (Kurrer 2021). Hence, simultaneously to air pollution, preventive measures are needed to protect the population from the harmful effects of noise on health (Hahad et al. 2019).

6.5 Conclusion

Overall, the achievements of this thesis are its contributions to epidemiological evidence on associations between environmental short-, as well as long-term air pollution exposure and cardiovascular morbidity and mortality in the Ruhr Area. Besides the overall weak associations with long-term concentrations from major air pollutants (PM_{10}, $PM_{2.5}$, and NO_2) regarding atherosclerotic progression, sub-group findings for those with no or only minor atherosclerotic burden were more consistent and supported adverse findings from cross-sectional investigations. These results provide biological plausibility of long-term adverse effects of air pollution on the cardiovascular system. Moreover, challenges with regard to population-based air pollution modelling were addressed, discussed, and transparently reported, as well as the role of simultaneous noise exposure. All studies presented in this thesis were conducted in the German Ruhr Area and used population-based data. As the home for roughly 5 million people, who are consistently exposed not only to rush-hour traffic and industrial hot spots, but also to air pollution from general traffic, industry, shipping, and agriculture within and outside of the Ruhr Area, even weak adverse health effects from air pollution exposure will have a strong impact on public health in this region.

7 References

Basagaña X, Rivera M, Aguilera I, Agis D, Bouso L, Elosua R, et al. 2012. Effect of the number of measurement sites on land use regression models in estimating local air pollution. Atmospheric Environment 54:634–642; doi:10.1016/j.atmosenv.2012.01.064.

Bauer M, Moebus S, Möhlenkamp S, Dragano N, Nonnemacher M, Fuchsluger M, et al. 2010. Urban Particulate Matter Air Pollution Is Associated With Subclinical Atherosclerosis. Journal of the American College of Cardiology 56:1803–1808; doi:10.1016/j.jacc.2010.04.065.

Beelen R, Hoek G, Vienneau D, Eeftens M, Dimakopoulou K, Pedeli X, et al. 2013. Development of NO2 and NOx land use regression models for estimating air pollution exposure in 36 study areas in Europe - The ESCAPE project. Atmospheric Environment 72:10–23; doi:10.1016/j.atmosenv.2013.02.037.

Bezirksregierung Arnsberg. 2011. Luftreinhalteplan Ruhrgebiet 2011. 1–185. Available: https://www.brd.nrw.de/umweltschutz/umweltzone%7B/_%7Dluftreinhaltung/pdf/Luftreinhalteplan-Ruhrgebiet-2011-i%7B/_%7Dd%7B/_%7DF%7B/_%7D-15%7B/_%7D06%7B/_%7D2015.pdf.

Birmili W, Weinhold K, Rasch F, Sonntag A, Sun J, Merkel M, et al. 2016. Long-term observations of tropospheric particle number size distributions and equivalent black carbon mass concentrations in the German Ultrafine Aerosol Network (GUAN). Earth System Science Data 8:355–382; doi:10.5194/essd-8-355-2016.

Bourdrel T, Bind M-A, Béjot Y, Morel O, Argacha J-F. 2017. Cardiovascular effects of air pollution. Archives of cardiovascular diseases 110:634–642; doi:10.1016/j.acvd.2017.05.003.

Brauer M, Brook JR, Christidis T, Chu Y, Crouse DL, Erickson A, et al. 2019. Mortality–Air Pollution Associations in Low-Exposure Environments (MAPLE): Phase 1. 5505.

Breiman L. 2001. Random Forests. In: *Machine learning* (R.E. Schapire, ed). Vol. 45 of. Kluwer Academic Publishers. 5–32.

Brokamp C, Jandarov R, Rao MB, LeMasters G, Ryan P. 2017. Exposure assessment models for elemental components of particulate matter in an urban environment: A comparison of regression and random forest approaches. Atmospheric Environment 151:1–11; doi:10.1016/j.atmosenv.2016.11.066.

Brook RD, Franklin B, Cascio W, Hong Y, Howard G, Lipsett M, et al. 2004. Air pollution and cardiovascular disease: A statement for healthcare professionals from the expert panel on population and prevention science of the American Heart Association. Circulation 109:2655–2671; doi:10.1161/01.CIR.0000128587.30041.C8.

Brook RD, Rajagopalan S. 2010. Particulate Matter Air Pollution and Atherosclerosis. Current Atherosclerosis Reports 12:291–300; doi:10.1007/s11883-010-0122-7.

Bruckmann P, Pfeffer U, Hoffmann V. 2014. 50 years of air quality control in Northwestern Germany - How the blue skies over the Ruhr district were achieved: Part I. Gefahrstoffe Reinhaltung der Luft 74: 37–44.

Brunekreef B, Holgate ST. 2002. Air pollution and health. Lancet 360:1233–1242; doi:10.1016/S0140-6736(02)11274-8.

Budoff MJ, Möhlenkamp S, McClelland R, Delaney JA, Bauer M, Jöckel HK, et al. 2013. A comparison of outcomes with coronary artery calcium scanning in unselected populations: The Multi-Ethnic Study of Atherosclerosis (MESA) and Heinz Nixdorf RECALL study (HNR). Journal of Cardiovascular Computed Tomography 7:182–191; doi:10.1016/j.jcct.2013.05.009.

Bundesministerium der Justiz und für Verbraucherschutz. 2010. 39. BImSchV - Neununddreißigste Verordnung zur Durchführung des Bundes-Immissionsschutzgesetzes.

Cesaroni G, Forastiere F, Stafoggia M, Andersen ZJ, Badaloni C, Beelen R, et al. 2014. Long term exposure to ambient air pollution and incidence of acute coronary events: Prospective cohort study and meta-analysis in 11 european cohorts from the escape project. BMJ (Online) 348; doi:10.1136/bmj.f7412.

Colette A, Granier C, Hodnebrog, Jakobs H, Maurizi A, Nyiri A, et al. 2011. Air quality trends in Europe over the past decade: A first multi-model assessment. Atmospheric Chemistry and Physics 11:11657–11678; doi:10.5194/acp-11-11657-2011.

Dominici F, Schwartz J, Di Q, Braun D, Choirat C, Zanobetti A. 2019. Assessing Adverse Health Effects of Long-Term Exposure to Low Levels of Ambient Air Pollution: Phase 1. Research report (Health Effects Institute) 1–51.

Eeftens M, Beelen R, De Hoogh K, Bellander T, Cesaroni G, Cirach M, et al. 2012. Development of land use regression models for PM2.5, PM 2.5 absorbance, PM10 and PMcoarse in 20 European study areas; Results of the ESCAPE project. Environmental Science and Technology 46:11195–11205; doi:10.1021/es301948k.

Erbel R, Möhlenkamp S, Moebus S, Schmermund A, Lehmann N, Stang A, et al. 2010. Coronary Risk Stratification, Discrimination, and Reclassification Improvement Based on Quantification of Subclinical Coronary Atherosclerosis. Journal of the American College of Cardiology 56:1397–1406; doi:10.1016/j.jacc.2010.06.030.

Estol CJ. 2020. Air Pollution and Cardiovascular Disease: A Proven Causality. In: *Health of people, health of planet and our responsibility.* 193–204.

European Commission. 2021. Air quality - Introduction. Available: https://ec.europa.eu/environment/air/quality/ [accessed March 5, 2021].

European Commission. 2019. Fitness check of the Ambient Air Quality Directives. Directive 2004/107/EC relating to arsenic, cadmium, mercury, nickel and polycyclic aromatic hydrocarbons in ambient air and Directive 2008/50/EC on ambient air quality and cleaner air for Europe. 1–27.

European Environment Agency (EEA). 2013. Europe's air today. Available: https://www.eea.europa.eu/signals/signals-2013/articles/europes-air-today [accessed March 5, 2021].

European Environmental Agency (EEA). 2013. Air pollution fact sheet 2013. 2. Available: http://www.eea.europa.eu/themes/air/air-pollution-country-fact-sheets [accessed March 5, 2021].

European Environmental Agency (EEA). 2017. Air quality in Europe - 2017 report. EEA Report 1–80; doi:10.2800/850018.

European Environmental Agency (EEA). 2020. Air quality in Europe - 2020 report. EEA Report 1–162; doi:10.2800/786656.

European Union. 2008. DIRECTIVE 2008/50/EC OF THE EUROPEAN PARLIAMENT AND OF THE COUNCIL of 21 May 2008 on ambient air quality and cleaner air for Europe. Official Journal of the European Union 152: 1–44 (BG, ES, CS, DA, DE, ET, EL, EN, FR, IT, LV).

Faustini A, Rapp R, Forastiere F. 2014. Nitrogen dioxide and mortality: review and meta-analysis of long-term studies. European Respiratory Journal 44:744–753; doi:10.1183/09031936.00114713.

Franklin BA, Brook R, Pope AC. 2015. Air Pollution and Cardiovascular Disease. Current Problems in Cardiology 40:207–238; doi:10.1016/j.cpcardiol.2015.01.003.

Fuks KB, Weinmayr G, Basagaña X, Gruzieva O, Hampel R, Oftedal B, et al. 2016a. Long-term exposure to ambient air pollution and traffic noise and incident hypertension in seven cohorts of the European study of cohorts for air pollution effects (ESCAPE). European Heart Journal 38:ehw413; doi:10.1093/eurheartj/ehw413.

Fuks KB, Weinmayr G, Hennig F, Tzivian L, Moebus S, Jakobs H, et al. 2016b. Association of long-term exposure to local industry- and traffic-specific particulate matter with arterial blood pressure and incident hypertension. International Journal of Hygiene and Environmental Health 219:527–535; doi:10.1016/j.ijheh.2016.05.008.

Gakidou E, Afshin A, Abajobir AA, Abate KH, Abbafati C, Abbas KM, et al. 2017. Global, regional, and national comparative risk assessment of 84 behavioural, environmental and occupational, and metabolic risks or clusters of risks, 1990–2016: a systematic analysis for the Global Burden of Disease Study 2016. The Lancet 390:1345–1422; doi:10.1016/S0140-6736(17)32366-8.

Hahad O, Beutel ME, Gilan DA, Michal M, Daiber A, Münzel T. 2020. Auswirkungen von Umweltrisikofaktoren wie Lärm und Luftverschmutzung auf die psychische Gesundheit: Was wissen wir? DMW - Deutsche Medizinische Wochenschrift 145:1701–1707; doi:10.1055/a-1201-2155.

Hahad O, Kröller-Schön S, Daiber A, Münzel T. 2019. Auswirkungen von Lärm auf das Herz-Kreislauf-System. Deutsches Arzteblatt International 116; doi:10.3238/arztebl.2019.0245.

Hebbinghaus H, Wurzler S, Memmesheimer M, Peikorz G, Friese E, Jakobs H, et al. 2014. The origin of PM10, PM2,5 and NO2background levels in Germany with focus on North-Rhine-Westphalia. Gefahrstoffe Reinhaltung der Luft 7.

HEI Panel on the Health Effects of Traffic-Related Air Pollution. 2009. Traffic-Related Air Pollution : A Critical Review of the Literature on Emissions , Exposure , and Health Effects. 1–394.

HEI Review Panel on Ultrafine Particles. 2013. Understanding the Health Effects of Ambient Ultrafine Particles. 122. Available: www.healtheffects.org%20http://pubs.healtheffects.org/view.php?id=394.

Hennig F, Fuks K, Moebus S, Weinmayr G, Memmesheimer M, Jakobs H, et al. 2014. Association between source-specific particulate matter air pollution and hs-CRP: Local traffic and industrial emissions. Environmental Health Perspectives 122:703–710; doi:10.1289/ehp.1307081.

Hennig F, Geisel MH, Kälsch H, Lucht S, Mahabadi AA, Moebus S, et al. 2020. Air pollution and progression of atherosclerosis in different vessel beds—results from a prospective cohort study in the ruhr area, germany. Environmental Health Perspectives 128:1–9; doi:10.1289/EHP7077.

Hennig F, Lucht S, Hoffmann B. 2018a. Improvement of LUR Model Predictions Using Chemistry-Transport Model Estimates. ISEE conference abstracts 2018; doi:10.1289/isesisee.2018.p01.1100.

Hennig F, Moebus S, Reinsch N, Budde T, Erbel R, Jöckel KH, et al. 2019. Investigation of air pollution and noise on progression of thoracic aortic calcification: results of the Heinz Nixdorf Recall Study. European Journal of Preventive Cardiology 0:1–9; doi:10.1177/2047487319854818.

Hennig F, Quass U, Hellack B, Küpper M, Kuhlbusch TAJ, Stafoggia M, et al. 2018b. Ultrafine and fine particle number and surface area concentrations and daily cause-specific mortality in the Ruhr area, Germany, 2009–2014. Environmental Health Perspectives 126:1–10; doi:10.1289/EHP2054.

Hennig F, Sugiri D, Tzivian L, Fuks K, Moebus S, Jöckel K-H, et al. 2016. Comparison of Land-Use Regression Modeling with Dispersion and Chemistry Transport Modeling to Assign Air Pollution Concentrations within the Ruhr Area. Atmosphere 7:48; doi:10.3390/atmos7030048.

Hoek G, Beelen R, Hoogh K de, Vienneau D, Gulliver J, Fischer P, et al. 2008. A review of land-use regression models to assess spatial variation of outdoor air pollution. Atmospheric Environment 42:7561–7578; doi:10.1016/j.atmosenv.2008.05.057.

Hoffmann B, Moebus S, Dragano N, Stang A, Möhlenkamp S, Schmermund A, et al. 2009. Chronic residential exposure to particulate matter air pollution and systemic inflammatory markers. Environmental Health Perspectives 117:1302–1308; doi:10.1289/ehp.0800362.

Hoffmann B, Moebus S, Möhlenkamp S, Stang A, Lehmann N, Dragano N, et al. 2007. Residential exposure to traffic is associated with coronary atherosclerosis. Circulation 116:489–496; doi:10.1161/CIRCULATIONAHA.107.693622.

Hoffmann B, Moebus S, Stang A, Beck EM, Dragano N, Möhlenkamp S, et al. 2006. Residence close to high traffic and prevalence of coronary heart disease. European Heart Journal 27:2696–2702; doi:10.1093/eurheartj/ehl278.

Hoffmann B, Roebbel N, Gumy S, Forastiere F, Brunekreef B, Jarosinska D, et al. 2020. Air pollution and health: Recent advances in air pollution epidemiology to inform the European green deal: A joint workshop report of ERS, WHO, ISEE and HEI. European Respiratory Journal 56; doi:10.1183/13993003.02575-2020.

Hoffmann B, Weinmayr G, Hennig F, Fuks K, Moebus S, Weimar C, et al. 2015. Air Quality, Stroke, and Coronary Events - Results of the Heinz Nixdorf Recall Study From the Ruhr Region. Deutsches Arzteblatt International 112:195–201; doi:10.3238/arztebl.2015.0195.

Hoogh K de, Chen J, Gulliver J, Hoffmann B, Hertel O, Ketzel M, et al. 2018. Spatial PM2.5, NO2, O3 and BC models for Western Europe – Evaluation of spatiotemporal stability. Environment International 120:81–92; doi:10.1016/j.envint.2018.07.036.

Hoogh K de, Korek M, Vienneau D, Keuken M, Kukkonen J, Nieuwenhuijsen MJ, et al. 2014. Comparing land use regression and dispersion modelling to assess residential exposure to ambient air pollution for epidemiological studies. Environment International 73:382–392; doi:10.1016/j.envint.2014.08.011.

Hvidtfeldt UA, Severi G, Andersen ZJ, Atkinson R, Bauwelinck M, Bellander T, et al. 2021. Long-term low-level ambient air pollution exposure and risk of lung cancer – A pooled analysis of 7 European cohorts. Environment International 146:106249; doi:10.1016/j.envint.2020.106249.

Jakobs H, Memmesheimer M, Ebel A. 2005. Daily Forecast of Air Quality over Europe with the EURAD Model System. Environmental Research 7.

Johnson CO, Nguyen M, Roth GA, Nichols E, Alam T, Abate D, et al. 2019. Global, regional, and national burden of stroke, 1990–2016: a systematic analysis for the Global Burden of Disease Study 2016. The Lancet Neurology 18:439–458; doi:10.1016/S1474-4422(19)30034-1.

Johnson M, Brook JR, Brook RD, Oiamo TH, Luginaah I, Peters PA, et al. 2020. Traffic-Related Air Pollution and Carotid Plaque Burden in a Canadian City With Low-Level Ambient Pollution. Journal of the American Heart Association 9:e013400; doi:10.1161/JAHA.119.013400.

Kaufman JD, Spalt EW, Curl CL, Hajat A, Jones MR, Kim S-Y, et al. 2016. Advances in Understanding Air Pollution and CVD. Global Heart 11:343; doi:10.1016/j.gheart.2016.07.004.

Kälsch H, Hennig F, Moebus S, Mohlenkamp S, Dragano N, Jakobs H, et al. 2014. Are air pollution and traffic noise independently associated with atherosclerosis: the Heinz Nixdorf Recall Study. European Heart Journal 35:853–860; doi:10.1093/eurheartj/eht426.

Kelly FJ, Fussell JC. 2015. Air pollution and public health: emerging hazards and improved understanding of risk. Environmental Geochemistry and Health 37:631–649; doi:10.1007/s10653-015-9720-1.

Klompmaker JO, Janssen N, Andersen ZJ, Atkinson R, Bauwelinck M, Chen J, et al. 2021. Comparison of associations between mortality and air pollution exposure estimated with a hybrid, a land-use regression and a dispersion model. Environment International 146:106306; doi:10.1016/j.envint.2020.106306.

Kurrer C. 2021. AIR AND NOISE POLLUTION. 1–6. Available: https://www.europarl.europa.eu/factsheets/en/sheet/75/air-and-noise-pollution [accessed March 5, 2021].

Künzli N, Jerrett M, Garcia-Esteban R, Basagaña X, Beckermann B, Gilliland F, et al. 2010. Ambient air pollution and the progression of atherosclerosis in adults. PLoS ONE 5; doi:10.1371/journal.pone.0009096.

Künzli N, Kaiser R, Medina S, Studnicka M, Chanel O, Filliger P, et al. 2000. Public-health impact of outdoor and traffic-related air pollution: a European assessment. The Lancet 356:795–801; doi:10.1016/S0140-6736(00)02653-2.

Lanki T, Hampel R, Tiittanen P, Andrich S, Beelen R, Brunekreef B, et al. 2015. Air pollution from road traffic and systemic inflammation in adults: A cross-sectional analysis in the European ESCAPE project. Environmental Health Perspectives 123:785–791; doi:10.1289/ehp.1408224.

LANUV. 2021. Messorte der Luftqualitätsüberwachung in NRW. Available: https://www.lanuv.nrw.de/umwelt/luft/immissionen/messorte-und-werte [accessed March 5, 2021].

Lehmann N, Erbel R, Mahabadi AA, Rauwolf M, Möhlenkamp S, Moebus S, et al. 2018. Value of progression of coronary artery calcification for risk prediction of coronary and cardiovascular events: Result of the hnr study (heinz nixdorf recall). Circulation 137:665–679; doi:10.1161/CIRCULATIONAHA.116.027034.

Libby P. 2012. Inflammation in atherosclerosis. Arteriosclerosis, Thrombosis, and Vascular Biology 32:2045–2051; doi:10.1161/ATVBAHA.108.179705.

Liu S, Jørgensen JT, Ljungman P, Pershagen G, Bellander T, Leander K, et al. 2021. Long-term exposure to low-level air pollution and incidence of chronic obstructive pulmonary disease: The ELAPSE project. Environment International 146:106267; doi:10.1016/j.envint.2020.106267.

Loizou CP, Nicolaides A, Kyriacou E, Georghiou N, Griffin M, Pattichis CS. 2015. A Comparison of Ultrasound Intima-Media Thickness Measurements of the Left and

Right Common Carotid Artery. IEEE Journal of Translational Engineering in Health and Medicine 3; doi:10.1109/JTEHM.2015.2450735.

Lucht SA, Hennig F, Matthiessen C, Ohlwein S, Icks A, Moebus S, et al. 2018. Air pollution and glucose metabolism: An analysis in non-diabetic participants of the Heinz Nixdorf recall study. Environmental Health Perspectives 126:047001-1-047001-10; doi:10.1289/EHP2561.

Lucht S, Hennig F, Moebus S, Ohlwein S, Herder C, Kowall B, et al. 2020. All-source and source-specific air pollution and 10-year diabetes Incidence: Total effect and mediation analyses in the Heinz Nixdorf recall study. Environment International 136:105493; doi:10.1016/j.envint.2020.105493.

Luo X, Yang Y, Cao T, Li Z. 2011. Differences in left and right carotid intima–media thickness and the associated risk factors. Clinical Radiology 66:393–398; doi:10.1016/j.crad.2010.12.002.

Memmesheimer M, Friese E, Ebel A, Jakobs HJ, Feldmann H, Kessler C, et al. 2004. Long-term simulations of particulate matter in Europe on different scales using sequential nesting of a regional model. International Journal of Environment and Pollution 22:108–132; doi:10.1504/ijep.2004.005530.

Münzel T, Schmidt FP, Steven S, Herzog J, Daiber A, Sørensen M. 2018. Environmental Noise and the Cardiovascular System. Journal of the American College of Cardiology 71:688–697; doi:10.1016/j.jacc.2017.12.015.

Nonnemacher M, Jakobs H, Viehmann A, Vanberg I, Kessler C, Moebus S, et al. 2014. Spatio-temporal modelling of residential exposure to particulate matter and gaseous pollutants for the Heinz Nixdorf Recall Cohort. Atmospheric Environment 91:15–23; doi:10.1016/j.atmosenv.2014.03.052.

Oberdörster G, Oberdörster E, Oberdörster J. 2005. Nanotoxicology: An emerging discipline evolving from studies of ultrafine particles. Environmental Health Perspectives 113:823–839; doi:10.1289/ehp.7339.

Ohlwein S, Kappeler R, Kutlar Joss M, Künzli N, Hoffmann B. 2019. Health effects of ultrafine particles: a systematic literature review update of epidemiological evidence. International Journal of Public Health 64:547–559; doi:10.1007/s00038-019-01202-7.

Papadogeorgou G, Kioumourtzoglou MA, Braun D, Zanobetti A. 2019. Low Levels of Air Pollution and Health: Effect Estimates, Methodological Challenges, and Future Directions. Current environmental health reports 6:105–115; doi:10.1007/s40572-019-00235-7.

Perez L, Wolf K, Hennig F, Penell J, Basagaña X, Foraster M, et al. 2015. Air pollution and atherosclerosis: A cross-sectional analysis of four European cohort studies in the ESCAPE study. Environmental Health Perspectives 123:597–605; doi:10.1289/ehp.1307711.

Pope CA, Coleman N, Pond ZA, Burnett RT. 2020. Fine particulate air pollution and human mortality: 25+ years of cohort studies. Environmental Research 183:108924; doi:10.1016/j.envres.2019.108924.

Provost EB, Madhloum N, Panis LI, De Boever P, Nawrot TS. 2015. Carotid intima-media thickness, a marker of subclinical atherosclerosis, and particulate air pollution exposure: The meta-analytical evidence. PLoS ONE 10:1–12; doi:10.1371/journal.pone.0127014.

Rodins V, Lucht S, Ohlwein S, Hennig F, Soppa V, Erbel R, et al. 2020. Long-term exposure to ambient source-specific particulate matter and its components and incidence of cardiovascular events – The Heinz Nixdorf Recall study. Environment International 142:105854; doi:10.1016/j.envint.2020.105854.

Rückerl R, Greven S, Ljungman P, Aalto P, Antoniades C, Bellander T, et al. 2007. Air pollution and inflammation (Interleukin-6, C-reactive protein, fibrinogen) in myocardial infarction survivors. Environmental Health Perspectives 115:1072–1080; doi:10.1289/ehp.10021.

Schmermund A, Möhlenkamp S, Stang A, Grönemeyer D, Seibel R, Hirche H, et al. 2002. Assessment of clinically silent atherosclerotic disease and established and novel risk factors for predicting myocardial infarction and cardiac death in healthy middle-aged subjects: Rationale and design of the Heinz Nixdorf RECALL Study. American Heart Journal 144:212–218; doi:10.1067/mhj.2002.123579.

Schraufnagel DE. 2020. The health effects of ultrafine particles. Experimental and Molecular Medicine 52:311–317; doi:10.1038/s12276-020-0403-3.

Stafoggia M, Cesaroni G, Peters A, Andersen ZJ, Badaloni C, Beelen R, et al. 2014. Long-term exposure to ambient air pollution and incidence of cerebrovascular events: Results from 11 European cohorts within the ESCAPE project. Environmental Health Perspectives 122:919–925; doi:10.1289/ehp.1307301.

Tétreault LF, Perron S, Smargiassi A. 2013. Cardiovascular health, traffic-related air pollution and noise: Are associations mutually confounded? A systematic review. International Journal of Public Health 58:649–666; doi:10.1007/s00038-013-0489-7.

Touboul PJ, Hennerici MG, Meairs S, Adams H, Amarenco P, Bornstein N, et al. 2012. Mannheim carotid intima-media thickness and plaque consensus (2004-2006-2011). Cerebrovascular Diseases 34:290–296; doi:10.1159/000343145.

Touboul PJ, Hennerici MG, Meairs S, Adams H, Amarenco P, Desvarieux M, et al. 2004. Mannheim intima-media thickness consensus. Cerebrovascular Diseases 18:346–349; doi:10.1159/000081812.

Tzivian L, Dlugaj M, Winkler A, Weinmayr G, Hennig F, Fuks KB, et al. 2016. Long-Term Air Pollution and Traffic Noise Exposures and Mild Cognitive Impairment in Older Adults: A Cross-Sectional Analysis of the Heinz Nixdorf Recall Study. Environmental Health Perspectives 124:1361–1368; doi:10.1289/ehp.1509824.

Umweltbundesamt. 2009. Feinstaubbelastung in Deutschland. 1–22. Available: http://www.env-it.de/luftdaten/map.%20https://www.umweltbundesamt.de/sites/default/files/medien/publikation/long/3565.pdf.

Viehmann A, Hertel S, Fuks K, Eisele L, Moebus S, Möhlenkamp S, et al. 2015. Long-term residential exposure to urban air pollution, and repeated measures of systemic blood markers of inflammation and coagulation. Occupational and Environmental Medicine 72:656–663; doi:10.1136/oemed-2014-102800.

Weinmayr G, Hennig F, Fuks K, Nonnemacher M, Jakobs H, Möhlenkamp S, et al. 2015. Long-term exposure to fine particulate matter and incidence of type 2 diabetes mellitus in a cohort study: effects of total and traffic-specific air pollution. Environmental Health 14:53; doi:10.1186/s12940-015-0031-x.

WHO European Centre for Environment and Health. 2013. Review of evidence on health aspects of air pollution - REVIHAAP. 1–309. Available: https://www.euro.who.int/%7B/_%7D%7B/_%7Ddata/assets/pdf%7B/_%7Dfile/0004/193108/REVIHAAP-Final-technical-report-final-version.pdf.

World Health Organization. 2011. Burden of disease from environmental noise - Quantification of healthy life years lost in Europe. 1–126. Available: https://www.euro.who.int/%7B/_%7D%7B/_%7Ddata/assets/pdf%7B/_%7Dfile/0008/136466/e94888.pdf.

World Health Organization. 2005. WHO Air quality guidelines for particulate matter, ozone, nitrogen dioxide and sulfur dioxide, Global update 2005 - Summary of risk assessment. 195: 491–498. Available: https://apps.who.int/iris/bitstream/handle/10665/69477/WHO%7B/_%7DSDE%7B/_%7DPHE%7B/_%7DOEH%7B/_%7D06.02%7B/_%7Deng.pdf?sequence=1%7B/&%7DisAllowed=y.

Acknowledgement

I am grateful for the time I was working in the group of Environmental Epidemiology, led by Barbara Hoffmann. This gratefulness is beyond the development of this thesis.

Barbara has introduced me to the topic of health effects of air pollution and also to the HNR study, which among Essen and Mülheim, is located in Bochum, which happens to be my hometown. So for me, this thesis is not only research but also research related to a place, I love - the Ruhr Area. She has thrown me into the deep end by giving me the lead of the research project "AIRCIMT" (Air pollution and carotid intima media thickness) and despite the challenges we had to face regarding cIMT measurements and monitoring for three examination periods, I am thankful for her taken this chance on me. She always discussed things at eye level, she has given an ear to me, and also, she has placed her trust in me. In addition, I am grateful for her introducing me to the International Society of Environmental Epidemiology (ISEE), which did not only bring me to places like Rome, Sydney or Ottawa, but also provided an excellent platform to discuss air pollution related research. Thank you.

I also would like to thank Oliver Kuss, who has inspired me, mostly because of his easy going way when it comes to research, methods and teaching.

I am truly thankful for each person that I have met during this path of interesting research, fruitful discussions, great collaborations, brain storming, writing, analysing, presenting, laughing, experiencing, learning, but also struggling. I am grateful for the friendships that have developed from this time.

Last but not least, I would like to thank my family and friends for always being by my side. You always listened to me when I was euphorically excited or doubted. Thank you for being there.